IDENTIFICATION OF SIRT1 (SILENT MATING TYPE INFORMATION REGULATION 2 HOMOLOG 1) MODIFIERS AS PROMISING THERAPEUTIC AGENTS FOR IMPROVING REDUCED WOUND HEALING IN TYPE II DIABETES

Thesis Submitted for the Award of the Degree of

DOCTOR OF PHILOSOPHY

in

Biochemistry

By

Rupal Dubey

Registration Number: 41800467

Supervised By	Co-Supervised By
Dr. Jeena Gupta	**Dr. Pranav Kumar Prabhakar**
Associate Professor	Professor
Department of Biochemistry	Department of Medical Laboratory Sciences
School of Bioengineering and Biosciences	School of Allied Medical Sciences
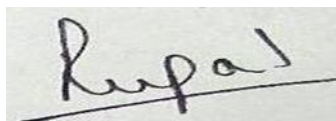
LOVELY PROFESSIONAL UNIVERSITY, PUNJAB
2024

DECLARATION

I, hereby declared that the presented work in the thesis entitled "Identification of SIRT1 (Silent mating type information regulation 2 homolog 1) modifiers as promising therapeutic agents for improving reduced wound healing in Type II Diabetes" in fulfilment of degree of **Doctor of Philosophy (Ph. D.)** is outcome of research work carried out by me under the supervision of Dr. Jeena Gupta, working as Associate Professor, in the Department of Biochemistry, School of Bioengineering and Biosciences of Lovely Professional University, Punjab, India. In keeping with general practice of reporting scientific observations, due acknowledgements have been made whenever work described here has been based on findings of other investigator. This work has not been submitted in part or full to any other University or Institute for the award of any degree.

(Signature of Scholar)

Name of the scholar: Rupal Dubey

Registration No.: 41800467

Department/school: Department of Biochemistry (School of Bioengineering and Biosciences)

Lovely Professional University,

Punjab, India

CERTIFICATE

This is to certify that the work reported in the Ph. D. thesis entitled "Identification of SIRT1 (Silent mating type information regulation 2 homolog 1) modifiers as promising therapeutic agents for improving reduced wound healing in Type II Diabetes" submitted in fulfillment of the requirement for the award of degree of **Doctor of Philosophy (Ph.D.)** in the Department of Biochemistry, School of Bioengineering and Biosciences, is a research work carried out by Rupal Dubey, 41800467, is bonafide record of her original work carried out under my supervision and that no part of thesis has been submitted for any other degree, diploma or equivalent course.
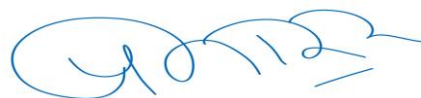

(Signature of Supervisor)   **(Signature of Co-Supervisor)**

Name of supervisor: Dr. Jeena Gupta   Name of Co-Supervisor: Dr. Pranav Kumar Prabhakar

Designation: Associate Professor   Designation: Professor

Department/school: Biochemistry,   Department/school: Medical Laboratory

School of Bioengineering and Biosciences   Sciences, School of Allied Medical Sciences

University: Lovely Professional University   University: Lovely Professional University

ABSTRACT

Diabetes mellitus (DM) poses a significant global public health challenge, impacting over 400 million individuals worldwide. This metabolic condition gradually gives rise to severe complications, including chronic microvascular, macrovascular, and neuropathic life-threatening issues. DM can arise from insufficient insulin secretion, pancreatic β cell damage, or insulin resistance associated with the non-utilization of insulin. The persistent increase in the global diabetic population may be attributed primarily to a growing preference for a sedentary lifestyle. DM gives rise to a range of complications, encompassing nephropathy, neuropathy, cardiovascular and renal issues, retinopathy, and disorders related to food intake, among others. Type 2 diabetes (T2D) results from the impairment of pancreatic beta cells, hindering an individual's ability to effectively use insulin. The rising pandemic has profound implications for individuals, society, and the economy, imposing substantial human and financial burdens. The expanding array of antihyperglycemic medications available for T2D, often characterized by diverse mechanisms of action and safety profiles, poses a challenge for clinicians. The growing complexity of diabetes management underscores the need for a well-informed strategy in both prevention and treatment.

Diabetic patients experience a diminished ability to metabolize glucose, leading to hyperglycemic conditions that complicate the wound-healing process, often resulting in prolonged chronic wounds. The incidence of delayed healing in diabetic patients is on the rise globally, primarily due to a lack of preventive and control measures. DM consumes a significant portion of worldwide health budgets, ranging from 2.5% to 15%, with diabetic wounds contributing substantially. According to a report, diabetes is anticipated to become the seventh leading cause of death by 2030. Shockingly, over 80% of diabetes-related deaths occur in low- and middle-income countries. Diabetic wounds account for approximately 50%–70% of all limb amputations, and it has been reported that one leg is amputated every 30 seconds worldwide due to impaired wound healing. Chronic wounds refer to tissue injuries that deviate from the typical organized stages of healing, persisting for more than 12 weeks. The usual healing process initiates with hemostasis, preventing blood loss and invasion of microbes into the wounded area. This phase swiftly transitions and overlaps with the inflammatory phase, where pro-inflammatory cells, initially neutrophils, are up-regulated. Subsequently, macrophages play a role in clearing debris and pathogens, along with the involvement of growth factors, cytokines, and other cells. The proliferative phase coincides with the inflammatory phase, during which the formation of new tissue, new blood vessels (angiogenesis), and the construction of a matrix are initiated to fill the wounded area. The subsequent remodeling phase further enhances the tensile strength of the extracellular matrix and diminishes the blood supply to the damaged area. Diabetic wounds manifests as delayed acute wounds and chronic wounds, revealing impaired healing characterized by a postponed, incomplete, or uncoordinated recovery process. These wounds exhibit a prolonged inflammatory phase, coupled with challenges in the formation of

mature granulation tissue and a decrease in wound tensile strength. Vascular damage resulting in ischemia may be a contributing factor.

Sirtuin 1 (SIRT1) belongs to a family of seven proteins that play a crucial role in the cellular response to inflammatory, metabolic, and oxidative stress. Its function involves NAD^+ dependent deacetylation of histones. Compounds that activate SIRT1 were discovered to safeguard and enhance the healing of diabetic wounds by regulating inflammation, cell migration, the response to oxidative stress, and the formation of granulation tissue at the wound site. However, the involvement of SIRT1 in enhancing delayed wound healing associated with diabetes is not fully comprehended. Consequently, scientists are actively researching to delve into this uncharted territory in translational research. Numerous medications are accessible in the market for treating DM and addressing delayed wound healing. However, synthetic drugs often come with side effects, prompting us to seek out phytochemicals capable of managing both DM and reduced wound healing.

This current investigation was conducted to identify natural SIRT1 modifiers with structural similarities to known phytochemicals used for managing DM and wound healing. The screening process involved utilizing ChEMBL and PubChem, followed by the assessment of SIRT1 activity through site-specific molecular docking using Autodock Vina 1.5.6. The results were visualized on a Python molecule viewer. Subsequently, promising molecules underwent further analysis using SwissADME to investigate Absorption, Distribution, Metabolism, and Excretion (ADME) properties. The efficacy of these potent molecules was then evaluated in both in vitro and in vivo models of diabetes and excision diabetic wounds. Following in silico and SwissADME investigations, Sinapic acid and o-Coumaric acid were chosen for additional study.

Both phytochemicals demonstrated notable antioxidant potential. The outcomes of the cell viability assay, conducted using the (3-(4,5-Dimethylthiazol-2-yl)-2,5-diphenyltetrazolium bromide (MTT) assay, revealed their impact on cell proliferation in the L929 cell line. It was found that the phytochemicals are non-toxic to normal cells ex-vivo. Moreover, both compounds exhibited the ability to enhance the migration of endothelial cells and restore the levels of antioxidant enzymes under hyperglycemic conditions. Therefore, our in vitro results suggest that the phytochemicals function as potent antioxidant compounds, potentially contributing to the mitigation of cellular damage. Due to the superior results observed with Sinapic acid compared to o-Coumaric acid, we have chosen Sinapic acid for further in vivo studies.

The outcomes of our in vivo study revealed that Sinapic acid effectively reduced elevated levels of blood plasma glucose, total cholesterol, serum triglycerides, very-low-density lipoprotein (VLDL), low-density lipoproteins (LDL), and Alkaline phosphatase (ALP). Histopathological findings revealed that critical factors essential for effective wound healing, such as re-epithelialization, thickening of the epidermis and dermis, and the maturation of fully developed granulation tissues, were disrupted in the diabetic wounded control group. In contrast, the administration of Sinapic acid at varying doses (20 mg/kg and 40 mg/kg) resulted in enhanced re-epithelization, mature and fully-developed granular tissues, and the formation of new blood vessels in

wounded tissues. However, when comparing diabetic wounds treated with 40 mg/kg of Sinapic acid to diabetic wound control groups, the 20 mg/kg dose of Sinapic acid proved effective in restoring all these parameters and expediting wound healing. This underscores the significance of undertaking pre-clinical investigations to discern the impact of different therapeutic dosages on the development of the disease. Consequently, to propel this product into clinical trials for potential applications in human health, additional research is essential. It is imperative to gain a deeper understanding of the molecular, cellular, and biochemical pathways through which this bioactive molecule facilitates wound healing.

ACKNOWLEDGEMENT

वक्रतुण्ड महाकाय सूर्यकोटि समप्रभ।

निर्विघ्नं कुरु मे देव सर्वकार्येषु सर्वदा॥

I am extremely grateful to **God** for his grace and wisdom during my academic path. The divine power has enlightened my path and given the fortitude to face the obstacles.

I dedicate this thesis to my beloved father, who resides in heaven, whose unwavering support and boundless love continue to inspire me every day. Your dreams became my guiding light, and I am immensely grateful for the values and aspirations you instilled in me. Your absence is deeply felt, yet your presence in my heart fuels my determination to fulfill the dreams we shared. This work stands as a tribute to your memory, a testament to the lessons you taught me, and a fulfillment of the aspirations you held my dear **Papa**. I am forever indebted to your enduring legacy.

I would like to express my gratitude and acknowledge my debt to my respected Supervisor **Dr. Jeena Gupta**, Associate Professor, Department of Biochemistry, School of Bioengineering and Biosciences, Lovely Professional University for her vigilant guidance, insightful criticism, extensive knowledge, helpful scientific advice, selfless demeanour, and unwavering support in completing this thesis. To work under her supervision has been an immense pleasure and honour.

I extend my deepest gratitude to my respected Co-Supervisor **Dr. Pranav Kumar Prabhakar**, Professor, Department of Medical Laboratory Sciences, School of Allied Medical Sciences, Lovely Professional University for his insightful feedback and guidance that propelled me through the challenges. I am immensely thankful for his mentorship.

I would like to express my sincere thanks to **Dr. Navneet Khurana**, Professor, Department of Pharmacology, School of Pharmaceutical Sciences, Lovely Professional University, for his diligent work in successfully completing my in vivo experiments and for kindly lending his time and expertise.

I would like to express my heartfelt gratitude to **Prof. Neeta Raj Sharma**, Head of the School, **Dr. Ashish Vyas**, Head of the Biochemistry Department, **Dr. Minhaj Ahmad Khan**, Head of Laboratory, and all other faculty members of the School of Bioengineering and Biosciences for providing me with the facilities to conduct my research and for their ongoing support.

I'd like to take this opportunity to thank **Dr. Ashok Mittal** (Honourable Chancellor), **Mrs. Rashmi Mittal** (Worthy Pro-Chancellor), **Dr. Lovi Raj Gupta** (Pro Vice Chancellor), and **Dr. Monica Gulati** (Registrar) for allowing me to serve at such a distinguished university.

TABLE OF CONTENT

LIST OF TABLES

LIST OF FIGURES

ABBREVIATIONS

ADME	Absorption, distribution, metabolism and excretion
AGEs	Advanced glycation end-products
AL-4	Angiopoietin-like 4
ALP	Alkaline Phosphatase
ANOVA	One-way analysis of variance
ATF-3	Activating transcription factor 3
BBB	Blood-brain barrier
BME	Basement membrane extract
BSA	Bovine serum albumin
BUN	Blood urea nitrogen
CDNB	1-chloro-2,4-dinitrobenzene
DDW	Double-distilled water
DFU	Diabetic foot ulcer
DMEM	Dulbecco's modified Eagle medium
DMSO	Dimethyl sulfoxide
DNMTs	DNA methyltransferases
DPPH	1,1-diphenyl-2-picrylhydrazyl
ECM	Extracellular matrix
EGF	Epidermal growth factor
EMT	Epithelial-to-mesenchymal transformation
eNOS	Endothelial nitric oxide synthase
EPCs	Endothelial progenitor cells
FBS	Fetal bovine serum
FGF	Fibroblast growth factor
GLP1R	Glucagon-like peptide 1 receptor
GSH	Glutathione (reduced)
GST	Glutathione-S-transferase
GWAS	Genome-wide association studies
H&E	Hematoxylin and Eosin
H3K4	Histone 3 lysine 4
HAT	Histone acetylation
HDAC	Histone deacetylase
HDL	High density lipoprotein
HFD	High-fat diet
HG	High glucose
HIA	Human intestinal absorption
HIF-1α	Hypoxia-inducible factor 1-alpha
HMECs	Human mammary epithelial cells
HMTs	Histone lysine methyltransferases
HRP	Horseradish peroxidase
HUVECs	Human umbilical vascular endothelial cells
IL	Interleukin
iNOS	Inducible nitric oxide synthase
IRAK1	Interleukin-1 receptor-associated kinase 1
IRF-4	Interferon regulatory factor-4
JMJ-C	Jumonji-C domain-containing demethylases
JNKs	c-Jun N-terminal kinases
LDL	Low density lipoprotein

LFT	Liver function test
LG	Low-glucose
LNA	Locked nucleic acid
LPO	Lipid peroxidation
LPS	Lipopolysaccharides
LPT	Lipid profile test
LSD	Lysine-specific demethylase
MCP-1	Monocyte chemoattractant protein 1
MDA	Malondialdehyde
MEF	Mouse embryonic fibroblast
miRNAs or miRs	MicroRNAs
MMP	Matrix metalloproteinase
MP	Macrophage polarization
MTT	3-(4,5-dimethylthiazol-2-yl)-2,5-diphenyltetrazolium bromide
NAD	Nicotine adenine dinucleotide
NBT	Nitro blue tetrazolium
NF-kB	Nuclear factor kappa B
NPD	Normal pellet diet
NR4A	Nuclear receptor subfamily 4 group A
NRF2	Nuclear factor erythroid 2-related factor
PBMC	Peripheral blood mononuclear cells
PBS	Phosphate buffered saline
PDB	Protein data bank
PDGF	Platelet-derived growth factor
PDHA1	Pyruvate dehydrogenase E1 alpha 1 subunit
PDX-1	Pancreatic and duodenal homeobox 1
P-gp	P-glycoprotein
PMN	Polymorphonuclear neutrophils
PMS	Post mitochondrial supernatant
PMV	Python molecule viewer
PNS	Post nuclear supernatant
PPARGC1α	Peroxisome proliferator-activated receptor gamma, coactivator 1 alpha
PUFA	Polyunsaturated fatty acids
QS	Quorum sensing
RMSD	Root mean square deviation
ROS	Reactive oxygen species
RPT	Renal profile test
SACs	SIRT1 activating compounds
SAM	S- adenosyl methionine
SD	Sprague-Dawley
SDF-1α	Stromal cell-derived factor 1α
SGOT	Serum glutamic oxaloacetic transaminase
SGPT	Serum glutamic pyruvic transaminase
SIRT1	Silent mating type information regulation 2 homolog 1
SOD	Superoxide dismutase
STAT3	Signal transducer and activator of transcription 3
STZ	Streptozotocin

T2D	Type 2 diabetes
TBA	Thiobarbituric acid
TET	Ten-eleven translocation
TGF-β1	Transforming growth factor-β1
TNF-α	Tumor necrosis factor- α
TRAF6	TNF receptor-associated factor 6
VCAM- 1	Vascular adhesion molecule-1
VEGF	Vascular endothelial growth factor
VLDL	Very low density lipoprotein

CHAPTER 1

INTRODUCTION

Diabetes is a metabolic dysfunction distinguished by elevated plasma glucose levels, stemming from impairments in either insulin action, insulin secretion, or a combination of both factors. According to a recent survey conducted by the International Diabetes Federation, approximately 537 million people worldwide are currently grappling with diabetes. Projections indicate that this number is anticipated to increase to 643 million by the year 2030 and further escalate to 783 million by 2045 (1). Individuals suffering from diabetes face an elevated likelihood of developing chronic wounds, especially in the foot region, commonly referred to as diabetic foot ulcer (DFU) (2). Approximately 15–20 % of patients with diabetes develop DFU annually, and almost 15 % of the health budget yearly is used to treat patients with diabetes and its complications worldwide. The decreased glucose metabolism was thought to affect the wound-healing process in patients with diabetes thereby installing chronic wounds (3).

The elevated level of blood glucose leads to poor blood flow, which prevents essential nutritional components from reaching the wounded area, and thus impairing the healing mechanism (4). Chronic inflammation and increased oxidative stress are characteristics of chronic wounds that result in causing extensive host tissue damage. For example, polymorphonuclear neutrophils (PMNs), immune cells, serve as potent effectors of inflammation as they display a first-line defence in case of tissue injury. However, excessive PMN activation results in increased reactive oxygen species (ROS) production at the site of inflammation, which affects the function of the vascular endothelium. The primary role of the vascular endothelium is to facilitate the transit of inflammatory cells from the bloodstream to the surrounding tissues. Nevertheless, in inflammatory situations, oxidative stress induced by PMNs disrupts the inter-endothelial junction, promoting the movement of inflammatory cells through the endothelial layer. Consequently, this process can result in tissue damage (5, 6). Therefore, disrupting the link between chronic inflammation and PMNs is imperative to reduce the increased incidence of diabetes-associated chronic wounds.

In addition to oxidative stress and chronic inflammation, impaired angiogenesis is another critical factor contributing to delayed wound healing in diabetic patients (7, 8). Angiogenesis, the formation of new blood vessels from pre-existing ones, is essential for delivering oxygen and nutrients to the wound site, thereby promoting tissue repair. However, in diabetic conditions, the angiogenic response is often blunted, leading to insufficient blood supply and delayed healing. This inadequate blood flow exacerbates hypoxia, a condition where tissues are deprived of sufficient oxygen, further impairing the wound healing process by limiting the energy available for cell proliferation and collagen synthesis (9-15). This impairment in angiogenesis is linked to the downregulation of key growth factors such as vascular endothelial growth factor (VEGF) and basic fibroblast growth factor (bFGF), which are crucial for endothelial cell proliferation and migration (16-19).

Furthermore, hyperglycemia-induced oxidative stress can directly damage endothelial cells, exacerbating vascular dysfunction and hindering the wound-healing process (20-22).

As aforementioned, fluctuation in blood glucose levels, oxidative stress, hypoxia, and impaired angiogenesis collectively contribute to chronic inflammation and delayed wound healing in patients with diabetes (23-27). Therefore, therapies that control blood glucose levels, reduce oxidative stress, and promote angiogenesis are critically needed to create a favourable microenvironment for wound healing. Since diabetic wound healing is a complex process, scientists developing pharmaceutical formulations have struggled to find scar-free wound healing treatments.

Over the past decades, sirtuins have attracted immense attention in diabetic wound healing because of their wide-ranging benefits. Sirtuins, a class of signaling proteins, play a crucial role in regulating various physiological pathways by interacting with their target molecules. Their involvement in processes such as inflammation, apoptosis, cellular senescence, and mitochondrial biogenesis highlights their importance in managing diabetes and its associated complications (28).

There are seven members in a conserved protein family known as sirtuins, which belong to class III histone deacetylases (HDACs) (29, 30). Mammals have seven sirtuins (SIRT1 to SIRT7) that display a wide range of different mechanisms and activities at the cellular level. Silent mating type information regulation 2 homolog 1 (SIRT1) regulates gene expression and DNA repair, while SIRT2 regulates cell division and the cell cycle. SIRT3 serves its purpose by regulating energy metabolism and protecting cells from oxidative stress, and SIRT4 regulates energy metabolism and insulin production. Furthermore, SIRT5 stimulates the regulation of metabolic pathways and eliminates post-translational modifications such as succinylation and malonylation, while SIRT6 is responsible for DNA repair, genomic integrity, and regulation of the inflammatory response. SIRT7, a distinct member of this family, controls the expression of ribosomal genes, essential for protein synthesis (31, 32).

Since sirtuins have shown potential involvement in aging, age-related diseases, and metabolic control, they have attracted significant attention in scientific studies. There is ongoing research and development of drugs aimed at controlling sirtuin activity as a strategy to prevent or delay aging and metabolic disorders (33, 34). Notably, SIRT1 is more extensively investigated in relation to diabetic wound healing than other members of the SIRT family. This is due to SIRT1's established roles in metabolism, inflammation, and cell survival, all of which are critical in the context to diabetes (35). Accumulating evidence indicates that disturbances in SIRT1 contribute to impairments in vessel development, while overexpression of SIRT1 improves the function and longevity of endothelial cells, which play a vital role in angiogenesis (36, 37). Recent discoveries propose that the pharmacological stimulation of SIRT1 not only boosts angiogenesis but also hastens the healing of wounds in individuals with diabetes by reducing ROS generation (38, 39). Studies have also highlighted the

potential mechanisms by which SIRT1 controls inflammation in diabetic lesions, making it a promising target for therapeutic interventions (40-43).

The endorsement of diabetic wound medications by regulatory agencies, such as the Food and Drug Administration, has led to a surge in the utilization of synthetic medications for treating DFU globally. However, the negative side effects of these medications, including blisters, skin peeling, excessive itching, and skin redness, have raised concerns about both their safety and effectiveness (44). This underscores the need for safer alternatives that may have minimal adverse effects. Naturally occurring phytochemicals are the most well-known option for the researchers to improve such medical problems. Plants are a growing source of natural epigenetic modifiers, including SIRT1 activators, which may provide numerous possibilities for researchers to identify new phytochemicals that could treat delayed wound healing in diabetic patients. To date, number of studies have been undertaken, with ongoing research aiming to elucidate the mechanism of SIRT1 in disease treatment. However, further in-depth investigations are necessary to unveil the association of SIRT1 with wound healing. Therefore, our objective is to identify a potent SIRT1 activator that could improve delayed wound healing associated with diabetes.

CHAPTER 2

REVIEW OF LITERATURE

2.1 Association between diabetes and diabetic wounds

Type 2 diabetes (T2D) is described as inveterately raised blood glucose levels, which occur due to insulin resistance associated with a halt in insulin release. T2D is increasing at an unprecedented pace across the world, and by 2035 the estimated occurrence of T2D is expected to rise to 592 million people (45). T2D is linked to various complications, whether micro or macrovascular, occurring in target organs, and is associated with a decrease in life expectancy. Chronic wounds in diabetes are a major source of concern, as they often result in atraumatic limb amputations (46). They are observed to impact approximately 15% of individuals with diabetes, constituting more than 27% of the $176 billion spent annually on healthcare services for diabetes in the United States (47, 48). Approximately 4-10% of individuals with diabetes are estimated to DFUs (49). Moreover, 56% of DFUs are prone to infection, with 20% of these cases requiring lower limb surgery (50). In recent times, it has been discovered that epigenetic pathways play a role in the development of cancer, diabetes, and related complications. Environmental factors modify the epigenetic machinery in individuals with diabetes, which is believed to be the fundamental cause of diabetic complications (51). Various factors in diabetes promote inflammation, hinder the proliferation of epithelial cells, and impede wound closure, leading to inadequate wound healing. Neutrophils and macrophages dispatched to the injured area are crucial elements of the healing process (52-54). In the initial phases of the standard healing process, macrophages assume a pro-inflammatory role before shifting to an anti-inflammatory form. This transition to an anti-inflammatory state promotes tissue regeneration and signifies advancement towards the subsequent stage of healing (53, 55, 56). In diabetic wounds, the typical transformation of macrophages is disrupted, causing them to persist in a pro-inflammatory state and impeding the healing process (57). Although the factors that cause the macrophage transition remains uncertain, new research indicates that epigenetic processes such as methylation of CpG islands (DNA) and histone tails (protein) are important for macrophage control in healthy as well as T2D wound healing (58-62). Owing to disrupted keratinocyte and fibroblast function caused by insulin resistance, production of advanced glycation end-products (AGEs), and re-epithelialization in diabetic wounds is delayed (63-66), thus the epigenetic control mechanisms are known to be involved in these processes (67-69).

2.2 Mechanism of wound healing in non-diabetics

Delayed healing of wound is a complex phenomenal defect that prevents the skin to regain its original shape, anatomical and morphological characteristics. The skin is an excellent barrier against microbial pathogens while chronic wounds are the active sites for microbiome to propagate by weakening the immune system (70). A total of four steps are mainly involved in the healing of wounds including hemostasis, and are represented in Fig 2.1.

2.2.1 Hemostasis: Excessive blood flow through the blood vessels after injury results in blood loss. However, damaged blood vessels at wounded tissue begin to constrict, resulting in the activation of the blood-clotting pathway. This cascade prevents the loss of blood thus maintaining the hemostasis of the body (71). Platelets are activated after encountering with vascular subendothelial matrix and play an important role during blood vessel damage. Glycoprotein VI is a well-known platelet receptor with the goal to interact with various proteins present in the extracellular matrix (ECM). These glycoproteins include Von Willebrand factor, fibronectin, and collagen that support platelet attachment to the damaged blood vessel wall (72). Thrombin, an enzyme acts as a bipolar molecule having procoagulant and anticoagulant properties and is responsible for activating the platelets. Thrombin exists in its zymogen form called prothrombin, an inactive enzyme present in the liver. Thrombin in its active state converts fibrinogen (an inactive form of fibrin) to fibrin (an active form of fibrinogen) and is thus involved in blood clotting (73). Three components factor V, thrombin, and prostacyclin together prevent the occurrence of platelet aggregation. Furthermore, endothelial and smooth muscle cells exhibit their function by releasing growth factors derived from platelets, and actively participates in the repair of the damaged vessel wall (74).

2.2.2 Inflammation: During any injury or pathogenic infection, the immune system signals the migrating cells and damaged tissue to release leukotrienes, prostaglandins, and histamines, leading to increased inflammation in the injured tissue. Neutrophils, monocytes, and macrophages are immune cells that play an important role during injury or infection. In wounds, the release of histamine is initiated by mast cells whose main function is to assist in the recruitment of neutrophils to the inflammation site (75). Neutrophils appear as specialized immune cells that immediately arrive at the site of infection or injury before any other immune cell. Damaged vessels are the major source of neutrophils in the injured area. At the time of injury, various inflammatory pathways are regulated and participate in the process. During this, neutrophils at the injury site begin to secrete cytokines that mediate the activation of nuclear factor kappa B (NF-kB) (76). Activation of inflammatory pathways by NF-kB and interleukin (IL) results in uncontrolled inflammation which ultimately delays the healing of an injury. In this scenario, circulating monocytes infiltrate the injured site and initiate their transformation into macrophages. Macrophages, being highly specialized immune cells, are capable of engulfing pathogens (also known as phagocytosis) and, as a result, play a primary role in the restoration of damaged tissues. The outer wall of Gram-negative bacteria contains lipopolysaccharides (LPS), which function as a strong stimulator of macrophages. A cascade of signal transduction is activated when macrophages are exposed to bacterial LPS which results in increased ROS, growth factors such as VEGF, platelet-derived growth factor (PDGF), and inflammatory cytokines such as tumor necrosis factor- α (TNF-α) and IL6 and thus increasing inflammation (77). Macrophages that are in an activated state also hasten the generation of pro-inflammatory cytokines, including IL-13, IL-10, and IL-4, at the site of the wound. Recent literature had also shown that circulating T-cells have the ability to resolve uncontrolled inflammation in wounds (78, 79).

2.2.3 Proliferation: During this phase, fibroblasts, macrophages, keratinocytes, and endothelial cells are activated and play important roles in matrix deposition, initiation of angiogenesis, and wound closure (80). It has been studied that, any kind of variation in electrical gradients or mechanical tension results in the activation of keratinocytes. Furthermore, the activation of keratinocytes during the proliferative phase of wound healing is facilitated by exposure to cytokines, hydrogen peroxide, and growth factors. As a result of this activation, keratinocytes mediate epithelial mesenchymal transitions and initiate re-epithelization in wounds (81). Keratinocytes support the dissociation of the integrin receptor which requires matrix metalloproteinase (MMP-1 and MMP-9) for them to migrate properly. Plasmin is a protease that degrades the fibrin-containing wound and thus helps in the movement of keratinocytes. As the movement of keratinocytes ceases, a thin layer formed by the epithelial cells (epithelial layer) is repaired (82). In addition to the epithelial layer, they also reform into the basement layer and eventually regenerate the epidermis followed by terminal differentiation. Fibroblast cells, another cell type, take over the replacement of the matrix by forming granulation tissue, which is abundant in proteoglycan, fibronectin, or immature collagen. This granulation tissue then facilitates the deposition of the mature ECM and angiogenesis, triggering the migration and differentiation of fibroblasts (83). These changes prompt endothelial cells to grow or fuse with new blood vessels in the wound area after proliferation to strengthen their network (84). During angiogenesis, macrophage governs the remodeling of new vasculature and generates MMP, which mediates the migration of endothelial cells (85).

2.2.4 Matrix remodeling: In this phase of wound healing, fibroblast cell uses fibronectin, hyaluronan, and proteoglycans to replace fibrin clots. With this removal, remodeling of the ECM begins at the injured site and, results in the formation of mature collagen fibrils that help in wound repair at later stages (86). Proteoglycans help in the migration of cells through the formation of mature and cross-linked collagen fibrils. Throughout the wound healing process, there is a substitution of type III collagen with type II collagen, which plays a role in strengthening the tensile strength essential for the formation of scars (87). Collagen mediates the growth of new tissues and initiates the process of angiogenesis and re-epithelization by attracting the fibroblast cells (87). In the ECM, collagen inactivates MMPs which helps in the faster healing of wounds (88).
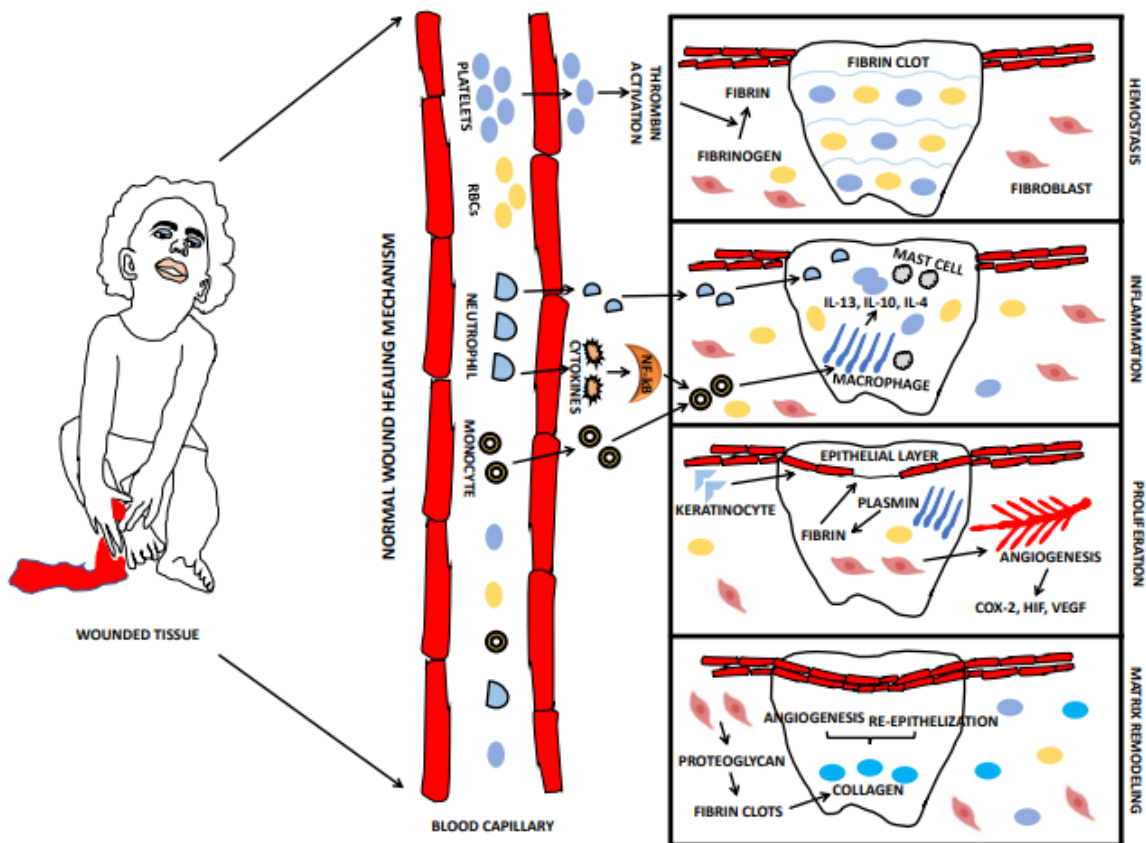
Fig 2.1: Different phases involved in wound healing mechanism: Upon injury, platelets and thrombin are activated and fibrin clots are formed. Platelets release several growth factors that initiate the first phase of wound healing. The second phase of wound healing is initiated when neutrophils adhere to endothelial cells in the vessel wall of the wound. In this phase, neutrophils activate NF-kB, leading to the entry of monocytes into the wound site. These monocytes then differentiate into macrophages, which play a crucial role in engulfing pathogens. The third phase of wound healing is characterized by the stimulation of angiogenesis, where the fibroblasts, and keratinocytes are released, and macrophages promote the deposition of the matrix. During angiogenesis, macrophages mediate the remodeling of new vasculature and produce matrix proteins that cause migration of endothelial cells. In the matrix remodeling phase, fibronectin dissolves the fibrin clot, which promotes collagen deposition and the remodeling of new vasculature to facilitate the wound healing.

2.3 Bacteria and biofilm: correlation in wound healing

Bacteria are categorized as unicellular microorganisms due to their absence of membrane-bound organelles and their capacity to adapt to diverse environments. Bacteria exist in the environment in two different states, one being sessile and the other being planktonic, whereas in the environment they are present in planktonic conditions (89). Bacterial biofilms are a composite mixture of microbiomes, the attachment of bacteria to any surface when they are present in the sessile form promotes biofilm growth, colonization, and dispersal, resulting in developing resistance to antibiotics and hence causing serious chronic skin infections.

2.3.1 Composition of biofilm

Polysaccharides, proteins, extracellular DNA, water, and biosurfactants constitute the primary components essential for the development of biofilms in chronic wounds. It is commonly noted that polysaccharides contributes to the mechanical characteristics of biofilms and are believed to form a significant portion of the exopolymeric material. Alginates are a class of natural exopolysaccharides produced by bacterial species like *Pseudomonas* and *Azotobacter* (90, 91). The primary role of alginate is to safeguard bacteria from stress by imparting mechanical strength to them in conditions characterized by limited water availability (92). Several proteins are secreted by bacteria in biofilms, for example, carbohydrate-binding proteins, also known as lectins or glycoproteins, which help in matrix formation and stabilization of biofilms. Extracellular DNA, vital for the development of biofilms, plays a crucial role in shielding bacteria from both antimicrobial agents and the host immune system. Extracellular DNA is released by a mechanism known as autolysis and is present in various bacterial species such as *Streptococcus*, *Staphylococcus*, *Enterococcus*, and more importantly *Pseudomonas aeruginosa* (93). An important function of extracellular DNA is to chelate cations that enhance cell lysis by stabilizing the LPS and outer membrane of bacteria. Additionally, biosurfactants help bacteria to attach and detach themselves from oil droplets, are also an important component of biofilms (94).

2.3.2 Mechanism of biofilm formation

The formation of biofilm is an intricate microbial collaboration encompassing distinct phases including attachment, growth, maturation, and dispersal (Fig 2.2).

2.3.2.1 Attachment and growth

The initial step in the biofilm formation is the adherence of a bacterium to any surface (95) i.e., free floating bacteria usually require pilli, fimbriae or flagella like structures for attachment (96-98). The adherence of these cells to the surface remains reversible, primarily attributed to weak attractive forces such as Van der Waals interactions. However, over time, cells develop strong attractive forces that increase resistance to physical displacement. They subsequently move into an unstressed phase and begin to produce an extracellular polymeric substance, indicating maturation and initiation of quorum sensing (QS) (99, 100).

2.3.2.2 Maturation and QS

The primary characteristics of this stage involve microorganisms forming an extensive networked colony, exhibiting traits that surpass individual cells. The extracellular polymeric substance, which includes DNA, proteins, and exopolysaccharides such as cellulose and N-acetylglucosamine, plays a vital role in the aggregation of bacterial cells, retention of water, and the cohesion of biofilms. Additionally, it serves functions such as providing nutrition and acting as a protective barrier (101). Before the extracellular polymeric substances are fully mature, the size of microscopic colonies rapidly increases until they develop into a three-dimensional colony of about 100 μm thick. QS is a major phenomenon exhibited by microorganisms to communicate with each other during biofilm formation. This process involves the regulation of several genes that initiate the cascade which leads to biofilm formation (102). Communication among bacteria is contingent on the concentration of "autoinducers," small signaling molecules synthesized during bacterial growth, that

assist in regulating the expression of specific genes (103). Upon reaching a concentration threshold, these autoinducers bind to their corresponding receptors, forming an autoinducer–receptor complex. This complex then binds to the target promoter, regulating QS genes, especially those associated with virulence (104). In Gram-positive and Gram-negative bacteria, respectively, the most comprehensively understood intra-species autoinducers are small post-translationally processed peptides and N-acyl homoserine lactone (105, 106). The bacterial QS system, which governs a broad spectrum of phenotypes, controls bioluminescence, pigment generation, and biofilm formation (107). QS governs the growth of biofilm and synthesis of virulence factor that promotes microbial resistance to the defence mechanism of the host immune system (108). It has been demonstrated that there is a contradictory regulation of QS in acute and chronic wounds. For instance, *Pseudomonas aeruginosa* increases the activity of protease enzyme and decrease the extracellular polymeric substance alginate activity and thereby causes dispersal of biofilm by antibiotics or host defence in acute wounds. But, the expression of this QS regulation system is decreased in chronic wounds due to mutation and as the wound progresses the expression is completely lost due to which dispersal capacity is vanished and biofilm growth and maturation occurs in chronic wounds (109). Numerous studies have demonstrated the pivotal role of QS in the chronicity of wounds. Consequently, blockers of QS have the potential to serve as therapeutic targets for the treatment of wounds assisted by biofilms (110, 111).

2.3.2.3 Dispersal

In this stage, the outermost cell layer can detach from the colony and disseminate to various surfaces within the host, potentially causing a systemic infection. Simultaneously, the inner cell layer is protected by extracellular polymeric substances. Consequently, individual cells or groups of cells migrate to the film's periphery due to limited nutritional availability, contributing to antibiotic resistance (112).
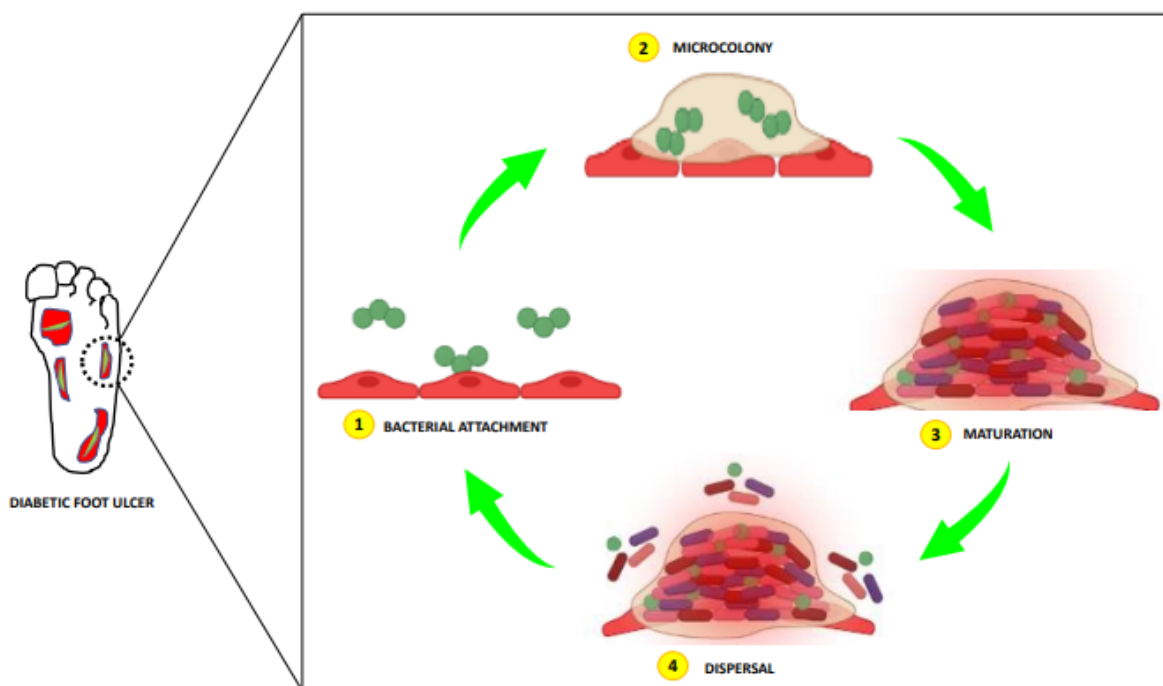
Fig 2.2: Mechanism of Biofilm maturation and attachment: The initial stage in the development of a biofilm involves the attachment of bacteria to a surface. Over time, cells move into an unstressed phase and begin to produce an extracellular polymeric substance, indicating maturation and initiation of QS. The external cell layer has the potential to separate from the colony and proceed to proliferate on different surfaces within the host. During dispersion, fluid accumulates inside the biofilm and cells move from place to place in this area.

2.4 Microbial contamination alters the wound healing

The role of microbial biofilm formation in inhibiting the healing phases and resulting in delaying wound healing in patients with diabetes has been elucidated by several investigations as discussed below (Fig 2.3):

2.4.1 Bacterial biofilms contribute to delayed wound healing

Bacteria in DFU are well organized into pathogroups with the purpose to mediate the close interaction of bacteria within the biofilm. Therefore, it is very important to investigate the interactions between bacteria when dealing with DFU. In the microbial community, *Staphylococcus aureus* and *Pseudomonas aeruginosa* are most studied bacteria that are known to have bacterial interactions with each other and increase infection in wounds of patients with diabetes (113). Individuals with diabetes are at high risk of being infected with chronic wounds because it is well known that high concentrations of glucose provide favourable conditions for the growth of bacteria in biofilms (114). This fact was later acknowledged when a team of researchers demonstrated that vancomycin-resistant *Staphylococcus aureus* biofilms formed only when glucose levels were increased in diabetic rats (115). During normal injury or any wound, the process of re-epithelization usually begins few hours after the injury. However, in chronic wounds, the movement of keratinocytes is disrupted by the development of biofilms. As a consequence of this disruption, cell proliferation at the wound site is impeded, leading to a delayed healing process. Altered migration of keratinocytes alone does not delay the repair of wounds in patients with diabetes. Other factors include the enhanced activity of proteases, hypoxia, fibroblast, aging, etc. Therefore, Kirker and colleagues used in vitro techniques to investigate whether the *Staphylococcus aureus* biofilms affects the migration of keratinocytes or not. The study results demonstrated that the presence of *Staphylococcus aureus* biofilm alters the keratinocyte migration and therefore delays wound healing in diabetics (116). The contribution of *Pseudomonas aeruginosa* biofilms in the delay of wound healing was identified by Zhao and his research team using db/db wounded mice model. They conducted a comparative study between the control group and the group with wounds to determine the rate of wound healing. The biochemical and histopathological analysis showed that the dermis and epidermis are thicker in the wounded rats. They found that mice which were not having diabetes healed wounds by day 28, but biofilm-induced mice having diabetes did not, which clearly indicates that biofilms delay the wound healing phases (117). In 2008, Schierle and colleagues investigated how Staphylococcal biofilms affect wound healing using a murine cutaneous wound model. The findings from this study suggest that biofilm formation by Staphylococcal slows down the epithelium formation in the wound area, and thus greatly impairs the normal

wound healing mechanism (118). Keratinocytes growth factor 1 is mainly produced from fibroblast cells in case of any injury. The prime function of this growth is to aid in the reepithelization of wounds by signaling the keratinocytes to initiate a cascade of proliferation and migration (119). Pastar and his team used the porcine model of diabetes associated wound to study the interaction between polymicrobial USA300 and *Pseudomonas aeruginosa*. Both of these species are involved to increase the infection by forming the biofilms in the wounded area when presenting together. Histological analysis of the study showed that *Pseudomonas aeruginosa* and USA300 results in downregulation of Keratinocytes growth factor 1 and thus delayed the epithelization of wound (120).

Watters and colleagues examined the protective impact of insulin treatment on wound healing associated with diabetes in rats. To this, streptozotocin (STZ) was introduced intraperitoneally into mice to induce diabetes followed by the insertion of *Pseudomonas aeruginosa* biofilms. The results demonstrated that wounds healed more quickly in rats without diabetes than in rats having diabetes. Furthermore, it was also found that insulin therapy in diabetic rats did not aid wound healing but resulted in an overall improvement in diabetes-associated complications (121). These results together reflect the role of biofilm to alter the healing mechanism of wounds in diabetics.

2.4.2 Fungal biofilms contribute to delayed wound healing

The emergence of a polymicrobial biofilm formed by fungal cells in the affected region tends to disrupt the typical physiological mechanisms of wound healing, leading to a delayed healing. The wound microbiome has majorly focused on bacterial biofilms, but insight into fungal contamination is also needed as it impairs wound healing and its associated complications. The microbiome of DFU is primarily composed of a mixture of commensal and pathogenic yeasts, such as *Candida* and *Trichosporon* spp., as well as fungi known for causing respiratory allergies, like *Cladosporium* spp (122). Exposure to fungus spores and antigens alone can initiate an immune response, leading to chronic inflammation and delayed recovery. The association between biofilm-forming yeasts, opportunistic skin fungal commensal infections, and wound necrosis, and unfavourable outcomes in DFU is notably linked to ischemia and reduced oxygenation. This correlation is attributed to a diverse array of microorganisms rather than a single species (123).

In 2007, a group of scientists conducted a study on diabetics to confirm the spread of fungal infections. They found that the uncontrolled glycemic index supports the incidence of fungal infections in diabetics (124). Similarly, Raiesi and colleagues conducted a comparative study by isolating the *Candida albicans* species and comparing the skin lesion and nail lesions with DFU in 122 patients. They found that a total of thirty individuals with diabetes were affected by fungal infections. Moreover, they also revealed that 28 % of diabetics who were suffering from skin or nail lesions were found to have fungal infections, while the frequency of being affected by fungal pathogens was found to be 19.1 % among individuals with DFU, which suggest that the prevalence of fungal infections in diabetes increases the disease severity (125). Likewise, another team of researchers isolated the fungi from patients suffering from T2D and lower-limb wounds. Upon

investigation, they found that the wounds contained a large number of microbes that were a mixture of bacterial-fungal flora (126). Scientists employed Internal Transcribed Spacer amplicon sequencing to investigate the involvement of fungi and their associations not only with clinical parameters but also with their bacterial counterparts. This approach aimed to provide a more comprehensive understanding of the prevalence of fungi in DFU (127). The fungal load was observed in 79 % of wounds, regardless of the mycobiome variations. A high majority of the bacterial populations associated with pathogenic fungus have been discovered in wounds that eventually lead to amputation or necrosis. In addition, cultured DFU isolates showed the potential to produce extensive, three-dimensional biofilms with close fungal-bacterial contact (128).
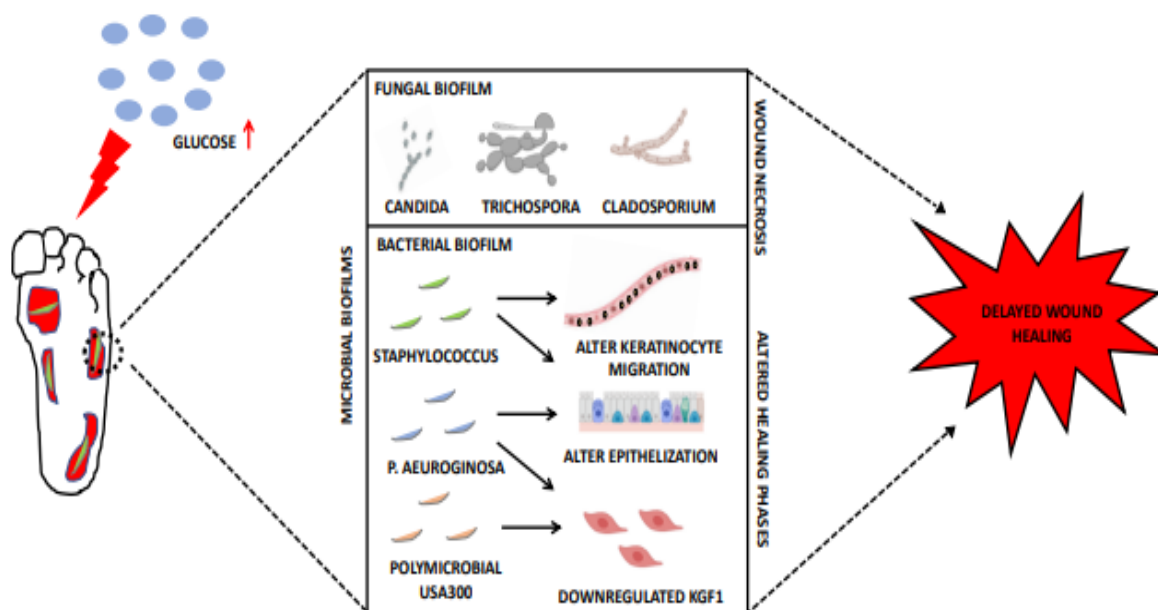
Fig 2.3: Role of high glucose (HG) in mediating the biofilm formation in wounded tissue: Under HG conditions, the wounds begin to form fungal and bacterial biofilm. Bacterial and fungal biofilm by *Candida, Trichospora, Cladosporium, Staphlyococcus, Pseudomonas aeuroginosa,* and *polymicrobial USA300* alters keratinocyte migration, epithelization, and downregulation of KGF-1 and thus inhibiting healing mechanism.

2.5 Factors known to alter healing mechanism in diabetics

2.5.1 Immune cells

In individuals without diabetes and its complications, like delayed wound healing, the acute phase is maintained through the coordinated activity of various cells, including immune system cells. These cells include macrophages, fibroblasts, platelets, endothelial cells, and keratinocytes and are related to the effective function of the immune system by mediating the release of chemokines and cytokines (129). Cytokines and chemokines primarily serve to communicate with the immune system, facilitating the directed movement of leukocytes, endothelial cells, and epithelial cells. When the wound vasculature is disrupted, an excessive number of inflammatory cells are carried to the site, making the injured area hypoxic and thereby increasing the oxygen demand (130). In addition, various cells that help maintain the immunity of the body are known as epithelial, macrophages, and fibroblasts that trigger the release of VEGF (131). This release prompts

endothelial nitric oxide synthase (eNOS) to be activated within the bone marrow with the aim of getting phosphorylated and increasing nitric oxide levels. Due to elevated levels of nitric oxide, endothelial progenitor cells (EPCs) are transported from the bone marrow into the bloodstream. Stromal cell-derived factor 1α (SDF-1α), serves as a chemoattractant that orchestrates the process, leading to the development of new blood vessels at damaged sites and facilitating expedited healing (132). But in diabetes conditions, macrophages and epithelial cells do not trigger the release of VEGF and as a result, eNOS phosphorylation and activation fail to occur. This failure inhibits the functioning of SDF-1α, which restricts the epithelial progenitor cells to access and heal the injured site (133).

2.5.2 Oxidative stress

Oxidative stress is a prominent and extensively studied factor in diabetes and its related complications, particularly in the context of delayed wound healing. One of the major consequences of excess ROS in chronic diabetes-associated wounds is damage to the endothelial layer, delaying the re-epithelization process and inhibiting the movement of keratinocytes (134). The increased presence of ROS directly influences the angiogenesis process by inflicting damage to the endothelial layer in wounds. While keratinocytes play a primary role, elevated levels of ROS disrupt the migration process of keratinocytes, thereby affecting the re-epithelization mechanism. The existence of ROS is associated with the tissue inhibition of MMPs, establishing a highly proteolytic environment conducive to chronic wounds (135). When biofilm formation takes place at the wound site, the chronic inflammatory response plays a role in eliminating the biofilm from the wound. In essence, the inflammatory response triggers the accumulation of neutrophils and macrophages around the biofilm. This accumulation leads to an elevated presence of ROS and proteases in chronic wounds. The basic function of the protease is to inhibit the interaction between biofilm and wounded tissue and thus helps in the removal of biofilm. Therefore, the higher the number of proteases such as Ficin, the greater the potential for biofilm removal from chronic wounds (136). Elevated levels of ROS do not facilitate the removal of biofilm; instead, they disrupt the healing and regeneration process of wounded tissue in individuals with diabetes. In recent decades, a growing body of evidence has substantiated the impact of oxidative stress and the modified activity of transcription factors in individuals with diabetes, contributing to the delayed mechanism of wound healing. In 2002, Mudge et al. performed a comparative study to examine the role of glutathione (GSH) in db/db diabetes associated wounded mice model. They demonstrated that the control group exhibited a higher concentration of the antioxidant GSH, leading to an accelerated capacity for healing diabetes-associated wounds when compared to the treatment group. Hence, this clarifies the crucial role of ROS in the process of wound healing, influencing the various steps involved (137). In addition, the activities of several antioxidant enzymes were analysed on diabetes-associated wounded rats in 2014 by Dhal and his team. This study unveiled that diabetic rats exhibit lower activity levels of essential antioxidant enzymes compared to nondiabetic rats (138). Nuclear factor erythroid 2-related factor (NRF2) is a transcription factor known to regulate the cellular resistance to oxidants. The process of repair and loss is regulated only when NRF2 is activated by oxidative

stress and HG levels. Several studies have well revealed the mechanism that oxidative stress in diabetes is progressively reduced by the activation of NRF2. When the glucose intake is high in the body, NRF2 reduces oxidative stress levels that promote a cascade of migration and proliferation. This mechanism favors a decrease in the level of MMP-9 and apoptosis by simultaneously increasing the level of transforming growth factor-β1 (TGF-β1) (139).

Another transcription factor called activating transcription factor 3(ATF-3), is expressed in quiescent cells at a steady state. The mRNA of this gene rapidly increases the stress of cells, due to which ATF-3 is also known as the stress-inducing gene. The heightened expression of ATF-3 and inducible nitric oxide synthase (iNOS) has been identified as a mechanism through which the body copes with elevated oxidative stress by diminishing antioxidant levels (140). There is speculation that inhibiting the activation of ATF-3 and iNOS could lower oxidative stress levels. This reduction in oxidative stress facilitates the mobilization of EPCs from the bone marrow, contributing to the prompt healing of wounds in diabetic conditions (141). Another transcription factor, known as STAT3 (Signal Transducer and Activator of Transcription 3), belongs to the STAT protein family and is specifically encoded by the STAT gene in humans. With this increase, nitric oxide levels from the keratinocytes present in the injured area are rapidly increased. Consequently, the increase in nitric oxide levels promotes the angiogenesis process, encouraging the formation of new blood vessels in the affected area, thereby contributing to the expedited healing of wounds associated with diabetes (142).

Angiopoietin-like 4, abbreviated as AL-4, is a protein that is encoded by the ANGPTL4 gene in humans. In diabetes conditions, the expression of AL-4 is gradually reduced resulting in impaired angiogenesis and re-epithelization and hence diabetes associated wounds take longer to heal (143). These reports suggested that the chronicity of wounds positively correlates with the increased level of oxidative stress. Moreover, oxidative stress also favors the formation of microbial biofilm resulting in the increased pathogenicity of chronic wounds. A prior study showed that when the biofilm extracted from chronic wounds was applied to newly excised wounds, it failed to induce chronic wounds in the absence of oxidative stress. Similarly, the absence of a microbiome did not lead to chronic wounds, even in the presence of high oxidative stress (144). Therefore, a combined approach involving manipulation of the microbiome and antioxidant treatment is necessary to address oxidative stress in the treatment of chronic wounds.

2.6 Epigenetic modifications in diabetic wound healing

Epigenetics is the study of changes in the DNA and histone proteins that leads to alteration in the gene expression but does not involve any change in the nucleotide sequences. Epigenetic modifications, such as DNA methylation, histone modifications, and microRNAs, are instances of inheritable yet reversible alterations in gene expression (145). Primarily affecting the promoter region of genes, these modifications lead to either increased or suppressed gene expression. Notably, environmental factors can induce these alterations, causing shifts in the expression of various proteins (146). Normal epigenetic modifications are required for cellular differentiation and growth, but abnormal changes result in a variety of diseases. Because

these epigenetic marks can be passed down through generations, they have the potential to expose coming generations to these maladies. Accumulating evidence suggests that epigenetic markers, including DNA methylation, histone modifications, and microRNAs, play a role in influencing the activity of numerous genes associated with the onset of T1D, T2D, and related complications (147-149). The following are the epigenetic mechanisms that can be targeted for improving diabetic wound healing were summarized in Fig 2.4.

2.6.1 DNA Methylation

DNA methylation is one form of epigenetic modification, in which methylation takes place at the cytosine residue of the CpG dinucleotide, with the help of an enzyme DNA methyltransferase (DNMTs). S- adenosyl methionine (SAM) acts as the methyl group donor for the methylation of a carbon atom at the 5th position in cytosine. DNA methylation leads to the inactivation of chromosomes, silencing of genes, and retrotransposons (150-152). DNMT1 is responsible for methylation in the somatic cells while DNMT3L in the germ cells (153). DNA demethylation can occur through the inhibition of methylation during DNA replication (154) or by a group of proteins referred to as ten-eleven translocation (TET) (155-157). Clusters of dinucleotides, specifically CpG islands (where p denotes the intervening phosphate group between cytosine and guanine), are exclusively found in the promoter region (158, 159) while they can also be present in the intragenic and enhancer regions (160-162). It has been observed that in normal cells, CpG islands in the promoter region remain unmethylated, and methylation in these regions results in the silencing of genes (159, 163, 164). It is documented that the extent of methylation is inversely proportional to the rate of gene transcription (165). This repression of transcription may be due to the activity of CpG binding proteins which recruit HDAC towards methylated DNA (166, 167), whereas unmethylated DNA does not have any attraction for the deacetylase enzyme and thereby cause the gene transcription (168-170). Some shreds of evidence have indicated that the occurrence of DNA methylation can increase with increasing age. A study was carried out with both young and elderly twins from the same population. The findings revealed that the promoter regions of genes related to the respiratory chain, specifically NDUFB6 and COX7A1, exhibited hyper-methylation in the elderly, resulting in lower mRNA expression. In contrast, the young twins demonstrated higher gene expression (171, 172).

DNA methylation has been shown to exhibit different patterns in both normal and abnormal cells, suggesting that it can be used as a biomarker (173). Evidence indicates that the PDX-1 (pancreatic and duodenal homeobox 1) gene, crucial for beta-cell differentiation, exhibits high methylation levels in the promoter and enhancer regions among individuals with T2D compared to non-diabetic individuals (174). Hence, in individuals with diabetes, there is reduced expression of PDX-1, resulting in diminished beta-cell differentiation. Studies indicate that elevated glucose levels activate DNA methyltransferase and concurrently inhibit TET proteins. In diabetic patients, the INS1 gene undergoes methylation at CpG islands in the promoter region, consequently reducing its mRNA expression (175). The genome-wide association study (GWAS) examining the methylation pattern in T2D revealed that the genes EXOC3L2, responsible for insulin secretion

from pancreatic beta-cells, and PPARGC1α (peroxisome proliferator-activated receptor gamma, coactivator 1 alpha), crucial for mitochondrial function, are positively correlated with glucose-stimulated insulin release. Both genes exhibit hypermethylation in individuals with T2D compared to controls, resulting in reduced expression and decreased insulin release from pancreatic beta-cells in diabetic individuals (176-178).

In the case of diabetes, alteration in DNA methylation is reported in the genes involved in inflammation, oxidative stress, glucose, and lipid metabolism (179). In a comparison done between T2D patients and control, it was found that hypermethylation of the heavy β-myosin chain, at the CpG site of gene β-MYH7 takes place in the diabetic heart that leads to dysfunctioning of the ventricles (180). Studies have demonstrated that altered methylation takes place in diabetic patients which leads to diabetes-associated cardiovascular complications. Recent research has identified oxidative stress as a significant contributor to diabetic complications. For instance, hypomethylation of the KEAP1 promoter takes place in patients with diabetic cardiomyopathy, which results in an increased level of KEAP1 protein. The KEAP1 protein binds to NRF2, which is subsequently engaged in the activation of various antioxidant enzymes. The interaction with KEAP1 results in the degradation of NRF2, diminishing the levels of antioxidant enzymes. This, in turn, disrupts the oxidation-reduction balance and contributes to oxidative stress in individuals with diabetes (181). At this time, it seems that the hyperglycemic environment promotes the methylation of DNA. In diabetes, DNMTs, enzymes sensitive to oxidoreduction, are readily influenced by superoxide and other free radical species. This influence leads to the hypermethylation of numerous genes (182). The suppression of immediate early genes, such as Nuclear Receptor Subfamily 4 Group A (NR4A), closely associated with glucose metabolism and insulin signaling, is a consequence of global hypermethylation attributed to the heightened activity of DNMT1 in diabetes. Additionally, elevating NR4A expression in pancreatic beta-cells through the use of the DNMT1 inhibitor aurintricarboxylic acid leads to effective glycemic regulation (183). Hypermethylation of *NR4A1* may then be a novel biomarker linked to the initiation and progression of T2D (183). The GLP1R (glucagon-like peptide 1 receptor) is a G protein-coupled receptor involved in regulating the insulin secretion pathway. In pancreatic islets from T2D donors, there was observed an excess of DNA methylation in the GLP1R gene. This suggests that such epigenetic alterations might contribute to the onset of T2D (184). In a correlated investigation, alterations in the methylation status of the p53-inducible promoter (p21WAF1/CIP1) were observed, leading to apoptosis and chronic heart disease in rats with diabetes (185). They postulated that oxidative stress was the principal factor behind the methylation of the p53-inducible p21WAF1/CIP1 gene. In diabetic ulcers, the inflammatory process resembles more of a disease than a typical biological response. Pro-inflammatory cytokines diminish the migration and activation of fibroblasts and EPCs, and notably, they "entice" these cells into committing suicide (186). Inflammation interferes with the synthesis of ECM by increasing matrix proteases and dismantling anabolic pathways through the NF-kB p65 and c-Jun N-terminal kinases (JNKs) signaling pathways (187). Another report showed that inhibiting DNMT1 with 5-aza-cytidine (5-aza-C) facilitated macrophage development, reduced inflammation, and defended against insulin resistance

in bone marrow-derived macrophages (60). Based on certain evidence, DNA demethylation is implicated in the process of diabetic wound healing. For instance, researchers identified that AGE-BSA (bovine serum albumin), generated as a result of HG, inhibits keratinocyte migration and proliferation by inducing TET expression, leading to the demethylation of the MMP9 promoter (64, 67, 188-190). TNFα enhances the activity of MMP9 in keratinocyte cell lines through the demethylation of its promoter at specific sites (68). This suggests that targeting DNA demethylation could be a promising therapeutic strategy for non-healing diabetic wounds. Further research is necessary to elucidate how DNA methylation and demethylation can be employed in treating complications induced by HG, especially in the context of wound healing.

2.6.2 Histone modifications

In eukaryotes, DNA is wrapped around multimeric histone proteins which form the repeating units called nucleosomes (191, 192). To form chromatin fibers, nucleosomes are organized in higher-order structures (193). The higher-order chromatin structure not only efficiently packages DNA but also regulates gene transcription. In a closely packed arrangement of nucleosomes, known as heterochromatin, transcription is impeded as it restricts the access of the transcriptional machinery to the nucleosomes (194-196). In a relaxed state of chromatin, known as euchromatin, nucleosomes resemble beads on a string. This condition is linked to active transcription (196). Every histone protein comprises an octamer consisting of two sets of H2A, H2B, H3, and H4 proteins linked together by a single histone H1 linker protein (192). The N-terminal "tail" of each histone subunit extends outward from the protein's surface, creating an exposed surface (197). Certain residues on the histone tail may be methylated, acetylated, phosphorylated, or ubiquitylated by histone-modifying enzymes (195). Transcription may be activated or repressed depending on the type of modification. Diabetes changes acetylation patterns across a wide range of tissues. Many of the processes caused by diabetes, such as inflammation, kidney disease, and retinopathy, are regulated by histone hyperacetylation. T2D is linked to protracted inflammation in tissues involved in metabolism like adipose tissue and the liver (198). Insulin resistance and T2D are caused by elevated levels of TNF-α, IL-1, and IL-6 (199, 200). This results from elevated phosphorylation of IRS-1 and IRS-2, coupled with the reduced capacity of the insulin receptor to activate downstream signaling pathways in the muscle, liver, and adipose tissue (201).

Hyperacetylation of proinflammatory genes in diabetic monocytes was discovered (202). According to studies, TNF-α and COX2 transcription are induced by HG, and this glucose-stimulated expression is regulated by an increase in H3K9, H3K14, H4K5, H4K8, and H4K12 acetylation (203, 204). Furthermore, histone acetylation (HAT) at inflammatory genes leads to renal fibrosis, which is linked to diabetic nephropathy. The accumulation of ECM in the nephrons and the transformation of epithelial-to-mesenchymal (EMT) cells lining the kidney tubules are prevalent complications in diabetes. Studies have indicated the involvement of HDAC-2 in the ECM build up and EMT in diabetic kidneys, with TGF-β1-induced activation of HDAC-2 being mediated by ROS. Additionally, elevated glucose levels led to increased H3HAT activity in the endothelial cells of the retina (205). Furthermore, augmented HAT activity at H3K9 and H3K23 was identified in mice

with T2D exhibiting renal disease or failure (206). Diabetes induces acetylation of histone H3 and H4 in the retina, consequently contributing to the development of diabetic retinopathy (206). Limited research has connected HAT to diabetes and the delayed healing of wounds. However, in diabetic mice, a comprehensive reduction in acetylation at H3K9 and H3K23 was observed (207). Diminished acetylation of H3K9 was identified in the promoter region of Glut2, a glucose transporter essential for maintaining glucose balance (208, 209), and this condition could be restored through treatment with the diabetic inhibitor exendin-4 (207). Furthermore, exendin-4 was discovered to induce acetylation of the H3 histone at the SOD3 promoter, leading to elevated expression of SOD3 in endothelial cells (210). These findings indicate that acetylation of histone contributes in disease progression, thereby therapeutics that target HAT may delay or stop disease progression. It is interesting to note that an increase in HDAC activity is often linked to diabetic complications. HG, for example, activates HDACs 1, 2, and 8 in the cells of the retina and capillaries. Elevated oxidative stress, hypoxia, and ischemia can also trigger disparity in HAT-HDAC function, resulting in diabetes target-organ disease (211). HDACs have also been associated with angiogenesis. Elevated expression of HDAC1 led to reduced transcription of the p53 genes, subsequently enhancing the activity of hypoxia-inducible factor 1-alpha (HIF-1α) and ultimately VEGF in a sample of primary endothelial cells (212). Furthermore, the inhibition of HDAC7 in human umbilical vascular endothelial cells (HUVECs) impeded the cells' capacity to migrate and form capillaries in vitro, along with inducing changes in cell morphology (213). Furthermore, evidence from experimental diabetic wound models showed that Sirtuin activators and class I HDAC inhibitors enhanced the healing process. Also, class I HDAC inhibitors were revealed to enhance oxidative metabolism, reduce body weight, and improve insulin sensitivity in diabetic mice, implying that these HDAC inhibitors may be beneficial. On the other side, the nonselective HDAC inhibitor, Trichostatin A, successfully reduced the incidence of diabetes when administered to female mice during the transition from the borderline to the diabetic stage. However, it proved ineffective in curing visibly diabetic mice (214). Furthermore, mice given HDAC inhibitors showed increased cellular proliferation and enhanced wound healing (215, 216). As a result, HAT influences numerous processes associated with diabetes, such as insulin resistance, inflammation, and various complications. Further research is needed to comprehensively explore the therapeutic potential of strategies targeting HAT and HDAC.

Methylation is another well-studied histone modification. In contrast to DNA methylation, which often results in transcriptional suppression, histone methylation either trigger or suppress transcription, based on the number of methyl groups added and target residues (195). Histone methylation, a crucial epigenetic marker influencing gene expression, is regulated by histone lysine methyltransferases (HMTs). These enzymes facilitate the transfer of a methyl group from SAM to specific lysine residues on histone proteins. Transient HG conditions can activate the Set7 enzyme, leading to alterations in histone 3 lysine 4 (H3K4) methylation at the NF-kB promoter. Consequently, the expression of inflammatory markers, including monocyte chemoattractant protein 1 (MCP-1) and vascular adhesion molecule-1 (VCAM-1), is increased (217).

Similarly, glucose has been shown to mediate the reduction in dimethylation and trimethylation of H3K9, as well as the rise in mono-methylation of H3K4, by recruiting lysine-specific demethylase-1 (LSD). Hence, these mechanisms collectively govern modifications at the NF-kB promoter sites. Conversely, histone demethylation is equally crucial in gene expression regulation. The enzymes overseeing this process fall into two categories: LSDs and Jumonji-C domain-containing demethylases (JMJ-C enzymes). Many researchers have been intrigued by the involvement of *Jmjd3* in diminishing essential inflammatory genes (62). *Jmjd3* plays a role in controlling the expression of interferon regulatory factor-4 (IRF-4), a critical factor for macrophage polarization (MP) toward the M2 state, making it vital for immune and inflammatory responses (58). The function of *Jmjd3* changes in diabetic patients, resulting in an overexpression of M1 markers. Increased *Jmjd3* activity was demonstrated to alter the methylation status of histone H3K27 in cells of wounded glucose-intolerant mice. Researchers identified a correlation between elevated Jmjd3 expression and accelerated inflammation at the wound site (58). This prevents MP from progressing to the M2 type, resulting in delayed wound healing in diabetics. The expression of *Jmjd3* seems essential for re-epithelization, as it facilitates the migration of keratinocytes to the injured site by promoting Notch1 expression (218, 219). Higher expression of *Jmjd3* was observed in epithelial cells of normal wounds, while Ezh2, the HMT crucial for H3K27 methylation, exhibited lower levels (219). *Jmjd3* levels were elevated on day 1 in wounds and decreased over time. In both macrophages and keratinocytes, Jmjd3 seems to be tightly regulated, showing increased expression during the early phases of wound healing that diminishes as the wound progresses. However, this coordination appears less distinct in diabetic wounds.

2.6.3 MicroRNAs

Besides DNA methylation and histone post-translational modifications, noncoding RNA assumes a crucial role within the cell. MicroRNAs (miRNAs or miRs), small non-coding RNAs comprising 21-23 nucleotides, intricately regulate post-transcriptional gene expression (220, 221). The seed sequence, a crucial 6-8 nucleotide segment responsible for recognizing target mRNA, is located at the 5′-end of each miRNA. Following processing, the mature miRNA binds to its target gene via complementary base pairing, leading to translational repression and/or mRNA destabilization (222). As a result, target protein amount gets reduced. miRNA is found within protein-coding genes or is generated in intergenic regions by noncoding transcription units. miRNAs are also related to diabetes and glucose homeostasis (223). miR-222, miR-27a, miR-195, miR-103, and miR-10b exhibit variations in insulin target tissues under HG conditions among rat strains with distinct diabetes propensities. This suggests that these miRNAs may contribute to the pathophysiology of T2D (224). miR-375, for example, is a pancreatic islet-specific miRNA whose overexpression reduces glucose-stimulated insulin release whereas its knockdown enhances secretion of insulin (225). miR-204 exhibits high expression in pancreatic cells and contributes to insulin production (226).

A large number of miRs have been linked to diabetes, and a better understanding of their functions can help us weed through possible therapeutic targets (223). Epigenetic changes, as well as prolonged exposure to HG

and/or hyperlipidemia, can impact the miRNA expression profile of beta cells. This alteration leads to impaired beta-cell function and survival, contributing to the progression of T2D. The study investigated the expression of eight miRNAs (miR-21, miR-122, miR-127-3p, miR-184, miR-195, miR-375, miR-492, and miR-493) in the islets of both normal and diabetic individuals (227). Glucose-intolerant individuals exhibited a significant elevation in miR-21 and miR-124a, with a tendency towards increased expression of miR-127-3p and miR-375. Additionally, a decrease in miR-184 expression was observed (228, 229). Studies have also reported an elevation in the expression of miR-130a, miR-130b, and miR-152 in the islets of patients with T2D (230). The above three miRNAs were found to be strongly associated with human islets. The elevated expression of these miRNAs led to a decrease in the levels of the pyruvate dehydrogenase E1 alpha 1 subunit (PDHA1), consequently reducing intracellular ATP and insulin secretion (226, 230-232). A decreased in miR-184 level promotes beta-cell proliferation (229, 232). Increase of miR-132 elicited similar effects, which were followed by an increase in pancreatic beta-cell secretory activity (232). Thus, improvements in miR-184 and miR-132 expression are likely to be a part of an integrated program that allows beta cells to release a high amount of insulin in order to compensate for the target tissue's decreased sensitivity. miR-7a is identified as a miRNA thought to participate in beta-cell adaptation to insulin resistance. It modulates the expression of several vital components essential for insulin exocytosis and is found in abundance within beta cells (233). During mild insulin resistance, the level of miR-7a diminishes in pancreatic cells, leading to increased insulin secretion. Conversely, in severe diabetic conditions, the expression of miR-7a gradually rises and can surpass levels observed in healthy individuals, potentially contributing to impaired insulin release and disease progression (233). Hence, methodologies enabling the correction of specific miRNA levels may eventually aid in preventing or even treating the disease.

It was found that mice lacking the miR-200 family were resistant to diabetes induced by STZ, and the absence of this family also prevented the onset of a severe form of diabetes (231). Numerous miRNA drug candidates are currently in phase 1 and phase 2 clinical trials, making this an exciting period for miRNA therapeutics. Ongoing trials include a phase 1 study of a Locked Nucleic Acid (LNA)-based drug targeting miR-92 for potential applications in wound healing and a phase 2 trial investigating miR-155 for patients with a specific type of T-cell lymphoma (234). The transient suppression of miR-200b, crucial for wound angiogenesis and normally induced by injury, is disrupted in diabetic wounds (235, 236). Fluid from wounds in diabetic individuals, unlike that from non-diabetic individuals, exhibited heightened activity of miR-200b in human mammary epithelial cells (HMECs). This observation supports the theory that the wound microenvironment is responsible for promoter hypomethylation and the consequent elevation of miR-200b. The potential of SAM, a recognized methyl donor, to counteract HG-induced hypomethylation of the miR-200b promoter was explored (237). The study demonstrated that SAM has the ability to reverse hypomethylation of the miR promoter induced by HG. This reversal proves effective in rescuing diabetic wound angiogenesis, thereby enhancing wound perfusion (238). SAM is recognized for impeding active DNA demethylation, thereby

providing protection against global hypomethylation, and it also nonenzymatically methylates DNA (237, 239). Recent discoveries have emphasized the significance of SAM as an intervention to prevent endothelial dysfunction (240). SAM treatment increased endothelium-derived relaxing factor while reducing serum triglycerides along with free fatty acids levels in high-fat diet (HFD) rats (241).

The identification of HG-induced hypomethylation as a contributor to endothelial dysfunction, posing a hindrance to diabetic wound angiogenesis, offers a new insight into the pathogenesis of diabetic vasculopathy. miR-146 is thought to regulate innate immune responses, including cytokines and Toll-like receptor signaling in monocytes, through negative feedback regulation of TNF receptor-associated factor 6 (TRAF6) and IL-1 receptor-associated kinase 1 (IRAK1), induced by the transcription factor NF-kB (242). NF-kB, on the other hand, blocks miR-125b transcription, which then targets and represses TNF-α, a key proinflammatory cytokine (243). miR-125b exerts epigenetic control over inflammatory genes in vascular smooth muscle cells derived from T2D mice by down-regulating the histone H3K9 methyltransferase Suv39h1 (244). The significance of miRNA in angiogenesis was initially illustrated in a study revealing that the expression of Dicer, a crucial regulatory helicase with an RNase motif and a member of the RNase III family essential for pre-microRNA cleavage, was indispensable for embryonic angiogenesis in mice (245-247). Depleting Dicer in human microvascular endothelial cells resulted in restricted angiogenesis, as observed in knock-out experiments (248). In HUVECs, miR-221 and miR-222 exhibit antiangiogenic effects by impeding the translation of c-Kit, a promoter of angiogenesis in tumors (249).
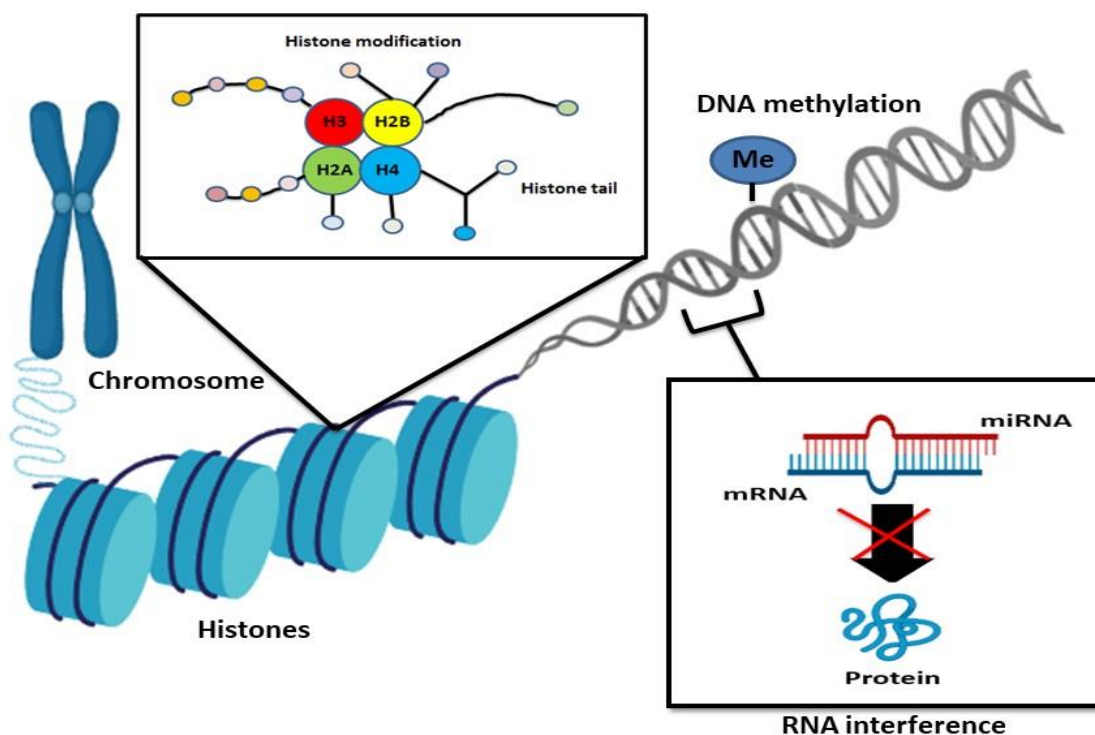
Fig 2.4: Illustration of different epigenetic pathways that may cause various metabolic ailments.

miRNAs contribute to keratinocyte function as well, miR-210, for example, has been linked to keratinocyte proliferation inhibition (250). HIF-1α regulates miR-210 transcription, which was found to target the transcription factor E2F3, which is the central promoter of keratinocyte proliferation (250, 251). Targeting miRs and non-coding RNAs, which can control the expression of several genes as well as gene families, could allow for the modulation of networks and entire pathways involved in disease development and could be used in conjunction with additional possible epigenetic therapies. A brief overview about the link of epigenetic with delayed wound healing has been summarized in Fig 2.5.
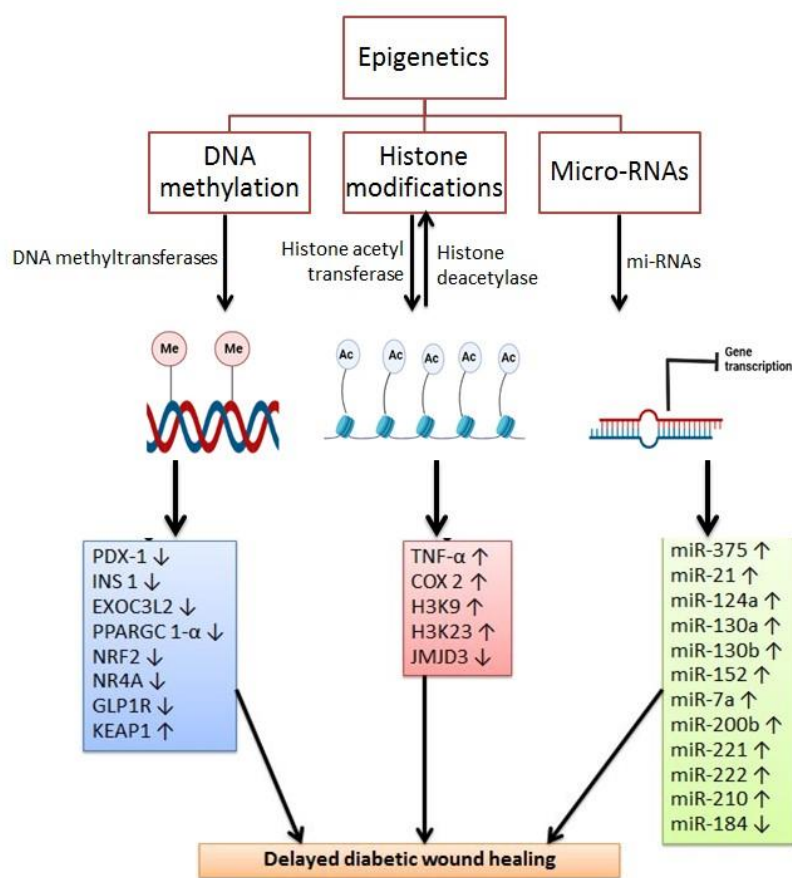
Fig 2.5: Overview of epigenetic changes responsible for delayed diabetic wound healing.

2.7 The involvement of SIRT1 in diabetic wound healing

The body's immune system starts an intricate biological reaction called inflammation when it detects noxious stimuli like infections, tissue injury, or irritants. By improving blood flow to the damaged area and providing vital nutrients and immune cells to aid tissue regeneration, this procedure accelerates the healing process. A study conducted by Huang et al. revealed that elevated hyperglycemia hampers the angiogenic activity of endothelial cells by diminishing SIRT1 expression, resulting in endothelial dysfunction. Moreover, their findings indicated that resveratrol treatment enhances the healing of diabetic wounds in experimental diabetic

animals. This is achieved by suppressing hyperglycemia-induced endothelial dysfunction and angiogenic dysfunction, achieved through an increase in c-Myc expression and FOXO1 degradation (252). An additional investigation by Li et al. demonstrated that individuals with diabetes exhibit decreased SIRT1 expression and chronic oxidative stress, resulting in impaired wound healing. They unveiled that diabetic mice undergoing treatment with SRT1720, a SIRT1 activator, exhibited substantial improvement in wound healing. This improvement was attributed to the reduction in ROS levels, enhanced angiogenesis, and increased migration of endothelial cells to the injured site (39). A similar study had shown an improvement in wound closure after receiving the treatment of a novel synthetic SIRT1 activator called NED416. In summary, exposure of NED416 to chronic wounds significantly activates Rac1/Cdc42 and ERK/JNK signaling pathways, thereby enhancing SIRT1 activity in fibroblast and keratinocyte cells to promote cell migration and angiogenesis in cutaneous wounds (253). Similarly, it was shown that treatment with novel 1,4-dihydropyridine led to skin restoration in a CD31 mouse model of wound healing by activating SIRT1, leading to faster wound healing (254).

Subsequent studies indicated that the application of an innovative berberine nanohydrogel to diabetic rats triggers the activation of SIRT1. This activation promotes the upregulation of SMA, CD31, and VEGF, coupled with a reduction in inflammatory markers such as IL-6, TNF-α, and NF-kB. Consequently, this intervention results in an expedited healing process for diabetes-associated wounds (255). Likewise, Shi et al. illustrated that exosomes derived from adipose-derived mesenchymal stem cells, treated with mmu_circ_0000250, enhance diabetic wound healing by elevating SIRT1 expression and diminishing the activity of miR-128-3p (256). An in-silico investigation conducted by Rupal et al. demonstrated that the docking of naturally occurring phytochemicals like Gossypetin and Herbacetin with the SIRT1 protein (PDB ID: 4ZZJ) exhibited binding energies of -7.5 kcal/mol, showing structural similarity to quercetin. This suggests that both these phytochemicals can be a lead compound for the activation of SIRT1 in improving diabetes-associated delayed wound healing (257). A study by Zhou et al. revealed that db/db mice receiving rosiglitazone therapy activate VEGF and SDF-1α activity, thereby leading to improvement in wound healing (258).

2.8 Therapeutic interventions for diabetes-associated wounds

Over decades of research and development, the efficacy and accuracy of wound infection detection has improved tremendously. To date, several treatment modalities have aroused great interest. However, growth factors, plant-based therapies (phytochemicals/essential oils), and nanodelivery systems are widely used to treat chronic wounds.

2.8.1 Growth factors

Growth factors are promising agents in aiding tissue healing because of their broad roles. Growth factors recruit cells to the wound site, promote their growth, and have important effects on the formation of ECM. Several studies have shown that since it has become possible to produce these cytokines on a large scale using

recombinant technology, growth factors can enhance all aspects of tissue restoration in both normal and impaired healing models (259). The recent rise in mortality has sparked significant interest in wound healing growth factors within the field of wound healing. According to a study by Zhu et al, roxadustat, a new HIF prolyl-4-hydroxylase inhibitor, dramatically reduces the severity of chronic wounds by promoting the expression of HIF-1α/VEGF/VEGFR2 signaling (260). In a double-blind, randomized, controlled experiment, PDGF was the only therapy found to aid treatment, and even then, the benefits were incredibly small (261). However, because there are so many altered growth factors and cytokines in a chronic wound, it may be beneficial to address some of these problems. As an illustration, older lesions frequently exhibit lower expression levels of IL-1 and -6, TNF, and VEGF compared to epidermal growth factor (EGF), fibroblast growth factor (FGF), TGF-β, and PDGF (78).

2.8.2 Plant-based therapies to improve wound healing

Dressings, which must comply with many standards, dominate the market of health care products used to treat chronic wounds. They include the ability to absorb wound fluid, maintain water permeability, pain relief, and wound pH optimization. The ability to treat open skin wounds with phytochemicals derived from plant extracts is currently gaining therapeutic importance. From past to present, plant-based natural remedies such as natural phytochemicals, essential oils and biological macromolecules have been extensively used to treat many diseases including chronic wounds.

2.8.2.1 Phytochemicals

A study by Huang and colleagues showed that epigallocatechin gallate supplements to diabetic rats improved LPS-induced inflammation and diabetic wound healing by binding to Notch-1 (262). In another study, it was demonstrated that the application of a 10-ppm dose of EGCG-incorporated collagen sponge led to an augmentation in CD31, Ki-67 expression, and α-smooth muscle actin. This resulted in an accelerated healing process for diabetic wounds by facilitating re-epithelialization, angiogenesis, and myofibroblast migration (263). Another study by Kant et al. showed that diabetic rats treated topically with quercetin at a concentration of 0.3 w/w exhibited expedited wound healing. This impact was ascribed to the decrease in TNF-α expression and an elevation in the expression of angiogenic markers, particularly IL-10 and VEGF (264). Another series of research highlighted that quercetin therapy to diabetic injured rats reduced oxidative stress by increasing the levels of superoxide dismutase (SOD), GSH peroxidase, catalase. Moreover, the administration of quercetin efficiently expedited the healing of wounds in diabetic rats by decreasing nitrite and malondialdehyde (MDA) levels, accompanied by the formation of granulation tissues around the wound (265). Likewise, the application of quercetin enhances fibroblast proliferation, migration, and the Wnt/β-catenin signaling pathway, contributing to an accelerated healing process in diabetic wounds by 94.6%, 97.31%, and 98.42%, respectively. Additionally, the use of quercetin is associated with reduced levels of inflammatory markers, including TNF-α and IL-6, in the treated animals (266).

Another naturally occurring phytochemical called curcumin was also evaluated to elucidate its potential in improving wound healing. For example, treating diabetic rats and genetically diabetic mice with curcumin significantly enhances neovascularization and the migration of fibroblasts, macrophages, and myofibroblast cells. They also showed that curcumin-treated rats had increased expression of TGF-β1, collagen deposition, which helps diabetic wounds heal faster (267). Similarly, angiogenesis, epithelialization, granulation tissue formation, and collagen accumulation were increased in rats receiving curcumin treatment (268). Another piece of evidence showed that dosing diabetic rats with curcumin (0.3% dose) for 19 consecutive days improved neovascularization with increased expression of VEGF, TGF-β1, and collagen deposition around the injured site (269). Whereas, curcumin treatment was found to decrease TNF-α, MMP-9 levels and increased angiogenesis, antioxidant enzyme levels and fibroblast migration towards the injured site, and hence helped in faster healing of cutaneous diabetic wounds (270).

In a different investigation, the administration of gallic acid to Mouse Embryonic Fibroblasts (MEF) cells led to heightened expression levels of focal adhesion kinase, extracellular signal-regulated kinases, JNKs in both keratinocyte and fibroblast cells. This suggests its involvement in the process of wound closure. Similarly, levels of antioxidant enzymes were restored after treating mice with gallic acid, highlighting the role of gallic acid in improving antioxidant activity at the wound site (271). Another series of shreds revealed that administration of luteolin to diabetic rats led to faster healing of cutaneous wounds by reducing MMP-9, TNF-α, IL-6, NF-kB signaling pathways. Additionally, treating diabetic rats with luteolin therapy led to an increased expression of antioxidant enzymes, such as GSH peroxidase, SOD1, and NRF2 (272). In another study, myricetin treatment was found to reduce MMP-1, -2, -9 and increase fibroblast proliferation and migration toward the wound site, thereby accelerating wound healing (273).

2.8.2.2 Essential oils

Essential oils have long been considered a potential complementary therapy for scar repair and wound healing. Despite the longstanding tradition of employing aromatic herbs for wound healing, the utilization of pure essential oils is uncommon (274). A number of researches have been published demonstrating the use of essential oils produced from plants in promoting the healing of chronic wounds. Some of these studies are discussed below.

According to a study by Ayuningtyas and colleagues, treatment with citrus limon peel essential oil gel dramatically increased the expression of VEGF and CD-31 markers in diabetic rats with painful ulcers (275). Another study found that giving citrus limon fruit peel Malang essential oil gel to diabetic rats with painful ulcers increased the production of FGF-2 and fibronectin, which led to ulcer healing (276). Similar efforts were made by Andjic and colleagues to investigate the function of an immortelle essential-oil based ointment, and they found that animals receiving this ointment had significantly longer wound healing times by 7 to 21 days compared to other groups. In summary, they said that the wound closure percentage in immortelle essential oil-based ointment-treated animals was 99.32%, while the wound closure ratio in the negative control

and ointment-based groups was 71.36% and 81.26%. Additionally, in vivo histopathology data showed that animals treated with immortelle essential-oil based ointment had greater collagen deposition than other groups (277). In a different investigation, Andjic et al. developed and assessed the potential of an essential oil and gel formulation based on *H. italicum* in an incision wound model. The results showed that the use of gel formulation and essential oil derived from *H. italicum* increased wound healing by 98% and 98.3%, respectively. Additionally, they demonstrated that animals receiving *H. italicum* essential oil therapy had higher amounts of hydroxyproline, collagen deposition, and antioxidant enzymes compared to the other groups (278). Conversely, *Hypericum scabrum* L. essential oil (*H. scabrum* L.) increases GSH, catalase and SOD activity while reducing MDA activity to restore antioxidant enzymes. Furthermore, diabetic rats had more wound healing ability, which highlights the importance of plant-derived essential oils in promoting the healing of chronic wounds (279). Similarly, it was shown that treatment of *Nigella sativa* L. essential oil of the plant improved wound contraction in experimental diabetic rats, followed by a significant decline in indicators of oxidative stress (280). Another study tested the effects of a herbal cream containing several essential oils including *Oliveria Decumbens* and *Pelargonium Graveolens* using an in vivo approach. The results of this experimental study showed a reduction in wound size and faster wound healing (281). Similarly, giving lavender oil to injured rats helped them deposit more collagen, migrate more fibroblasts, and express more TGF-β compared to the control group (282).

2.8.2.3 Biological macromolecules-based nanoformulations

As biofilms mature, they develop a visible protective matrix that adheres to the wound surface. This matrix impedes the penetration of antimicrobial agents into the wound, enabling the prolonged survival of microbes in wounds (283). At the genetic level, any bacteria present inside the biofilm changes their phenotypic expression, either by exchanging their genetic material or by QS and therefore delay wound healing. This shows that the combination therapies targeting microbes and QS to inhibit biofilm formation is highly required. Nowadays, biological macromolecules-based nanomaterials have attracted much attention because they exhibit antibacterial, anti-inflammatory and angiogenic activities and can activate a variety of cellular and molecular mechanism that promote rapid healing of chronic wounds (284). Chitosan, cellulose, and polylactic acid are among the well-known polymers that have been widely employed in the development of nanoformulations for addressing delayed wound healing associated with diabetes. The mechanism by which these nanoformulations ameliorate the local wound microenvironment by inhibiting biofilm formation are shown in Fig 2.6 and Table 2.1.

2.8.2.3.1. The role of chitosan-based nanoformulations in improving diabetic wounds

Chitosan, a well-known biological macromolecule, is the N-deacetylated product of chitin. Structurally chitosan is formed of β-(1-4)- linked D-glucosamine and N-acetyl-D-glucosamine (285). Several preclinical investigations have emphasized the positive effects of the use of chitosan for the treatment of diabetes-associated delayed wound healing. Teaima and colleagues prepared the polyurethane modified chitosan

nanofibers, loaded them with linezolid and investigated their potential in healing diabetic wounds in Sprague-Dawley (SD) rats. They showed that diabetic rats receiving polyurethane modified chitosan nanofibers-loaded linezolid nanofibers therapy showed downregulation in levels of NF-kB, homocysteine, and neutrophil elastase, which led to reduced inflammation at the wound site. Furthermore, diabetic rats receiving polyurethane modified chitosan nanofibers-loaded linezolid nanofiber therapy showed 79.9 %, 86.6 %, 95.5 % improvement in diabetic wounds and controlled microbial growth. Besides wound healing and antimicrobial activity, the developed nanoformulation was also found to improve reduced GSH levels and decrease MDA and nitric oxide levels, thus demonstrating its antioxidant potential to scavenge free radicals (286). Similarly, Wang et al. formulated and evaluated the efficacy of novel chitosan nanoparticles loaded with calcium alginate hydrogel to improve local wound healing environment. Experimental analysis revealed that the developed nanoparticles mediate a change in the permeability of *Escherichia coli* and *Staphylococcus aureus* and lead to bacterial death, therefore exhibiting antibacterial activity. Likewise, animals treated with chitosan nanoparticles-loaded calcium hydrogel exhibit a modulation in ROS production, promoting the growth and relocation of vascular endothelial cells, and facilitating neovascularization to enhance the process of wound healing (287). A study by Wang et al. shown that insulin, a polypeptide hormone significantly improves diabetic wounds under HG conditions (288). Later, Ribeiro et al. proposed the hypothesis of combinational therapy and designed insulin-loaded chitosan nanoparticles which were further examined for their potential to improve diabetic wound healing using a female Wistar rat model. They demonstrated that administration of insulin-loaded chitosan nanoparticle resulted in reduced fibroplasia and increased fibrosis in diabetic rats. In addition, increase in the density of blood vessels further indicates that the presence of insulin in chitosan nanoparticles effectively improved fibroblast migration, angiogenesis, and the local wound environment (289). Similarly, another group developed human EGF loaded chitosan hydrogel which was further conjugated with sodium carboxymethyl chitosan nanoparticles followed by subsequently treatment of diabetic rats with the developed hydrogel on cut wound, which enhance fibroblast proliferation and accelerated wound healing (290). The deposition of collagen plays a crucial role in the healing of diabetic wounds. However, individuals with diabetes often show reduced expression of collagen, leading to prolonged healing times for wounds in diabetic patients (291). Focusing on this aspect, Tallapaneni et al. choose a naturally occurring phytochemical called resveratrol and develop a nanocomposite for the management of diabetic wounds. They select resveratrol based on its antioxidant potential because it improves fibroblast function and promotes the proliferation of dermal cells, thereby accelerating collagen formation. Treatment of resveratrol microparticles encapsulated within chitosan-collagen scaffold-associated doxycycline accelerates diabetic wounds by improving the functioning of fibroblast and proliferation of dermal cells (292). Similarly, Shah et al. prepared another series of hydrogels and investigated their potential to heal diabetic wounds. For instance, they prepared curcumin-chitosan carboxymethyl cellulose-g-PF172 injectable hydrogels and showed that the designed hydrogels exhibit good biocompatibility with 3T3- fibroblast cells. Furthermore, animals receiving curcumin-

chitosan carboxymethyl cellulose-g-PF172 hydrogel therapy showed a spontaneous increase in fibroblast, keratinocyte expression, and collagen deposition, which promote diabetes-associated wound healing (293). Another in vivo experimental study by Arantes et al. showed that solid lipid nanoparticles loaded with retinoic acid surrounded by a chitosan film effectively reduced leukocyte infiltration into the wound, causing collagen accumulation and improved wound closure in diabetic mice with no sign of skin irritation (294). A similar study by Correa et al. showed diabetic rats supplemented with melatonin loaded lecithin-chitosan nanoparticle therapy had higher fibroblast cell motility, proliferation of angiogenic factors and collagen deposition (295). Several reports have well-discussed the role of topical formulations for the management of diabetic wounds, either clinically as a treatment for infected wound, or preventive measure to prevent infection in wounds (296-298). For instance, Terkelsen and colleagues demonstrated that applying cod liver oil topically promotes the healing of wounds in mice by improving the processes of re-epithelization and angiogenesis (299). Subsequently, a different team of innovative scientists employed the microwave-assisted electrospinning method to create nanoscaffolds made of polylactic acid and chitosan, incorporating 30% cod liver oil. These nanoscaffolds were designed for addressing delayed wound healing associated with diabetes. They revealed that male mice treated with cod liver oil containing nanoscaffolds for 14 days, had good wound healing properties up to 94.5 %, while animals receiving only cod liver oil had wound healing properties up to 86 %. They also showed that polylactic acid and chitosan prevents the early degradation of cod liver oil and helps the drug to reach its target site, which suggests that chitosan is a biocompatible polymer and may improve the local diabetic wound environment (300). Recently, a Chinese group of scientists developed the chitosan-based POSS-PEG hybrid hydrogel which was further cross-linked with hydroxypropyltrimethyl ammonium chloride chitosan. The efficacy and potential of the developed hydrogels were subsequently evaluated using a mice model of diabetes-associated delayed wound healing. The in vivo result of this study showed that hydrogel treatment resulted in increased cell migration and proliferation, epithelial regeneration, collagen accumulation and VEGF expression, resulting in improving local environment of diabetic wounds (301). Neurotensin is a 13 amino acid neuropeptide which functions as an inflammatory modulator in wound healing mechanism (302). Moura et al. prepared chitosan derivatives-based novel dressing loaded with neurotensin with the aim to ameliorate delayed wound healing associated with diabetes. They showed that among N-carboxymethyl chitosan, 5-methyl pyrrolidinone chitosan and N-succinyl chitosan, only 5-methyl pyrrolidinone chitosan exhibits good healing properties. Interestingly, neurotensin-loaded 5-methyl pyrrolidinone chitosan has been shown to downregulate TNF-α and MMP-9 level, while promoting fibroblast migration and increasing collagen accumulation (COL1A1, COL1A2, and COL3A1). This acceleration contributes to the healing of diabetes-associated delayed wounds (303). The modified ionic gelation method proved effective in synthesizing chitosan alginate nanoparticles, offering significant improvements in diabetic wound healing. The nanoparticles demonstrated a notable reduction in the inflammation index and a simultaneous increase in collagen levels. This suggests that a nanoformulation based on chitosan holds promise as a therapeutic strategy

to enhance wound healing in individuals with diabetes (304). In a separate investigation, chitosan nanoparticles loaded with curcumin demonstrated effective suppression of inflammation markers stimulated by macrophages, including TLR-4, NF-kB, TNF-α, and IL-6, along with an enhancement in angiogenesis in diabetic rats induced by STZ. Additionally, observations on day 14 revealed collagen deposition and fibroblast migration in rats subjected to nanoparticle therapy, indicating a positive impact on wound healing in diabetic animals (305). Curcumin, a naturally occurring polyphenol derived from the perennial turmeric plant (Curcuma longa), is renowned for its antioxidant and anti-inflammatory properties (306). A study conducted by Kant et al. demonstrated that curcumin expedited wound healing by suppressing the expression of TNF-α and MMP-9. Similarly, the administration of curcumin increased the levels of antioxidant enzymes, such as SOD, GSH peroxidase, and catalase, in STZ-induced diabetic rats (270). However, the poor bioavailability and stability of curcumin restricts its clinical use for the treatment of disease (307). Therefore, to improve the clinical efficacy of curcumin, Karri et al. prepared curcumin-loaded chitosan nanoparticles and fused them in collagen-alginate scaffolds to investigate their potential in impaired diabetes-associated wound healing. The preclinical findings indicated that adult male Wistar rats treated with topical scaffolds exhibited enhanced fibroblast migration, increased collagen deposition, reduced inflammation, and accelerated wound healing. These results suggest that the enhanced clinical application of curcumin could be attributed to its improved bioavailability and stability, reflecting the potential role of nanotechnology in enhancing the clinical effectiveness of therapeutic drugs for disease management (308).

2.8.2.4 The role of cellulose-based nanoformulations in improving diabetic wounds

Aside from chitosan, the most prevalent biopolymer on the planet is cellulose, which is mostly derived from plants. It is a linear homopolysaccharide or homopolymer composed of D-glucose residues linked together by β-1,4-glycosidic linkages (309). Several cellulose-based novel formulations have been designed and tested pre-clinically to find a safer treatment strategy for the management of diabetes-associated delayed wound healing (310). For instance, Loh and colleagues formulated hydrogels using bacterial cellulose, incorporating keratinocytes and fibroblasts to improve local wound environment. In vivo findings indicated that male athymic mice treated with keratinocytes-loaded cellulose hydrogel demonstrated accelerated wound healing, attributed to the rapid attachment and migration of keratinocytes in the wound tissues. It concludes that cellulose, a polysaccharide can be used to deliver keratinocytes and fibroblast to stimulate rapid wound healing (311). Similarly, Yang et al. prepared an injectable hydrogel by loading melatonin and γ-cyclodextrin in carboxymethyl cellulose. The potential of developed hydrogel was subsequently confirmed on 7-week male Wistar rats as a model of diabetic wound. In vivo results showed that animals receiving hydrogel therapy aided epithelial regeneration, and collagen accumulation around the wound site on day 14, whereas no such effect was observed in other groups. Furthermore, male Wistar rats treated with the hydrogel exhibited a decrease in the production of ROS and an enhancement in blood vessel density, contributing to the expedited wound healing in diabetic rats in vivo (312). Cellulose acetate is a poorly soluble cellulose derivate which is a partially

acetylated cellulose product (313). Cellulose acetate is a slowly degradable biomaterial which enhances its use to deliver bioactive materials for treating diabetic wounds (314, 315). Recently, a group of scientists developed cellulose acetate loaded crude annatto extract nanofibers and examine its potential for improving local wound environment. They showed that Wistar rats receiving cellulose acetate loaded crude annatto extract nanofibers treatment modulates inflammatory phases and enhance migration and proliferation rate of fibroblasts, suggesting cellulose acetate as a dressing strategy for the treatment of chronic wounds (316).

2.8.2.5 Exploring the Involvement of Alternative Nanoformulations in Enhancing Wound Healing Linked to Diabetes

Since the presence of microbial species and biofilm formation alters normal healing mechanism in diabetics and exacerbates antibiotic resistance, therefore, nanoformulations that targets microbial colonization and biofilm formation have become the primary treatment option for diabetic wounds globally. For instance, a study by Anjum et al. showed that PLGA nanoparticles loaded-xylitol penetrates the biofilm's extracellular polymeric substances matrix and exhibit antibiofilm activity by inhibiting biofilm formation (317). Another investigation conducted by Kalishwaralal et al. confirmed that silver nanoparticles inhibit the growth of *Pseudomonas aeruginosa* and *Staphylococcus epidermidis*, consequently impeding the formation of biofilms (318). In a study, Singh et al. used the soil fungus *Rhizopus arrhizus* BRS-07 metabolites by mycofabricating the silver nanoparticles and evaluated their potential as antibiofilm. The function of QS-regulated genes, N-acyl homoserine lactones, and various virulence factors like LasA protease, LasB elastase, pyocyanin, pyoverdin, pyochelin, rhamnolipid, and alginate was observed to decrease after nanoparticle treatment, leading to the inhibition of biofilm formation by *Pseudomonas aeruginosa* (318). In another study, silver nanoparticles at 100 μg ml^{-1} concentrations prepared from *Gelidiella acerosa* inhibited biofilm formation and reduce colonies of *Vibrio parahaemolyticus* (71 %) and *Vibrio vulnificus* (83 %) by suppressing QS (319). In a recent study, Li et al. developed the ciprofloxacin-loaded lactose modified azocalix[4]arene nanoformulation and showed its potential to accelerate wound healing by inhibiting biofilm formation against Pseudomonas aeruginosa infected diabetic ulcer. The animals receiving nanoformulation therapy showed increased expression of VEGF and CD31, which promote angiogenesis at wound site whereas no such result was observed in other groups. Moreover, the hastening of wound healing was noticed due to an increase in collagen deposition, coupled with a simultaneous decrease in the expression of TNF-α, resulting in a reduced inflammatory state. The number of neutrophils and macrophages were also found to decrease when receiving nanoformulation therapy, which promotes reduction of oxidative stress (320). Another study by McLaughlin and colleagues showed that treatment of sprayable silver nanoparticles coated antimicrobial peptide LL-37 and collagen significantly inhibits biofilm by reducing *Pseudomonas aeruginosa* colonies in mouse model of wound, thus act as a barrier against bacterial colonization in biofilm (321). In a parallel study conducted by Lazurko et al., it was demonstrated that the application of a sprayable solution containing silver nanoparticles and antimicrobial peptide CLKRS on injured diabetic mice effectively hinders biofilm formation. This

inhibition was particularly notable against *Staphylococcus aureus* (ATCC 25923) and *Pseudomonas aeruginosa* (PA14), with no comparable outcomes observed in other experimental groups (322). Richter and colleagues demonstrated that the application of quasi-spherical nanoparticles leads to a significant decrease in the activity of *Pseudomonas aeruginosa*, *Staphylococcus aureus*, and methicillin-resistant *Staphylococcus aureus* (MRSA), achieving a 96% inhibition of biofilm formation (323). The treatment of alginate film containing silica-silver nanoparticles showed no cytotoxicity for human keratinocytes and fibroblast cells. Similarly, their treatment was also found effective in demonstrating the antibiofilm activity by reducing the *Pseudomonas aeruginosa* and *Staphylococcus aureus* species (324). Besides, the frequency of *Pseudomonas aeruginosa* species was decreased and biofilms were broken in 2D-bacterial biofilm cell monolayers model and 3D human model of infected skin, when chronic wounds were treated with copper-containing mesoporous glass nanoparticles (325). In another study, Yang et al. showed that treatment with aminosaccharide-based gold nanoparticles resulted in a 68 % reduction in wound size in MRSA-infected skin of female BALB/c mice (326). Mir and colleagues conducted a study that uncovered the effectiveness of employing bacteria-responsive PCL nanoparticles containing carvacrol, along with microneedles. This approach resulted in a noteworthy reduction in the prevalence of bacterial strains such as *Staphylococcus aureus* and *Pseudomonas aeruginosa*. The findings, derived from an ex vivo pig skin wound model, suggest promising potential for addressing polymicrobial biofilms at infected wound sites (327). Another series of study by Sancineto et al. renders that diphenyl diselenide derivatives such as bis[ethylN-(2′-selenobenzoyl) glycinate] and bis[2′-seleno-N-(1-methyl-2-phenylethyl) benzamide] possess good antibacterial and antioxidant potential by inhibiting the activity of *Staphylococcus aureus* and *Staphylococcus epidermidis* in wounds. Additionally, their discovery indicates that the suppression of microbial biofilm formation and reduction of oxidative stress contribute to expedited wound healing. This suggests that diphenyl diselenide derivatives emerge as promising candidates for enhancing the wound healing process (328). Since, the DapE protein is important in peptidoglycan synthesis, there is a great need for therapeutic strategies that inhibit or reduce the activity of this protein. One such attempt was done by Khan et al. by synthesizing the zinc oxide nanoparticles. They showed that release of zinc ions from zinc oxide nanoparticles inhibits biofilm formation by reducing the DapE protein activity and exhibits antibiofilm and antimicrobial applications against *Rothia dentocariosa* and *Rothia mucilaginosa* pathogens (329). EGF stands out as a crucial growth factor plentiful in the epidermis, playing an essential role in the synthesis of collagen, elastin, and hyaluronic acid (330). However, studies have confirmed that patients with diabetes lack this growth factor, which makes wound healing difficult (331, 332). Therefore, administering EGF conjugated with nanoparticles is one of the leading therapeutic strategies to avoid delayed wound healing. Considering this, Qi and colleagues synthesized the stable EGF via polylactic acid/glycolic acid copolymer and evaluated its efficacy in diabetic rat ulcers. The outcomes indicated that in animals undergoing nanoparticle therapy, diabetic wounds exhibited an accelerated healing process attributed to the increased proliferation and migration of fibroblasts. In contrast, the group receiving EGF therapy did

not show similar results, likely due to the short half-life of EGF (333). Likewise, Chu and colleagues developed a set of poly(lactic-co-glycolic acid) nanoparticles encapsulating recombinant human EGF through the double-emulsion method. In vivo findings from this investigation demonstrated that administering these nanoparticles to diabetic mice led to heightened fibroblast proliferation and an accelerated rate of wound healing (333). Similarly, the combinational therapy of VEGF-encapsulated PLGA nanoparticles in a diabetic mouse showed epithelial and blood vessel remodeling that promoted a faster healing rate due to the presence of lactate and VEGF. Furthermore, this treatment increases the migration of keratinocytes and VEGFR2 levels while the untreated groups show poor dermal remodeling (334). On the contrary, Li and colleagues revealed that coupling keratinocyte growth factor with gold nanoparticles enhanced the proliferation and mobility of keratinocytes at the wound site. This led to an elevated expression of Col-I, α-SMA, and TGF-β1, contributing to epithelial remodeling and the closure of wounds in female SD rats (335).

TNF-α, a widely recognized inflammatory cytokine, plays a pivotal role in the expedited healing of diabetic wounds by facilitating the proliferation of fibroblasts (336). Whereas continuous production of this cytokine increases the cell apoptosis and thus alter the normal healing mechanism which suggest that TNF-α must be present in small amounts to accelerate wound healing (337, 338). Focusing on this aspect, Kasiewicz and colleagues showed that topical therapy of siRNA-loaded lipid nanoparticles accelerates wound healing by reducing TNF-α mRNA expression in diabetic (C57BL/6) mice (339). Since oxidative stress in diabetic wounds leads to the ulcer development (340), scavenging free radicals is essential for improving the local wound microenvironment. Based on this, Xu et al. prepared by incorporating thermosensitive poly(d, L-lactide)-poly (ethylene glycol)-poly(d, L-lactide) hydrogel into prussian blue nanoparticles against diabetic wound healing. The use of these nanoparticles was noted to accelerate the healing of diabetic wounds by diminishing the expression of ROS, IL-6, and TNF-α, while simultaneously fostering angiogenesis (341). In a recent study, a significant reduction in the presence of inflammatory cells and a simultaneous increase in blood vessel density were observed in diabetes-induced Wistar rats undergoing treatment with gold nanoparticles loaded with dicer substrate siRNA (342).
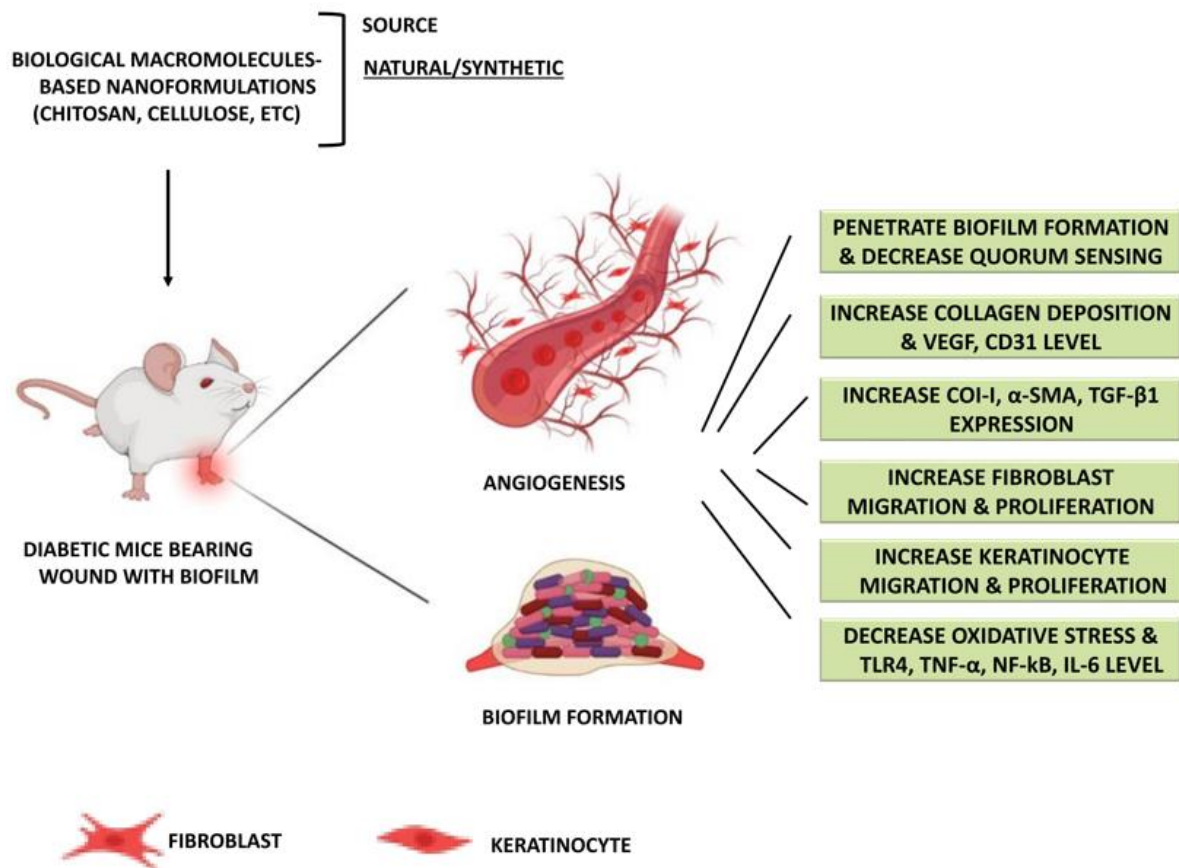
Fig 2.6: Nanoformulation in healing diabetes-associated wounds: Nanoformulation can be prepared from natural or synthetic origin. Treatment of these nanoformulations in diabetic wound alter many factors and improves the healing mechanism. Treatment with nanoformulation decrease the QS by penetration of biofilm formation, and increase collagen deposition. In addition, they also support angiogenesis by increasing the expression of VEGF, CD-31, COI-I, α-SMA, TGF-β1. In addition, nanoparticle treatment decreases oxidative stress and TLR4, TNF-α, NF-kB, IL-6 level in diabetic-wounds.

Table 2.1: List of experimental studies conducted using nanoparticles in various *in vivo* and *in vitro* model of diabetes and biofilm

S. No.	Nanoformulation	Type of model	Mechanism	Outcome	Reference
1.	Polyurethane-modified chitosan nanofibers loaded linezolid	SD model of diabetic wound	• Downregulate NF-kB, homocysteine, neutrophil elastase	• Decrease inflammation and oxidative stress	(286)

33

			• Reduce GSH, MDA, and nitric oxide levels • Control microbial growth		
2.	Chitosan nanoparticles loaded calcium alginate hydrogel	Chronic wound	• Change permeability of *Escherichia coli* and *Staphylococcus aureus* • Decrease ROS level • Helps in proliferation and migration of vascular endothelial cells	• Decrease oxidative stress • Accelerate wound healing	(287)
3.	Insulin-loaded chitosan nanoparticles	Female Wistar rat model of diabetic wound	• Reduced fibroplasia and increased fibrosis	• Improve wound healing	(289)
4.	Human EGF-loaded chitosan hydrogel-conjugated sodium carboxymethyl chitosan nanoparticle	Diabetic wound	• Enhance fibroblast proliferation • reduced fibroplasia and increased fibrosis	• Improve wound healing	(290)
5.	Resveratrol microparticles encapsulated chitosan-collagen scaffold associated doxycycline	Diabetic wound	• Enhance fibroblast functioning and dermal cell proliferation • Enhance collagen formation	• Improve wound healing	(292)

6.	Curcumin-chitosan-carboxymethyl cellulose-g-PF172 injectable hydrogels	Diabetic wound	• Enhance fibroblast proliferation, keratinocyte and collagen deposition	• Accelerate wound healing	(293)
7.	Solid lipid nanoparticles loaded retinoic acid surrounded by chitosan film	Diabetic wound	• Reduce leukocyte infiltration • Cause collagen deposition • Improve wound closure	• Accelerate wound healing	(294)
8.	Melatonin loaded lecithin-chitosan nanoparticle	Diabetic wound	• Enhance fibroblast cell motility • Enhance proliferation of angiogenic factor • Enhance collagen deposition	• Accelerate wound healing	(295)
9.	Polylactic acid/chitosan nanoscaffolds containing 30% cod liver oil	Diabetic wound	• Heal wound up to 94.5% • Improve delivery of cod liver oil	• Accelerate wound healing	(300)
10.	Chitosan-based POSS-PEG hybrid hydrogel cross-linked with hydroxypropyltrimethyl ammonium chloride chitosan	Diabetic wound	• Increase cell migration, proliferation, epithelial regeneration, collagen accumulation and VEGF expression	• Improve local wound environment	(301)

#				
11.	5-methyl pyrrolidinone chitosan loaded neurotensin	Diabetic wound	• Downregulate TNF-α, MMP-9 level • Enhance fibroblast migration and collagen deposition (i.e., COL1A1, COL1A2 and COL3A1),	• Accelerate wound healing	(303)
12.	Chitosan alginate nanoparticles	Diabetic wound	• Decrease inflammation • Enhance collagen levels	• Promote wound healing	(304)
13.	Curcumin-loaded chitosan nanoparticles	Diabetic wound	• Reduce TLR-4, NF-kB, TNF-α, and IL-6 expression • Enhance angiogenesis, collagen deposition and fibroblast migration	• Accelerate wound healing	(305)
14.	Curcumin-loaded chitosan nanoparticles fused in collagen-alginate scaffolds	Adult male Wistar rat model of diabetic wound	• Enhance fibroblast migration, collagen deposition • Reduce inflammation • Improve bioavailability of curcumin	• Improve drug delivery • Accelerate wound healing	(308)

15.	Bacterial cellulose hydrogels-loaded with human epidermal keratinocytes and dermal fibroblasts	Male athymic mice model of diabetic wound	• Enhance migration of keratinocyte • Quick cell attachment	• Stimulate rapid wound healing	(311)
16.	Injectable hydrogel by loading melatonin and γ-cyclodextrin in carboxymethyl cellulose	7-week male Wistar rat model of diabetic wound	• Enhance epithelial regeneration and collagen accumulation • Reduce oxygen species generation • Enhance blood vessel density	• Accelerate wound healing	(312)
17.	Cellulose acetate loaded crude annatto extract nanofibers	Wistar rat	• Modulate inflammatory phase • Enhance migration and proliferation of fibroblast	• Accelerate wound healing	(316)
18.	PLGA nanoparticles loaded-xylitol	Polymicrobial bacterial biofilm strains	• Penetrates the biofilm extracellular polymeric substances matrix and inhibit biofilm formation	• Promote antibiofilm activity in infected wounds	(317)
19.	Silver nanoparticles	*In vitro* biofilm model	• Reduce *Pseudomonas aeruginosa* and *Staphylococcus epidermidis* growth up to 95%	Inhibit biofilm formation	(318)

No.				
20.	Mycofabricated biosilver nanoparticles	*In vitro* biofilm model	• Decrease the activity of QS regulated genes, N-acyl homoserine lactones and several virulence factors such as LasA protease, LasB elastrase, pyocyanin, pyoverdin, pyochelin, rhamnolipid, and alginate	Inhibit biofilm formation by *Pseudomonas aeruginosa* (343)
21.	Silver nanoparticle	*In vitro* and *in vivo* biofilm model	• Inhibit *Vibrio parahaemolyticus* (71%) and *Vibrio vulnificus* (83%) mediated biofilm formation at 100μg mL^{-1} concentrations by suppressing QS	Inhibit biofilm formation (319)
22.	Ciprofloxacin-loaded lactose-modified azocalix[4]arene	*In vivo* diabetic rat wound model	• Inhibit biofilm formation in *Pseudomonas aeruginosa* infected diabetic ulcer • Enhance collagen deposition to accelerate wound healing	Improve diabetic wounds and inhibit biofilm formation (320)

			Enhance VEGF and CD31 expression to promote angiogenesis		
			• Decrease TNF-α expression to reduce inflammation		
			• Reduce the number of neutrophils and macrophages and alleviates oxidative stress		
23.	Sprayable silver nanoparticles coated antimicrobial peptide LL-37 and collagen	Mouse model of wound	• Inhibit biofilm formation by reducing *Pseudomonas aeruginosa* colonies	• Inhibit biofilm formation and accelerate wound healing	(321)
24.	Sprayable silver nanoparticles coated antimicrobial peptide CLKRS	Diabetic wound mice	• Inhibit biofilm formation by reducing *Staphylococcus aureus* (ATCC 25923) and *Pseudomonas aeruginosa* (PA14) colonies	• Improve diabetic wound healing	(322)
25.	Quasi-spherical nanoparticles	*In vitro* biofilm model	• Inhibit biofilm formation by reducing *Pseudomonas aeruginosa,*	• Inhibit biofilm formation	(323)

			Staphylococcus aureus and MRSA by 96%		
26.	Alginate film containing silica-silver nanoparticles	*In vitro* biofilm model	• Inhibit biofilm formation by reducing *Pseudomonas aeruginosa* and *Staphylococcus aureus* colonies	• Inhibit biofilm formation	(324)
27.	Copper-containing mesoporous glass nanoparticles	2D-bacterial biofilm cell monolayers model and 3D human model of infected skin	• Inhibit biofilm formation by reducing *Pseudomonas aeruginosa* species	• Inhibit biofilm formation and accelerate wound healing	(325)
28.	Aminosaccharide-based gold nanoparticles	MRSA skin-infected female BALB/c mice model	• Reduce wound size by 68%	• Improve local wound microenvironment	(325)
29.	Carvacrol-loaded bacteria-responsive PCL nanoparticles	*Ex vivo* pig skin wound model	• Inhibit biofilm formation by reducing *Pseudomonas aeruginosa* and *Staphylococcus aureus* colonies	• Improve polymicrobial-biofilms infected wound	(327)
30.	bis[ethylN-(2'-selenobenzoyl) glycinate] and bis[2'-seleno-N-(1-methyl-2-phenylethyl) benzamide]	*In vitro* biofilm model of Staphylococcus epidermidis, Staphylococcus aureus	• Inhibit biofilm formation by reducing *Staphylococcus aureus* and *Staphylococcus epidermidis*	• Improve wound healing	(328)

				• Inhibit oxidative stress		
31.	Zinc oxide nanoparticles	Biofilm model of Rothia dentocariosa and Rothia mucilaginosa	• Inhibit biofilm formation by reducing DapE protein activity • Exhibit antimicrobial activity by inhibiting *Rothia dentocariosa* and *Rothia mucilaginosa* pathogens	• Inhibit biofilm formation	(329)
32.	EGF via polylactic acid/glycolic acid copolymer	Diabetic rat ulcer	• Enhance proliferation and migration of fibroblasts	• Improve diabetic ulcer	(333)
33.	Recombinant human EGF encapsulated poly(lactic-co-glycolic acid) nanoparticles	Diabetic mice	• Enhance fibroblast proliferation and accelerate healing rate	• Improve local diabetic wound microenvironment	(344)
34.	VEGF-encapsulated PLGA nanoparticles	Diabetic mouse	• Enhance epithelial and blood vessel remodeling due to the presence of lactate and VEGF • Enhance migration of keratinocytes and VEGFR2 levels	• Accelerate healing rate and improve diabetic wound healing	(334)

35.	Keratinocyte growth factor conjugated gold nanoparticles	Female SD rat model of wound	• Increase proliferation and migration of keratinocytes toward wound • Increase Col-I, α-SMA and TGF-β1 expressions and helps in epithelial remodeling and wound closure	• Improve local wound microenvironment	(335)
35.	siRNA-loaded lipid nanoparticles	C57BL/6 diabetic mice	• Reduce TNF-α mRNA expression	• Accelerate wound healing	(339)
36.	Thermosensitive poly(d, L-lactide)-poly(ethylene glycol)-poly(d, L-lactide) hydrogel into prussian blue nanoparticles		• Decrease ROS • Decrease IL-6, TNF-αand increase remodeling of angiogenesis	• Improve wound healing	(341)
37.	Dicer substrate small interfering RNA loaded gold nanoparticles	Diabetes-induced wistar rats	• Decrease inflammation and increase blood vessel density	• Improve wound healing	(342)

CHAPTER 3
HYPOTHESIS

Diabetes, a metabolic disorder typically arising from deficiencies in insulin secretion or action, results from a complex interplay of genetic and environmental factors. A recent study conducted by the International Diabetes Federation indicates that currently, 537 million people worldwide are dealing with diabetes. Projections suggest a rise to 643 million by 2030 and 783 million by 2045, highlighting the epidemic scale of diabetes prevalence. Individuals with diabetes face a higher likelihood of developing chronic wounds, particularly in the feet, referred to as DFU. The substantial worldwide rise in DFU incidence carries significant socio-economic consequences. For example, around 15% of the global health budget is dedicated annually to the treatment of individuals with diabetes and the associated complications, including DFU patients. The reduced glucose metabolism is believed to hinder the wound-healing process in diabetic individuals, resulting in the development of chronic wounds. Moreover, heightened blood sugar levels impede blood circulation, preventing crucial nutrients from reaching the affected area and impeding healing mechanisms. The typical characteristics of chronic lesions, which contribute to substantial damage to host tissue, include persistent inflammation and heightened oxidative stress. Numerous reports have provided evidence for the engagement of epigenetic mechanisms, including DNA methylation, histone post-translational modifications, and miRNAs, in the formation of diabetic lesions. While extensive research has been conducted to elucidate the involvement of inflammatory and angiogenic markers in diabetic wounds, there is still a considerable amount to be revealed. The approval of anti-diabetic wound drugs by the United States Food and Drug Administration has prompted a widespread adoption of synthetic drugs globally for the treatment of DFU. Becaplermin and Omnigraft are some common examples of drugs that were used in clinical practice to prevent the pathogenesis of DFU. Concerns about the safety and effectiveness of these medications have arisen due to their adverse side effects, which encompass blisters, skin peeling, intense itching, and skin redness. As previously mentioned, while the utilization of synthetic drugs has decreased the risk of developing DFU, doubts about their safety and efficacy persist due to various unwanted effects. This underscores the importance of exploring safer alternatives with fewer or minimal side effects, with naturally occurring phytochemicals emerging as the primary candidates among researchers for addressing such medical conditions. Since plants are a potent source of natural epigenetic modifiers, these may open up many opportunities for scientists to discover and validate novel phytochemicals with the potential to improve DFU using in vitro and in vivo diabetic wound models.

As a result, we speculate that naturally occurring phytochemicals may reverse the epigenetic changes that lead to diabetes and diabetes associated delayed wound healing. To accomplish this, we used a hypothesis called **"similar structures will have similar biological activities"** to screen potential phytochemicals against diabetic wounds.

CHAPTER 4

AIMS AND OBJECTIVES

The use of synthetic medications to treat diabetic wounds raised questions about their safety and efficacy as they have adverse side effects that include blisters, skin peeling, intense itching, and skin redness. This highlights the necessity to explore safer alternatives with fewer side effects, with naturally occurring phytochemicals being the foremost candidates among researchers for addressing such medical conditions. Since plants are an emerging source of natural epigenetic modifiers, these may open up many opportunities for scientists to discover and validate novel phytochemicals (SIRT1 activator) using a recent approach of structural similarity and binding energy through molecular docking. Compounds finalized from molecular docking will be further taken into consideration for validating their potential in reducing diabetes-associated delayed wound healing and oxidative stress using in vitro and in vivo diabetic wound models. Based on this, following objectives were created to elucidate the potential of selected phytochemicals in improving wound healing:

1. Molecular docking studies of the promising SACs (SIRT1 activating compounds) to find out the potential binding interactions and binding energies with SIRT1.
2. In vitro migration, proliferation and tube formation assay in endothelial cells to evaluate wound healing activity of potential SACs.
3. In vivo evaluation of the potential SACs in improving wound healing in type 2 diabetic animal models.

<div align="center">

CHAPTER 5

MATERIALS AND METHODS

</div>

5.1 Material, Method, and Experimentation

5.1.1 Chemicals and Reagents

The analysis employed analytical quality chemicals, namely 99% pure Sinapic acid, 99% pure o-Coumaric acid obtained from Sigma-Aldrich chemicals, and cholesterol procured from Hi Media Lab Mumbai, India. DL-Methionine, carboxymethyl cellulose, casein from Saras Casein (Orai), vitamin and mineral combination from a nearby vendor, and yeast powder from S.D Fine Chemicals and HiMedia India Ltd. were obtained for study.

5.2 In silico studies

5.2.1 Analyzing similarities and compiling data in silico

To find structures similar to the parent compound, we look for their similar structures using various aspects, as discussed below:

• Several databases related to chemicals and natural products, including ZINC, ChEMBL, PubChem, ChemSpider, and Drug Bank, were explored to compile information on SMILE notation, 2D and 3D structures, experimental data related to various biological activities, and physicochemical parameters.

• Using a filter of similarity index >0.8, each phytochemical structure was used as a query to search chemical and natural similar compound.

• Furthermore, we investigated the biological activities of compounds selected from the reviewed literature and used for docking.

5.2.2 Molecular docking studies

Using a method called molecular docking, it can be predicted how a query structure will bind to the active site of a protein (345, 346). The human SIRT1 protein three-dimensional structure was extracted from the protein data bank (PDB). After a comprehensive review of the literature, we identified several phytochemicals that show biological activities. To identify ligands with the highest likelihood of activating SIRT1, we employed the web-based docking program AutoDock-Vina (347). The SIRT1 protein structure was searched using the PDB (https://www.rcsb.org/). We employed similar parameters to compare these related structures. For docking, we used PDB ID: 4ZZJ in this case. For molecular docking studies, preparation of the ligand and receptor was carried out according to the 2019 Bashary and Khatik protocol (348).

5.2.2.1 Preparation of receptor

After obtaining the protein 4ZZJ PDB file in PDB format from the PDB database, we opened it for editing in the AutoDock Edit window. As the protein was repaired, the protein structure appeared on the screen, missing

atoms were replaced, water molecules were removed, and polar hydrogens were inserted. The original ligand was excluded from the active site, leaving only the cofactors typically bound to the protein chain. Following these transformations, the protein was saved in the PDBQT format.

5.2.2.2 Ligand preparation

The PubChem database was searched for ligands as SDF files, which were then converted to pdbqt format using the software Open Babel. Ligand energies were minimized using ChemBio Office software. The ligand was added to the PDB file in AutoDock-Vina by selecting the input molecule in the edit panel. For each ligand, non-polar hydrogen and Gesture charges were specified. The last step entailed choosing the torsion tree and finding the root in addition to saving the produced ligands in the pdbqt format.

5.2.2.3 Finding the active site of the receptor and observing docking interactions

Prior to docking, we must know the binding cavity in which our ligand will bind. In order to construct the receptor 4ZZJ and determine its active site, Python Molecule Viewer (PMV) was utilised. The binding site was examined when the natural ligand was inserted into our receptor 4ZZJ in PMV in PDB format. Every naturally occurring ligand that has formed a cocrystal with the receptor possesses a binding site cavity. After identifying the active site cavity, we incorporated its corresponding X, Y, and Z coordinates (-0.827, 45.618, -0.853, respectively) in the configuration file for AutoDock Vina. The process of locating the binding cavity and preparing both the protein and ligand for docking enables the loading of the ligand in PDBQT format and the selection of the map type. The option to centre on the ligand in the panel has to be chosen in order to construct the grid box. The search was conducted inside a 0.375 Angstrom space. The protein was saved in pdbqt format with all of these parameters. The configuration file was created using the same X, Y, and Z coordinates i.e. -0.827, 45.618, -0.853. A command line was used to carry out the docking process and analyse the results. The docking scores were generated as binding affinity values (kcal/mol) in the output file accessed through the command prompt. The docking data presented conformational poses, with an allowable Root Mean Square Deviation (RMSD) of 1.5 (349). The simulated structure is considered excellent when the RMSD value is below 2.0, and over 80% of the residues are positioned in the optimal locations.

5.2.3 SWISS-ADME studies

The SwissADME tool was used to predict absorption, distribution, metabolism and excretion (ADME) characteristics of compounds (350). In silico ADME properties were supposed to evaluate the toxicity of a compound by correlating its lipophilicity and water solubility. We used Swiss ADME to establish the drug's pharmacokinetics, physiochemical properties, water solubility, and lipophilicity (http://www.swissadme.ch/index.php). As an alternative to experimental approaches to predict ADME, in silico models have been widely used where chemical structures are abundant but resources and their availability are issues (351).

A molecule is considered suitable and efficacious when it reaches its target site, maintaining its bioactive state long enough for the required therapeutic effects to occur, ensuring its effectiveness as a drug. Drug development requires ADME assessment, especially when dealing with numerous compounds and a limited supply of physical samples. To tackle this challenge, in silico computer models like SwissADME are preferred. For instance, the boiling egg representation in SwissADME is a key method for determining whether a compound is blood-brain barrier (BBB) permeant or GI absorbed. Additionally, spider web graphs are used to display information across multiple dimensions. ADME evaluations were conducted on several comparable phytochemicals for each parent molecule. Canonical SMILES were obtained from the ChEMBL database and utilized in the SwissADME tool to perform ADME analysis.

5.3 In vitro studies

5.3.1 DPPH free radical scavenging activity

To assess the efficacy of 1,1-diphenyl-2-picrylhydrazyl (DPPH) in neutralizing free radicals, we followed the procedure outlined by Sharma et al. in 2009. Sinapic acid and o-Coumaric acid were added in different amounts to the sample mixture containing 0.1 mM of total DPPH radicals. The solution was vigorously stirred at 2,500 rpm for one minute and then allowed to stand in the dark for sixty minutes. The scavenging capacity was measured at 517 nm, with ascorbic acid serving as the positive control. A plot was generated by correlating the sample concentration with the percentage of inhibition in the reaction system (352).

5.3.2 Cell line toxicity test

To visualize cell cytotoxicity and quantify cell death in culture, we followed the procedure for the 3-(4,5-dimethylthiazol-2-yl)-2,5-diphenyltetrazolium bromide (MTT) test as described by Gerlier & Thomasset (1986). In preclinical drug development, potential therapeutic compounds are regularly assessed on cell lines to detect any potential adverse effects on the cells (353).

Principle

The MTT test is used to assess cellular metabolic activity, providing a measure of cell viability, proliferation, and cytotoxicity. In this colorimetric experiment, a yellow tetrazolium salt, MTT, undergoes reduction to form purple formazan crystals in metabolically active cells. The conversion of MTT to formazan is facilitated by NAD(P)H-dependent oxidoreductase enzymes within living cells. Following the dissolution of insoluble formazan crystals in a solubilization solution, the colored solution's absorbance is measured at 540 nm using a multi-well spectrophotometer. A deeper color indicates higher cellular activity and, consequently, increased metabolic activity.

Reagents

MTT

DMSO (Dimethyl sulfoxide)

Procedure

- Initially, a seeding of 1 x 10^8 cells per well was performed in each well of a 96-well plate, allowing for attachment over a 24-hour period at 37 °C in a CO2 incubator.

- Afterwards, the culture media were replaced with a new medium.

- Subsequently, the cells were exposed to varying doses of the test medication for 24 hours at 37 °C in a CO2 incubator. Following this exposure, the cells were transitioned from the old medium to a fresh one.

- Following the exposure, a working solution with 10 mg/ml of MTT was added to the 96-well plates, which were then placed in a CO2 incubator for 4 hours at 37 °C.

- After removing the medium, add DMSO in each well to dissolve the formazan crystals for 30 minutes at 37 °C in a CO2 incubator.

- In conclusion, the magnitude of the purple formazan crystals was assessed using an ELISA plate reader set to 540 nm. Since a positive correlation existed between the number of viable cells and the absorbance at 540 nm, cell viability was represented as the percentage of viable cells in both treated and untreated cell samples.

5.3.3 Tube formation assay

This assay entails seeding endothelial cells onto a substrate resembling a basement membrane, leading to the formation of tubules within 6 to 12 hours. These tubules typically include a lumen, and the cells establish strong cell-to-cell and cell-matrix connections. Quantification can be achieved by measuring the tube area, length, and/or the number of branch points, with area measurement being the most commonly employed and straightforward method. This robust semi-quantitative assay offers numerous advantages. It is rapid and uncomplicated, adaptable for high-throughput analysis, and allows the introduction of exogenous factors into the medium, transfection into the cells, or knockdown procedures. Additionally, this assay closely replicates the in vivo environment, serving as a potent tool for assessing angiogenesis promoters and inhibitors before their application in in vivo assays (354).

Method of analyzing cell migration

- HUVECs were cultured and allowed to achieve 70-90% confluency.

- Basement membrane extract (BME) was thawed overnight at 4°C after being removed from the freezer.

- A 96-well plate was labeled and placed in the refrigerator overnight for pre-cooling.

- PBS, trypsin, and growth medium were brought to room temperature, and the tube containing thawed BME was kept on ice.

- Pre-cooled 96-well plate wells were loaded with 50-80 μl of BME, followed by a 1-hour incubation.
- Endothelial cells (100,000 - 150,000) were poured to 15 ml centrifuge tubes, followed by centrifugation at 300 x g for 3 minutes, and pellet was resuspended in 1 ml of the corresponding test or control medium.
- 100 μl of each single cell suspension was added per well on top of the gelled BME.
- The 96-well plate was incubated in CO2 incubator with 37°C, 5% CO2 for continuous 6 hours. Cell monitoring occurred at specified time points using an inverted microscope.
- The tubular network in the wells was imaged without fixation or labeling using an inverted microscope.
- The pictures were examined for the quantification of overall tube length and branches using the Angiogenesis Analyzer plugin by Gilles Carpentier in the ImageJ software.

5.3.4 Cell scratch assay/ Cell migration assay

The scratch-wound assay is frequently employed to assess fundamental cell migration characteristics. In this assay, HUVEC cells are cultured and after achieving the confluency, a narrow "wound" is created with a pipette tip. Cells positioned at the edge of the wound undergo polarization and migrate towards the injured region (355).

Method of analyzing cell migration

- HUVECs were cultivated in a 12-well plate until they formed a monolayer.
- When the cells reached approximately 60-70% confluency, a scratch was generated to create a wound.
- The monolayer was rinsed twice with 1 ml of phosphate buffered saline (PBS).
- Subsequently, 2 ml of medium, with or without test drugs, was introduced to each well and incubated for 24 hours.
- Periodic images were captured using an inverted phase-contrast microscope.

The percentage of cell migration was determined by comparing the final gap width with the initial gap width.

5.3.5 In vitro induction of diabetes in L929 cell line

Material

- DMEM
- Mannitol
- Glucose
- Antibiotic/AB
- Fetal bovine serum/ FBS
- PBS
- Distilled water/DW

Procedure

- L929 cell line was supplied by the cell bank of NCCS, Pune.

- Cells were cultured following standard procedures and established methodologies, using Dulbecco's modified Eagle medium (DMEM) at suitable concentrations. This involved either low/normal glucose conditions (5 mM + 20 mM mannitol for osmotic balance) or HG conditions (25 mM), as per established protocols. Following the inclusion of antibiotics (penicillin 100 IU/mL and streptomycin 100 mg/mL), cells were cultured at 37 °C with 5% CO2 and 10% fetal bovine serum.

- Cell cycle arrest in the G0 phase occurred when cells achieved 80–90% confluence, resembling conditions associated with hyperglycemia and hyperinsulinemia. The procedure was done in triplicate.

Procedure for in vitro model establishment (in 6 well plates)

- To prepare a low-glucose (LG) plate, cells were allowed to grow in a 6-well plate with 5 mmol glucose. Once the cells reached 70% confluence, the group was given the appropriate treatment.

- For the creation of a HG plate, cells were loaded in a 6-well plate with HG (30 mmol). When the cells reached 70% confluence, the group underwent the necessary treatment. (Fig 5.1).
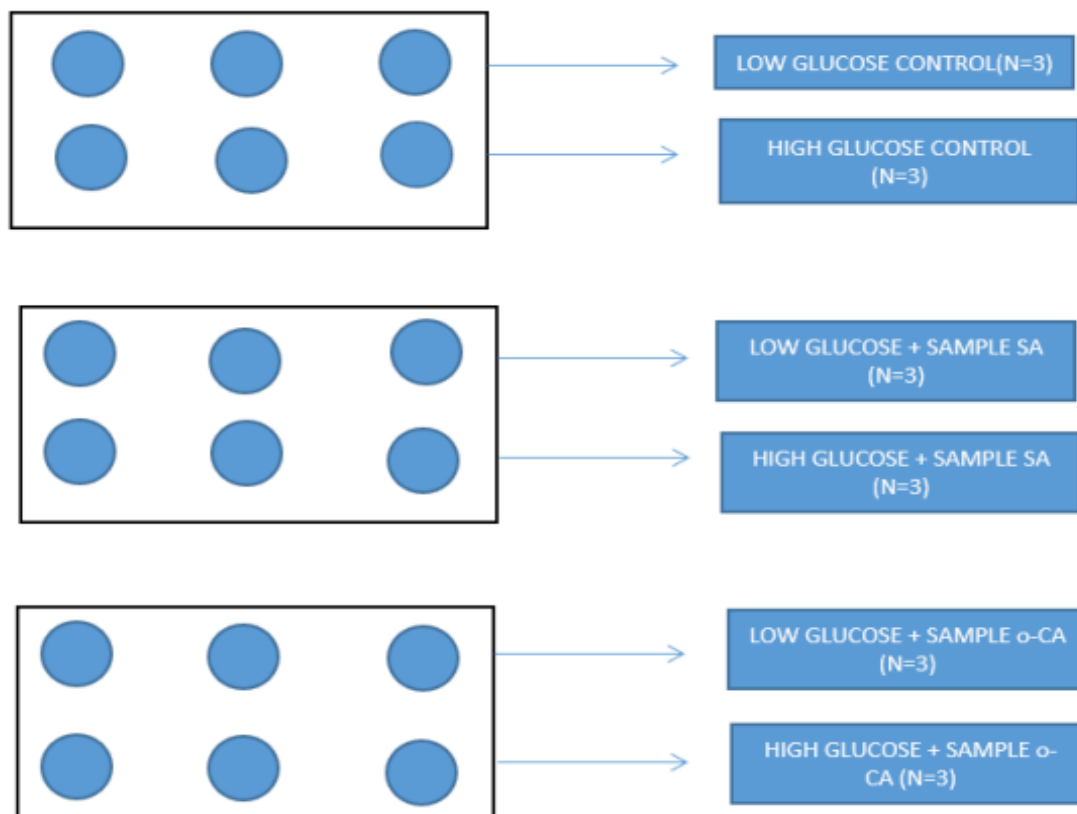
Fig 5.1: Cell culture study schematics for developing diabetic condition.

Procedure for lysing the cells and preparing the lysate for the protein array (6-well format)

- In order to maximize protein yield in cell analysis, we initially introduced protease and phosphatase inhibitors into the analysis solution to prevent the breakdown and modification of isolated proteins. Following the application of the experimental protocol to treat cells on a 6-well plate, they were subsequently rinsed with ice-cold PBS. Afterwards, the plate was filled with lysis buffer. After scraping the cells using a cell scraper, the lysate was collected into microcentrifuge tubes. With this, the cell lysate was centrifuged for seven minutes at 1700 rpm in a cold microcentrifuge.
- The pellet was disposed off and preserved the supernatant for further analysis.

5.3.5.1 Preparation of tissue/cell homogenate

To do this, we combined both solutions and adjusted the pH to 7.4 to create a buffer of ethylenediamine tetra acetic acid (0.1M) – Tris chloride (0.1M), which we then homogenized using a Dounce homogenizer. Before homogenizing the cells and tissues, beta-mercaptoethanol was immediately added to the solution. The homogenization tube was placed in a beaker filled with ice to prevent protein denaturation. Cell homogenization was carried out utilizing a motorized Teflon pestle rotating at 3000 revolutions per minute. Following homogenization, the resulting mixture underwent filtration through cotton gauze and was then stored in properly labelled plastic vials at -18 °C in the refrigerator until subsequent use. Using this 10% homogenate (1 g cell in 9 ml buffer) as the starting homogenate, the working homogenate fraction was obtained by required dilution using appropriate buffers as required.

5.3.5.2 Preparation of Post nuclear supernatant (PNS)

The cell homogenate was subjected to centrifugation at 10,000 rpm for five minutes at 4°C in a C-24 REMI cold centrifuge to separate the nuclear pellet and supernatant. The PNS was then isolated and stored at -18°C for subsequent use.

5.3.3.3 Preparation of Post mitochondrial supernatant (PMS)

To generate the PMS, the nuclear pellet was eliminated, and the supernatant underwent centrifugation for 10 minutes at 10,000 g at 4 °C to separate the mitochondrial pellet. The resulting PMS was then stored at -18°C for various assays.

5.4 Estimation of protein

To determine the protein content, we used the method described by Lowry et al. (1951), employing a standard curve constructed with BSA (356).

Principle

This approach relies on the presence of amino acids such as tryptophan and tyrosine. For this, a reagent called Lowry's reagent was used, which reacts with the protein to form a coloured complex. The color is formed due

to the reduction of phosphomolybdate by amino acids in the protein reacting with copper (an alkaline substance). The intensity of the color is determined by the amount of aromatic amino acids present.

Reagents

Various reagents were prepared and used to estimate protein concentrations, as listed below:

Reagent A consists of 2% sodium carbonate in 0.1N NaOH. Reagent B comprises 1% CuSO4 in double-distilled water (DDW), and Reagent C is composed of 2% sodium potassium tartrate in DDW. Lowry's Reagent is prepared by combining Reagent A, Reagent B, and Reagent C in a ratio of 49:0.5:0.5 (v/v).

For Folin's Ciocalteau's Reagent, dilution with DDW should be done at a ratio of 1:1 (v/v). To create a stock protein standard, 20 mg of BSA should be dissolved in 1 ml of DDW.

Procedure

Sample preparation for protein estimation

Table 5.1: Method for estimating protein concentration

Reagents	Blank (ml)	Standard (ml)	Test (ml)
DDW	1	0.9	0.9
Standard	-	0.1	-
Test Sample	-	-	0.1
Lowry's Reagent	5 ml	5 ml	5 ml

Add the test sample and necessary reagents, incubate the tubes for 15 minutes at 37 °C, and then add 0.5 ml Folin Ciocalto reagent. Again, incubate the tubes at 37°C for a short period of 30 minutes and read the absorbance at 670 nm.

5.5 Estimation of Catalase activity

To assess the activity of catalase, a vital antioxidant enzyme, we followed the procedure outlined by Chance et al. (1995), and was performed using the PNS (357).

Principle

The underlying principle of this test involves the dissociation of hydrogen peroxide to release oxygen and water, serving as a means to detect the presence of the catalase enzyme.

Reagents

- Phosphate Buffer (pH=7.0, 0.2M)
- Add 1.79 g of KH2PO4 to 200 ml of DDW to get Solution A

- Add 3.52 g of NaHPO4.2H2O to 300 ml of DDW to get Solution B
- Combine Solutions A and B in a 3:7 ratio (pH = 7.0)
- Add 160µl of H2O2 to 100 ml of phosphate buffer to obtain working phosphate buffer

Procedure

Table 5.2: Method for estimating catalase activity

Reagents	Blank	Test
Sample	25 µl	25 µl
Phosphate buffer+ H_2O_2	-	3.0 ml
Phosphate buffer- H_2O_2	3.0 ml	-

Following the addition of the aforementioned chemicals, absorbance was measured every 30 seconds for two minutes at 240 nm.

By employing the molar extinction coefficient of 43.6 $M^{-1}cm^{-1}$, the enzyme activity of catalase was approximated. The outcome is expressed as micromoles of H_2O_2 decomposed per minute per milligram of protein.

5.6 Estimation of Glutathione-S-transferase (GST) activity

To investigate the activity of glutathione S-transferase (GST), an important antioxidant enzyme involved in the detoxification process, we followed the procedure described by Habig et al. (1974), using the PMS (358).

Principle

This enzyme functions by catalysing the interaction between glutathione's sulfhydryl group and 1-chloro-2,4-dinitrobenzene (also known as CDNB). At 340 nm, the CDNB-glutathione conjugate absorbs.

Reagents

- 100mM Phosphate Buffer (pH 6.5)
- Reduced GSH (1 mM; pH = 6.5)
- Mix 5.0 ml of distilled alcohol with 61 mg of CDNB (1 mM CDNB)

Procedure

Table 5.3: Method for estimating GST activity

Reagents	Blank (ml)	Test (ml)
Buffer	1	1
DDW	1.65	1.55
GSH	0.3	0.3
Sample	-	0.1
CDNB	0.05	0.05

Following the addition of the aforementioned chemicals, absorbance was measured from 1 minute to 5 minutes at 240 nm.

5.7 Estimation of lipid peroxidation (LPO)

To estimate the level of LPO, we used the procedure outlined by Beuge and Aust (1978) (359).

Principle

Polyunsaturated fatty acids (PUFAs) can be damaged by peroxidation due to free radicals, mainly by OH^- and O_2^-. MDA, a byproduct of LPO, undergoes a reaction with thiobarbituric acid (TBA) resulting in the formation of a complex that exhibits an absorption peak at 535 nm.

Reagents

- 150mM Tris-HCl buffer(pH=7.1)
- Tris-HCl buffer (150 mM; pH=7.1)
- Ascorbic acid (1.5 mM)
- 10% trichloroacetic acid; 1 mM FeSO4
- TBA (pH=7), 0.375%

Procedure

Table 5.4: Method of estimating LPO

Reagent	Blank (ml)	Test (ml)
Tris-HCl buffer	0.1	0.1
FeSO$_4$	0.1	0.1
Ascorbic acid	0.1	0.1
DDW	0.7	0.6
Sample	-	0.1
Let the mixture incubate at 37°C for 15 minutes, and then halt the reaction by introducing TCA and TBA.		
TCA	1	1
TBA	2	2

Once all the ingredients and test sample are mixed, place the mixture in a boiling water bath for 15 minutes. Then, let it cool and centrifuge for 10 minutes at 3000 rpm. Using the supernatant, absorbance measurements were made at 535 nm. After calculating the LPO concentration, the result was represented as n moles of MDA produced per millilitre.

5.8 Estimation of SOD activity

To estimate the activity of SOD in the cell homogenate, we followed the protocol described by Kono (1978) (360).

Principle

The fundamental mechanism underlying the experiment involves the reduction of the blue Tetrazolium dye Nitroblue to formazan, a process regulated by superoxide radicals. The auto-oxidation of hydroxylamine hydrochloride results in the production of these radicals. It prevents Nitro Blue Tetrazolium (NBT) from being decreased and mediated by hydroxylamine hydrochloride in addition to SOD. The degree of inhibition serves as a factor for measuring enzyme activity.

Reagents

- 0.1 mM EDTA with 50 mM sodium carbonate buffer (pH=10.8)
- 95% ethanol with 96μM NBT
- In DDW, add 0.6% Triton X-100
- Hydroxylamine HCl (20 mM; pH = 6.0)

Procedure

Table 5.5: Method of estimating SOD activity

Reagents	Blank (ml)	Test (ml)
Buffer	1.35	1.3
Hydroxylamine HCl	0.1	0.1
Triton X-100	0.1	0.1
NBT	0.5	0.5
	Allow the mixture to incubate for 2 min	
Sample	-	0.05

After mixing all the components and the test sample the entire mixture appeared blue in color. Afterwards, measure the absorbance at 560 nm, for a period of 30 seconds to 2 minutes. The half-maximal inhibition of NBT reduction at an enzyme concentration is known as a unit of enzyme activity.

5.9 In vivo animal studies

Rats, aged 7 weeks and weighing around 250g, were obtained from the Animal House Facility at Lovely Professional University, India (Protocol no: LPU/IAEC/2022/07). They were accommodated in groups of 6 and 8 individuals per cage within a room maintaining a 12/12-hour light/dark cycle and an ambient temperature fluctuating between 22 to 25°C. After a one-week acclimatization period, the rats were segregated into two dietary groups: one receiving a normal pellet diet (NPD) as controls and the other having HFD (58% fat, 25% protein, and 17% carbohydrate) ad libitum for a duration of 4 weeks.

On the 7th day, a solitary dose of STZ was given to the rats consuming the HFD. After another 7 days, blood glucose levels were measured, and rats with levels surpassing 250 mg/dl were classified as diabetic. Excision wounds were then created on the diabetic rats following a reported procedure, with the wound's initiation considered as day 0. Subsequently, from day 1 to day 14, the diabetic rats received the following treatments: HFD + Sinapic acid (low dose) and HFD + Sinapic acid (high dose). The composition and preparation of the HFD followed the procedure outlined by Gaikwad et al. (2010) (361). The test groups were orally administered with lower dose (20 mg/kg) and higher dose (40 mg/kg) of Sinapic acid (Fig 5.2) (Table 5.6).

5.9.1. Excision wound model

The animals underwent anesthesia administered with ketamine (70 mg/kg, i.p.) and xylazine (10 mg/kg, i.p.), after which the hair was cleaned from the dorsal thoracic region. Subsequently, excision wounds were generated by removing skin sections from the shaved area, resulting in wounds approximately 200 mm^2 in size. The entire wound remained exposed, with certain groups receiving daily drug administration over a period of 14 days. The measurement of wound size was conducted on the 3rd, 7th, and 14th days, and the percentage of wound closure was determined using the methodology outlined by Ahmed et al. (2018) (362).

Table 5.6: Animal grouping and diet plan

S. No.	Group Name	Diet + Dose and route of drug treatment	No. of animals
Group 1	Non-diabetic non-wounded control	NPD for 4 weeks + 0.5% CMC (p.o.) (Vehicle)	6
Group 2	Non-diabetic non-wounded control + Sinapic acid *per se*	NPD for 4 weeks + 40 mg/kg of Sinapic acid (p.o.)	6
Group 3	Non-diabetic wounded control	NPD for 4 weeks + 0.5% CMC (p.o.) (Vehicle)	6
Group 4	Non-diabetic wounded + Low dose of Sinapic acid	NPD for 4 weeks + 20 mg/kg of Sinapic acid (p.o.)	6
Group 5	Non-diabetic wounded + High dose of Sinapic acid	NPD for 4 weeks + 40 mg/kg of Sinapic acid (p.o.)	6
Group 6	Diabetic wounded control	HFD for 4 weeks + 40 mg/kg STZ (i.p) + 0.5% CMC (p.o.) (Vehicle)	8
Group 7	Diabetic wounded + Low dose of Sinapic acid	HFD for 4 weeks + 40 mg/kg STZ (i.p) + 20 mg/kg of Sinapic acid (p.o.)	8
Group 8	Diabetic wounded + High dose of Sinapic acid	HFD for 4 weeks + 40 mg/kg STZ (i.p) + 40 mg/kg of Sinapic acid (p.o.)	8

Total	54

*NPD = Normal Pellet Diet; **HFD = High Fat Diet; ***STZ = Streptozotocin
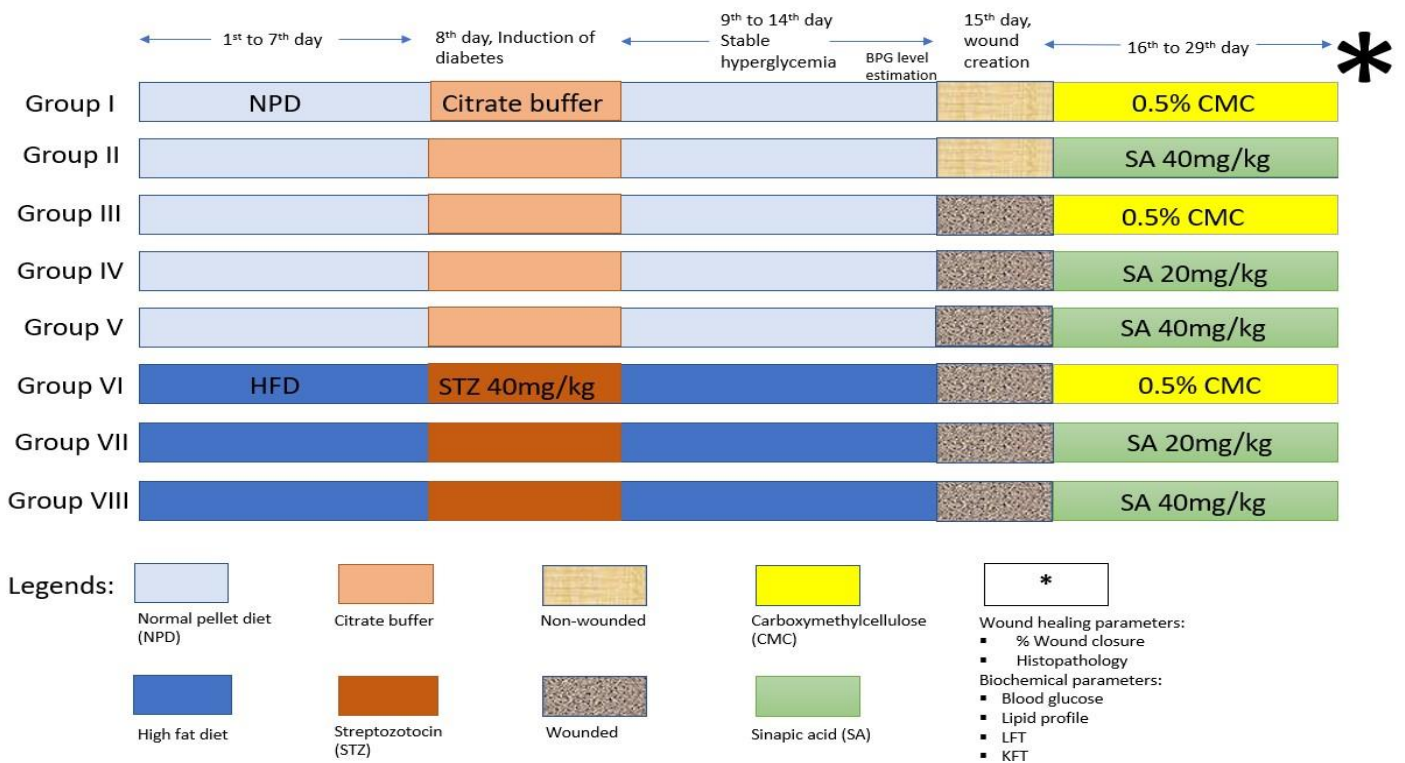
Fig 5.2: Representation of treatment schedule of different groups.

5.9.2. % Wound Closure

The determination of wound contraction percentage relied on the reduction percentage of the wound from its initial size. The assessment of wound closure percentage was performed on the 3rd, 7th, and 14th days.

Percentage wound closure = Wound area on day 0 - wound area on day (n) x 100

Wound area on day 0

where n = number of days (3, 7 and 14).

5.9.3. Parameter of evaluation

The following parameters were assessed at the conclusion of the research to determine the impact of the phytochemical treatment:

5.9.3.1. Bodyweight estimation

Prior to conducting in vivo research, the rats' body weights were estimated, and after the study began, body weights were tracked weekly.

5.9.3.2. Blood plasma glucose

With the use of the counter equipment Accu Check, rat's tail was used to extract 0.1 millilitre of blood for the blood glucose estimation.

5.9.3.3. Lipid profile test (LPT), Liver function test (LFT) and Renal profile test (RPT)

Total cholesterol, high density lipoprotein (HDL), low density lipoprotein (LDL), very low density lipoprotein (VLDL), and triglycerides are all components of lipid profiles. Liver profile constitutes total, direct and indirect bilirubin, serum glutamic oxaloacetic transaminase (SGOT), serum glutamic pyruvic transaminase (SGPT) and alkaline phosphatase (ALP) estimation. Serum uric acid, serum creatinine, and blood urea are examples of renal profiles. The clinical chemistry laboratory at Gargi Laboratory in Jalandhar employed a fully automated biochemistry and electrolyte analyzer (which includes testing for lithium) as well as an ELISA system for conducting these tests.

Protocol

- Blood samples were obtained using the retro-orbital technique after the animals had fasted for 12 hours.
- The samples were placed in tubes coated with heparin. In a centrifuge, serum and blood were separated by centrifugation at 300 x g.
- The serum was transferred to the Gargi laboratory in Jalandhar for a lipid, renal, and liver profile after being kept at 4°C.

5.9.4. Oxidative biomarkers

At the culmination of the study on the final day of care, animals designated for biochemical investigations were humanely euthanized via cervical dislocation. Subsequently, tissues were extracted and homogenized to create a 10% (w/v) tissue homogenate in 0.1 M phosphate buffer (pH 7.4). The clear supernatant that was left over after centrifugation for 15 minutes at 3000 rpm was employed in a number of biochemical analyses to determine the amount of GST, LPO, GSH, SOD and catalase. The methodology for assessing GST, LPO, SOD, and catalase was previously explained in the in vitro evaluation of antioxidant enzymes. While the GSH experiment relies on the interaction between GSH and DTNB (also referred to as Ellman's reagent), resulting in the formation of the TNB chromophore. This chromophore displays its highest absorbance at 412 nm, and the assay determines the concentration of GSH in the sample by measuring the rate of TNB formation at this wavelength. Additionally, the oxidized GSH–TNB adduct (GS–TNB) is formed. Following this, GSH reductase, in the presence of NADPH, reduces the disulfide product (GS–TNB), efficiently recycling GSH back into the reaction (363).

5.9.5. Histopathology

After euthanasia and decapitation, rats underwent dissection, and the skin surrounding the wound sites was immediately removed and preserved in 10% neutral buffered formalin for 48 hours. The fixed skin from each rat was subjected to wax blocking and sectioning. Sections, cut at a thickness of 5 μm using a microtome, underwent processing through a xylene alcohol-series and were stained with alum

hematoxylin and eosin (H&E). Microscopic examination of the sections was performed to evaluate histopathological changes, following the procedure outlined by Ahmed et al. (2017) (362).

5.10. SIRT1 assay

Principle

The wells were pre-coated with an anti-SIRT1/SIR2L1 antibody, which immobilized any SIRT1/SIR2L1 present in standards and samples. Following the removal of any unbound substances, a biotin-conjugated antibody that specifically targets SIRT1/SIR2L1 was added to the wells. Subsequently, the microplate was filled with horseradish peroxidase (HRP) coupled with avidin. After rinsing off any unbound avidin-enzyme reagent, a substrate solution was applied to the wells. The development of color was directly proportional to the quantity of SIRT1/SIR2L1 initially bound. The color development process was then terminated, and its intensity was measured. The experiment was conducted following the instructions outlined in the SIRT1 kit.

Procedure

- Pour 100µl of the standard and sample into each well and applied a covering using the included adhesive strip. Incubated for two hours at 37 °C.
- Discarded each well's contents without cleaning.
- Poured 100µl of Biotin-antibody (1x) into each well and incubated for an hour at 37 °C.
- Took out everything and gave it three thorough washing. Using a squirt bottle, added 200µl of Wash Buffer to each well and let it stand for two minutes before washing.
- Following the final wash, remove any residual wash buffer by aspiration or decantation.
- Repeated washing five times.
- Filled each well with 100µl of HRP-avidin (1x).
- Incubated for one hour at 37 °C.
- After adding 90µl of TMB substrate to each well and covering them from the light, we incubated them at 37°C for 15 to 30 minutes.
- Next, 50µl of Stop Solution was added.
- Within a five-minute timeframe, assess the optical density of each well using a microplate reader configured to 450 nm.

5.11. Statistical analysis

The mean ± SEM of all the data was expressed. Behavioral and biochemical data statistics were analyzed using Sigma Stat software. Initially, a one-way analysis of variance (ANOVA) was conducted, followed by a Tukey test. Differences were considered statistically significant at the 5% level of significance ($p < 0.05$).

CHAPTER 6
RESULTS

6.1. Data mining and similarity searching

Over the past several decades, it has been established that the goal of drug discovery is to develop new molecules with certain chemical characteristics that may have the potential to treat a variety of diseases. Drug discovery largely depends on the assumption of molecular similarity, which has often been employed in the development of new compounds. It relies on the idea that two molecules with similar structural features often exhibit similar physical characteristics and biological functions. Utilizing two-dimensional similarity in molecular analysis has been employed to improve the effectiveness and kinetics of lead compounds by exploring the correlation between their structure and biological activities (364). Recently there has been an emphasis on the creation of techniques to represent and contrast small molecule conformations in three dimensions for molecular target prediction, drug repurposing, and scaffold hopping. Due to the declining frequency of new drug approvals and rising costs, new drug innovation is facing significant difficulties. This situation has encouraged us to develop a revolutionary integrated drug discovery strategy, where Ayurvedic knowledge can work together with drug development from plant sources. Identification of suitable candidate plants using Ayurvedic knowledge, historical recorded use, tribal undocumented use, and extended literature search should be the first step in developing novel plant-based medicines (365, 366).

Considering all the above factors and the statement that **"similar structures have similar biological activities"**, we conducted an extensive literature search to identify potential phytochemicals that have previously been shown to improve delayed wound healing associated with diabetes. To accomplish this, we begin with successful data mining by structural similarity search and molecular docking by Autodock vina. The results obtained from the similarity search were run on AutoDock vina with the goal of identifying the potential of the docked molecule with target protein in improving diabetic wounds in terms of binding energy. The outcomes associated with the most favourable binding energy will undergo assessment regarding ADME. The objective of this assessment is to ascertain whether the molecule with the highest binding energy in the docking process meets the criteria as a promising drug candidate for diabetic wound treatment. Following a thorough examination of results from previously published reports primarily centered on diabetes and wound healing, a total of 16 chemical compounds were scrutinized to identify potential candidates for further investigation through in silico, in vitro, and in vivo studies. The names of these chemical compounds are **Quercetin, Resveratrol, Ellagic acid, Naringenin, Baicalein, Glabridin, Naringin, Capsaicin, Diosgenin, Amygdalin, Kaempferol, Ferulic acid, Vanillic acid, Coumaric acid, Apigenin, and Genistein.** In this study, we used various tools such as ChEMBL, NCBI, PubChem, ChemSpider, and Drug Bank to search for similar structures of these compounds one by one, and the below-attached tables shows the similar structures of the above-mentioned compounds:
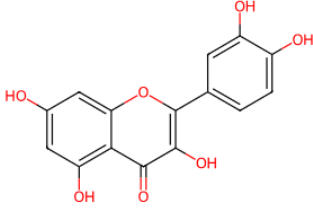
Table 6.1: Compounds similar to Quercetin
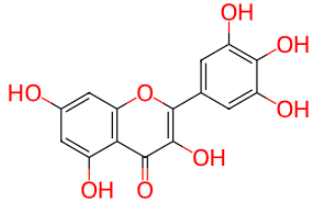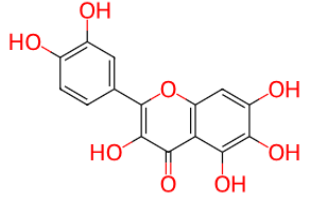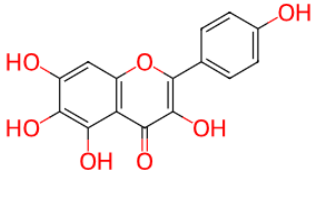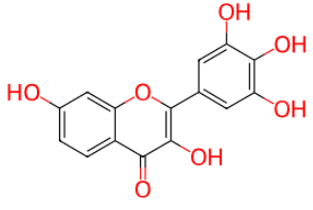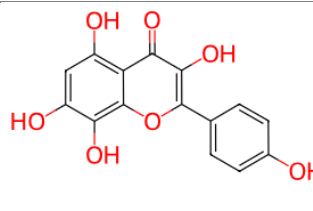
Chemical compound	IUPAC Name	ChEMBL ID	Chemical structure	Similarity index
Quercetin (Parent compound)	"2-(3,4-dihydroxyphenyl)-3,5,7-trihydroxychromen-4-one"	CHEMBL50		
Myricetin	"3,5,7-trihydroxy-2-(3,4,5-trihydroxyphenyl)chromen-4-one"	CHEMBL164		99.53
Quercetagetin	"2-(3,4-dihydroxyphenyl)-3,5,6,7-tetrahydroxychromen-4-one"	CHEMBL413552		98.88
Gossypetin	"2-(3,4-dihydroxyphenyl)-3,5,7,8-tetrahydroxychromen-4-one"	CHEMBL253570		98.70
6-Hydroxykaempferol	"3,5,6,7-tetrahydroxy-2-(4-hydroxyphenyl)chromen-4-one"	CHEMBL455504		97.86
Robinetin	"3,7-dihydroxy-2-(3,4,5-trihydroxyphenyl)chromen-4-one"	CHEMBL170405		97.76
Herbacetin	"3,5,7,8-tetrahydroxy-2-(4-hydroxyphenyl)chromen-4-one"	CHEMBL611029		97.68

Table 6.2: Compounds similar to Resveratrol
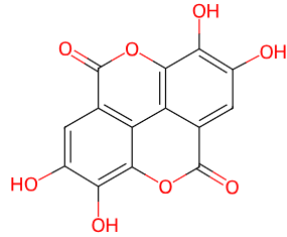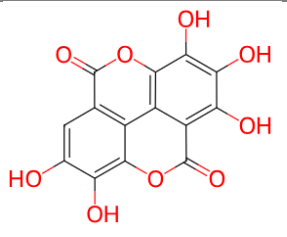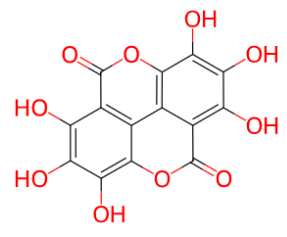
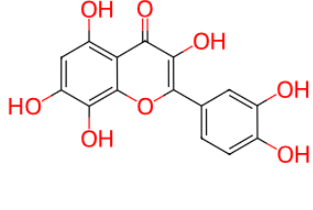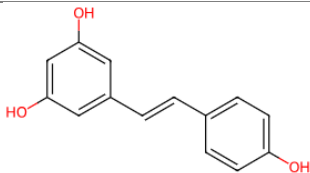| Chemical compound	IUPAC Name	ChEMBL ID	Chemical structure	Similarity index
Resveratrol (Parent compound)	"5-[(*E*)-2-(4-hydroxyphenyl)ethenyl]benzene-1,3-diol"	CHEMBL165		
Pinosylvin	"5-[(*E*)-2-phenylethenyl]benzene-1,3-diol"	CHEMBL101506		83.57

Table 6.3: Compounds similar to Ellagic acid

Chemical compound	IUPAC Name	ChEMBL ID	Chemical structure	Similarity index
Ellagic acid (Parent compound)	"6,7,13,14-tetrahydroxy-2,9-dioxatetracyclo[6.6.2.0^{4,16}.0^{11,15}]hexadeca-1(15),4,6,8(16),11,13-hexaene-3,10-dione"	CHEMBL6246		
Flavellagic acid	"3,5,6,10,13-pentahydroxy-2,9-dioxatetracyclo[6.6.2.0^{4,16}.0^{11,15}]hexadeca-1(15),3,5,8(16),10,12-hexaene-7,14-dione"	CHEMBL1688543		96.52
Coruleoellagic acid	"3,5,6,10,12,13-hexahydroxy-2,9-dioxatetracyclo[6.6.2.0^{4,16}.0^{11,15}]hexadeca-1(15),3,5,8(16),10,12-hexaene-7,14-dione"	CHEMBL1688544		96.13
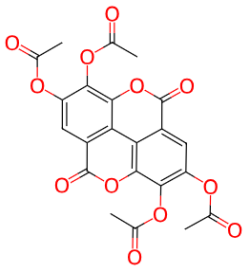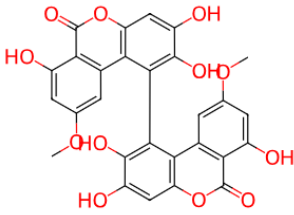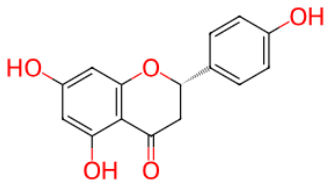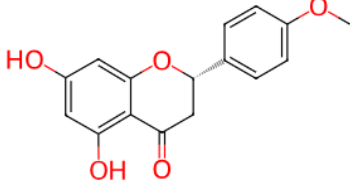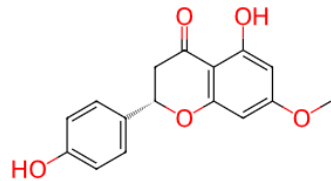
Ellagic acid tetraacetate	"(7,13,14-triacetyloxy-3,10-dioxo-2,9-dioxatetracyclo[6.6.2.$0^{4,16}.0^{11,15}$]hexadeca-1(15),4,6,8(16),11,13-hexaen-6-yl) acetate"	CHEMBL244617		88.57
Verrulactone A	"2,3,7-trihydroxy-9-methoxy-1-(2,3,7-trihydroxy-9-methoxy-6-oxobenzo[c]chromen-1-yl)benzo[c]chromen-6-one"	CHEMBL2011360		87.81

Table 6.4: Compounds similar to Naringenin

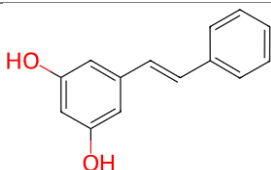| Chemical compound	IUPAC Name	ChEMBL ID	Chemical structure	Similarity index
Naringenin (Parent compound)	"(2*S*)-5,7-dihydroxy-2-(4-hydroxyphenyl)-2,3-dihydrochromen-4-one"	CHEMBL9352		
Isosakuranetin	"(2*S*)-5,7-dihydroxy-2-(4-methoxyphenyl)-2,3-dihydrochromen-4-one"	CHEMBL470266		97.15
Sakuranetin	"(2*S*)-5-hydroxy-2-(4-hydroxyphenyl)-7-methoxy-2,3-dihydrochromen-4-one"	CHEMBL448297		95.84
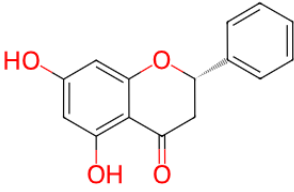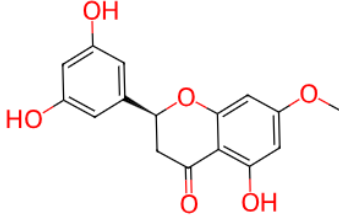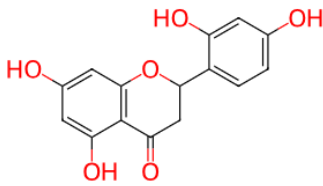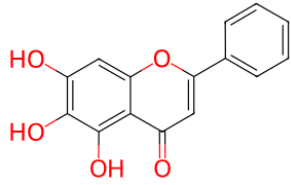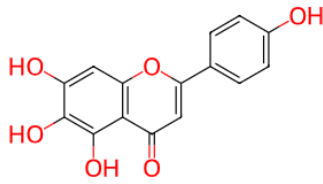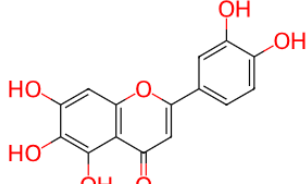
Pinocembrin	"(2S)-5,7-dihydroxy-2-phenyl-2,3-dihydrochromen-4-one"	CHEMBL399910		95.76
Blumeatin	"(2S)-2-(3,5-dihydroxyphenyl)-5-hydroxy-7-methoxy-2,3-dihydrochromen-4-one"	CHEMBL2037158		94.97
Steppogenin	"(2S)-2-(2,4-dihydroxyphenyl)-5,7-dihydroxy-2,3-dihydrochromen-4-one"	CHEMBL465194		94.22

Table 6.5: Compounds similar to Baicalein

Chemical compound	IUPAC Name	ChEMBL ID	Chemical structure	Similarity index
Baicalein (Parent compound)	"5,6,7-trihydroxy-2-phenylchromen-4-one"	CHEMBL8260		
Scutellarein	"5,6,7-trihydroxy-2-(4-hydroxyphenyl)chromen-4-one"	CHEMBL55415		98.9
6-Hydroxyluteolin	"2-(3,4-dihydroxyphenyl)-5,6,7-trihydroxychromen-4-one"	CHEMBL464107		97.45
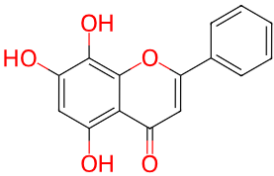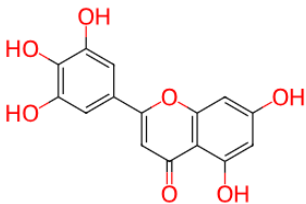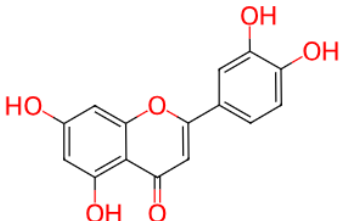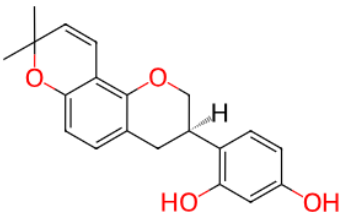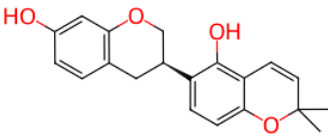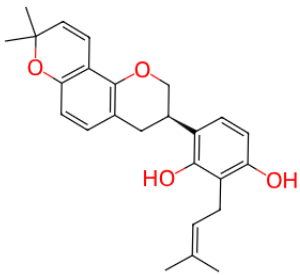
Norwogonin	"5,7,8-trihydroxy-2-phenylchromen-4-one"	CHEMBL485250		97.26
Tricetin	"5,7-dihydroxy-2-(3,4,5-trihydroxyphenyl)chromen-4-one"	CHEMBL247484		97.23
Luteolin	"2-(3,4-dihydroxyphenyl)-5,7-dihydroxychromen-4-one"	CHEMBL151		96.05

Table 6.6: Compounds similar to Glabridin

Chemical compound	IUPAC Name	ChEMBL ID	Chemical structure	Similarity index
Glabridin (Parent compound)	"4-[(3*R*)-8,8-dimethyl-3,4-dihydro-2*H*-pyrano[2,3-f]chromen-3-yl]benzene-1,3-diol"	CHEMBL480477		
Phaseollinisoflavan	"6-[(3*R*)-7-hydroxy-3,4-dihydro-2*H*-chromen-3-yl]-2,2-dimethylchromen-5-ol"	CHEMBL465812		94.39
Hispaglabridin A	"4-[(3*R*)-8,8-dimethyl-3,4-dihydro-2*H*-pyrano[2,3-f]chromen-3-yl]-2-(3-methylbut-2-enyl)benzene-1,3-diol"	CHEMBL464581		92.73
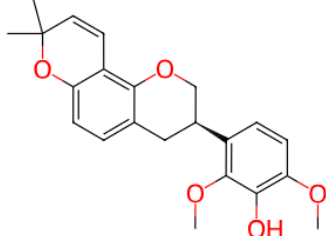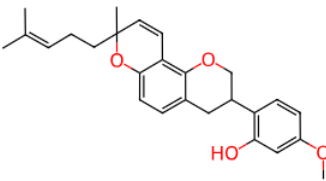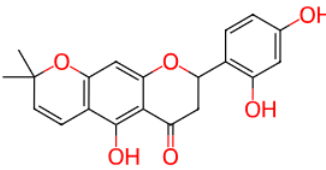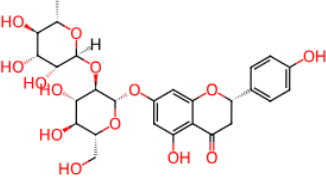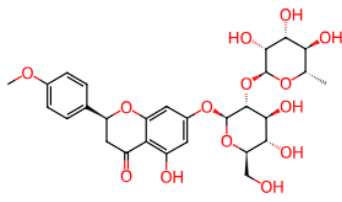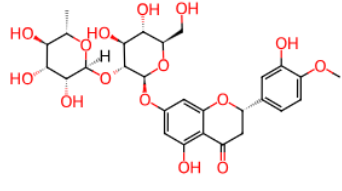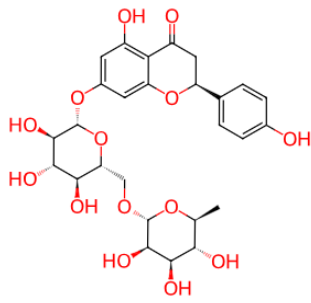
Glyasperin H	"3-[(3R)-8,8-dimethyl-3,4-dihydro-2H-pyrano[2,3-f]chromen-3-yl]-2,6-dimethoxyphenol"	CHEMBL49872 5		91.89
Heminitidulan	"5-methoxy-2-[8-methyl-8-(4-methylpent-3-enyl)-3,4-dihydro-2H-pyrano[2,3-f]chromen-3-yl]phenol"	CHEMBL51667 2		89.78
Dalenin	"8-(2,4-dihydroxyphenyl)-5-hydroxy-2,2-dimethyl-7,8-dihydropyrano[3,2-g]chromen-6-one"	CHEMBL21471 65		89.05

Table 6.7: Compounds similar to Naringin

Chemical compound	IUPAC Name	ChEMBL ID	Chemical structure	Similarity index
Naringin (Parent compound)	"(2S)-7-[(2S,3R,4S,5S,6R)-4,5-dihydroxy-6-(hydroxymethyl)-3-[(2S,3R,4R,5R,6S)-3,4,5-trihydroxy-6-methyloxan-2-yl]oxyoxan-2-yl]oxy-5-hydroxy-2-(4-hydroxyphenyl)-2,3-dihydrochromen-4-one"	CHEMBL45153 2		

Poncirin	"(2S)-7-[(2S,3R,4S,5S,6R)-4,5-dihydroxy-6-(hydroxymethyl)-3-[(2S,3R,4R,5R,6S)-3,4,5-trihydroxy-6-methyloxan-2-yl]oxyoxan-2-yl]oxy-5-hydroxy-2-(4-methoxyphenyl)-2,3-dihydrochromen-4-one"	CHEMBL45105 0		99.4
Neohesperi din	"(2S)-7-[(2S,3R,4S,5S,6R)-4,5-dihydroxy-6-(hydroxymethyl)-3-[(2S,3R,4R,5R,6S)-3,4,5-trihydroxy-6-methyloxan-2-yl]oxyoxan-2-yl]oxy-5-hydroxy-2-(3-hydroxy-4-methoxyphenyl)-2,3-dihydrochromen-4-one"	CHEMBL50639 8		98.8
Narirutin	"(2S)-5-hydroxy-2-(4-hydroxyphenyl)-7-[(2S,3R,4S,5S,6R)-3,4,5-trihydroxy-6-[[(2R,3R,4R,5R,6S)-3,4,5-trihydroxy-6-methyloxan-2-yl]oxymethyl]oxan-2-yl]oxy-2,3-	CHEMBL44624 6		97.8
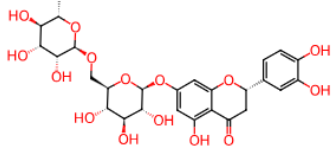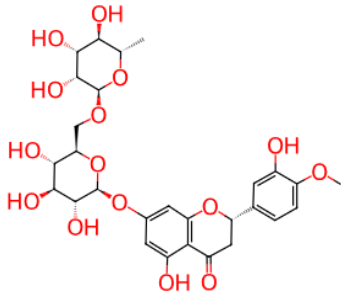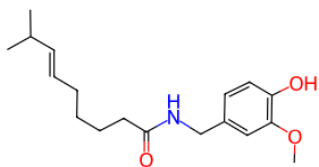
	dihydrochromen-4-one"			
Eriocitrin	"(2*S*)-2-(3,4-dihydroxyphenyl)-5-hydroxy-7-[(2*S*,3*R*,4*S*,5*S*,6*R*)-3,4,5-trihydroxy-6-[[(2*R*,3*R*,4*R*,5*R*,6*S*)-3,4,5-trihydroxy-6-methyloxan-2-yl]oxymethyl]oxan-2-yl]oxy-2,3-dihydrochromen-4-one"	CHEMBL2165586		97.4
Hesperidin	"(2*S*)-5-hydroxy-2-(3-hydroxy-4-methoxyphenyl)-7-[(2*S*,3*R*,4*S*,5*S*,6*R*)-3,4,5-trihydroxy-6-[[(2*R*,3*R*,4*R*,5*R*,6*S*)-3,4,5-trihydroxy-6-methyloxan-2-yl]oxymethyl]oxan-2-yl]oxy-2,3-dihydrochromen-4-one"	CHEMBL449317		96.7

Table 6.8: Compounds similar to Capsaicin

Chemical compound	IUPAC Name	ChEMBL ID	Chemical structure	Similarity index
Capsaicin (Parent compound)	"(*E*)-*N*-[(4-hydroxy-3-methoxyphenyl)methy	CHEMBL294199		
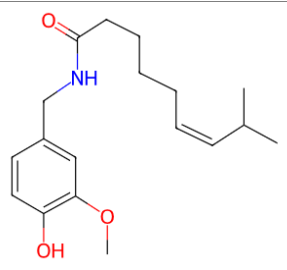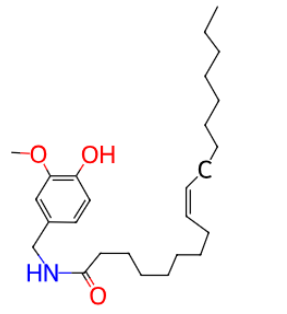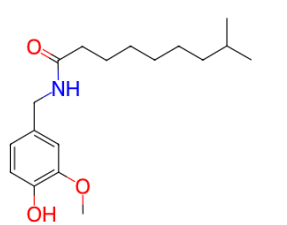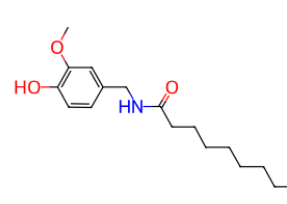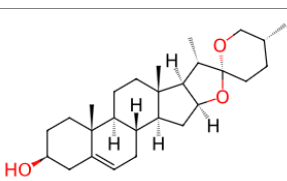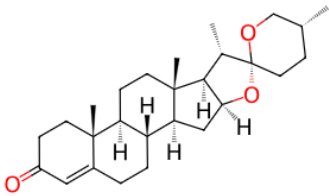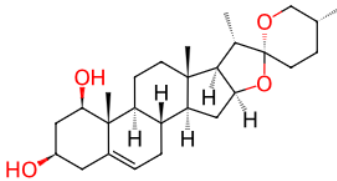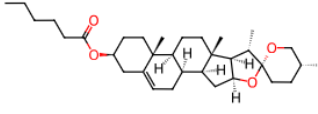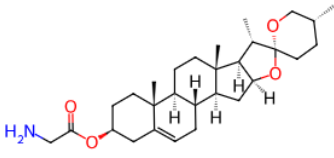
	l]-8-methylnon-6-enamide"			
Zucapsaicin	"(Z)-N-[(4-hydroxy-3-methoxyphenyl)methyl]-8-methylnon-6-enamide"	CHEMBL313971		100
Olvanil	"(Z)-N-[(4-hydroxy-3-methoxyphenyl)methyl]octadec-9-enamide"	CHEMBL76903		87.2
Dihydrocapsaicin	"N-[(4-hydroxy-3-methoxyphenyl)methyl]-8-methylnonanamide"	CHEMBL311158		86.7
Nonivamide	"N-[(4-hydroxy-3-methoxyphenyl)methyl]nonanamide"	CHEMBL75124		82.7

Table 6.9: Compounds similar to Diosgenin

Chemical compound	IUPAC Name	ChEMBL ID	Chemical structure	Similarity index
Diosgenin (Parent compound)	"(1S,2S,4S,5'R,6R,7S,8R,9S,12S,13R,16S)-5',7,9,13-tetramethylspiro[5-oxapentacyclo[10.8.0.0^{2,9}.0^{4,8}.0^{13,18}]icos-18-ene-6,2'-oxane]-16-ol"	CHEMBL412437		

Diosgenone	"(1S,2S,4S,5'R,6R,7S,8R,9S,12S,13R)-5',7,9,13-tetramethylspiro[5-oxapentacyclo[10.8.0.0^{2,9}.0^{4,8}.0^{13,18}]icos-17-ene-6,2'-oxane]-16-one"	CHEMBL1915879		95.73
Ruscogenin	"(1S,2S,4S,5'R,6R,7S,8R,9S,12S,13R,14R,16R)-5',7,9,13-tetramethylspiro[5-oxapentacyclo[10.8.0.0^{2,9}.0^{4,8}.0^{13,18}]icos-18-ene-6,2'-oxane]-14,16-diol"	CHEMBL1169820		94.87
Caprospinol	"[(1S,2S,4S,5'R,6R,7S,8R,9S,12S,13R,16S)-5',7,9,13-tetramethylspiro[5-oxapentacyclo[10.8.0.0^{2,9}.0^{4,8}.0^{13,18}]icos-18-ene-6,2'-oxane]-16-yl]hexanoate"	CHEMBL2386881		94.67
Glycine Diosgenyl Ester	"[(1S,2S,4S,5'R,6R,7S,8R,9S,12S,13R,16S)-5',7,9,13-tetramethylspiro[5-oxapentacyclo[10.8.0.0^{2,9}.0^{4,8}.0^{13,18}]icos-18-ene-6,2'-oxane]-16-yl]2-aminoacetate"	CHEMBL2207420		93.23
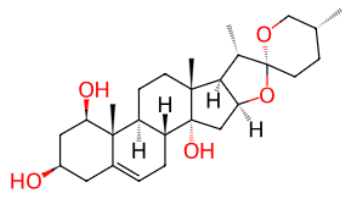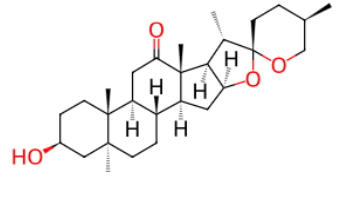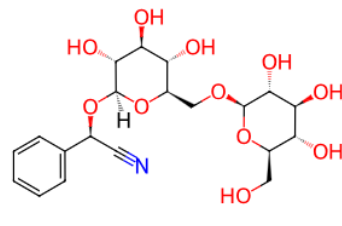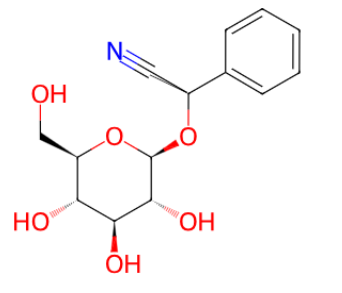
Chemical compound	IUPAC Name	ChEMBL ID	Chemical structure	Similarity index
Namogenin B	"(1R,2R,4S,5'R,6R,7S,8R,9R,12S,13R,14R,16R)-5',7,9,13-tetramethylspiro[5-oxapentacyclo[10.8.0.0^{2,9}.0^{4,8}.0^{13,18}]icos-18-ene-6,2'-oxane]-2,14,16-triol"	CHEMBL458574		93.2
Hecogenin	"(1R,2S,4S,5'R,6R,7S,8R,9S,12S,13S,16S,18S)-16-hydroxy-5',7,9,13-tetramethylspiro[5-oxapentacyclo[10.8.0.0^{2,9}.0^{4,8}.0^{13,18}]icosane-6,2'-oxane]-10-one"	CHEMBL44125		91.36

Table 6.10: Compounds similar to Amygdalin

Chemical compound	IUPAC Name	ChEMBL ID	Chemical structure	Similarity index
Amygdalin (Parent compound)	"(2R)-2-phenyl-2-[(2R,3R,4S,5S,6R)-3,4,5-trihydroxy-6-[[(2R,3R,4S,5S,6R)-3,4,5-trihydroxy-6-(hydroxymethyl)oxan-2-yl]oxymethyl]oxan-2-yl]oxyacetonitrile"	CHEMBL461727		
Prunasin	"(2R)-2-phenyl-2-[(2R,3R,4S,5S,6R)-3,4,5-trihydroxy-6-(hydroxymethyl)oxan-2-yl]oxyacetonitrile"	CHEMBL1778417		90.1
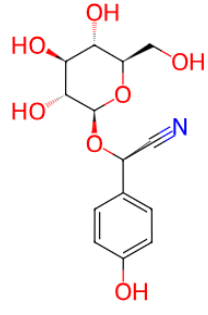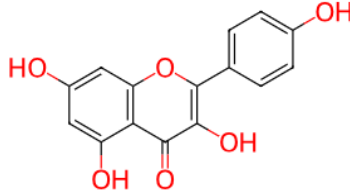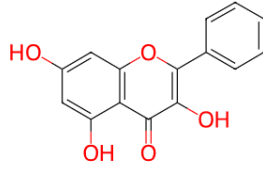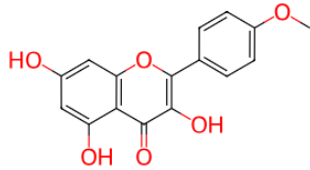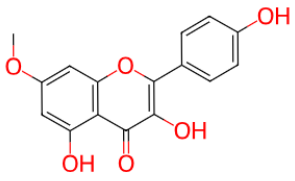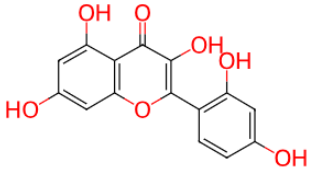
Taxiphyllin	"(2R)-2-(4-hydroxyphenyl)-2-[(2R,3R,4S,5S,6R)-3,4,5-trihydroxy-6-(hydroxymethyl)oxan-2-yl]oxyacetonitrile"	CHEMBL469825		88.64

Table 6.11: Compounds similar to Kaempferol

Chemical compound	IUPAC Name	ChEMBL ID	Chemical structure	Similarity index
Kaempferol (Parent compound)	"3,5,7-trihydroxy-2-(4-hydroxyphenyl)chromen-4-one"	CHEMBL150		
Galangin	"3,5,7-trihydroxy-2-phenylchromen-4-one"	CHEMBL309490		98.5
Kaempferide	"3,5,7-trihydroxy-2-(4-methoxyphenyl)chromen-4-one"	CHEMBL40919		98.4
Rhamnocitrin	"3,5-dihydroxy-2-(4-hydroxyphenyl)-7-methoxychromen-4-one"	CHEMBL442289		97.3
Morin	"2-(2,4-dihydroxyphenyl)-3,5,7-trihydroxychromen-4-one"	CHEMBL28626		97.2
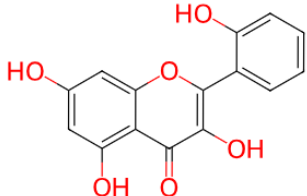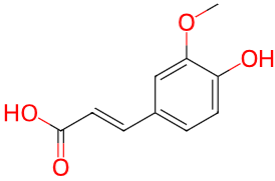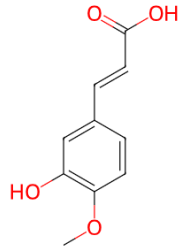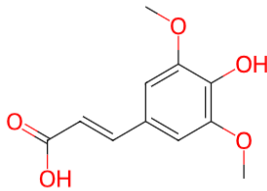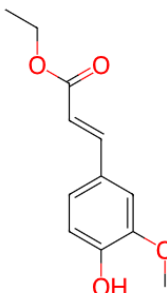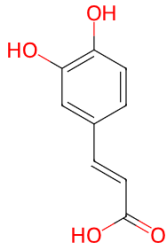
| Datiscetin | "3,5,7-trihydroxy-2-(2-hydroxyphenyl)chromen-4-one" | CHEMBL503168 | | 96.4 |

Table 6.12: Compounds similar to Ferulic acid

Chemical compound	IUPAC Name	ChEMBL ID	Chemical structure	Similarity index
Ferulic acid (Parent compound)	"(*E*)-3-(4-hydroxy-3-methoxyphenyl)prop-2-enoic acid"	CHEMBL32749		
Isoferulic acid	"(*E*)-3-(3-hydroxy-4-methoxyphenyl)prop-2-enoic acid"	CHEMBL233295		98
Sinapic acid	"(*E*)-3-(4-hydroxy-3,5-dimethoxyphenyl)prop-2-enoic acid"	CHEMBL109341		94
Ethyl ferulate	"ethyl (*E*)-3-(4-hydroxy-3-methoxyphenyl)prop-2-enoate"	CHEMBL286796		90
3,4-dihydroxyc inna mic acid	"(*E*)-3-(3,4-dihydroxyphenyl)prop-2-enoic acid"	CHEMBL145		88
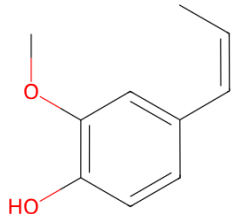
Isoeugenol	"2-methoxy-4-[(E)-prop-1-enyl]phenol"	CHEMBL44520 6		79

Table 6.13: Compounds similar to Vanillic acid
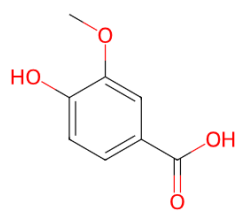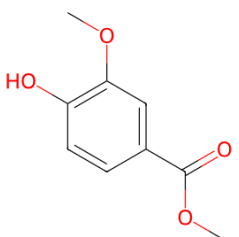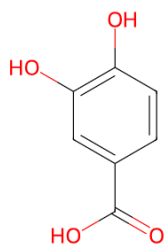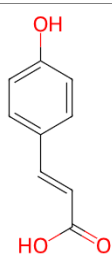
Chemical compound	IUPAC Name	ChEMBL ID	Chemical structure	Similarity index
Vanillic acid (Parent compound)	"4-hydroxy-3-methoxybenzoic acid"	CHEMBL12056 8		
Methyl vanillate	"methyl 4-hydroxy-3-methoxybenzoate"	CHEMBL48621 4		89
Protocatehuic acid	"3,4-dihydroxybenzoic acid"	CHEMBL37537		84

Table 6.14: Compounds similar to Coumaric acid

Chemical compound	IUPAC Name	ChEMBL ID	Chemical structure	Similarity index
Coumaric acid (Parent compound)	"(E)-3-(4-hydroxyphenyl)prop-2-enoic acid"	CHEMBL66879		
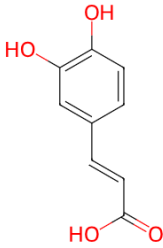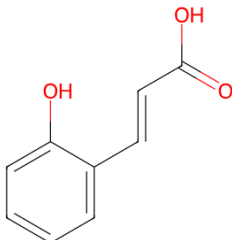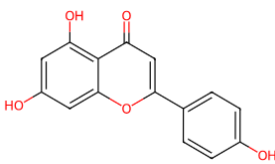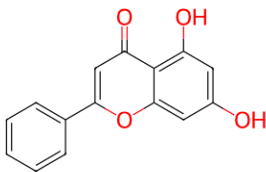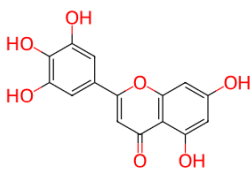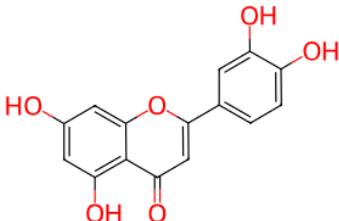
| Caffeic Acid | "(E)-3-(3,4-dihydroxyphenyl)prop-2-enoic acid" | CHEMBL145 | | 87 |
| o-Coumaric acid | "(E)-3-(2-hydroxyphenyl)prop-2-enoic acid" | CHEMBL52564 | | 83 |

Table 6.15: Compounds similar to Apigenin

Chemical compound	IUPAC Name	ChEMBL ID	Chemical structure	Similarity index
Apigenin (Parent compound)	"5,7-dihydroxy-2-(4-hydroxyphenyl)chromen-4-one"	CHEMBL28		
Chrysin	"5,7-dihydroxy-2-phenylchromen-4-one"	CHEMBL117		98
Tricetin	"5,7-dihydroxy-2-(3,4,5-trihydroxyphenyl)chromen-4-one"	CHEMBL247484		93
Luteolin	"2-(3,4-dihydroxyphenyl)-5,7-dihydroxychromen-4-one"	CHEMBL151		93
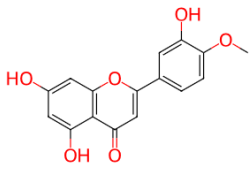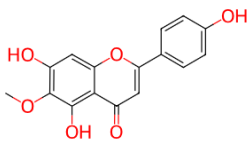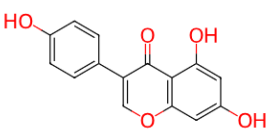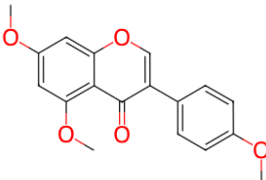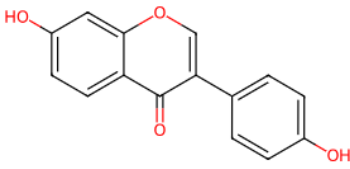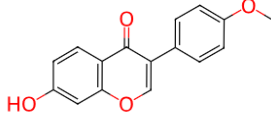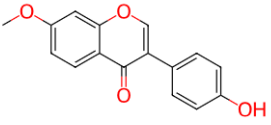
| Diosmetin | "5,7-dihydroxy-2-(3-hydroxy-4-methoxyphenyl)chromen-4-one" | CHEMBL90568 | | 89 |
| Hispidulin | "5,7-dihydroxy-2-(4-hydroxyphenyl)-6-methoxychromen-4-one" | CHEMBL293776 | | 87 |

Table 6.16: Compounds similar to Genistein

Chemical compound	IUPAC Name	ChEMBL ID	Chemical structure	Similarity index
Genistein (Parent compound)	"5,7-dihydroxy-3-(4-hydroxyphenyl)chromen-4-one"	CHEMBL44		
Biochanin A	"5,7-dihydroxy-3-(4-methoxyphenyl)chromen-4-one"	CHEMBL13097		96
Daidzein	"7-hydroxy-3-(4-hydroxyphenyl)chromen-4-one"	CHEMBL8145		94
Formononetin	"7-hydroxy-3-(4-methoxyphenyl)chromen-4-one"	CHEMBL242341		91
Isoformononetin	"3-(4-hydroxyphenyl)-7-methoxychromen-4-one"	CHEMBL453280		89

NATURAL EPIGENETIC MODIFIERS

- QUERCETIN
- RESVERATROL
- ELLAGIC ACID
- NARINGENIN
- BAICALEIN
- GLABRIDIN
- NARINGIN
- CAPSAICIN
- DISOGENIN
- AMYGDALIN
- KAEMPFEROL
- FERULIC ACID
- VANILLIC ACID
- COUMARIC ACID
- APIGENIN
- GENISTEIN

SEARCH FOR SIMILAR COMPOUNDS WITH 80% SIMILAR INDEX →

DOCKING WITH CRYSTAL STRUCTURE OF SIRT1 PROTEIN
↓
REDOCKED PROTEIN WITH INBOUND LIGAND TO STANDARDISE DOCKING SOFTWARE TO ENSURE IT BOUNDS IN THE SIMILAR MANNER
↓
COMPARE BINDING ENERGIES OF ALL SIMILAR MOLECULES
↓
SIMILAR MOLECULES HAD NEARLY THE SAME BINDING ENERGIES WITH THEIR PARENT COMPOUND

Fig 6.1: Natural SIRT1 molecules selected for in silico evaluation.

6.2 Molecular docking

After a thorough evaluation of the literature, we found a total of 16 natural molecules that may have the potential to reduce delayed wound healing. Subsequently, the selected molecules were processed in various databases to search for their similar compounds. These compounds were then combined with the ligand binding domain of SIRT1 protein (PDB ID: 4ZZJ) using the AutoDock Vina program, which screened for potent molecules based on their binding energy. So, first, we docked the SIRT1 protein (PDB ID: 4ZZJ) with the standard ligand (4TQ) bound to it. The docking of standard ligand (4TQ) with SIRT1 protein (PDF ID: 4ZZJ) showed the binding energy of -8.0 kcal/mol with GLU477, PHE474, ARG649, GLU467, PRO468, LEU469, PRO470, VAL657, and ARG274 as interacting amino acids.

The docking of Quercetin (parent compound) with SIRT1 protein (PDB ID: 4ZZJ) showed the binding energy of -7.5 kcal/mol with ARG274, VAL657, SER442, PRO468, LYS444, LEU469 as interacting amino acids, with two hydrogen bonds formation. Next, we sought to dock the compounds similar to quercetin with SIRT1 protein (PDB ID: 4ZZJ). For instance, the docking of Gossypetin with protein 4ZZJ showed the binding energy of -7.5 kcal/mol with VAL657, ARG274, LYS444, PRO468, LEU469, SER442 as an interacting amino acid, whereas -7.5 kcal/mol of binding energy and LEU469, PRO468, HIS471, LYS444, ARG274, VAL657 amino acids were observed when Herbacetin was docked with this SIRT1 protein 4ZZJ. The molecular docking of

Gossypetin and Herbacetin with 4ZZJ leads to the formation of two hydrogen bonds. In addition, the docking of Myricetin and 6-hydoxykaempferol showed a similar binding energy of -7.2 kcal/mol. When Myricetin was docked with 4ZZJ protein, only one hydrogen bond formation was reported, whereas two hydrogen bonds formation were reported upon docking of 6-hydroxykaempferol with SIRT1 protein 4ZZJ. The docking of Myricetin and 6-hydroxykaempferol with 4ZZJ protein nearly had different interacting amino acid residues such as ARG274, VAL657, LYS444, SER442, PRO468, LEU469, and VAL657, ARG274, GLU467, PRO468, HIS471, LEU469 respectively. On the contrary, docking of Quercetagetin and Robinetin with SIRT1 protein (PDB ID: 4ZZJ) almost had similar binding energies of -7.1 kcal/mol, whereas they have been reported to have different interacting amino acids and hydrogen bonds. For instance, interacting amino acid residues such as ARG199, LEU202, LYS203, THR209, ILE210 were observed when Quercetagetin was docked with 4ZZJ protein, whereas GLU477, ARG649, PRO468, PRO470, HIS473, and PHE474 amino acids and one hydrogen bond formation was observed when Robinetin was docked with SIRT1 protein 4ZZJ.

The docking of Resveratrol (parent compound) with SIRT1 protein (PDB ID: 4ZZJ) showed the binding energy of -6.8 kcal/mol with SER453, LYS233, ARG234, HIS473, LEU472, HIS471 as interacting amino acids, and only one hydrogen bond formation. Next, we sought to dock the compounds similar to resveratrol with SIRT1 protein (PDB ID: 4ZZJ). For instance, the docking of Pinosylvin with SIRT1 protein 4ZZJ showed the binding energy of -6.8 kcal/mol with SER453, ARG234, HIS473, LEU472, HIS471, LYS233, with one hydrogen bond formation.

After analyzing the binding energies of quercetin and resveratrol, we evaluate the binding energy of parent compound Ellagic acid, followed by its structurally similar compounds. The docking of Ellagic acid (parent compound) with selected SIRT1 protein 4ZZJ had the binding energy of -7.2 kcal/mol with LYS203, LEU206, ILE210 as interacting amino acids. Next, we perform the molecular docking of compounds similar to Ellagic acid with SIRT1 protein (PDB ID: 4ZZJ). For instance, the docking of Flavellagic acid and Coruleoellagic acid with SIRT1 protein 4ZZJ showed a similar binding energy of -7.5 kcal/mol with different interacting amino acids. When Flavellagic acid and Coruleoellagic acid was docked with SIRT1 protein (PDB ID: 4ZZJ), interacting amino acids such as LYS203, LEU206, THR209, ILE210, and SER453, LYS233, LEU472, HIS471, ARG446, ALA449 were observed. In addition, molecular docking of Coruleoellagic acid with 4ZZJ protein leads to the formation of two hydrogen bonds, whereas no such hydrogen bond formation was observed upon docking of Flavellagic acid with 4ZZJ protein. On the contrary, the docking of Ellagic acid tetraacetate and Verrulactone A had binding energies of -6.8 kcal/mol and -8.5 kcal/mol respectively. The amino acid results which are interacting when Ellagic acid tetraacetate and Verrulactone A were GLU477, PHE474, HIS473, ARG649, LEU472, LEU469, PRO470, PRO468, and ARG649, PRO470, HIS473, LYS236, and PHE474. Additionally, only one hydrogen bond was formed when Ellagic acid tetraacetate was docked with 4ZZJ protein, whereas no such hydrogen bond formation occurred upon docking of Verrulactone A with SIRT1 4ZZJ protein.

Besides this, the molecular docking of Naringenin (parent compound) with SIRT1 protein (PDB ID: 4ZZJ) showed a binding energy of -7.4 kcal/mol with the formation of only one hydrogen bond. Interacting amino acids such as VAL657, PRO468, LEU469, SER442, LYS444, and ARG274 were observed when Naringenin was docked with 4ZZJ protein. Next, we sought to dock the compounds similar to Naringenin with SIRT1 protein (PDB ID: 4ZZJ) to analyze the potent molecule on the basis of their binding energy. For instance, the docking of Isosakuranetin with SIRT1 protein 4ZZJ showed the binding energy of –7.5 kcal/mol with ARG274, LYS444, SER442, VAL657, PRO468, LEU469, with no hydrogen bond formation. Similarly, the docking of Sakuranetin with SIRT1 protein 4ZZJ showed the binding energy of –6.9 kcal/mol with ILE210, PRO211, ARG199, THR209, LYS203, whereas the binding energy (-7.6 kcal/mol) and interacting amino acid residues such as HIS473, PRO468, PHE474 was observed when Blumeatin was docked with 4ZZJ protein. On the contrary, the docking of Steppogenin with 4ZZJ protein showed the binding energy of -7.4 kcal/mol with various interacting amino acid residues such as LEU469, PRO468, VAL657, ARG274, SER442, and LYS444 was observed.

The docking of Baicalein (parent compound) with SIRT1 protein (PDB ID: 4ZZJ) showed the binding energy of -7.2 kcal/mol with ARG274, GLU467, PRO468, LEU469 as interacting amino acids, with one hydrogen bond formation. Next, we sought to dock the compounds similar to Baicalein with SIRT1 protein (PDB ID: 4ZZJ). For instance, the docking of Scutellarein with protein 4ZZJ showed the binding energy of -6.9 kcal/mol with PRO211, ARG199, LYS203, THR209, ILE210 as an interacting amino acid, whereas -6.9 kcal/mol of binding energy and ARG274, LYS444, HIS471 amino acids were observed when 6-Hydroxyluteolin was docked with this SIRT1 protein 4ZZJ. On the contrary, the docking of Norwogonin with SIRT1 protein (PDB ID: 4ZZJ) showed the -7.5 kcal/mol binding energy with varying amino acids such as VAL657, ARG274, LYS444, PRO468, LEU469, whereas the binding energy of -7.1 kcal/mol and interacting amino acids such as LEU469, PRO468, SER442, LYS444, VAL657, and ARG274, and one hydrogen bond formation was observed upon docking of Tricetin with 4ZZJ protein.

After predicting the binding energy and interacting amino acid residues of aforementioned compounds, we perform the docking of Glabridin (parent compound) with 4ZZJ protein and found the binding energy of -7.7 kcal/mol with ARG199, LYS203, THR209, and ILE210 as interacting amino acids. Next, we sought to dock the compounds similar to Glabridin with SIRT1 protein (PDB ID: 4ZZJ). For instance, the docking of Phaseollinisoflavan with protein 4ZZJ showed the binding energy of -7.8 kcal/mol with ARG199, PRO211, ILE210, LYS203, THR209 as interacting amino acid, whereas -8.2 kcal/mol of binding energy and LYS236, HIS473, LEU472, LEU469, PRO468 amino acids were observed when Hispaglabridin A was docked with this SIRT1 protein 4ZZJ. On the contrary, docking of Glyasperin H with 4ZZJ protein had binding energy of -7.5 kcal/mol with ARG199, LEU202, LYS203, THR209, ILE210, PRO211 as interacting amino acids, whereas -7.6 kcal/mol of the binding energy and LYS236, ARG469, PRO468, PRO470, and HIS473 amino acid residues were observed when Heminitidulan was docked with 4ZZJ protein. Furthermore, the molecular

docking of Dalenin with 4ZZJ SIRT1 protein leads to the formation of two hydrogen bonds, with the binding energy and interacting amino acids of -8.3 kcal/mol, and PRO468, GLU467, VAL657, ARG274, LYS444, HIS471, PRO470.

Similarly, we perform the docking of Naringin (parent compound) with 4ZZJ protein and found the binding energy of -7.8 kcal/mol with GLU467, ARG274, LYS444, ALA449, HIS471, PRO470, ARG446 as interacting amino acids. Next, we sought to dock the compounds similar to Naringin with SIRT1 protein (PDB ID: 4ZZJ). For instance, the docking of Poncirin with protein 4ZZJ showed the binding energy of -7.8 kcal/mol with GLU467, ARG274, LYS444, SER442, HIS471, ALA449, ARG446 as interacting amino acid, whereas -7.8 kcal/mol of binding energy and GLU467, LYS444, ARG446, ALA449, HIS471, PRO470 amino acid residues were observed when Neohesperidin was docked with this SIRT1 protein 4ZZJ. On the contrary, docking of Narirutin with 4ZZJ protein had binding energy of -8.1 kcal/mol with ARG649, LEU469, PRO470, GLU477, PHE474, LEU472, HIS473, LYS236 as interacting amino acids, whereas -8.3 kcal/mol of the binding energy and PRO647, ASN648, GLU477, PHE474, ARG649, LYS236, LEU469, PRO470, HIS473, and LEU472 amino acid residues were observed when Eriocitrin was docked with 4ZZJ protein. Furthermore, the docking of Hesperidin with 4ZZJ SIRT1 protein had the binding energy (-8.1 kcal/mol) and interacting amino acids of -8.3 kcal/mol, and LYS235, HIS473, LEU472, PRO470, LEU469, LYS236, PHE474, GLU477, ARG649 respectively. The molecular docking of Neohesperidin, Narirutin, Eriocitrin, and Hesperidin with 4ZZJ SIRT1 protein leads to the formation of two hydrogen bonds.

Next, we sought to analyze the binding energies and interacting amino acid residues of Capsaicin (parent compound) and its similar structures after docked them with SIRT1 protein (PDB ID: 4ZZJ). The results showed that docking of Capsaicin with 4ZZJ protein had -6.1 kcal/mol of binding energy and interacting amino acids which takes place were THR209, LYS203, LEU202, THR200, PRO211, ILE210, and ARG199. The docking of Zucapsaicin with protein 4ZZJ showed the binding energy of -5.9 kcal/mol with THR209, ILE210, PRO211, LEU202, LYS203, THR200, ARG199 as interacting amino acids, whereas -6.2 kcal/mol of binding energy and LEU479, ALA655, GLU477, PHE474, ARG649, LEU469, LEU472, HIS473, PRO470, PRO468 amino acid residues were observed when Olvanil was docked with this SIRT1 protein 4ZZJ. On the contrary, the docking of Dihydrocapsaicin with 4ZZJ protein exhibit the -5.6 kcal/mol binding energy and GLU477, PHE474, LYS236, LYS238, HIS473, LEU472, LEU469, PRO468 as interacting amino acid residues, whereas -5.3 kcal/mol of binding energy, and GLU467, PRO468, VAL657, ARG274, HIS471 interacting amino acids were observed upon docking of Nonivamide with 4ZZJ protein, and it leads to the formation of only one hydrogen bond.

The docking of Diosgenin (parent compound) with SIRT1 protein (PDB ID: 4ZZJ) showed the binding energy of -10.1 kcal/mol with GLY183, PRO184, PHE187, LEU228 as interacting amino acid residues. Similarly, compounds similar to Diosgenin were also docked with 4ZZJ protein to evaluate the binding energy. For

instance, the docking of Diosgenone with this protein shows the binding energy of -10.2 kcal/mol with GLY183, PHE187, LEU228 as interacting amino acids, with one hydrogen bond formation, whereas docking of Ruscogenin with this SIRT1 protein showed the similar binding energy (-9.8 kcal/mol) with PHE187, GLY183, LEU228 as interacting amino acids. The docking of Diosgenin and Ruscogenin leads to the formation of one hydrogen bond when docked with 4ZZJ SIRT1 protein. On the contrary, the docking of Caprospinol with 4ZZJ protein exhibits the -9.1 kcal/mol binding energy and ARG446, LYS444, ALA449, HIS471, GLU467, VAL657 as interacting amino acid residues, whereas -9.3 kcal/mol of binding energy, and GLY183, PHE187, LEU228 interacting amino acids were observed upon docking of Glycine Diosgenyl Ester with 4ZZJ protein. In addition, the docking of Namogenin B with 4ZZJ protein had the -9.1 kcal/mol binding energy, and ASP204, LEU228, PHE187, GLY183 amino acids residues were observed, whereas -10.0 kcal/mol of binding energy and LEU228, PHE187, GLY183 interacting amino acid residues were observed upon docking of Hecogenin with 4ZZJ SIRT1 protein. The docking of Namogenin B with 4ZZJ protein leads to the formation of one hydrogen bond formation.

Besides this, the molecular docking of Amygdalin (parent compound) with SIRT1 protein (PDB ID: 4ZZJ) showed a binding energy of -7.2 kcal/mol with the formation of two hydrogen bonds. Interacting amino acids such as HIS473, LEU472, LEU469, PRO468, ARG649, and LYS236 were observed when Amygdalin was docked with 4ZZJ protein. Next, we sought to dock the compounds similar to Amygdalin with SIRT1 protein (PDB ID: 4ZZJ) to analyze the potent molecule on the basis of their binding energy. For instance, the docking of Prunasin with SIRT1 protein 4ZZJ showed a binding energy of –6.1 kcal/mol withLEU469, PRO468, GLU467, VAL657, ARG274, SER442, with no hydrogen bond formation. Similarly, the docking of Taxiphyllin with 4ZZJ protein exhibits a binding energy of -6.4 kcal/mol with interacting amino acid residues such as GLU477, ASN648, PHE474, LEU469, LEU472, LYS236, and forms one hydrogen bond.

The docking of Kaempferol (parent compound) with SIRT1 protein (PDB ID: 4ZZJ) showed the binding energy of -7.7 kcal/mol with VAL657, ARG274, LYS444, SER442, PRO468, LEU469 as interacting amino acid residues. The docking of Kaempferol with 4ZZJ protein leads to the formation of only one hydrogen bond. Similarly, compounds similar to Kaempferol were also docked with 4ZZJ protein to evaluate the binding energy. For instance, the docking of Galangin with this protein shows the binding energy of -7.8 kcal/mol with LEU469, VAL657, ARG274, LYS444, SER442, and PRO468 as interacting amino acids, whereas docking of Kaempferide with this SIRT1 protein showed the similar binding energy to Galangin (-7.7 kcal/mol) with VAL657, ARG274, LYS444, SER442, PRO468, LEU460 as interacting amino acids. The molecular docking of Galangin and Kaempferide with SIRT1 protein (PDB ID: 4ZZJ) leads to the formation of two hydrogen bonds. In addition, the binding energy of -7.0 kcal/mol and interacting amino acids such as LYS203, LEU202, THR209, ILE210, PRO211, and ARG199 was observed when Rhamnocitrin was docked with 4ZZJ protein, whereas docking of Morin with 4ZZJ protein exhibits binding energy of -7.6 kcal/mol and several interacting amino acid residues were also involved such as LEU469, PRO468, SER442, LYS444, ARG274, VAL657. On

the contrary, the docking of Datiscetin with 4ZZJ (SIRT1 protein) had a binding energy of -7.8 kcal/mol with LEU469, PRO468, VAL657, ARG274, LYS444, and SER442 as interacting amino acids. The docking of Morin with 4ZZJ protein leads to the formation of two hydrogen bonds, while only one hydrogen bond was formed when Datiscetin was docked with 4ZZJ protein.

The docking of ferulic acid (parent compound) with SIRT1 protein (PDF ID: 4ZZJ) showed the binding energy of -5.5 kcal/mol with LYS203, THR209, ILE210, PRO211, ARG199 as interacting amino acids. Similarly, compounds similar to ferulic acid were also docked with SIRT1 protein (PDB ID: 4ZZJ) to evaluate the binding energy. For example, the docking of Isoferulic acid with this protein shows the binding energy of -5.5 kcal/mol with LEU202, LYS203, THR209, ILE210, and ARG199 as interacting amino acids, with one hydrogen bond formation, whereas docking of Sinapic acid with this SIRT1 protein showed the similar binding (-5.5 kcal/mol) with ARG199, PRO211, ILE210, THR209, and LYS203 as interacting amino acids with no formation of hydrogen bond. Similarly, the docking of ethyl ferulate with this SIRT1 protein showed the binding energy of -5.6 kcal/mol with ILE210, PRO211, THR209, and LYS203 as interacting amino acids, and one hydrogen bond formation; whereas, the docking of isoeugenol with this protein showed the binding energy of -5.6 kcal/mol with ARG234, PRO452, LEU472, HIS471, HIS473, and LYS233, with no formation of hydrogen bond.

The docking of vanillic acid (parent compound) with SIRT1 protein (PDF ID: 4ZZJ) showed the binding energy of -5.7 kcal/mol with LYS233, SER453, PRO452, ARG234, HIS473, and LEU472 as interacting amino acids, and one hydrogen bond formation. Similarly, compounds similar to vanillic acid were also docked with SIRT1 protein (PDB ID: 4ZZJ) to evaluate the binding energy. For example, the docking of methyl vanillate with this protein shows the binding energy of -5.3 kcal/mol with LYS233, SER453, PRO452, ARG234, HIS473, and LEU472 as interacting amino acids, with one hydrogen bond formation, whereas docking of protocatehuic acid with this SIRT1 protein (PDB ID: 4ZZJ) showed the similar binding (-6.1 kcal/mol) with LYS233, PRO452, ARG234, GLN461, and HIS473 as interacting amino acids with one hydrogen bond formation.

Next, we sought to analyze the binding energy and interacting amino acids of coumaric acid and its similar compounds with 4ZZJ protein. Our results showed -6.1 kcal/mol of binding energy and SER453, LYS233, PRO452, ARG234, GLN461, HIS473, and LEU472 interacting amino acid residues when coumaric acid (parent compound) was docked with SIRT1 protein i.e., 4ZZJ. Similarly, the docking of caffeic acid with protein 4ZZJ showed -5.6 kcal/mol of binding energy with PRO211, ILE210, THR209, LEU202, LYS203 as interacting amino acids, whereas -5.9 kcal/mol and ILE210, PRO211, THR209, LEU206, LYS203, and LEU202 of binding energy and interacting amino acids were observed upon docking of o-Coumaric acid with 4ZZJ protein.

We also found that docking of Apigenin (parent compound) with SIRT1 protein i.e., 4ZZJ exhibit binding energy (-7.4 kcal/mol) and interacting amino acids (SER442, LYS444, ARG274, PRO468, LEU469, VAL657), while the binding energy (-7.6 kcal/mol), and interacting amino acid residues such as VAL657, ARG274, LYS444, PRO468, LEU469, SER442 was found when Chrysin was docked with 4ZZJ protein. In addition, the molecular docking of Tricetin with 4ZZJ protein exhibits the binding energy of -7.1 kcal/mol with several interacting amino acid residues such as VAL657, ARG274, LYS444, SER442, GLU467, PRO468, LEU469, whereas -7.4 kcal/mol and ARG274, SER442, VAL657, PRO468, LEU469, and LYS444 of binding energy, and interacting amino acid residues was observed when Luteolin was docked with 4ZZJ protein. After this, the molecular docking of Diosmetin with 4ZZJ protein showed the binding energy (-7.3 kcal/mol) and SER442, ARG274, VAL657, PRO468, LEU469, while -6.7 kcal/mol and LYS444, HIS471, LEU469, PRO470, ARG274, VAL657, GLU467, and PRO468 of binding energy and interacting amino acids were found when Hispidulin was docked with 4ZZJ protein. The molecular docking of Luteolin, Diosmetin, and Hispidulin with SIRT1 protein (PDB ID: 4ZZJ) leads to the one hydrogen bond each.

At last, we sought to predict the binding energy and interacting amino acid residues of Genistein and similar compounds with 4ZZJ protein. We found that docking of Genistein (parent compound) with 4ZZJ protein showed the binding energy of -7.0 kcal/mol and interacting amino acids such as ARG199, LEU202, LYS203, PRO211, ILE210 were present, whereas only -6.5 kcal/mol of binding energy and ILE210, THR209, LYS203, and ARG199 was found when Biochanin A was docked with 4ZZJ protein. Similarly, the binding energy (-6.9 kcal/mol) and LYS203, ARG199, THR209, PRO211, and ILE210 were observed upon docking of Daidzein with 4ZZJ (SIRT1 protein), while the molecular docking of 4ZZJ protein with Formononetin exhibit the -6.5 kcal/mol of binding energy with ILE210, THR209, LEU206, LYS203, and ARG199 as interacting amino acids. The docking of Daidzein and Formononetin with this SIRT1 protein leads to the formation of one hydrogen bond each. On the contrary, the docking of Isoformononetin with 4ZZJ (SIRT1 protein) showed the binding energy of -6.8 kcal/mol and interacting amino acid residues of ILE210, THR209, PRO211, ARG199, LEU202, and LYS203.
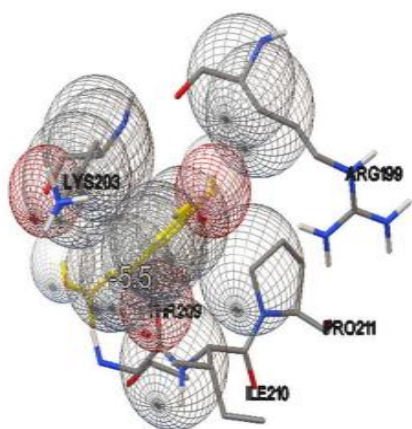
Fig 6.2: Docking of the SIRT1 protein (PDB ID:4ZZJ) with Ferulic acid
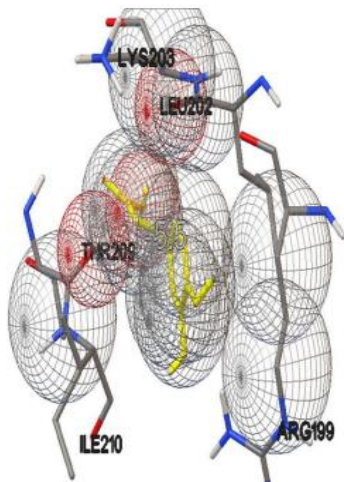
Fig 6.3: Docking of the SIRT1 protein (PDB ID:4ZZJ) with Isoferulic acid
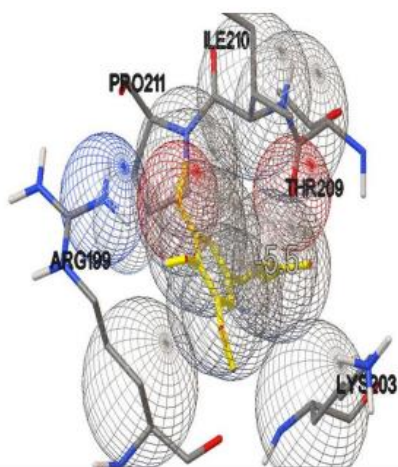
Fig 6.4: Docking of the SIRT1 protein (PDB ID:4ZZJ) with Sinapic acid
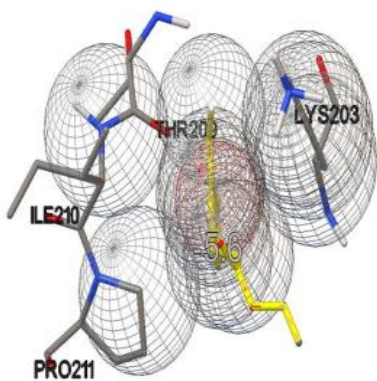
Fig 6.5: Docking of the SIRT1 protein (PDB ID:4ZZJ) with Ethyl ferulate
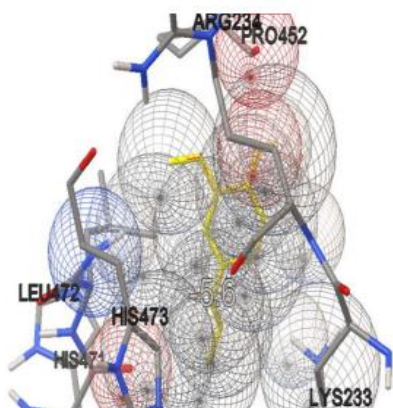
Fig 6.6: Docking of the SIRT1 protein (PDB ID:4ZZJ) with Isoeugenol
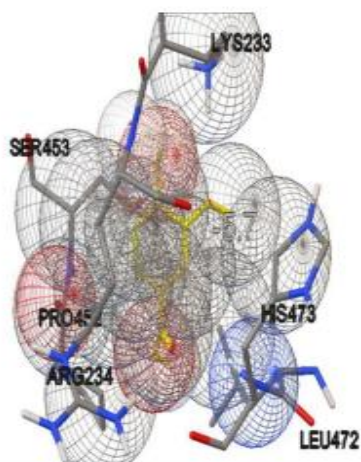
Fig 6.7: Docking of the SIRT1 protein (PDB ID:4ZZJ) with Vanillic acid
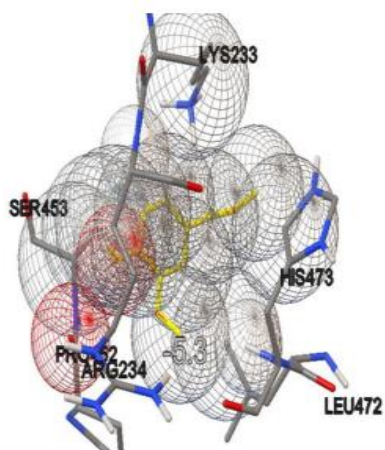
Fig 6.8: Docking of the SIRT1 protein (PDB ID:4ZZJ) with Methyl vanillate
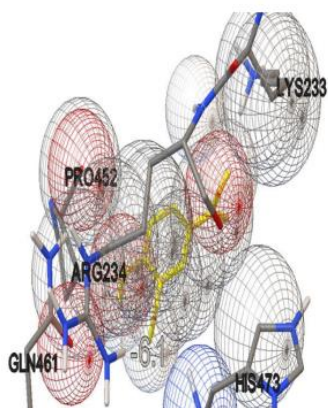
Fig 6.9: Docking of the SIRT1 protein (PDB ID:4ZZJ) with Protocatechuic acid
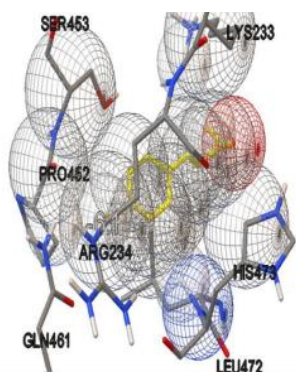
Fig 6.10: Docking of the SIRT1 protein (PDB ID:4ZZJ) with Coumaric acid
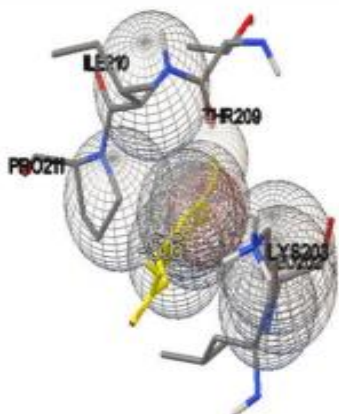
Fig 6.11: Docking of the SIRT1 protein (PDB ID:4ZZJ) with Caffeic acid
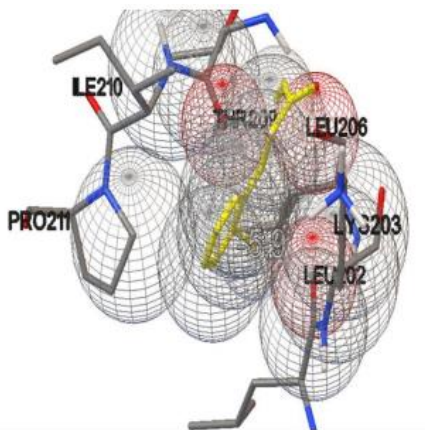
Fig 6.12: Docking of the SIRT1 protein (PDB ID:4ZZJ) with o-Coumaric acid
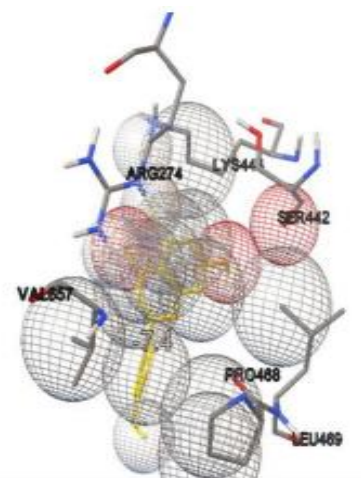
Fig 6.13: Docking of the SIRT1 protein (PDB ID:4ZZJ) with Apigenin
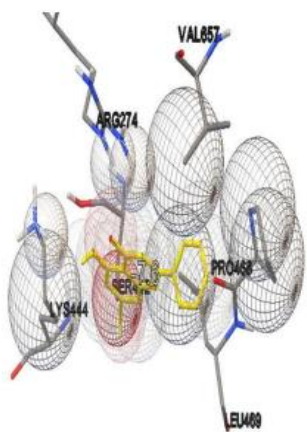
Fig 6.14: Docking of the SIRT1 protein (PDB ID:4ZZJ) with Chrysin
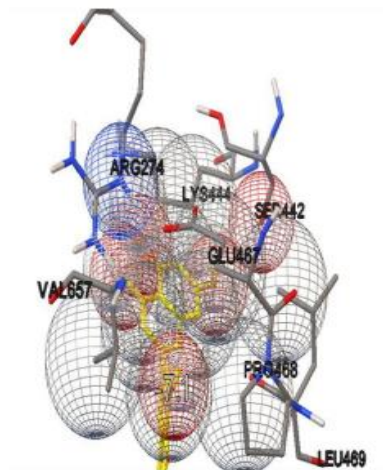
Fig 6.15: Docking of the SIRT1 protein (PDB ID:4ZZJ) with Tricetin
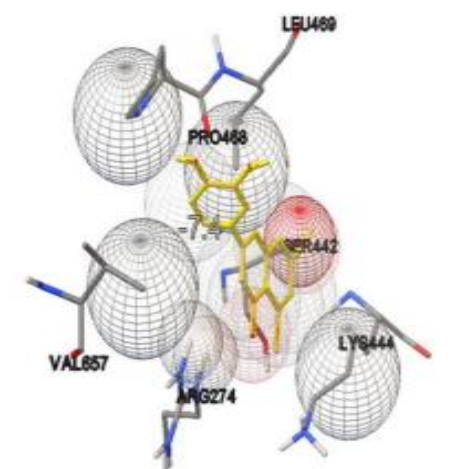
Fig 6.16: Docking of the SIRT1 protein (PDB ID:4ZZJ) with Luteolin
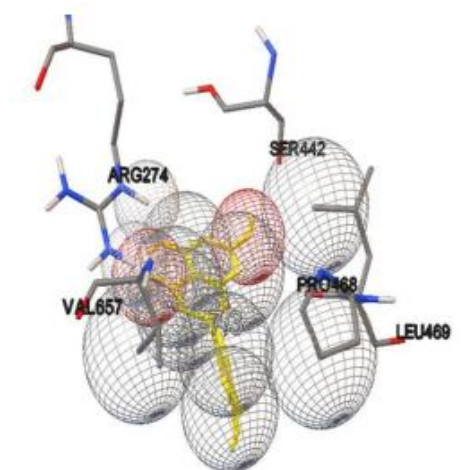
Fig 6.17: Docking of the SIRT1 protein (PDB ID:4ZZJ) with Diosmetin
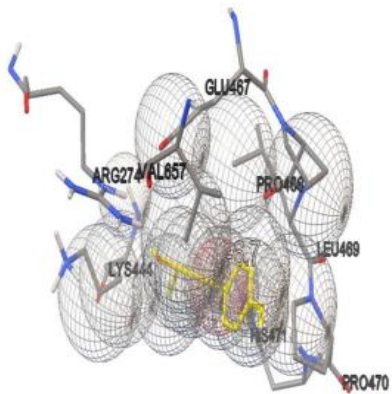
Fig 6.18: Docking of the SIRT1 protein (PDB ID:4ZZJ) with Hispidulin
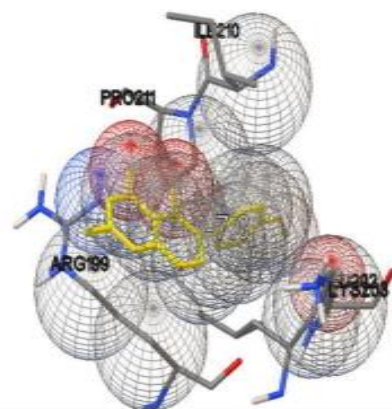
Fig 6.19: Docking of the SIRT1 protein (PDB ID:4ZZJ) with Genistein
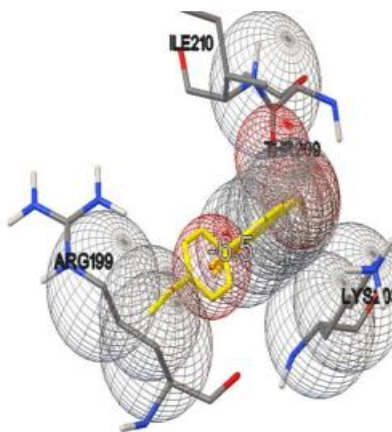
Fig 6.20: Docking of the SIRT1 protein (PDB ID:4ZZJ) with Biochanin A
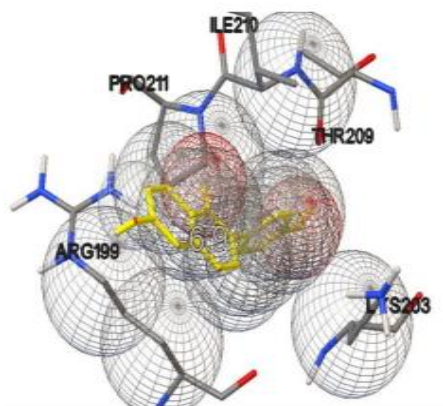
Fig 6.21: Docking of the SIRT1 protein (PDB ID:4ZZJ) with Daidzein
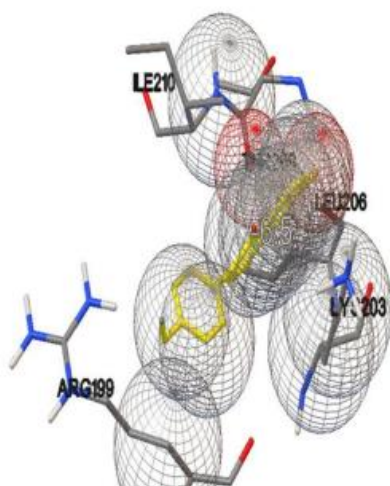
Fig 6.22: Docking of the SIRT1 protein (PDB ID:4ZZJ) with Formononetin
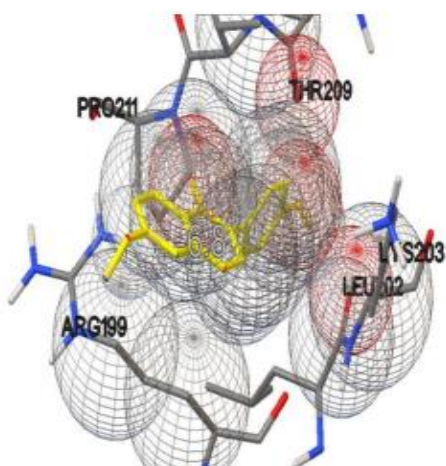
Fig 6.23: Docking of the SIRT1 protein (PDB ID:4ZZJ) with Isoformononetin

6.3. In-silico ADME prediction

We used the SwissADME online tool to assess the pharmacokinetics, drug-likeness, and physicochemical characteristics of the screened compounds through molecular docking.

Table 6.17: Physicochemical property

Phytochemical	Molecular weight (g/mol)	Number of heavy atoms	Number of aromatic heavy atoms	Number of H-bond acceptor	Number of H-bond donors	Molar Refractivity
Herbacetin	302.24	22	16	7	5	78.03
Robinetin	302.24	22	16	7	5	78.03
Hecogenin	430.62	31	0	4	1	122.27
Galangin	270.24	20	16	5	3	73.99
Rhamnocitrin	300.26	22	16	6	3	80.48
Sinapic acid	224.21	16	6	5	2	58.12
Isoeugenol	164.20	12	6	2	1	49.86
Protocatehuic acid	154.12	11	6	4	3	37.45
Caffeic acid	180.16	13	6	4	3	47.16
o-Coumaric acid	164.16	12	6	3	2	45.13

Table 6.18: Water solubility

Phytochemical	Log S (ESOL)	Solubility (mg/ml)	Class
Herbacetin	-3.55	8.46e-02	Soluble
Robinetin	-3.20	1.91e-01	Soluble
Hecogenin	-5.55	1.21e-03	Moderately soluble
Galangin	-3.46	9.39e-02	Soluble
Rhamnocitrin	-3.51	9.36e-02	Soluble
Sinapic acid	-2.16	1.54e+00	Soluble
Isoeugenol	-3.01	1.60e-01	Soluble
Protocatehuic acid	-1.86	2.14e+00	Very soluble
Caffeic acid	-1.89	2.32e+00	Very soluble
o-Coumaric acid	-2.37	6.93-01	Soluble

Table 6.19: Pharmacokinetic

Phytochemical	GI Absorption	BBB Permeant	P-gp substrate	CYP1A2 Inhibitor	CYP2C19 inhibitor	CYP2C9 inhibitor	Log K_p Skin Permeation (cm/s)
Herbacetin	High	No	No	No	No	Yes	-6.60
Robinetin	High	No	No	No	No	Yes	-7.00
Hecogenin	High	Yes	Yes	No	No	No	-5.50
Galangin	High	No	No	No	No	Yes	-6.35
Rhamnocitrin	High	No	No	No	No	Yes	-6.56
Sinapic acid	High	No	No	No	No	No	-6.63
Isoeugenol	High	Yes	No	No	No	No	-5.14
Protocatehuic acid	High	No	No	No	No	No	-6.42
Caffeic acid	High	No	No	No	No	No	-6.58
o-Coumaric acid	High	Yes	No	No	No	No	-5.86

Table 6.20: Drug-likeness

Phytochemical	Lipinski	Ghose	Veber	Egan	Muegge	Bioavailability Score
Herbacetin	Yes	Yes	Yes	Yes	Yes	0.55
Robinetin	Yes	Yes	Yes	Yes	Yes	0.55
Hecogenin	Yes	No	Yes	Yes	Yes	0.55
Galangin	Yes	Yes	Yes	Yes	Yes	0.55
Rhamnocitrin	Yes	Yes	Yes	Yes	Yes	0.55
Sinapic acid	Yes	Yes	Yes	Yes	Yes	0.56
Isoeugenol	Yes	Yes	Yes	Yes	No	0.55
Protocatehuic acid	Yes	No	Yes	Yes	No	0.56
Caffeic acid	Yes	Yes	Yes	Yes	No	0.56
o-Coumaric acid	Yes	Yes	Yes	Yes	No	0.85

Table 6.21: Medicinal Chemistry

Phytochemical	PAINS	Brenk	Leadlikeness	Synthetic accessibility

Herbacetin	1	2	Yes	3.20
Robinetin	1	1	Yes	3.21
Hecogenin	0	0	No	6.70
Galangin	0	0	Yes	3.12
Rhamnocitrin	0	0	Yes	3.21
Sinapic acid	0	1	No	2.17
Isoeugenol	0	0	No	1.81
Protocatehuic acid	1	1	No	1.07
Caffeic acid	1	2	No	1.81
o-Coumaric acid	0	1	No	1.85

6.4. Boiled-egg representation

The Boiled-Egg diagram is used for a straightforward assessment of passive gastrointestinal absorption indicated by the white section and BBB indicated by the yellow section. Additionally, blue and red points represent P-glycoprotein (P-gp) positivity and negativity concerning the position of small molecules in the WLOGP-versus-TPSA graph. The Boiled Egg plots in Fig 6.24 depict Herbacetin, Robinetin, Hecogenin, Galangin, and Rhamnocitrin, while Fig 6.25 illustrates the Boiled Egg plot for Sinapic acid, Isoeugenol, Protocatechuic acid, Caffeic acid, and o-Coumaric acid (2-Hydroxycinnamic acid).
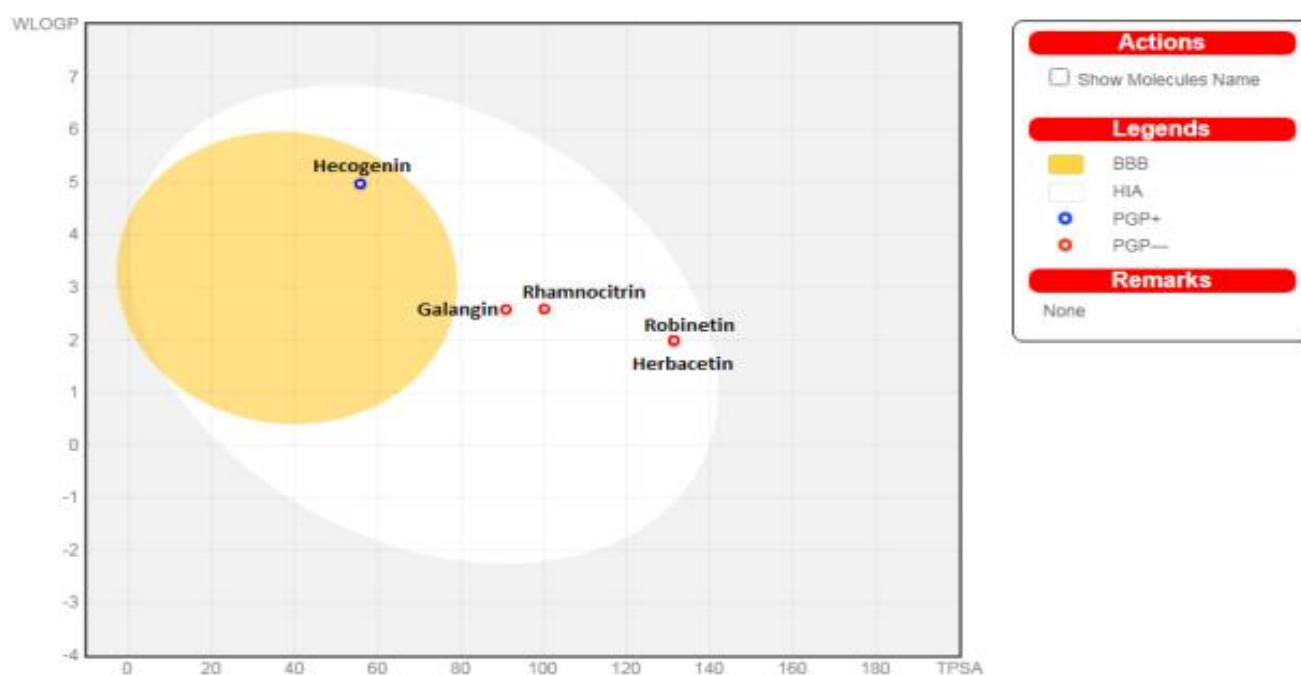
Fig 6.24: Boiled egg representation of Herbacetin, Robinetin, Hecogenin, Galangin and Rhamnocitrin.
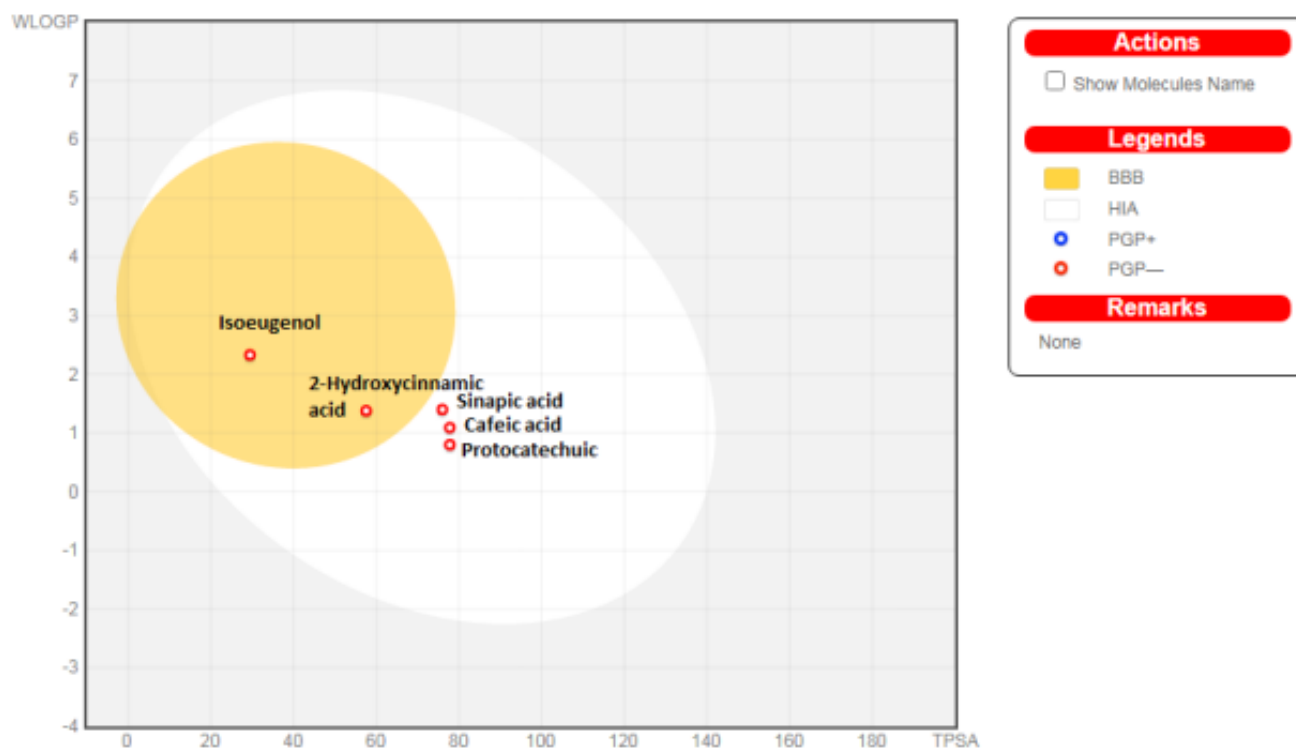
Fig 6.25: Boiled egg representation of Sinapic acid, Isoeugenol, Protocatechuic acid, Caffeic acid and o-Coumaric acid (2-Hydroxycinnamic acid).

From a pool of 66 phytochemicals, a selection was made based on cost considerations, resulting in the inclusion of 10 chemical compounds. These include Herbacetin, Robinetin, Hecogenin, Galangin, Rhamnocitrin, Sinapic acid, Isoeugenol, Protocatechuic acid, Caffeic acid and o-Coumaric acid. Of the 10 compounds selected, an additional ADME analysis was performed to determine which two phytochemicals would be the best candidates for use in future. The outcomes from the ADME study indicated that all phytochemicals, with the exception of Hecogenin, exhibit water solubility, where Hecogenin is moderately soluble. Notably, Protocatechuic acid is highly soluble in water. Pharmacokinetic analysis revealed that all the phytochemicals demonstrate high gastrointestinal absorption. However, only Hecogenin, Isoeugenol, and o-Coumaric acid were observed to permeate the BBB. Compared to all other selected compounds, a compound called Hecogenin was found to be a P-gp substrate. Four compounds, including Herbacetin, Robinatin, Galangin, and Rhamnocitrin, displayed inhibition of one of the CYP-450 isoforms, while the others did not. This implies that there were no drug-drug interactions or accumulation that could result in drug toxicity. Among all the phytochemicals, Robinetin exhibits the lowest permeability to the skin, while Isoeugenol demonstrates high skin permeability. The majority of phytochemicals have a bioavailability score of 0.55, with exceptions such as o-Coumaric acid (0.85) and Sinapic acid, Protocatechuic acid, and Caffeic acid (0.56). Upon scrutinizing various parameters, chemical compounds including Herbacetin, Robinetin, Galangin, and Rhamnocitrin were identified as promising candidates with lead-like properties.

Regarding synthetic accessibility, Protocatechuic acid stands out as readily synthesizable. The boiled-egg model illustrates that all molecules have a high likelihood of absorption in the gastrointestinal tract, with Hecogenin demonstrating BBB penetration. Since the chemical compound has been identified as a P-gp substrate, our intention was to choose the top two compounds out of the ten based on the comprehensive studies conducted, including similarity search, molecular docking, ADME, and cost considerations. The two compounds selected for further investigation are Sinapic acid and o-Coumaric acid.
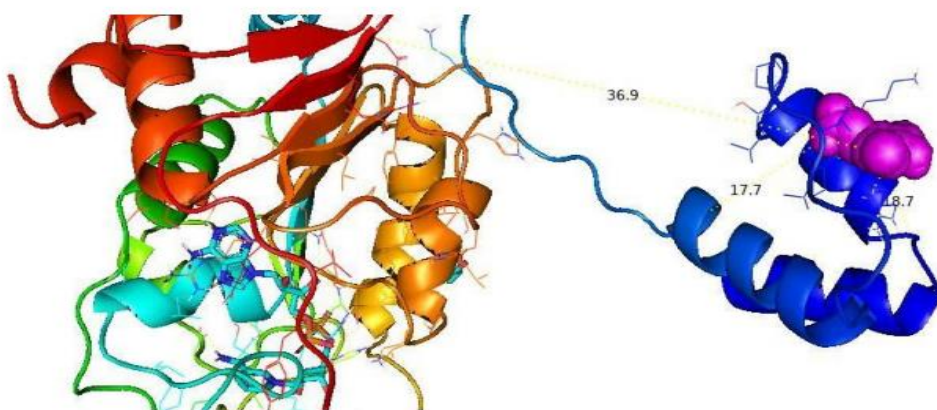
Fig 6.26: Visualization of binding interactions between target protein (cartoon structure) and Sinapic acid (magenta sphere) using Pymol software.
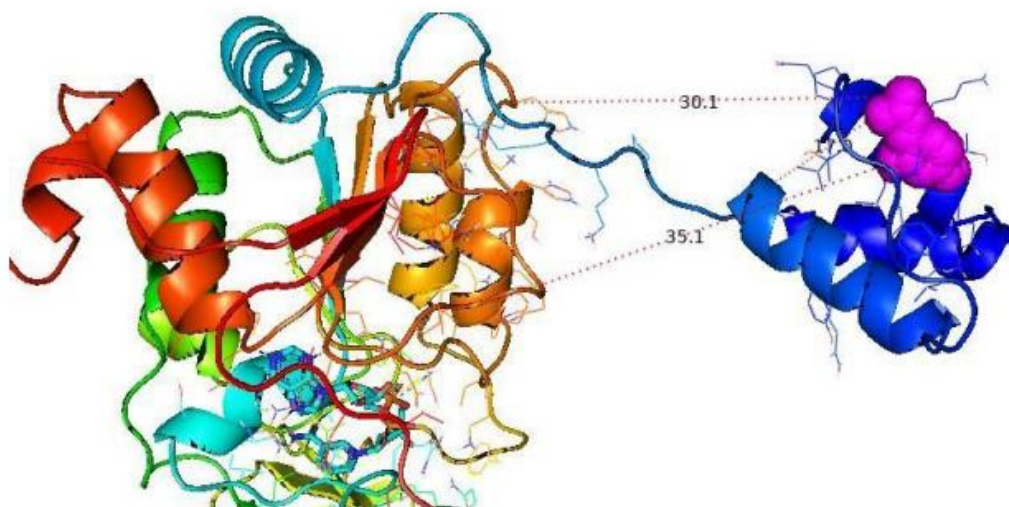
Fig 6.27: The Pymol software was employed to visualize the binding interactions between the target protein (depicted in a cartoon structure) and o-Coumaric acid (represented as a magenta sphere).

6.5. In vitro study

6.5.1 DPPH free radical scavenging activity

We employed the approach outlined by Sharma and colleagues to assess the free radical scavenging capability of Sinapic acid and o-Coumaric acid (352). Our result showed that Sinapic acid shows 50% inhibition at 35.6 µg/mL while o-Coumaric acid shows 50% inhibition at 106 µg/mL. In comparison to Sinapic acid and o-

Coumaric acid, Ascorbic acid as a standard was found to show 50% inhibition at 44.26 µg/mL (Fig 6.28, 6.29, and 6.30). This leads to the conclusion that compared to o-Coumaric acid and Ascorbic acid, Sinapic acid treatment has greater antioxidant capacity by eliminating free radical generation at lower concentrations.

% Inhibition Sinapic Acid

$y = 0.4091x + 35.421$
$R^2 = 0.9194$
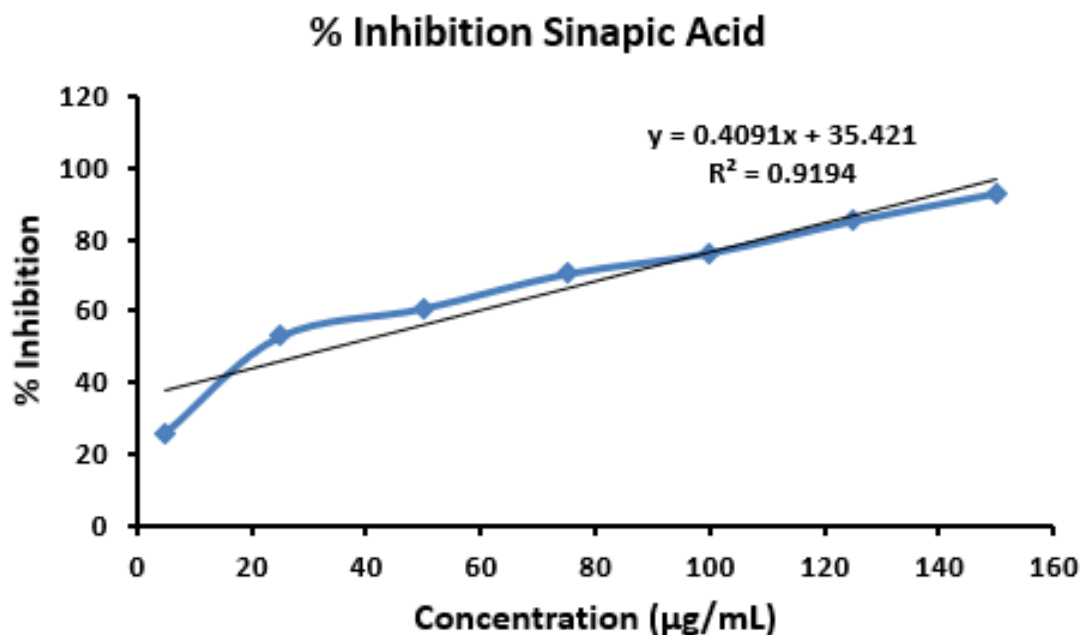
Fig 6.28: DPPH scavenging activity of Sinapic acid. The data is presented as the Mean±SEM from three independent tests.

% Inhibition o-Coumaric Acid

$y = 0.441x + 3.2708$
$R^2 = 0.9711$
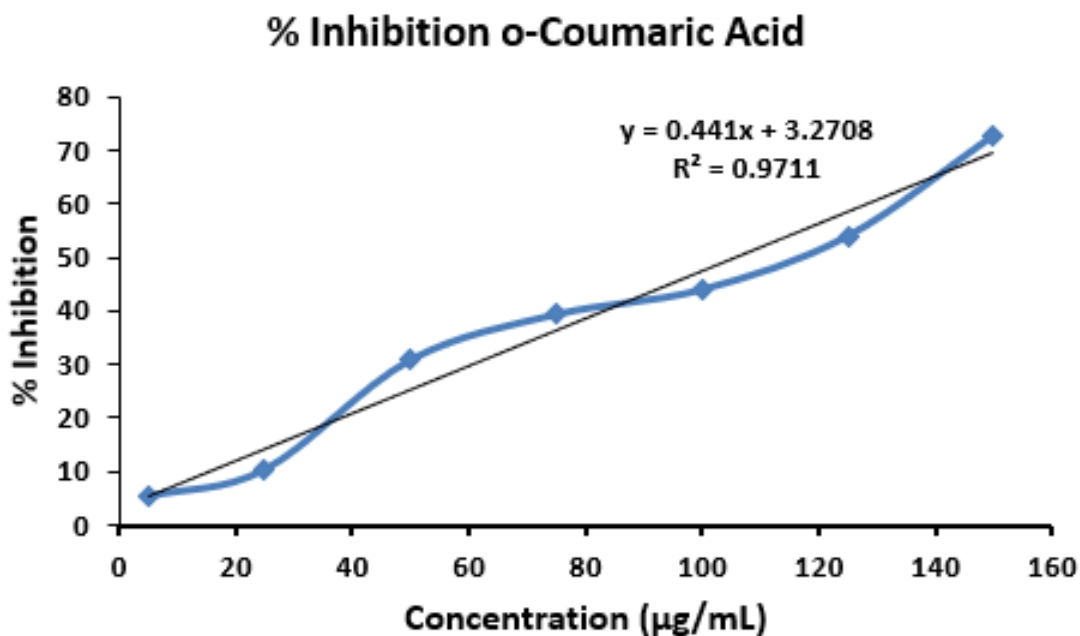
Fig 6.29: DPPH scavenging activity of o-Coumaric acid. The data is presented as the Mean±SEM from three independent tests.
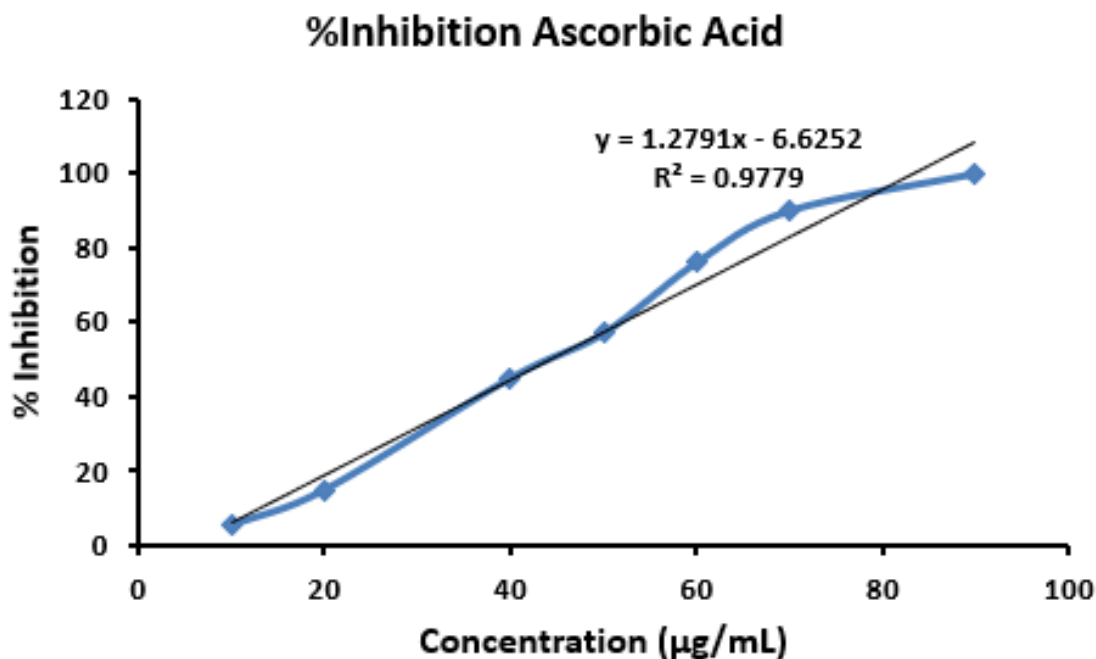
Fig 6.30: DPPH scavenging activity of Ascorbic acid. The data is presented as the Mean±SEM from three independent tests.

6.5.2. Cell line toxicity assay

To assess the impact of Sinapic acid and o-Coumaric acid on cell viability, we conducted the MTT assay on L929 cells, employing different concentrations ranging 50, 100, 150, 200, 250, 300, 350, 400, 450, and 500 µM. In-vitro cytotoxicity studies are the most recommended approach in pre-clinical drug development to assess the toxicity of a potential drug candidate on cell lines. According to our findings, compared to all other concentrations, cells treated with Sinapic acid at a concentration of 50, 100, 150, and 200 µM displayed maximum cell viability with values of 96.29±55.60, 90.72±52.36, 86.35±49.66, and 81.90±47.26 respectively (Fig 6.31). Similarly, compared to all other concentrations, o-Coumaric acid treatment to cells at a concentration of 50, 100, 150, and 200 µM displayed maximum cell viability with values of 96.50±55.61, 89.51±51.57, 83.73±48.36, and 80.82±46.62 respectively (Fig 6.32; Table 6.22). The experiment was conducted in triplicate, and the results were presented as the Mean±SEM. The IC_{50} values for Sinapic acid and o-Coumaric acid were found to be **467µM** and **427µM**.

Table 6.22: The cell viability percentage following treatment with Sinapic acid and o-Coumaric acid at various concentrations in the L929 cell line is presented as Mean ± SEM, n=3.

Concentration of Sinapic acid (µM)	% Cell viability Sinapic acid	Concentration of o-Coumaric acid (µM)	% Cell viability o-Coumaric acid
50	96.29±55.60	50	96.50±55.61

100	90.72±52.36	**100**	89.51±51.57
150	86.72±49.66	**150**	83.73±48.36
200	81.90±47.26	**200**	80.82±46.62
250	76.91±44.34	**250**	73.12±42.14
300	70.34±40.65	**300**	65.51±37.78
350	64.30±37.18	**350**	60.52±34.97
400	59.10±34.17	**400**	51.99±29.92
450	53.07±30.55	**450**	46.83±26.96
500	43.21±24.95	**500**	40.72±23.51

y = -0.1151x + 103.77
R^2 = 0.9947
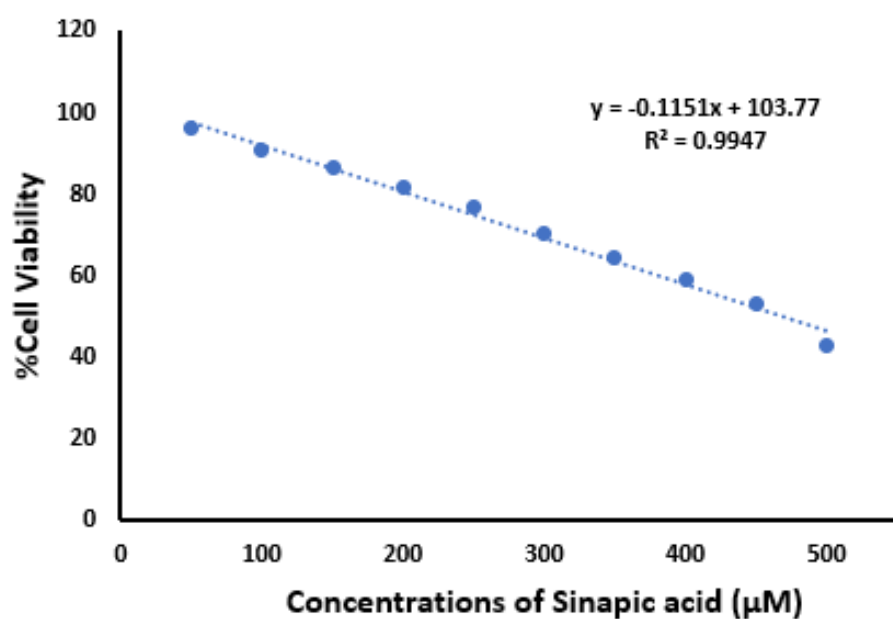
Fig 6.31: Cell line toxicity assay using L929 cell line.

Percentage cell viability after Sinapic acid treatment at the different concentrations on L929 cell line, all the value are shown as Mean±SEM, (n=3).
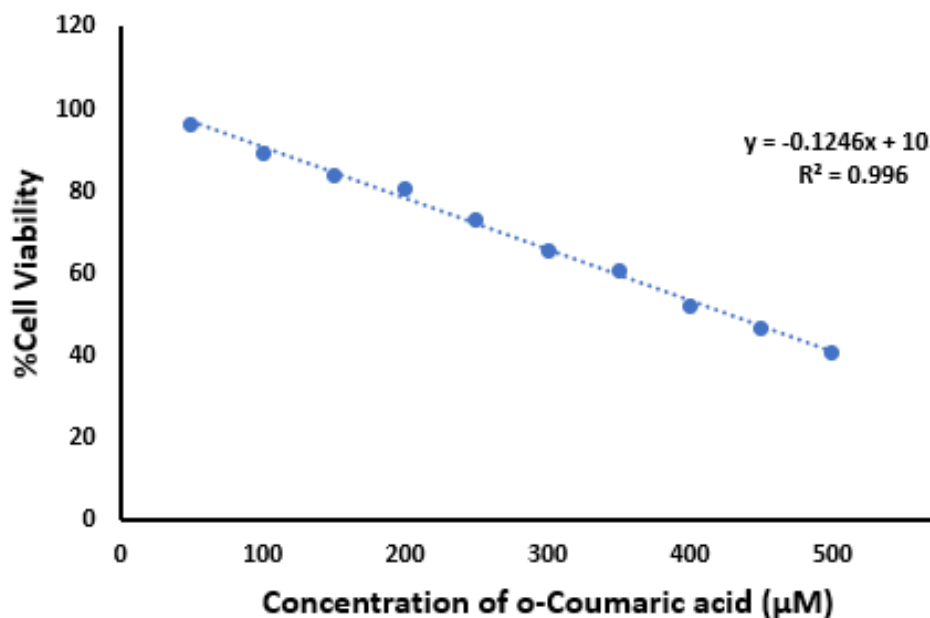
Fig 6.32: Cell line toxicity assay using L929 cell line.

Percentage cell viability after o-Coumaric acid treatment at the different concentrations on L929 cell line, all the value are shown as Mean±SEM, (n=3).

6.5.3 Tube formation assay

As studies over the past decades have shown that enhancing angiogenesis and revascularization in diabetic wounds is important to accelerate wound healing, our objective was to assess the capability of Sinapic acid and o-Coumaric acid in enhancing angiogenesis for accelerated wound healing. Our findings showed that groups receiving treatment of Sinapic acid and o-Coumaric acid at both 10 µM and 50 µM enhanced the number of branches, and tube length, compared to the untreated HG treated group (Fig 6.33 and 6.34). In addition, we also showed that there was a significant variation in the HUVEC morphology such as reduced branching and thinning of capillaries in the HG treated group, whereas the group receiving treatment of Sinapic acid and o-Coumaric acid at 10 µM and 50 µM doses reversed these parameters by increasing branching and thickening of capillaries, and thus supporting the initiation of angiogenesis (Fig 6.35).
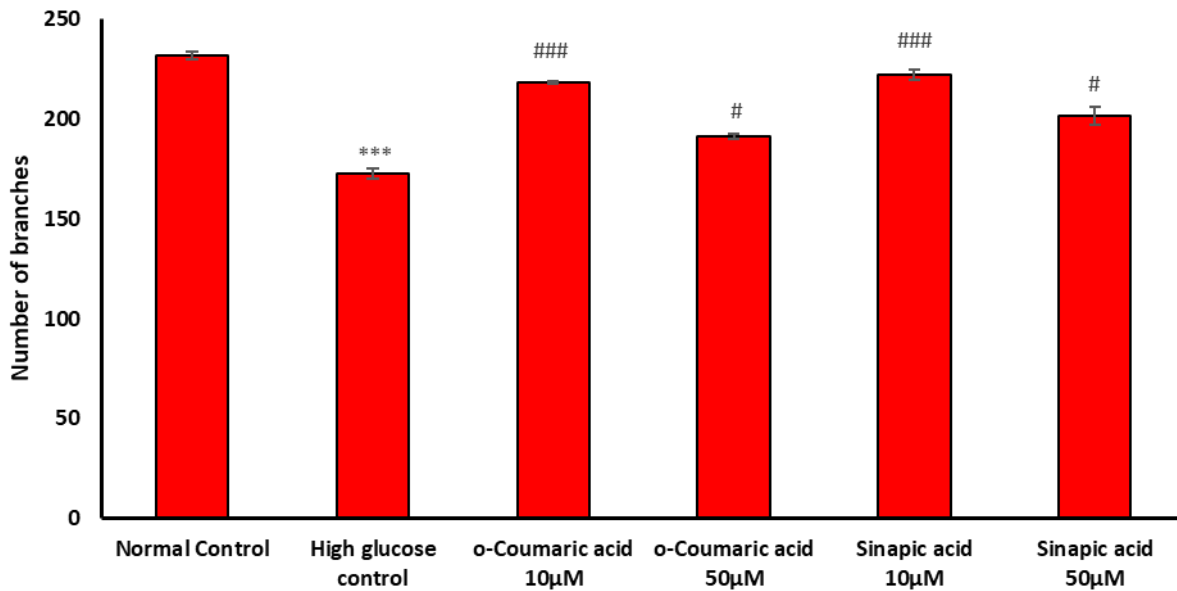
Fig 6.33: Graph between number of branches and different concentration of treatment compounds.

All the values were represented as Mean ± S.E.M. (n=3), ***p<0.001, vs normal control and ###p<0.001, and #p<0.05, vs high glucose control.
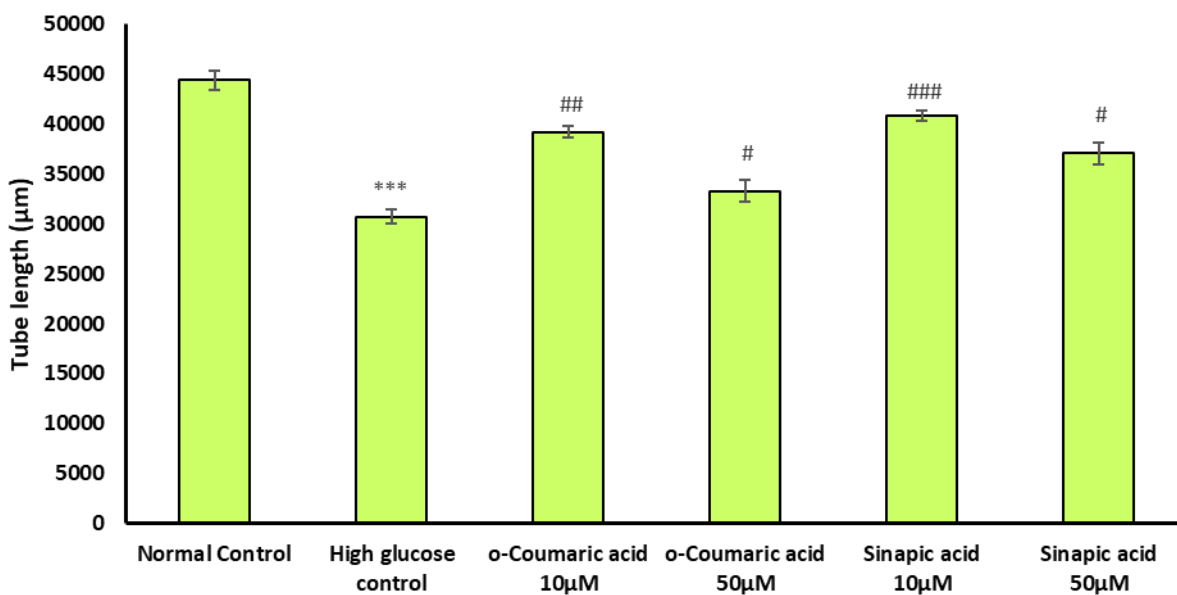
Fig 6.34: Graph between tube length and different concentration of treatment compounds.

All the values were represented as Mean ± S.E.M. (n=3), ***p<0.001, vs normal control and ###p<0.001, ##p<0.01 and #p<0.05, vs high glucose control.
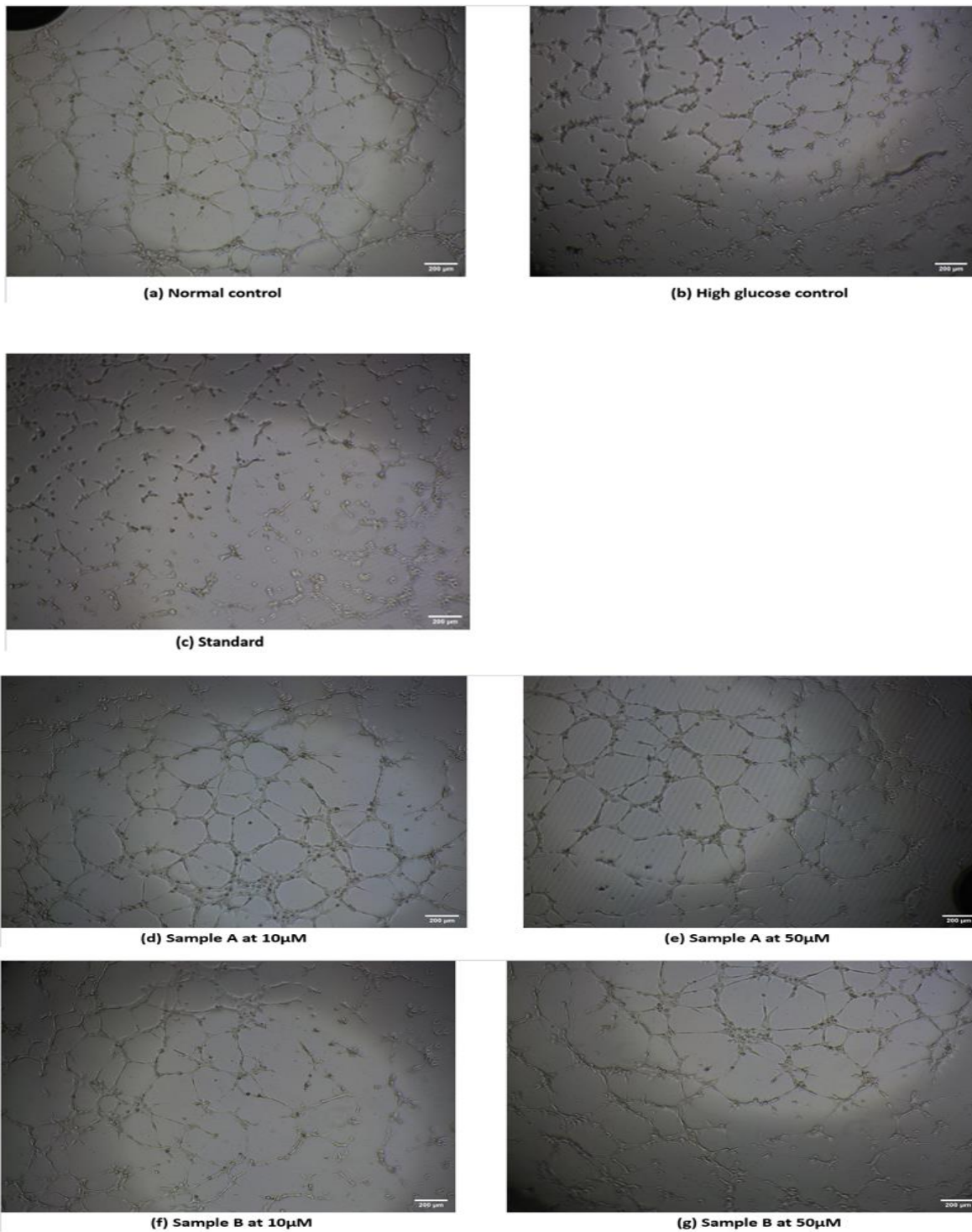
Fig. 6.35: Figure showing tube formation initiation under different conditions (control, untreated and treated) Sample A: o-Coumaric acid; Sample B: Sinapic acid.

6.5.4 Scratch assay

We next attempted to investigate the ability of Sinapic acid and o-Coumaric acid to promote cell migration to accelerate wound healing because research over the past several decades has shown that cell migration is essential to accelerate wound healing. Our results showed that the untreated hyperglycemic/HG group displayed lower potential to improve wound healing compared to both Sinapic acid and o-Coumaric acid

treated HG/LG group. Briefly, the treatment of Sinapic acid to the LG treated group at 10 µM and 50 µM concentrations had higher wound healing capacity up to 77.07±1.32 and 72.09±1.32, compared to the control untreated LG group i.e. 54.0±5.26. This suggests that, in comparison to the LG treated group without intervention, the administration of Sinapic acid to the LG treated group notably enhances wound healing. Similarly, the treatment of Sinapic acid to the HG treated group at 10 µM and 50 µM concentrations effectively enhance wound healing up to 77.83±2.08 and 69.86±3.43, compared to control untreated HG group i.e. 52.33±3.50 respectively. Whereas, the treatment of o-Coumaric acid to the LG treated group at 10 µM and 50 µM concentrations for 24 hours effectively increase wound healing up to 78.82±0.39 and 74.63±2.58, compared to o-Coumaric acid treated HG group at both concentrations i.e. 68.82±1.91 and 60.38±1.66 respectively. This indicates that the treatment of Sinapic acid and o-Coumaric acid at both concentrations for 24 hours significantly enhanced wound healing, as shown in Fig 6.36, 6.37, and 6.38).

(a) Wound at 0 hour (10µM) (b) Wound at 24 hour (10µM)

(c) Wound at 0 hour (50µM) (d) Wound at 24 hour (50µM)
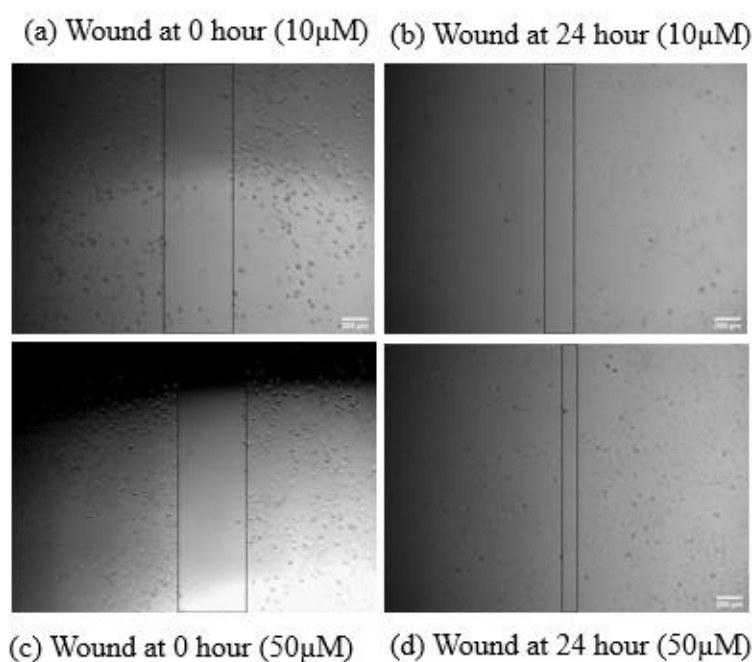
Fig 6.36: Cell migration of cells after Sinapic acid treatment at different concentrations (a) 0 hour at 10µM (b) 24 hour at 10 µM (c) 0 hour at 50µM (d) 24 hour at 50µM.

(a) Wound at 0 hour (10μM)   (b) Wound at 24 hour (10μM)

(c) Wound at 0 hour (50μM)   (d) Wound at 24 hour (50μM)
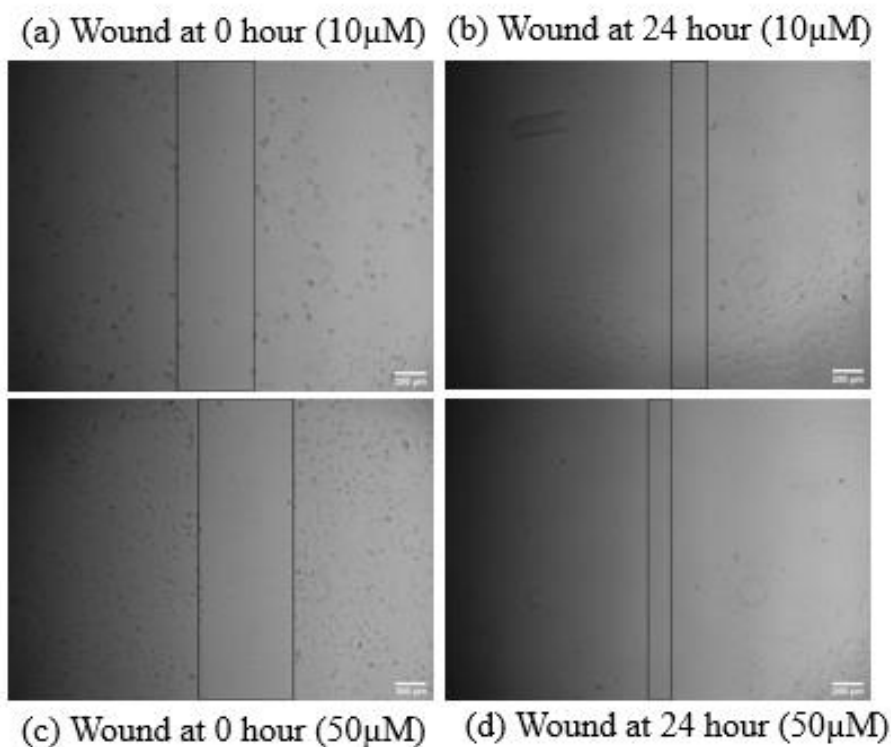
Fig 6.37: Cell migration of cells after o-Coumaric acid treatment at different concentrations (a) 0 hour at 10μM (b) 24 hour at 10 μM (c) 0 hour at 50μM (d) 24 hour at 50μM.
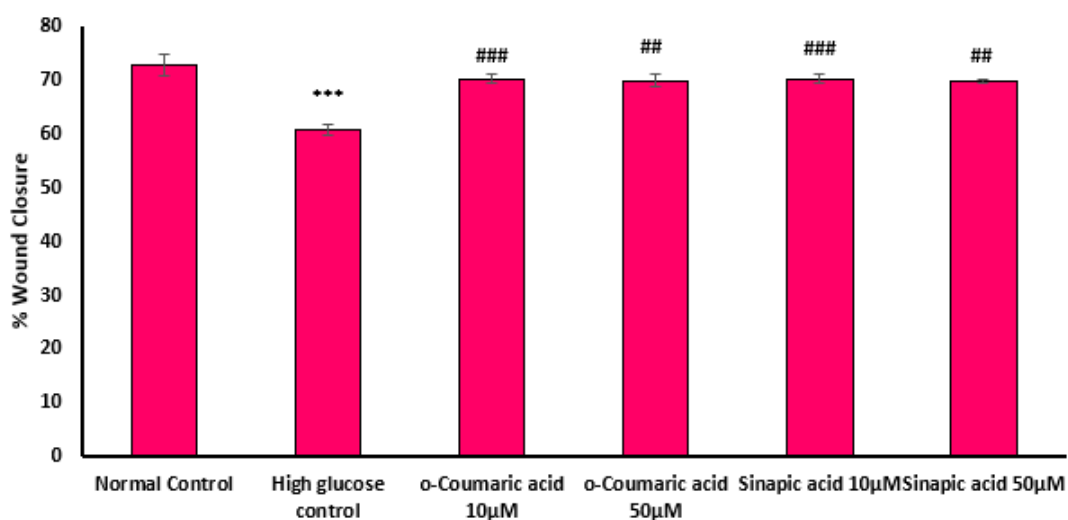
Fig 6.38: Graph showing the % migration of cells (wound closure) after receiving treatment of Sinapic acid and o-Coumaric acid under LG and HG conditions.

All the values were represented as Mean ± S.E.M. (n=3), ***$p < 0.001$, vs normal control and ###$p < 0.001$, ##$p < 0.01$, and ##$p < 0.01$, vs high glucose control.

6.6 In vitro oxidative biomarkers analysis

6.6.1 Total protein estimation in cells using the Lowry method

The protein content (BSA) was quantified using the procedure described by Lowry et al. (1951), employing a standard curve established with BSA (Fig 6.39). It is crucial to assess the quantity of total protein content in the sample before initiating the assay, as the percentage of total protein content serves as a parameter for defining enzyme activity (367).

$$y = 2.8857x + 0.0247$$
$$R^2 = 0.9993$$
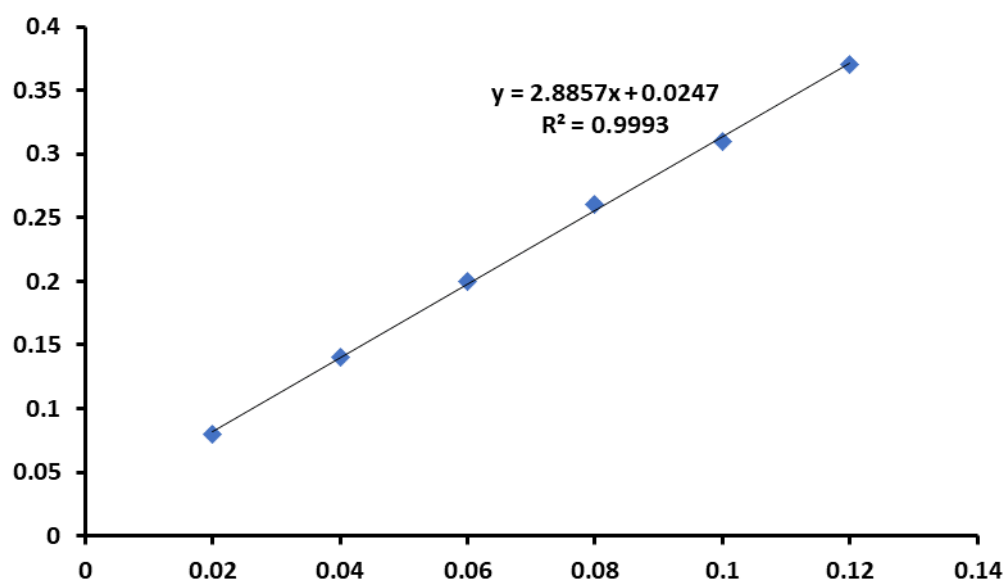
Figure 6.39: Protein estimation using the Lowry method.

6.6.2 LPO

LPO is a process in which oxidants, including free radicals, break down lipids that contain carbon-carbon double bonds, with a particular focus on PUFAs. This investigation explores the evaluation of the protective capabilities of Sinapic acid and o-Coumaric acid against oxidative stress. Our results showed that the untreated hyperglycemic/ HG group displayed higher amounts of MDA compared to both Sinapic acid and o-Coumaric acid-treated HG/LG groups. Briefly, the treatment of Sinapic acid to the LG treated group at 100 µM and 150 µM concentrations had MDA levels of 2.74±0.239 µmol MDA/mg and 2.98±0.232 µmol MDA/mg, compared to control untreated LG group i.e. 2.099±0.095 µmol MDA/mg. This implies that the introduction of Sinapic acid to the LG treated group did not result in a significant decrease in MDA levels compared to the untreated LG treated group. Similarly, the administration of Sinapic acid to the HG treated group at concentrations of 100 µM and 150 µM effectively lowers MDA levels to 6.65±0.288 µmol MDA/mg and 5.33±0.274 µmol MDA/mg, respectively, compared to the control untreated HG group, which recorded 8.68±0.463 µmol MDA/mg. Whereas, the treatment of o-Coumaric acid to the LG treated group at 100 µM and 150 µM concentrations effectively reduces the MDA level to 6.4762±0.394 µmol MDA/mg and 5.101±0.347 µmol MDA/mg, compared to untreated HG group i.e. 8.688±0.164 µmol MDA/mg. Based on our findings, the administration of Sinapic acid and o-Coumaric acid at both concentrations demonstrated a notable reduction in oxidative stress, evidenced by the decrease in MDA levels, as depicted in the Fig 6.40.

	Control LG	LG (100µM)	LG (150µM)	Control HG	HG (100µM)	HG (150µM)
Sinapic acid	2.099	2.74	2.98	8.68	6.65	5.33
o-Coumaric acid	2.0999	2.164	2.08	8.6889	6.4762	5.101
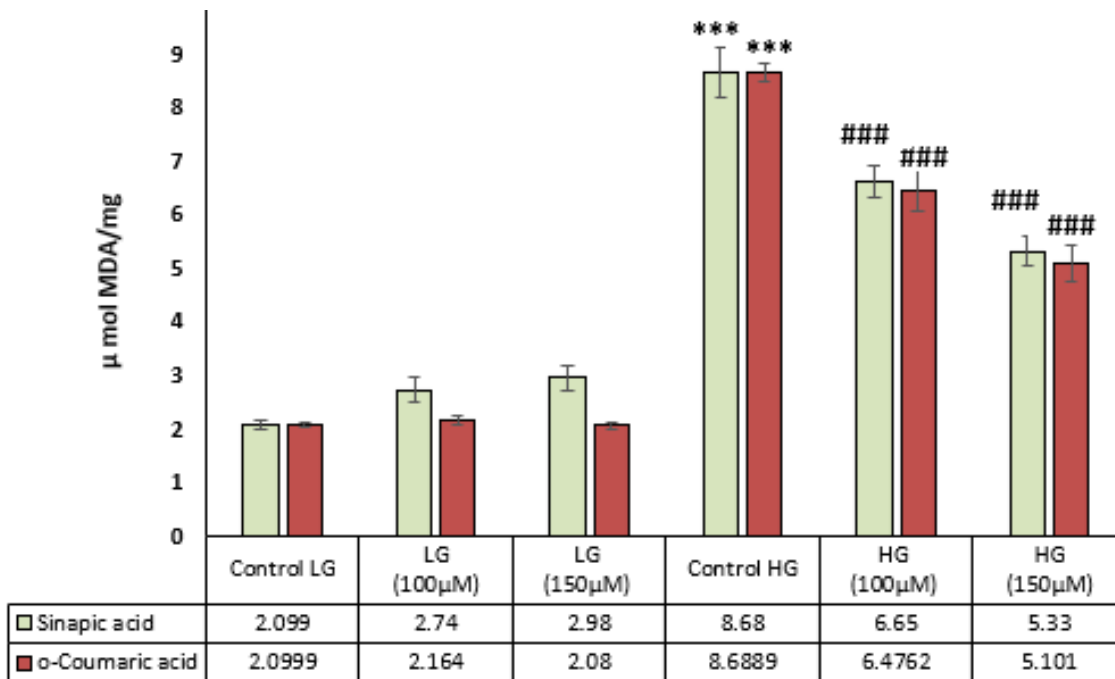
Fig 6.40: The impact of Sinapic acid and o-Coumaric acid at concentrations of 100 µM and 150 µM on LPO was assessed under both LG and HG conditions, utilizing PNS obtained after cell lysis.

All the values were represented as Mean ± S.E.M. (n=3), ***p<0.001, vs control LG and ###p<0.001, vs control HG.

6.6.3 GST

Intracellular detoxification of xenobiotics and harmful products formed within the cell is significantly facilitated by GST. Our results showed that the untreated hyperglycemic/HG group displayed lower amounts of GST compared to both Sinapic acid and o-Coumaric acid treated HG/LG group. Briefly, treatment with Sinapic acid in the LG treated group at 100 µM and 150 µM concentrations resulted in comparatively negligible change in GST levels up to 24.046±1.07 U/mg and 21.851±1.19 U/mg, compared to control untreated LG group i.e. 25.682±2.43 U/mg. Similarly, the treatment of Sinapic acid to the HG treated group at 100 µM and 150 µM concentrations effectively restored the GST levels to 13.064±0.37 U/mg and 12.319±0.35 U/mg, compared to control untreated HG group i.e. 7.221±0.622 U/mg respectively. Whereas, the treatment of o-Coumaric acid to the LG treated group at 100 µM and 150 µM concentrations effectively restored the GST levels to 24.05±0.978 U/mg and 24.054±0.978 U/mg, compared to untreated LG treated group i.e. 25.682±0.401 U/mg. Similarly, the treatment of o-Coumaric acid to the HG treated group at 100 µM and 150 µM concentrations effectively restored the GST levels to 15.908±0.769 U/mg and 16.909±0.522 U/mg, compared to control untreated HG group i.e. 7.76±0.769 U/mg respectively. As per our findings, the administration of Sinapic acid and o-Coumaric acid at both concentrations notably diminished oxidative stress by restoring GST levels, as illustrated in Fig 6.41.

	Control LG	LG (100µM)	LG (150µM)	Control HG	HG (100µM)	HG (150µM)
Sinapic acid	25.68	24.046	21.85	7.27	9.54	12.319
o-Coumaric acid	25.682	24.05	24.054	7.76	15.908	16.909
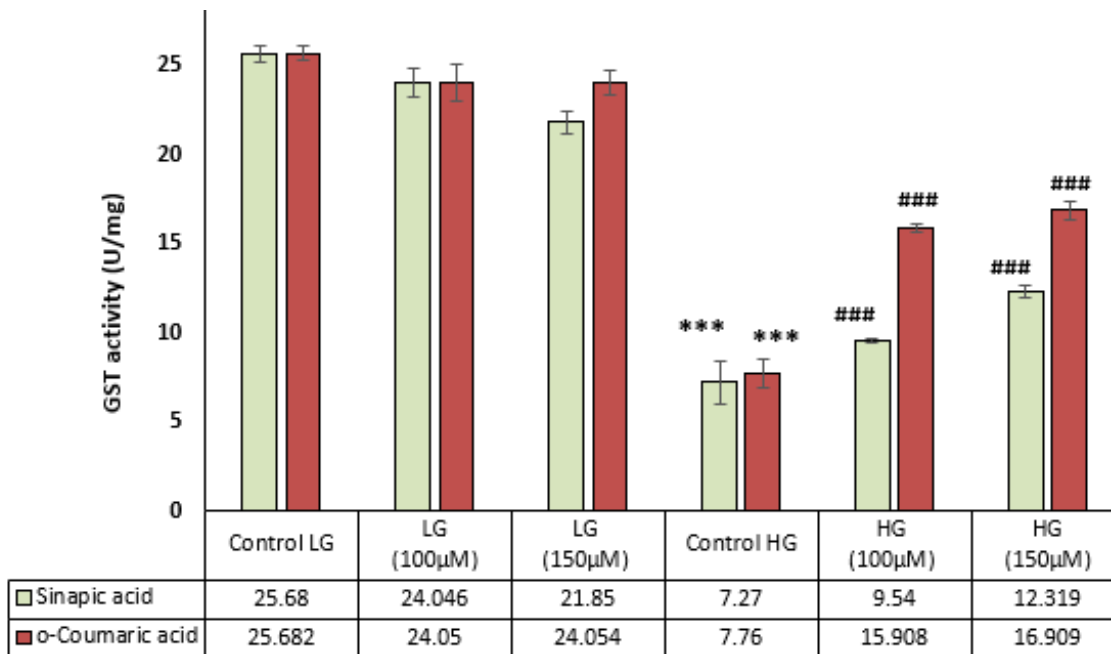
Fig 6.41: Effect of Sinapic acid and o-Coumaric acid at 100 µM and 150 µM concentrations on GST activity under LG and HG condition using PNS after cell lysis.

All the values were represented as Mean ± S.E.M. (n=3), ***p<0.001, vs control LG and ###p<0.001, vs control HG.

6.6.4 SOD

Maintaining cellular health is a crucial role of SOD, as it safeguards cells from harmful free radicals, excessive oxygen radicals, and other substances that hasten cellular aging or death. Our results showed that the untreated hyperglycemic/ HG group displayed lower amounts of SOD compared to both Sinapic acid and o-Coumaric acid treated HG or LG group. Briefly, the treatment of Sinapic acid to the LG treated group at 100 µM and 150 µM concentrations did not increase SOD levels i.e. 191.65±3.81 U/mg and 197±0.75 U/mg, although, there was a minor change in the SOD levels when compared to the control untreated LG group i.e. 206.82±3.14 U/mg. Similarly, the treatment of Sinapic acid to the HG treated group at 100 µM and 150 µM concentrations effectively restored the SOD levels to 109.66±1.189 U/mg and 90.04±2.621 U/mg, compared to control untreated HG group i.e. 44.67±1.763 U/mg respectively. Whereas, the treatment of o-Coumaric acid to the LG treated group at 100 µM and 150 µM concentrations effectively restored the SOD levels to 70.44±0.3 U/mg and 72.29±1.529 U/mg, compared to untreated LG treated group i.e. 73.75±0.36 U/mg. Similarly, the treatment of o-Coumaric acid to the HG treated group at 100 µM and 150 µM concentrations effectively restored the SOD levels to 37.57±0.487 U/mg and 29.72±1.04 U/mg, compared to control untreated HG group i.e. 10.21±0.704 U/mg respectively. Based on our results, the application of Sinapic acid and o-Coumaric acid at both concentrations led to a significant reduction in oxidative stress by restoring SOD levels, as depicted in Fig 6.42.

	Control LG	LG (100µM)	LG (150µM)	Control HG	HG (100µM)	HG (150µM)
Sinapic acid	206.82	191.65	197	44.67	109.66	90.04
o-Coumaric acid	73.75	70.44	72.29	10.21	37.57	29.72
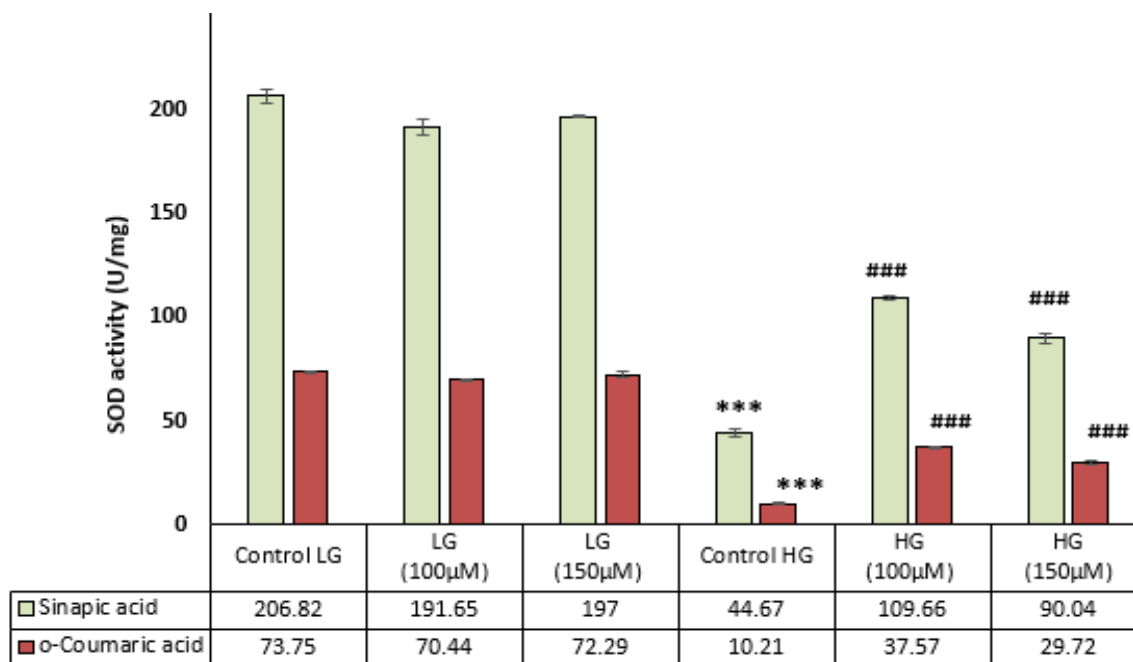
Fig 6.42: Effect of Sinapic acid and o-Coumaric acid at 100 µM and 150µM concentrations on SOD activity under LG and HG condition using PNS after cell lysis.

All the values were represented as Mean ± S.E.M. (n=3), ***$p<0.001$, vs control LG and ###$p<0.001$, vs control HG.

6.6.5 Catalase

An enzyme called catalase helps eliminate hydrogen peroxide (H_2O_2) from living cells. The impairment of pancreatic cells caused by elevated levels of H2O2 results in an insulin production and signaling imbalance. This, in turn, disrupts glucose metabolism and contributes to the onset of diabetes. Our results showed that the untreated hyperglycemic/HG group displayed lower amounts of catalase compared to both Sinapic acid and o-Coumaric acid treated HG or LG group. Briefly, the treatment with Sinapic acid in the LG treated group at 100 µM and 150 µM concentrations showed a negligible change in catalase levels up to 77.9±3.81 U/mg and 78.12±0.75 U/mg, compared to the control untreated LG group i.e. 78.65±0.36 U/mg. Similarly, the treatment of Sinapic acid to the HG treated group at 100 µM and 150 µM concentrations effectively restored the catalase levels to 23.005±1.189 U/mg and 35.028±2.621 U/mg, compared to control untreated HG group i.e. 12.36±0.704 U/mg respectively. Whereas, the treatment of o-Coumaric acid to the LG treated group at 100 µM and 150 µM concentrations effectively restored the SOD levels to 78.328±0.3 U/mg and 78.547±1.529 U/mg, compared to the untreated LG treated group i.e. 78.65±0.36 U/mg. Similarly, the treatment of o-Coumaric acid to the HG treated group at 100 µM and 150 µM concentrations effectively enhanced the catalase levels to 36.05±0.487 U/mg and 40.99±1.04 U/mg, compared to control untreated HG group i.e. 12.36±0.704 U/mg respectively. Based on our findings, the administration of Sinapic acid and o-Coumaric acid at both

concentrations led to a significant reduction in oxidative stress, as evidenced by the restoration of catalase levels, as depicted in the Fig 6.43.

	Control LG	LG (100µM)	LG (150µM)	Control HG	HG (100µM)	HG (150µM)
Sinapic acid	78.65	77.9	78.12	12.36	23.005	35.028
o-Coumaric acid	78.65	78.328	78.547	12.36	36.05	40.99
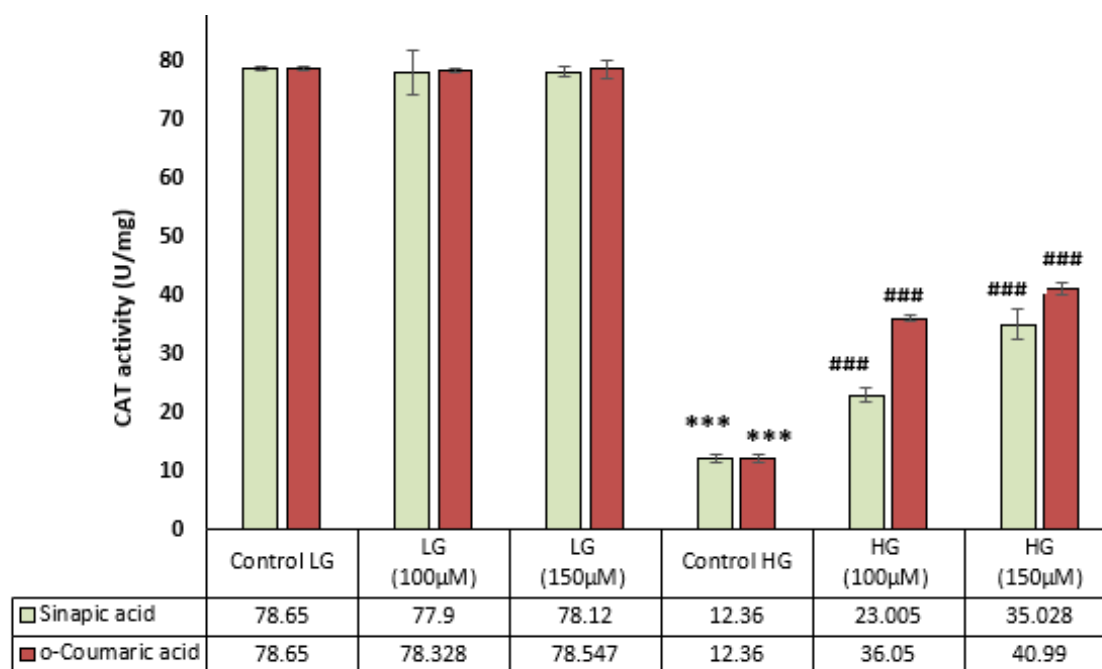
Fig 6.43: Effect of Sinapic acid and o-Coumaric acid at 100 µM and 150µM concentrations on catalase activity under LG and HG condition using PNS after cell lysis.

All the values were represented as Mean ± S.E.M. (n=3), ***$p < 0.001$, vs control LG and ###$p < 0.001$, vs control HG.

6.7 In vivo experimental data

Given the promising antioxidant, anti-diabetic, and wound-healing properties demonstrated by both compounds in our in vitro findings, we opted to evaluate the potential of only Sinapic acid in the animal model, as it exhibited more significant results than o-Coumaric acid. For the in vivo study, a total of 54 SD rats were procured, divided into 8 groups, and administered various nutritional supplements, including NPD and HFD.

6.7.1 Body weight estimation

The body weight was recorded on a weekly basis throughout the entire duration of the study, starting from its commencement and concluding at its endpoint. During the first week, where all rats were on a NPD, and the second week, when the diabetic group rats were transitioned to HFD, there was not a substantial difference in the body weight. Following the third week of the HFD, there was an observable increase in the rats' body weight, and after 14 days of treatment, a reduction in body weight was also noted, as depicted in Fig 6.44.
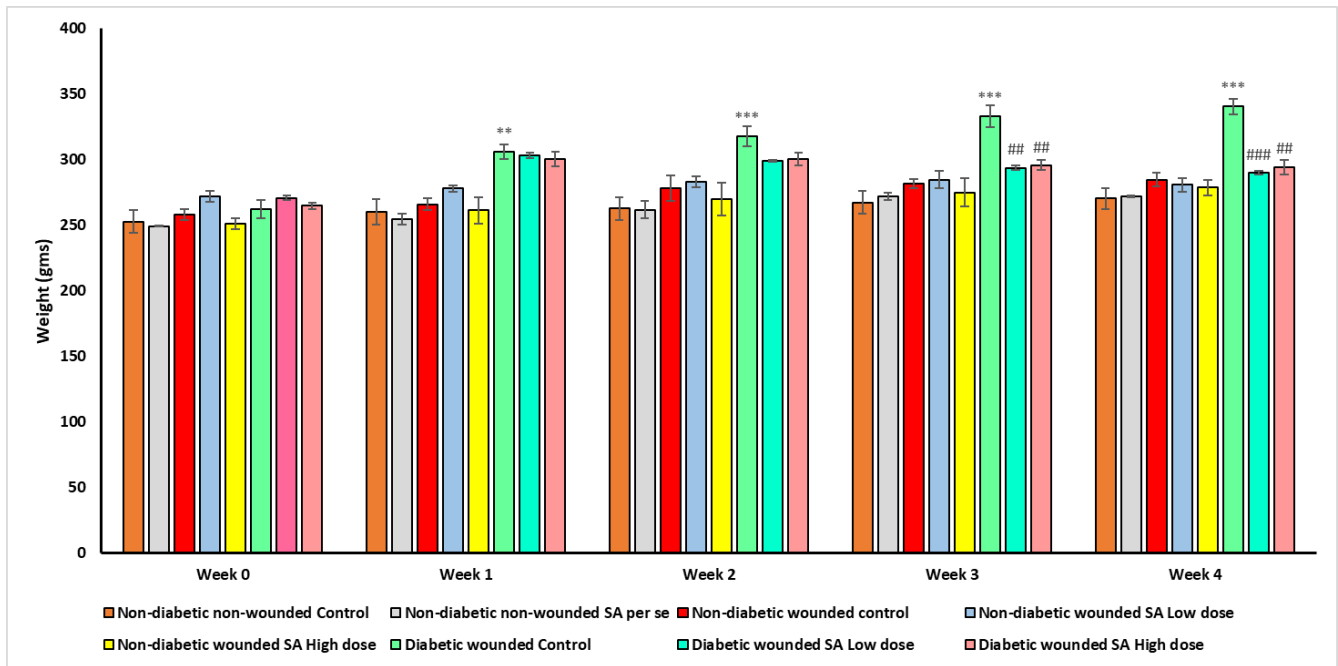
Fig 6.44: Impact of various treatments on the body weight of rats.

The data is represented as Mean ± S.E.M. (n=3), ***symbolises $p<0.001$, **symbolises $p<0.01$, when in comparison with the non-diabetic non-wounded control group; ###symbolises $p<0.001$, ##symbolises $p<0.01$, when in comparison to the diabetic wounded control group.

6.7.2 Blood glucose estimation

Blood glucose levels were measured at the initiation of the study (prior to treatment) and its conclusion (post-treatment) utilizing a glucometer. In the HFD/STZ-induced diabetic rats, the 40 mg/kg, i.p. dose of STZ led to heightened hyperglycemia, with blood glucose levels exceeding 250 mg/dl indicating the onset of diabetes. Following the induction of diabetes, a wound was generated, and treatment commenced from the subsequent day. Rats in Group 6, the vehicle control (0.5% carboxy methyl cellulose), exhibited elevated glucose levels throughout the study duration. In Group 7, rats administered a low dose (20 mg/kg) of Sinapic acid exhibited a decline in blood glucose levels. Meanwhile, Group 8 rats, treated with a high dose (40 mg/kg) of Sinapic acid, displayed a noteworthy reduction in blood glucose levels, as depicted in Fig 6.45.
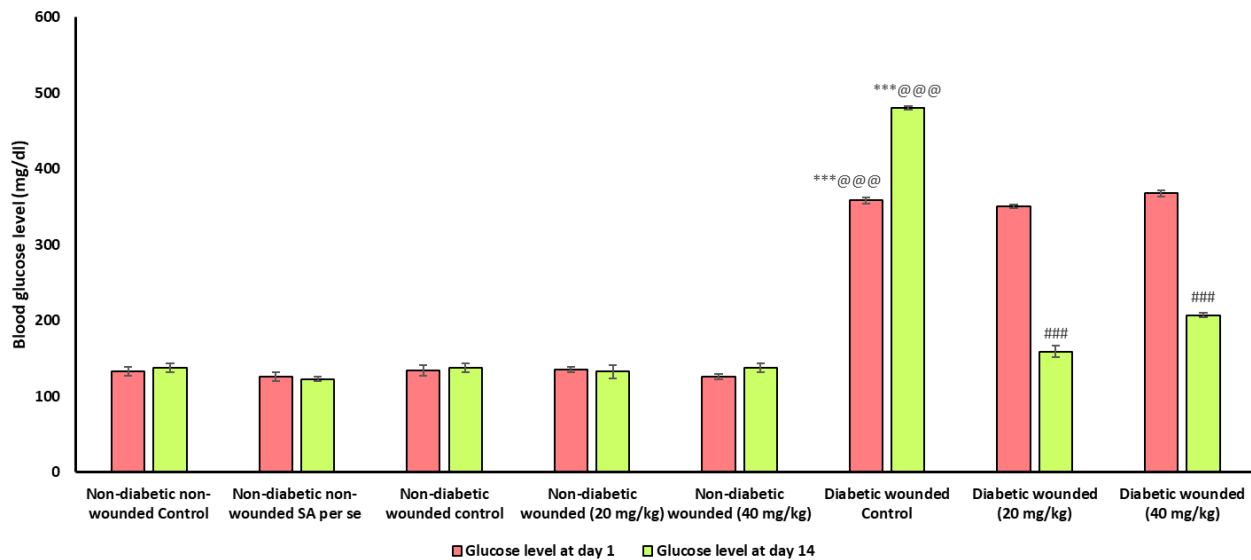
Fig 6.45: Impact of Sinapic acid on blood glucose of rats.

The data is represented as Mean ± S.E.M. (n=3), ***symbolises $p<0.001$, when in comparison with the non-diabetic non-wounded control group; @@@symbolises $p<0.001$, when in comparison to the non-diabetic wounded control group; ###symbolises $p<0.001$, when in comparison to the diabetic wounded control group.

6.7.3 Biochemical parameters

6.7.3.1 Lipid profile estimation

Insulin resistance and impaired lipid metabolism are closely linked to lipid accumulation in diabetes. During hyperglycemia, the body's cells become less sensitive to the actions of insulin, which is the primary symbol of T2D. These metabolic disorders cause lipid build-up, especially in organs such as the liver and skeletal muscles. In the present study, the levels of cholesterol, triglyceride, HDL, VLDL and LDL in the blood serum of overnight fasted animals were tested.

6.7.3.1.1 Cholesterol estimation

Our results showed that non-diabetic non-wounded control rats receiving NPD had lower levels of cholesterol i.e. 70±2 mmol/L, whereas the feeding of NPD to non-diabetic wounded rats had increased level of cholesterol i.e. 92±1 mmol/L. Similarly, compared to non-diabetic wounded rats (70±2 mmol/L), the level of cholesterol was reduced upon receiving the treatment of Sinapic acid at both 20 mg/kg and 40 mg/kg doses i.e. 85.5±50.5 mmol/L and 91±1 mmol/L respectively. On the contrary, the feeding of HFD to diabetic rats exhibit higher cholesterol levels up to 111.5±0.5 mmol/L, when compared to non-diabetic rats i.e. 92±1 mmol/L. In addition, the levels of cholesterol in diabetic wounded rats were significantly reduced upon receiving the treatment of Sinapic acid at both 20 mg/kg and 40 mg.kg i.e. 99±1 mmol/L and 101±2 mmol/L, compared to diabetic wounded rats receiving HFD treatment i.e. 111.5±0.5 mmol/L (Fig 6.46). The outcomes of this experiment

revealed that the administration of Sinapic acid, at both dosage levels, led to a significant reduction in cholesterol levels in diabetic wounded rats.
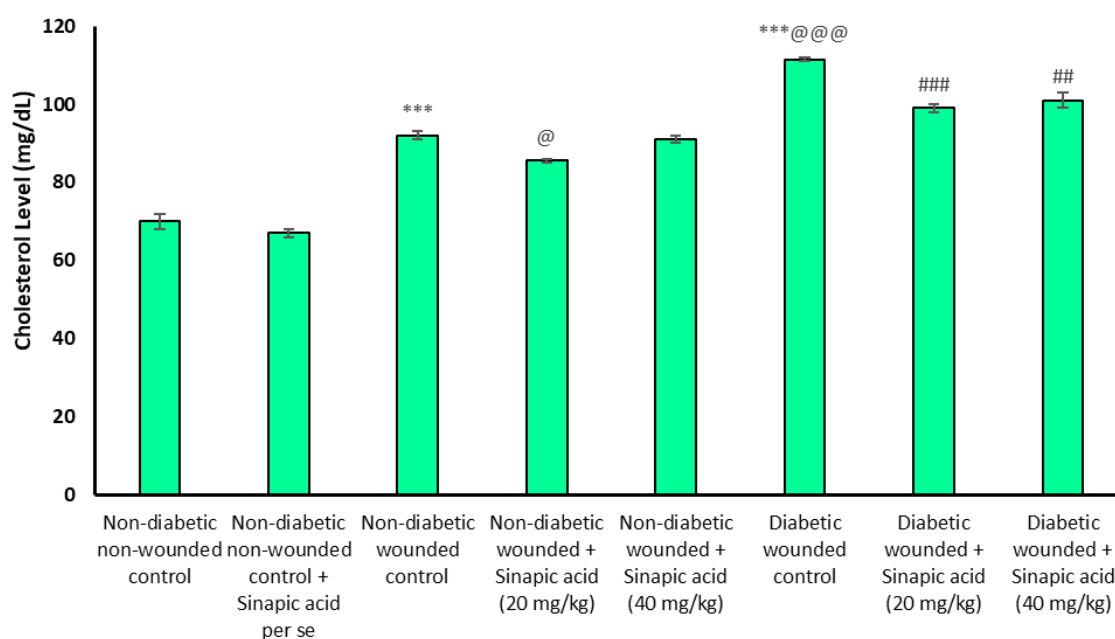
Fig 6.46: Graph showing variation in cholesterol level on different groups.

The data is represented as Mean ± S.E.M. (n=3), ***symbolises $p < 0.001$, when in comparison with the non-diabetic non-wounded control group; @@@symbolises $p < 0.001$, and @symbolizes $p < 0.05$, when in comparison with the non-diabetic wounded control group; ###symbolises $p < 0.001$, and ##symbolises $p < 0.01$, when in comparison to the diabetic wounded control group.

6.7.3.1.2 Triglyceride estimation

Subsequently, we endeavored to investigate the impact of Sinapic acid on triglyceride levels in diabetic wounded rats. Our results showed that non-diabetic non-wounded control rats receiving NPD had lower levels of triglycerides i.e. 77.5 ± 1.5 mg/dL, whereas the feeding of NPD to non-diabetic wounded rats had increased level of triglycerides i.e. 87 ± 1 mg/dL. Similarly, compared to non-diabetic wounded rats (87 ± 1 mg/dL), the level of triglycerides was reduced upon receiving the treatment of Sinapic acid at both 20 mg/kg and 40 mg/kg doses i.e. 82.5 ± 0.5 mg/dL and 85.5 ± 1.5 mg/dL respectively. On the contrary, the feeding of HFD to diabetic rats shows higher triglycerides levels up to 148.5 ± 2.5 mg/dL, when compared to non-diabetic rats i.e. 87 ± 1 mg/dL. In addition, the levels of triglycerides in diabetic wounded rats were significantly reduced upon receiving the treatment of Sinapic acid at both 20 mg/kg and 40 mg.kg i.e. 129.5 ± 1.5 mg/dL and 138.5 ± 2.5 mg/dL, compared to diabetic wounded rats receiving HFD i.e. 148.5 ± 2.5 mg/dL (Fig 6.47). In summary, our findings indicate that the administration of Sinapic acid treatment, at both dosage levels, resulted in a significant reduction in triglyceride levels in diabetic wounded rats.

Fig 6.47: Graph showing variation in triglyceride level in different treatment groups.

The data is represented as Mean ± S.E.M. (n=3), ***symbolises $p<0.001$, and *symbolizes $p<0.05$, when in comparison with the non-diabetic non-wounded control group; @@@symbolises $p<0.001$, when in comparison with the non-diabetic wounded control group; ###symbolises $p<0.001$, and #symbolises $p<0.05$, when in comparison to the diabetic wounded control group.

6.7.3.1.3 HDL estimation

In addition to cholesterol and triglyceride levels, we also analyzed HDL levels in diabetic wounded rats receiving Sinapic acid. Our results showed that non-diabetic non-wounded control rats receiving NPD had higher levels of HDL i.e. 34±1 mg/dL, whereas the feeding of NPD to non-diabetic wounded rats had reduced level of HDL i.e. 27±1 mg/dL. Similarly, compared to non-diabetic wounded rats (27±1 mg/dL), the level of HDL (29±1 mg/dL) was increased upon receiving the treatment of Sinapic acid at 20 mg/kg, whereas at 40 mg/kg doses their levels were reduced i.e. 23.5±1.5 mg/dL. On the contrary, the feeding of HFD to diabetic rats exhibit lower HDL levels up to 21.5±1.5 mg/dL, when compared to non-diabetic rats i.e. 27±1 mg/dL. In addition, the levels of HDL in diabetic wounded rats were significantly restored upon receiving the treatment of Sinapic acid at both 20 mg/kg and 40 mg.kg i.e. 29.5±0.5 mg/dL and 27±1 mg/dL, compared to diabetic wounded rats receiving HFD treatment i.e. 21.5±1.5 mg/dL (Fig 6.48). Consequently, our data revealed that the therapy of Sinapic acid at 20 mg/kg yielded more favourable results compared to the 40 mg/kg dose.

Fig 6.48: Graph showing variation in HDL level in different treatment groups.

The data is represented as Mean ± S.E.M. (n=3), ***symbolises $p<0.001$, and *symbolises $p<0.05$, when in comparison with the non-diabetic non-wounded control group; @symbolises $p<0.05$, when in comparison to the non-diabetic wounded control group; ##symbolises $p<0.01$, and #symbolises $p<0.05$, when in comparison to the diabetic wounded control group.

6.7.3.1.4 VLDL estimation

Continuing these lipid parameters, we also analyzed VLDL levels in the diabetic and treated groups. Our results showed that non-diabetic non-wounded control rats receiving NPD had lower levels of VLDL i.e. 15.6±0.4 mg/dL, whereas the feeding of NPD to non-diabetic wounded rats had increased level of VLDL i.e. 20±1 mg/dL. Similarly, compared to non-diabetic wounded rats (20±1 mg/dL), the level of VLDL (17.3±0.7 mg/dL) was reduced upon receiving the therapy of Sinapic acid at 20 mg/kg, and these levels were further reduced to 14.1±1.9 mg/dL upon receiving Sinapic acid treatment at 40 mg/kg doses. On the contrary, the feeding of HFD to diabetic rats exhibit higher VLDL levels up to 30.9±0.1 mg/dL, when compared to non-diabetic rats i.e. 20±1 mg/dL. Furthermore, the administration of Sinapic acid at both 20 mg/kg and 40 mg/kg significantly decreased the levels of VLDL in diabetic wounded rats, measuring 24.15±0.15 mg/dL and 25.4±0.4 mg/dL, respectively, in comparison to diabetic wounded rats treated with a HFD, which recorded 30.9±0.1 mg/dL (Fig 6.49). Consequently, our data indicate that the administration of Sinapic acid at a dose of 20 mg/kg produces more favourable results compared to the 40 mg/kg dose.

Fig 6.49: Graph showing variation in VLDL level in different treatment groups.

The data is represented as Mean ± S.E.M. (n=3), ***symbolises p<0.001, when in comparison with the non-diabetic non-wounded control group; @@@symbolises p<0.001, and @@symbolises p<0.01, when in comparison to the non-diabetic wounded control group; ##symbolises p<0.01, and #symbolises p<0.05, when in comparison to the diabetic wounded control group.

6.7.3.1.5 LDL estimation

Besides cholesterol, triglycerides, HDL, VLDL levels, we also analyzed the level of LDL in diabetic wounded and treated groups. Our results showed that non-diabetic non-wounded control rats receiving NPD had lower levels of LDL i.e. 30.9±0.1 mg/dL, whereas the feeding of NPD to non-diabetic wounded rats had increased level of LDL i.e. 47.7±0.7 mg/dL. Similarly, compared to non-diabetic wounded rats (47.7±0.7 mg/dL), the level of LDL (43.7±0.7 mg/dL) was reduced upon receiving the treatment of Sinapic acid at 20 mg/kg, and these levels were not much reduced upon receiving Sinapic acid treatment at 40 mg/kg doses i.e. 47.4±1.4 mg/dL. On the contrary, the feeding of HFD to diabetic rats exhibit higher LDL levels up to 67±2 mg/dL, when compared to non-diabetic rats i.e. 47.7±0.7 mg/dL. Moreover, the levels of LDL in diabetic wounded rats exhibited a significant reduction with the treatment of Sinapic acid at both 20 mg/kg and 40 mg/kg, measuring 59.5±0.5 mg/dL and 61±1 mg/dL, respectively, in contrast to diabetic wounded rats treated with a HFD, which registered 67±2 mg/dL (Fig 6.50). In summary, our data indicate that the therapy of Sinapic acid at a dose of 20 mg/kg yields more favourable results compared to the 40 mg/kg dose.

Fig 6.50: Graph showing variation in LDL level in different treatment groups.

The data is represented as Mean ± S.E.M. (n=3), ***symbolises p<0.001, when in comparison with the non-diabetic non-wounded control group; @@@symbolises p<0.001, when in comparison to the non-diabetic wounded control group; ##symbolises p<0.01, and #symbolises p<0.05, when in comparison to the diabetic wounded control group.

6.7.3.2 Kidney profile estimation

The kidneys' tiny filters, known as glomeruli, help remove waste and excess fluid from the blood. Due to increased pressure on the kidneys due to diabetes, elevated blood sugar levels can cause an increase in pressure inside the glomeruli. This excess pressure has the potential to damage the filtration system over time. Therefore, after analyzing the impact of Sinapic acid at both doses on lipid parameters, it was essential to evaluate its effect on nephrotoxicity markers in diabetic animals to determine whether it had a beneficial or detrimental effect on disease progression.

6.7.3.2.1 Urea estimation

Our results showed that non-diabetic non-wounded control rats receiving NPD had lower levels of urea i.e. 38.5±0.5 mg/dL, whereas the feeding of NPD to non-diabetic wounded rats had increased level of these kidney parameters i.e. 55±1 mg/dL. Similarly, compared to non-diabetic wounded rats (55±1 mg/dL), the level of urea was reduced upon receiving the treatment of Sinapic acid at 20 mg/kg dose i.e. 53±2 mg/dL. Compared to Sinapic acid treatment at 20 mg/kg dose, the level of urea was found to increase upon treatment with Sinapic acid at 40 mg/kg dose i.e. 54.25±0.25 mg/dL. On the contrary, the feeding of HFD to diabetic rats exhibited higher levels of urea up to 74.5±0.5 mg/dL, when compared to non-diabetic rats i.e. 55±1 mg/dL. In addition, the levels of this kidney functioning markers in diabetic wounded rats were significantly reduced upon receiving the treatment of Sinapic acid at both 20 mg/kg and 40 mg/kg i.e. 66±1 mg/dL and 67.5±0.5 mg/dL, compared to diabetic wounded rats receiving HFD treatment i.e. 74.5±0.5 mg/dL (Fig 6.51). Overall, our data revealed a notable enhancement in the function of nephrotoxicity markers in diabetic rats receiving Sinapic

acid treatment at both dosage levels. However, more pronounced results were observed when treated with Sinapic acid at a dose of 20 mg/kg.

Fig 6.51: Graph showing variation in urea level in different treatment groups.

The data is represented as Mean ± S.E.M. (n=3), ***symbolises p<0.001, when in comparison with the non-diabetic non-wounded control group; @@@symbolises p<0.001, when in comparison to the non-diabetic wounded control group; ##symbolises p<0.01, and #symbolises p<0.05, when in comparison to the diabetic wounded control group.

6.7.3.2.2 Creatinine estimation

Our results showed that non-diabetic non-wounded control rats receiving NPD had lower levels of creatinine i.e. 0.445±0.005 mg/dL, whereas the feeding of NPD to non-diabetic wounded rats had increased level of these kidney parameters i.e. 0.51±0.02 mg/dL. Similarly, compared to non-diabetic wounded rats (0.51±0.02 mg/dL), the level of creatinine was reduced upon receiving the treatment of Sinapic acid at 20 mg/kg dose i.e. 0.475±0.005 mg/dL. Compared to Sinapic acid treatment at 20 mg/kg dose, the level of creatinine was found to increase upon treatment with Sinapic acid at 40 mg/kg dose i.e. 0.48±0.01 mg/dL. On the contrary, the feeding of HFD to diabetic rats exhibited higher levels of creatinine up to 0.565±0.015 mg/dL, when compared to non-diabetic rats i.e. 0.51±0.02 mg/dL. In addition, the levels of these kidney functioning markers in diabetic wounded rats were significantly reduced upon receiving the treatment of Sinapic acid at both 20 mg/kg and 40 mg/kg i.e. 0.475±0.005 mg/dL, and 0.495±0.015 mg/dL, compared to diabetic wounded rats receiving HFD treatment i.e. 0.565±0.015 mg/dL (Fig 6.52). Overall, our data illustrated a substantial enhancement in the performance of nephrotoxicity markers in diabetic rats treated with Sinapic acid at both dosage levels. However, more notable outcomes were observed when the treatment involved Sinapic acid at a dose of 20 mg/kg.
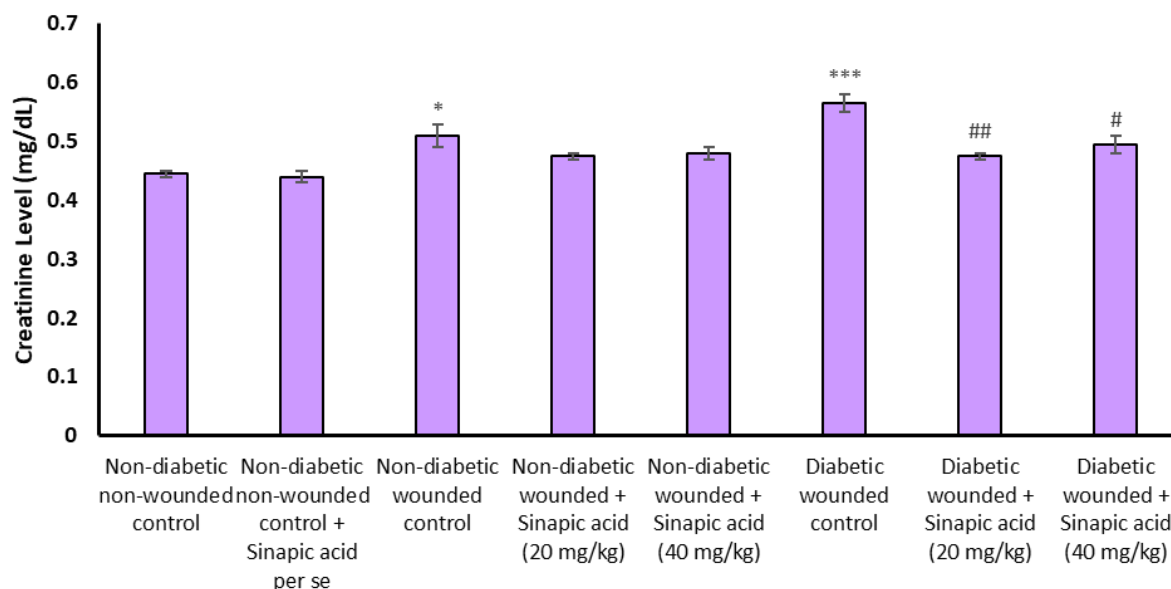
Fig 6.52: Graph showing variation in creatinine level in different treatment groups.

The data is represented as Mean ± S.E.M. (n=3), ***symbolises p<0.001, and *symbolizes p<0.05, when in comparison with the non-diabetic non-wounded control group; ##symbolises p<0.01, and #symbolises p<0.05, when in comparison to the diabetic wounded control group.

6.7.3.2.3 Uric acid estimation

Our results showed that non-diabetic non-wounded control rats receiving NPD had lower levels of uric acid i.e. 1.75±0.05 mg/dL, whereas the feeding of NPD to non-diabetic wounded rats had increased level of these kidney parameters i.e. 1.85±0.05 mg/dL. Similarly, compared to non-diabetic wounded rats (1.85±0.05 mg/dL), the level of urea, creatinine, and uric acid were reduced upon receiving the treatment of Sinapic acid at 20 mg/kg dose i.e. 1.65±0.15 mg/dL. Compared to Sinapic acid treatment at 20 mg/kg dose, the level of uric acid was found to increase upon treatment with Sinapic acid at 40 mg/kg dose i.e. 1.6±0.1 mg/dL respectively. On the contrary, the feeding of HFD to diabetic rats exhibited higher levels of uric acid up to 2.75±0.05 mg/dL, when compared to non-diabetic rats i.e. 1.85±0.05 mg/dL. In addition, the levels of these kidney functioning markers in diabetic wounded rats were significantly reduced upon receiving the treatment of Sinapic acid at both 20 mg/kg and 40 mg/kg i.e. 1.85±0.05 mg/dL, and 2±0.2 mg/dL, compared to diabetic wounded rats receiving HFD treatment i.e. 2.75±0.05 mg/dL (Fig 6.53). Broadly, our data indicated a noteworthy enhancement in the performance of nephrotoxicity markers in diabetic rats treated with Sinapic acid at both dosage levels. However, more pronounced results were observed when the treatment involved Sinapic acid at a dose of 20 mg/kg.
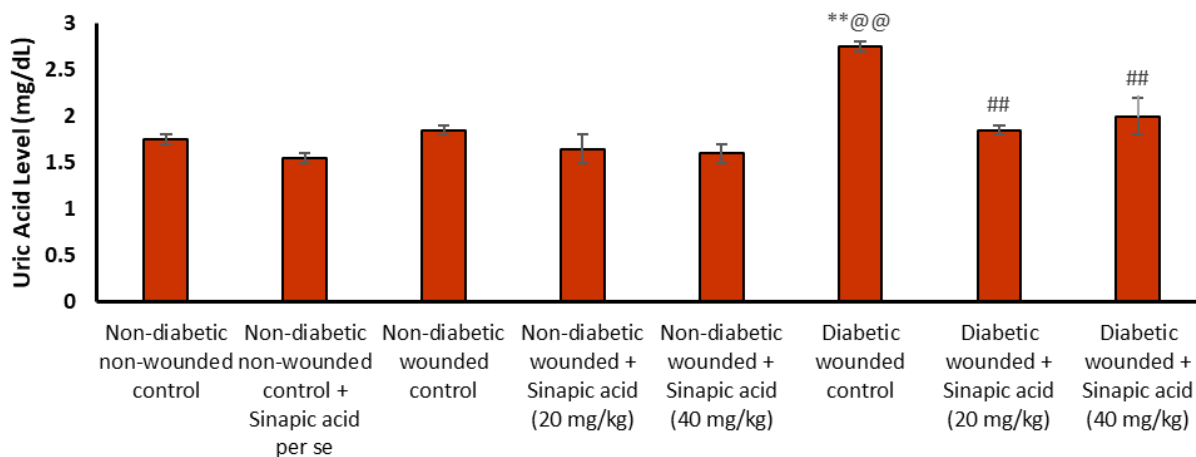
Fig 6.53: Graph showing variation in uric acid level in different treatment groups.

The data is represented as Mean ± S.E.M. (n=3), **symbolises $p < 0.01$, when in comparison with the non-diabetic non-wounded control group; @@symbolises $p < 0.01$, when in comparison with the non-diabetic wounded control group; ##symbolises $p < 0.01$, when in comparison to the diabetic wounded control group.

6.7.3.3 Hepatic profile estimation

HFDs, particularly those rich in saturated fat, have been associated with insulin resistance. For instance, insulin resistance may lead to heightened insulin secretion, potentially facilitating the hepatic fat storage process. Liver damage, including non-alcoholic fatty liver disease, can result from excess fat in the liver. Thus, it is important to analyze the hepatic profile of animals receiving HFD.

6.7.3.3.1 SGPT estimation

Besides lipid accumulation and renal profile, we sought to analyze the effect of Sinapic acid treatment at both doses (20 mg/kg and 40 mg/kg) in improving hepatic profile by measuring SGPT levels in diabetes rats. Our results showed that non-diabetic non-wounded control rats receiving NPD had lower levels of SGPT i.e. 75.5±0.5 U/L, whereas the feeding of NPD to non-diabetic wounded rats had increased level of SGPT i.e. 83±1 U/L. Similarly, compared to non-diabetic wounded rats (83±1 U/L), the level of SGPT (78.5±1.5 U/L) was reduced upon receiving the treatment of Sinapic acid at 20 mg/kg, and these levels were not much reduced upon receiving Sinapic acid treatment at 40 mg/kg doses i.e. 87±1 U/L. On the contrary, the feeding of HFD to diabetic rats exhibit higher SGPT levels up to 123±2 U/L, when compared to non-diabetic rats i.e. 83±1 U/L. In addition, the levels of SGPT in diabetic wounded rats were significantly reduced upon receiving the treatment of Sinapic acid at both 20 mg/kg and 40 mg.kg i.e. 105.5±1.5 U/L and 115.5±1.5 U/L, compared to diabetic wounded rats receiving HFD treatment i.e. 123±2 U/L (Fig 6.54). Overall, our data revealed a substantial enhancement in the performance of hepatotoxicity markers in diabetic rats treated with Sinapic acid at both dosage levels. However, more notable results were observed with Sinapic acid administered at a dose of 20 mg/kg.
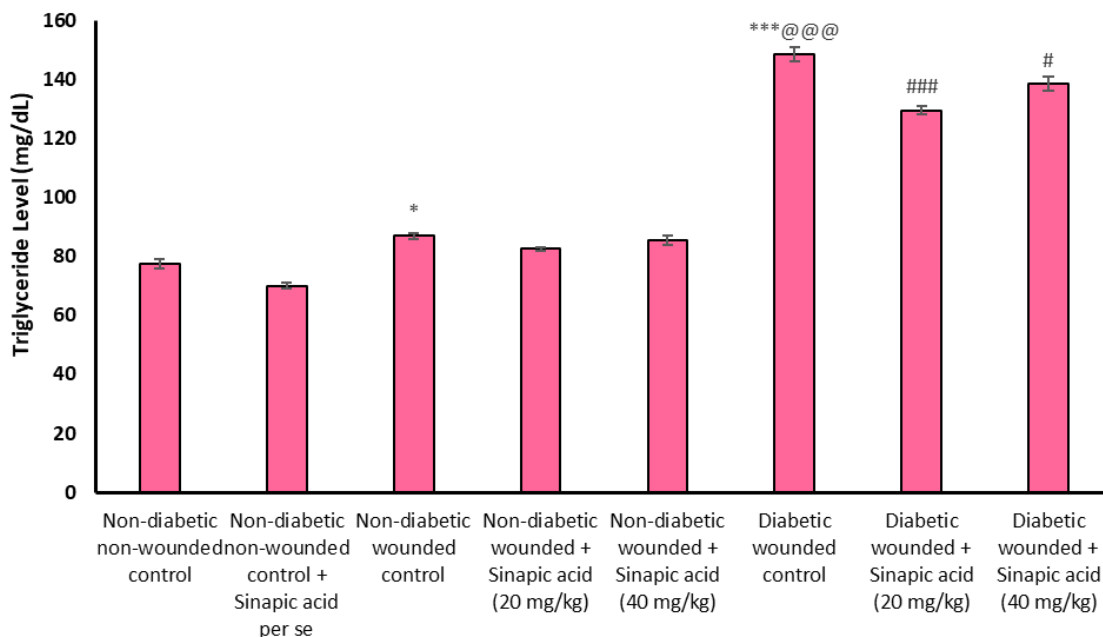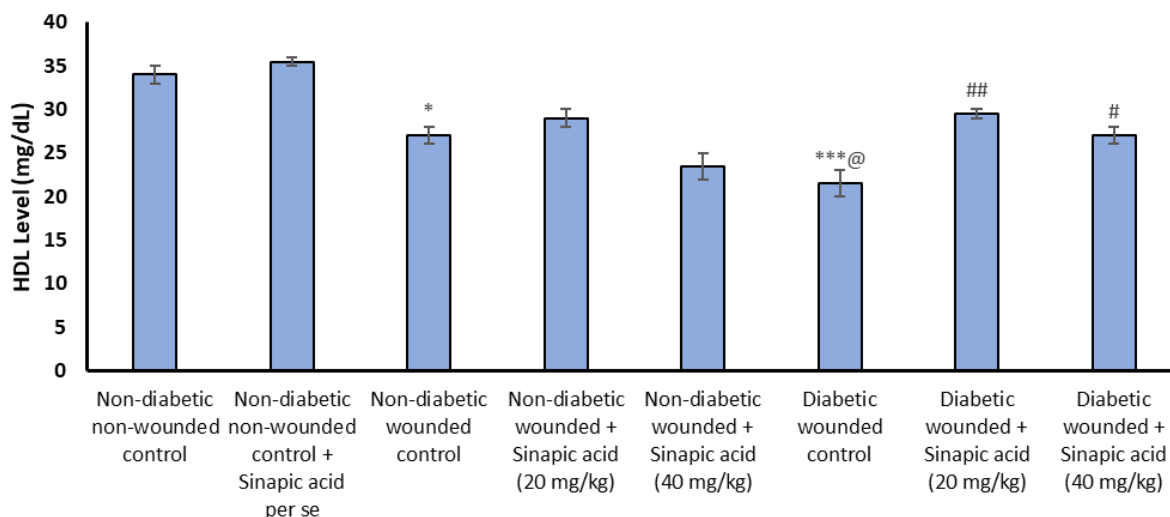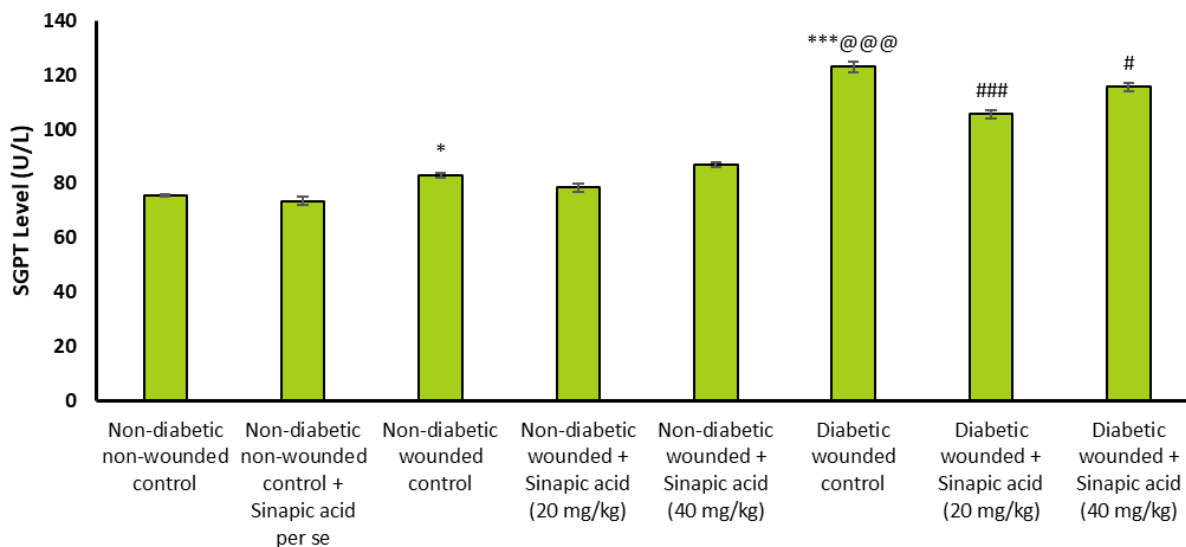
Fig 6.54: Graph showing variation in SGPT level in different treatment groups.

The data is represented as Mean ± S.E.M. (n=3), ***symbolises p<0.001, and *symbolises p<0.05, when in comparison with the non-diabetic non-wounded control group; @@@symbolises p<0.001, when in comparison to the non-diabetic wounded control group; ###symbolises p<0.001, and #symbolises p<0.05, when in comparison to the diabetic wounded control group.

6.7.3.3.2 SGOT estimation

Next, we sought to analyze the level of SGOT in diabetic rats after receiving the treatment of Sinapic acid with 20 mg/kg and 40 mg/kg doses. Our results showed that non-diabetic non-wounded control rats receiving NPD had lower levels of SGOT i.e. 91±1 U/L, whereas the feeding of NPD to non-diabetic wounded rats had increased level of SGOT i.e. 97±1 U/L. Similarly, compared to non-diabetic wounded rats (97±1 U/L), the level of SGOT (91.5±0.5 U/L) was reduced upon receiving the treatment of Sinapic acid at 20 mg/kg, and these levels were not much reduced upon receiving Sinapic acid treatment at 40 mg/kg doses i.e. 102±1 U/L. On the contrary, the feeding of HFD to diabetic rats exhibit higher SGOT levels up to 148±1 U/L, when compared to non-diabetic rats i.e. 97±1 U/L. In addition, the levels of SGOT in diabetic wounded rats were significantly reduced upon receiving the treatment of Sinapic acid at both 20 mg/kg and 40 mg.kg i.e. 137±1 U/L and 140.5±1.5 U/L, compared to diabetic wounded rats receiving HFD treatment i.e. 148±1 U/L (Fig 6.55). Overall, our data indicated a noteworthy enhancement in the performance of hepatotoxicity markers in diabetic rats treated with Sinapic acid at both dosage levels. However, more pronounced results were observed when the treatment involved Sinapic acid at a dose of 20 mg/kg.
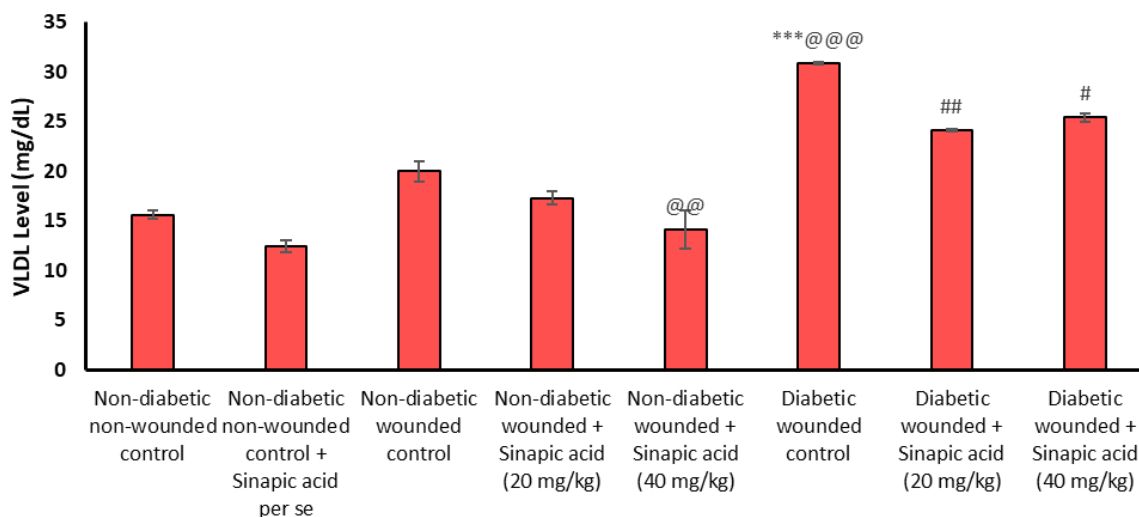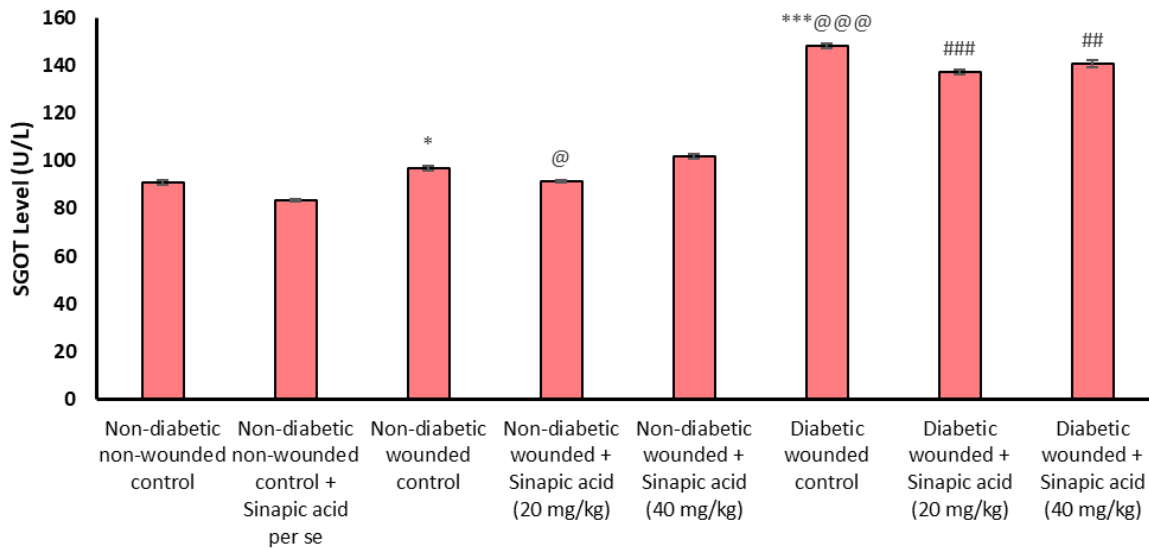
Fig 6.55: Graph showing variation in SGOT level in different treatment groups.

The data is represented as Mean ± S.E.M. (n=3), ***symbolises p<0.001, and *symbolises p<0.05, when in comparison with the non-diabetic non-wounded control group; @@@symbolises p<0.001, and @symbolises p<0.05, when in comparison to the non-diabetic wounded control group; ###symbolises p<0.001, and ##symbolises p<0.01, when in comparison to the diabetic wounded control group.

6.7.3.3.3 Bilirubin estimation

As hemoglobin, the oxygen-carrying protein in red blood cells, breaks down, bilirubin, a yellow pigment, is produced. It is a key element of the body's waste removal system and plays an imperative role in the liver. High level of bilirubin can lead to the hepatic failure, therefore, we sought to analyze the level of bilirubin in diabetic rats after receiving the treatment of Sinapic acid with 20 mg/kg and 40 mg/kg doses. Our results showed that non-diabetic non-wounded control rats receiving NPD had lower levels of bilirubin i.e. 0.065±0.005 U/L, whereas the feeding of NPD to non-diabetic wounded rats had increased level of bilirubin i.e. 0.115±0.005 U/L. Similarly, compared to non-diabetic wounded rats (0.115±0.005 U/L), the level of bilirubin (0.1±0.01 U/L) was reduced upon receiving the Sinapic acid at 20 mg/kg, and these levels were not much reduced upon receiving Sinapic acid treatment at 40 mg/kg doses i.e. 0.125±0.015 U/L. On the contrary, the feeding of HFD to diabetic rats exhibit higher bilirubin levels up to 0.175±0.015 U/L, when compared to non-diabetic rats i.e. 0.115±0.005 U/L. In addition, the levels of bilirubin in diabetic wounded rats were significantly reduced upon receiving the treatment of Sinapic acid at both 20 mg/kg and 40 mg.kg i.e. 0.115±0.005 U/L and 0.125±0.005 U/L, compared to diabetic wounded rats receiving HFD treatment i.e. 0.175±0.015 U/L (Fig 6.56). Broadly, our data indicated a substantial enhancement in the performance of hepatotoxicity markers in diabetic rats treated with Sinapic acid at both dosage levels. However, more notable results were observed when the treatment involved Sinapic acid at a dose of 20 mg/kg.
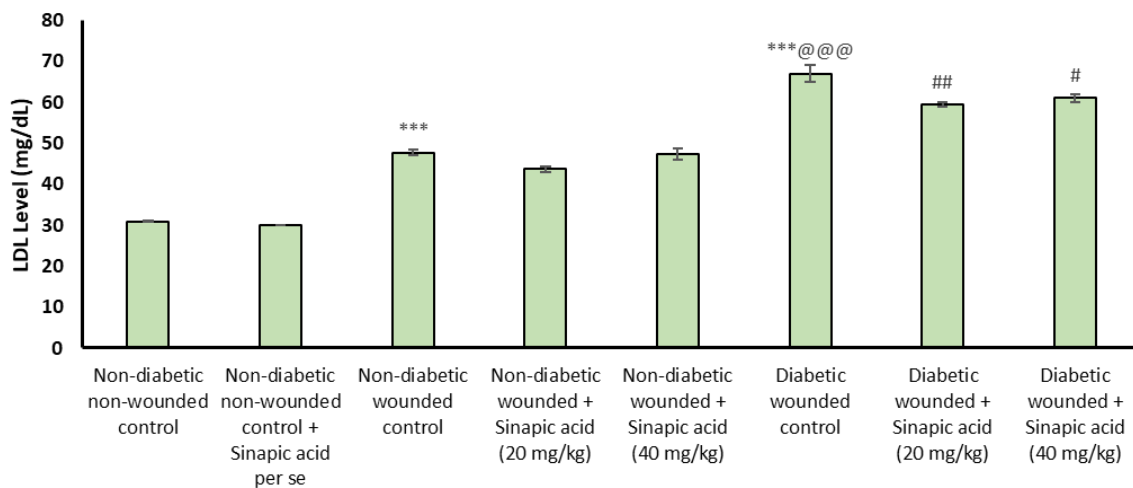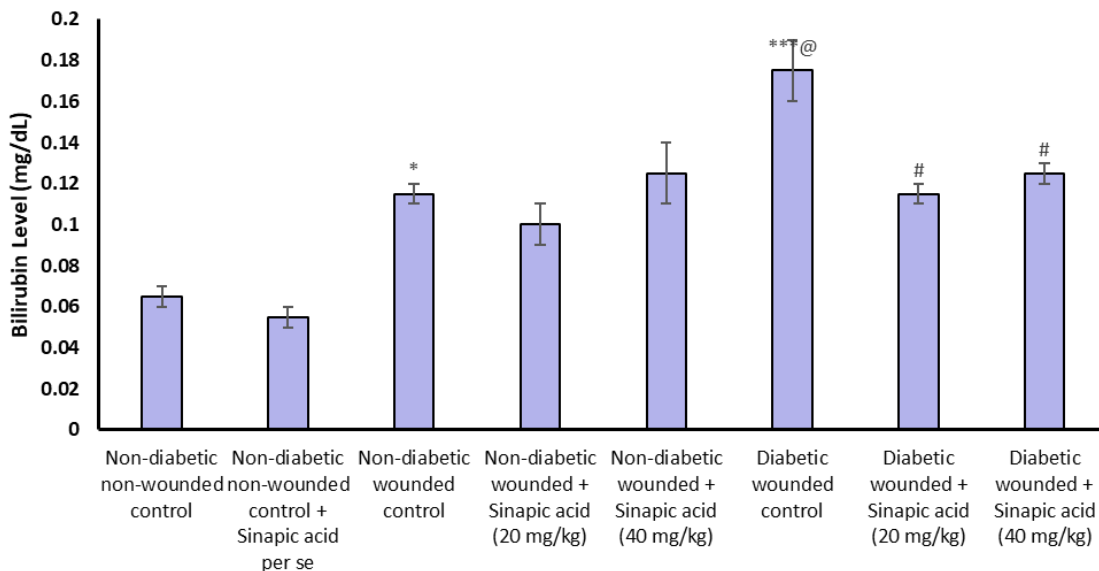
Fig 6.56: Graph showing variation in Bilirubin level in different treatment groups.

The data is represented as Mean ± S.E.M. (n=3), ***symbolises $p<0.001$, and *symbolises $p<0.05$, when in comparison to the non-diabetic non-wounded control group; @symbolises $p<0.05$, when in comparison to the non-diabetic wounded control group; #symbolises $p<0.05$, when in comparison to the diabetic wounded control group.

6.7.3.3.4 ALP estimation

Another important enzyme called ALP is present in many bodily tissues, but it is especially abundant in the liver, bone, bile ducts, and placenta during pregnancy. Since, the high level of this enzyme can lead to hepatic injury; therefore, it is important to investigate the level of this enzyme after treating the diabetic rats with Sinapic acid at both doses (20 mg/kg and 40 mg/kg). Our results showed that non-diabetic non-wounded control rats receiving NPD had lower levels of ALP i.e. 311±1 U/L, whereas the feeding of NPD to non-diabetic wounded rats had increased level of ALP i.e. 377.5±1.5 U/L. Similarly, compared to non-diabetic wounded rats (377.5±1.5 U/L), the level of ALP (356±1 U/L) was reduced upon receiving the treatment of Sinapic acid at 20 mg/kg, and these levels were not much reduced upon receiving Sinapic acid treatment at 40 mg/kg doses i.e. 370±1 U/L. On the contrary, the feeding of HFD to diabetic rats exhibit higher ALP levels up to 506.5±2.5 U/L, when compared to non-diabetic rats i.e. 377.5±1.5 U/L. In addition, the levels of ALP in diabetic wounded rats were significantly reduced upon receiving the treatment of Sinapic acid at both 20 mg/kg and 40 mg.kg i.e. 486±3 U/L and 492.5±1.5 U/L, compared to diabetic wounded rats receiving HFD treatment i.e. 506.5±2.5 U/L (Fig 6.57). Broadly, our data indicated a substantial enhancement in the performance of hepatotoxicity markers in diabetic rats treated with Sinapic acid at both dosage levels. However, more notable results were observed when the treatment involved Sinapic acid at a dose of 20 mg/kg.
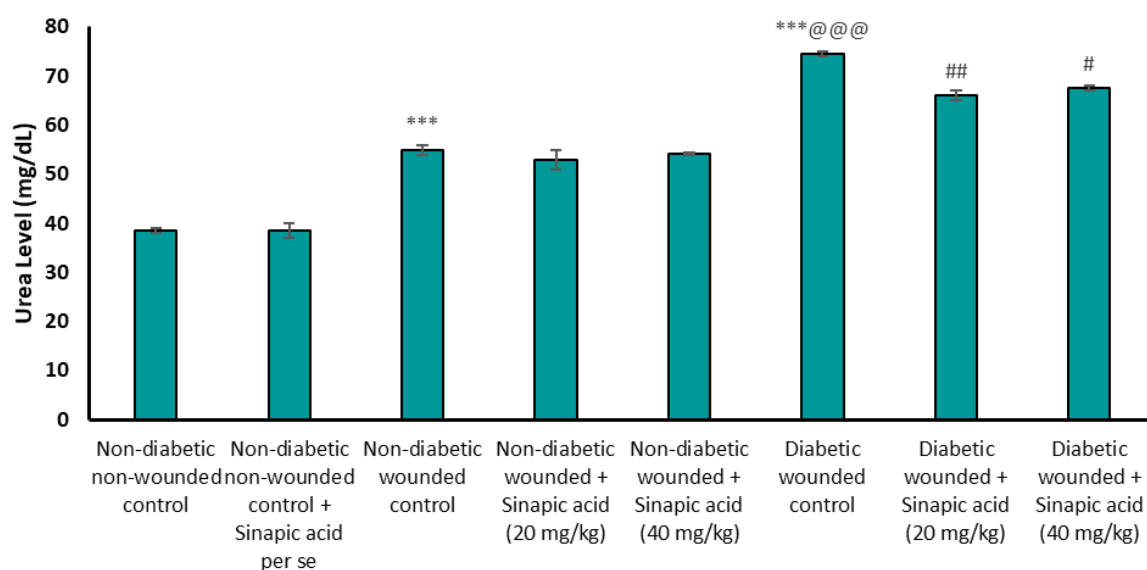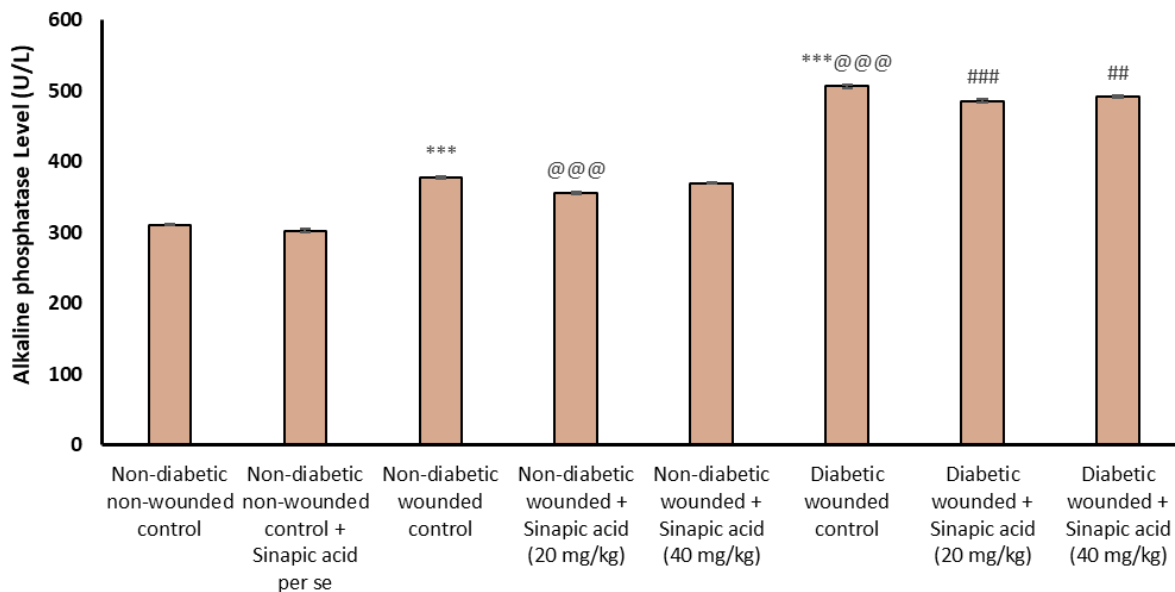
Fig 6.57: Graph showing variation in ALP level in different treatment groups.

The data is represented as Mean ± S.E.M. (n=3), ***symbolises $p < 0.001$, when in comparison to the non-diabetic non-wounded control group; @@@symbolises $p < 0.001$, when in comparison to the non-diabetic wounded control group; ###symbolises $p < 0.001$, and ##symbolises $p < 0.01$, when in comparison to the diabetic wounded control group.

6.7.4 In vivo oxidative marker

6.7.4.1 Protein estimation in tissue homogenate using Lowry's method

The total protein content, crucial for expressing enzyme-specific activity, is determined using the established technique described by Lowry et al. (Fig 6.58).
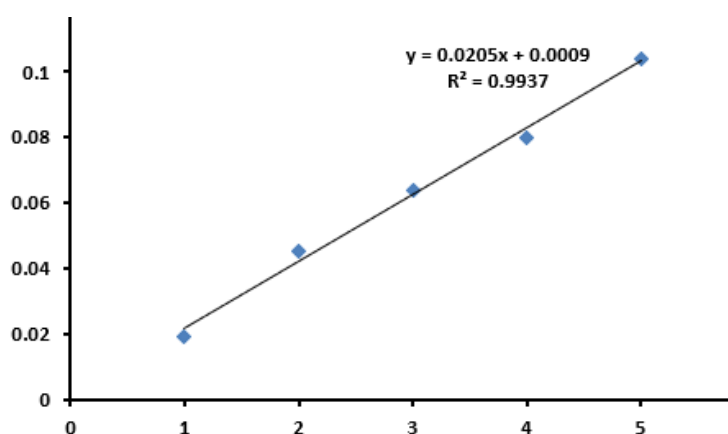
Fig 6.58: Protein estimation using the Lowry method.

6.7.4.2 LPO

Excessive LPO can result from hyperglycemia. Consequently, we aimed to assess the extent of LPO in the kidney and skin tissues of male diabetic rats following the Sinapic acid therapy at doses of 20 mg/kg and 40

122

mg/kg. Our results showed that non-diabetic non-wounded control rats receiving NPD had lower levels of LPO in kidney and skin tissues i.e. 0.014±0.001 µmol MDA/mg and 0.012±0.0006 µmol MDA/mg, whereas the feeding of NPD to non-diabetic wounded rats had increased level of LPO i.e. 0.030±0.0007 µmol MDA/mg and 0.020±0.0001 µmol MDA/mg respectively. Similarly, compared to non-diabetic wounded rats (0.030±0.0007 µmol MDA/mg and 0.020±0.0001 µmol MDA/mg), the level of LPO in kidney and skin tissues (0.017±0.0043 µmol MDA/mg and 0.015±0.0002 µmol MDA/mg) was reduced upon receiving the treatment of Sinapic acid at 20 mg/kg, and these levels were not much reduced upon receiving Sinapic acid treatment at 40 mg/kg doses i.e. 0.020±0.001 µmol MDA/mg and 0.020±0.001 µmol MDA/mg. On the contrary, the feeding of HFD to diabetic rats exhibit higher level of LPO in kidney and skin tissues up to 0.059±0.001 µmol MDA/mg and 0.049±0.008 µmol MDA/mg, when compared to non-diabetic rats i.e. 0.030±0.0007 µmol MDA/mg and 0.020±0.0001 µmol MDA/mg. In addition, the levels of LPO in kidney and skin tissues of diabetic wounded rats were significantly reduced upon receiving the treatment of Sinapic acid at both 20 mg/kg and 40 mg/kg i.e. 0.036±0.003 µmol MDA/mg, 0.045±0.004 µmol MDA/mg, and 0.027±0.001 µmol MDA/mg, 0.028±0.003 µmol MDA/mg, compared to diabetic wounded rats receiving HFD treatment i.e. 0.059±0.001 µmol MDA/mg and 0.049±0.008 µmol MDA/mg (Fig 6.59). In summary, our findings indicate that the administration of Sinapic acid at both dosage levels significantly mitigated the risk of oxidative stress by reducing LPO (MDA levels) in diabetic rats. Notably, more pronounced results were observed with Sinapic acid at a dose of 20 mg/kg.

	Non-Diabetic Non-wounded control	Non-Diabetic Non-wounded + Per se	Non-Diabetic wounded control	Non-Diabetic wounded + Sinapic acid (20 mg/kg)	Non-Diabetic wounded + Sinapic acid (40 mg/kg)	Diabetic wounded control	Diabetic wpunded control + Sinapic acid (20 mg/kg)	Diabetic wounded control + Sinapic acid (40 mg/kg)
Kidney	0.0145	0.0121	0.0303	0.017	0.02	0.0591	0.0362	0.0455
Skin	0.0122	0.011	0.0205	0.0151	0.0202	0.0491	0.0271	0.028
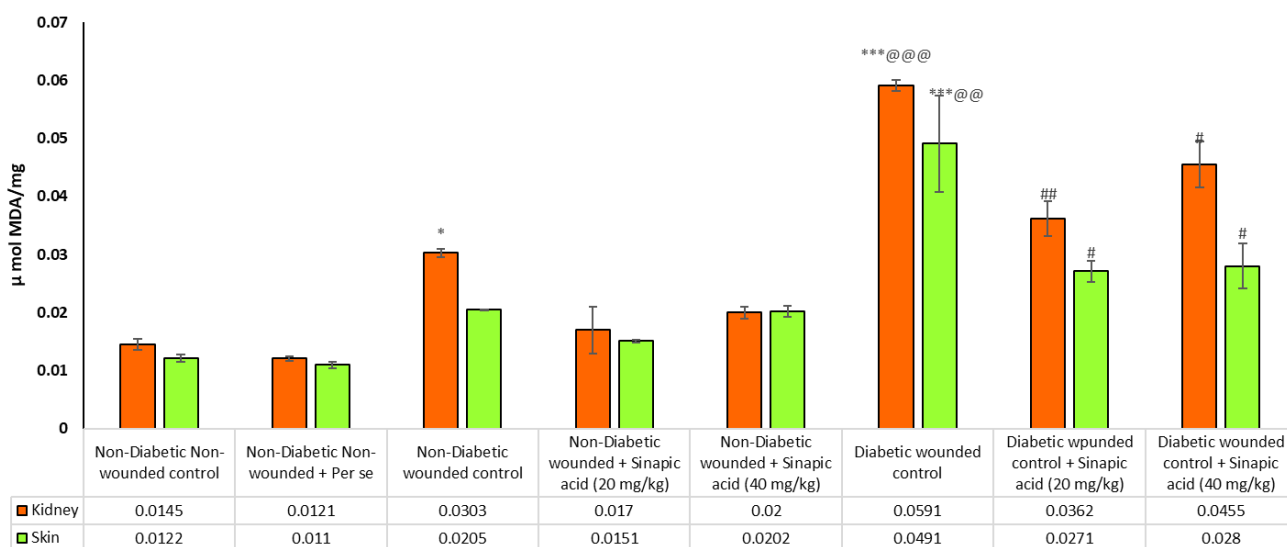
Fig 6.59: Graph showing variation in LPO in kidney and skin tissues of different treatment groups.

The data is represented as Mean ± S.E.M. (n=3), ***symbolises $p<0.001$, and *symbolises $p<0.05$, when in comparison with the non-diabetic non-wounded control group; @@@symbolises $p<0.001$, and @@symbolises $p<0.01$, when in comparison to the non-diabetic wounded control group; ##symbolises $p<0.01$, and #symbolises $p<0.05$, when in comparison to the diabetic wounded control group.

6.7.4.3 Catalase estimation

Chronic hyperglycemia has been linked to reduced catalase levels. Thus, we aimed to examine the catalase levels in the kidney and skin tissues of male diabetic rats following the Sinapic acid at doses of 20 mg/kg and 40 mg/kg. Our results showed that non-diabetic non-wounded control rats receiving NPD had higher levels of catalase in kidney and skin tissues i.e. 3.79±0.123 U/mg and 3.93±0.064 U/mg, whereas the feeding of NPD to non-diabetic wounded rats had reduced level of catalase i.e. 3.28±0.178 U/mg and 3.09±0.119 U/mg respectively. Similarly, compared to non-diabetic wounded rats (3.28±0.178 U/mg and 3.09±0.119 U/mg), the level of catalase in kidney and skin tissues (3.59±0.195 U/mg and 3.90±0.025 U/mg) was increased upon receiving the Sinapic acid at 20 mg/kg, and these levels were not much increased upon receiving Sinapic acid treatment at 40 mg/kg doses i.e. 3.30±0.172 U/mg and 3.65±0.192 U/mg. On the contrary, the feeding of HFD to diabetic rats exhibit lower level of catalase in kidney and skin tissues up to 1.36±0.17 U/mg and 1.77±0.164 U/mg, when compared to non-diabetic rats i.e. 3.28±0.178 U/mg and 3.09±0.119 U/mg. In addition, the levels of catalase in kidney and skin tissues of diabetic wounded rats were significantly increased upon receiving the treatment of Sinapic acid at both 20 mg/kg and 40 mg/kg i.e. 2.99±0.092 U/mg, 3.24±0.177 U/mg, and 2.45±0.330 U/mg, 2.49±0.200 U/mg, compared to diabetic wounded rats receiving HFD treatment i.e. 1.36±0.17 U/mg and 1.77±0.164 U/mg (Fig 6.60). In summary, our results indicate that the Sinapic acid at both dosage levels significantly mitigated the risk of oxidative stress by enhancing catalase activity in diabetic rats. Notably, more pronounced results were observed with the administration of Sinapic acid at a dose of 20 mg/kg.

	Non-Diabetic Non-wounded control	Non-Diabetic Non-wounded + Per se	Non-Diabetic wounded control	Non-Diabetic wounded + Sinapic acid (20 mg/kg)	Non-Diabetic wounded + Sinapic acid (40 mg/kg)	Diabetic wounded control	Diabetic wpunded control + Sinapic acid (20 mg/kg)	Diabetic wounded control + Sinapic acid (40 mg/kg)
Kidney	3.79	3.755	3.285	3.596	3.3	1.361	2.99	2.458
Skin	3.93	3.98	3.09	3.9	3.65	1.77	3.24	2.49
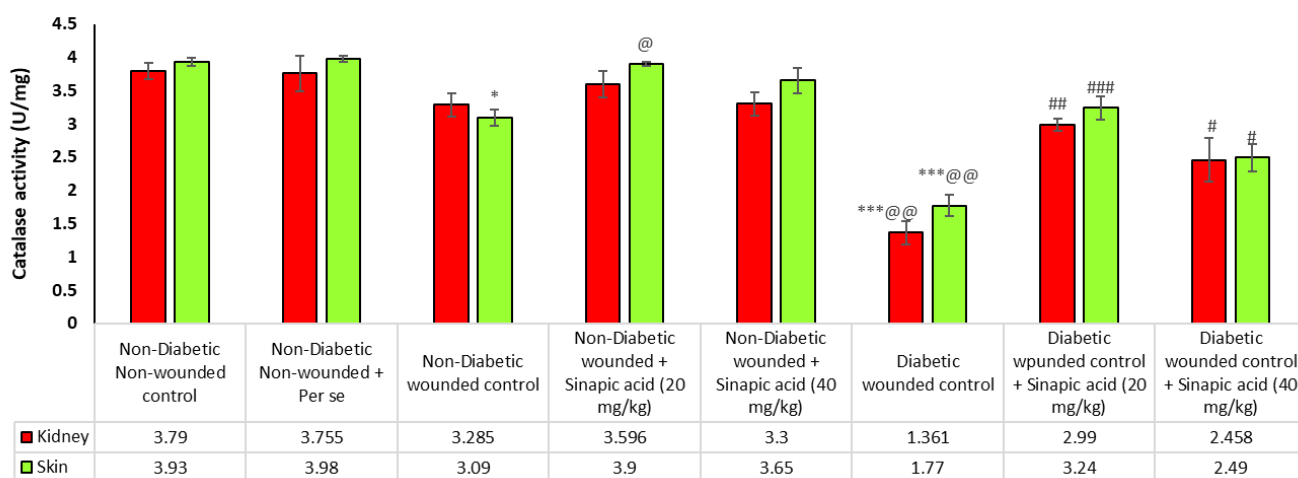
Fig 6.60: Graph showing variation in catalase levels in kidney and skin tissues of different treatment groups

The data is represented as Mean ± S.E.M. (n=3), ***symbolises $p<0.001$, and *symbolises $p<0.05$, when in comparison to the non-diabetic non-wounded control group; @@symbolises $p<0.01$, and @symbolises $p<0.05$, when in comparison to the non-diabetic wounded control group; ###symbolises $p<0.001$, ##symbolises $p<0.01$, and #symbolises $p<0.05$, when in comparison to the diabetic wounded control group.

6.7.4.4 SOD estimation

Reduced levels of SOD have been linked to chronic hyperglycemia. Consequently, we aimed to examine the SOD levels in the kidney and skin tissues of male diabetic rats following the Sinapic acid at doses of 20 mg/kg and 40 mg/kg. Our results showed that non-diabetic non-wounded control rats receiving NPD had higher levels of SOD in kidney and skin tissues i.e. 21.99 ± 0.98 U/mg and 10.81 ± 6.19 U/mg, whereas the feeding of NPD to non-diabetic wounded rats had reduced level of SOD i.e. 17.66 ± 0.53 U/mg and 6.19 ± 0.33 U/mg respectively. Similarly, compared to non-diabetic wounded rats (17.66 ± 0.53 U/mg and 6.19 ± 0.33 U/mg), the level of SOD in kidney and skin tissues (28.82 ± 0.81 U/mg and 10.47 ± 0.30 U/mg) was increased upon receiving the treatment of Sinapic acid at 20 mg/kg, and these levels were not much increased upon receiving Sinapic acid treatment at 40 mg/kg doses i.e. 20.71 ± 0.55 U/mg and 8.20 ± 0.76 U/mg. On the contrary, the feeding of HFD to diabetic rats exhibit lower level of SOD in kidney and skin tissues up to 9.20 ± 2.23 U/mg and 3.23 ± 0.46 U/mg, when compared to non-diabetic rats i.e. 17.66 ± 0.53 U/mg and 6.19 ± 0.33 U/mg. In addition, the levels of SOD in kidney and skin tissues of diabetic wounded rats were significantly increased upon receiving the treatment of Sinapic acid at both 20 mg/kg and 40 mg/kg i.e. 22.51 ± 0.25 U/mg, 7.42 ± 0.43 U/mg, and 16.07 ± 1.06 U/mg, 6.31 ± 0.77 U/mg, compared to diabetic wounded rats receiving HFD treatment i.e. 9.20 ± 2.23 U/mg and 3.23 ± 0.46 U/mg (Fig 6.61). In summary, our findings indicate that the administration of Sinapic acid at both dosage levels significantly diminished the risk of oxidative stress by enhancing catalase activity in diabetic rats. Notably, more substantial results were observed with Sinapic acid at a dose of 20 mg/kg.

	Non-Diabetic Non-wounded control	Non-Diabetic Non-wounded + Per se	Non-Diabetic wounded control	Non-Diabetic wounded + Sinapic acid (20 mg/kg)	Non-Diabetic wounded + Sinapic acid (40 mg/kg)	Diabetic wounded control	Diabetic wpunded control + Sinapic acid (20 mg/kg)	Diabetic wounded control + Sinapic acid (40 mg/kg)
Kidney	21.99	21.94	17.66	28.22	20.71	9.2	22.51	16.07
Skin	10.81	8.64	6.19	10.47	8.2	3.23	7.42	6.31
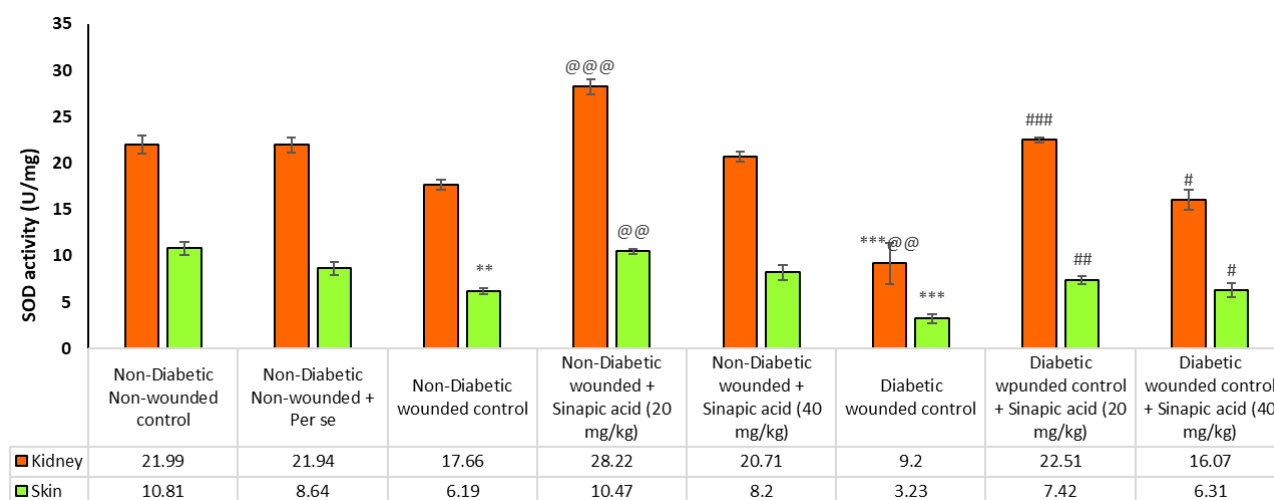
Fig 6.61: Graph showing variation in SOD levels in kidney and skin tissues of different treatment groups.

The data is represented as Mean ± S.E.M. (n=3), ***symbolises $p<0.001$, and **symbolises $p<0.01$, when in comparison to the non-diabetic non-wounded control group; @@@symbolises $p<0.001$, and @@symbolizes $p<0.01$, when in comparison to the non-diabetic wounded control group; ###symbolises $p<0.001$, ##symbolises $p<0.01$, and #symbolises $p<0.05$, when in comparison to the diabetic wounded control group.

6.7.4.5 GST estimation

Reduced levels of GST have been linked to chronic hyperglycemia. Consequently, we aimed to examine the GST levels in the kidney and skin tissues of male diabetic rats following the Sinapic acid at doses of 20 mg/kg and 40 mg/kg. Our results showed that non-diabetic non-wounded control rats receiving NPD had higher levels of GST in kidney and skin tissues i.e. 0.0004±1.88E U/mg and 0.0015E±0.0001 U/mg, whereas the feeding of NPD to non-diabetic wounded rats had reduced level of GST i.e. 0.0003±2.02 U/mg and 0.0013±0.0001 U/mg respectively. Similarly, compared to non-diabetic wounded rats (0.0003±2.02 U/mg and 0.0013±0.0001 U/mg), the level of GST in kidney and skin tissues (0.0005±4.66E U/mg and 0.0019±2.65 U/mg) was increased upon receiving the treatment of Sinapic acid at 20 mg/kg, and these levels were not much increased upon receiving Sinapic acid treatment at 40 mg/kg doses i.e. 0.0004±1.31E U/mg and 0.0016±0.00 U/mg. On the contrary, the feeding of HFD to diabetic rats exhibit lower level of GST in kidney and skin tissues up to 0.0001±1.21E U/mg and 0.0006±1.63E U/mg, when compared to non-diabetic rats i.e. 0.0004±1.88E U/mg and 0.0015±0.001 U/mg. In addition, the levels of GST in kidney and skin tissues of diabetic wounded rats were significantly increased upon receiving the treatment of Sinapic acid at both 20 mg/kg and 40 mg/kg i.e. 0.0003±3.55e U/mg, 0.0015±0.0001 U/mg, and 0.0002±2.52E U/mg, 0.0013±0.0001 U/mg, compared to diabetic wounded rats receiving HFD treatment i.e. 0.0001±1.21E U/mg and 0.0006±1.63E U/mg (Fig 6.62). In summary, our findings indicate that the administration of Sinapic acid at both dosage levels significantly diminished the risk of oxidative stress by enhancing GST activity in diabetic rats. Notably, more substantial results were observed with the Sinapic acid at a dose of 20 mg/kg.
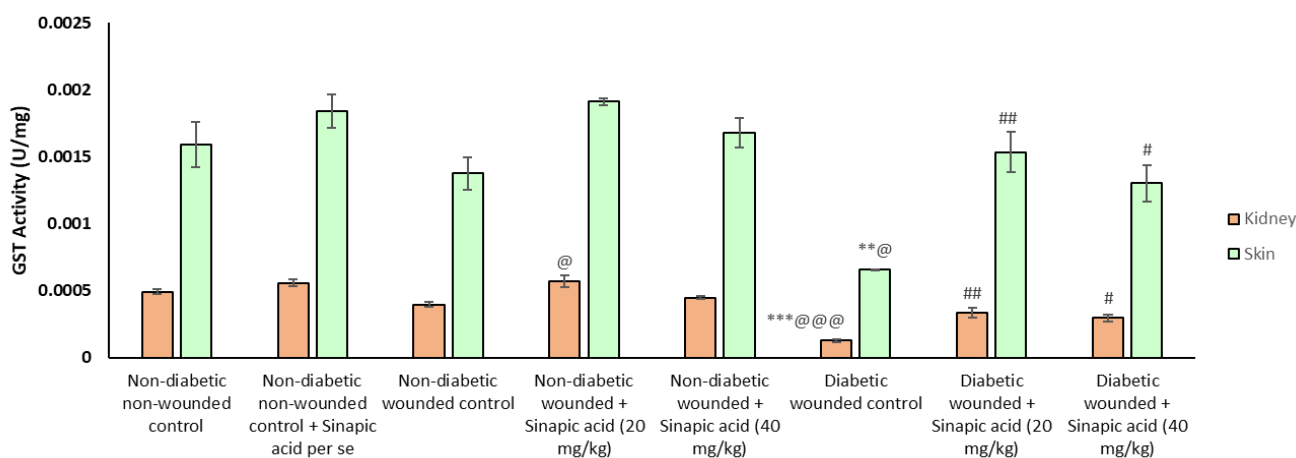
Fig 6.62: Graph showing variation in GST levels in kidney and skin tissues of different treatment groups.

The data is represented as Mean ± S.E.M. (n=3), ***symbolises $p<0.001$, and **symbolises $p<0.01$, when in comparison to the non-diabetic non-wounded control group; @@@symbolises $p<0.001$, and @symbolizes $p<0.05$, when in comparison to the non-diabetic wounded control group; ##symbolises $p<0.01$, and #symbolises $p<0.05$, when in comparison to the diabetic wounded control group.

6.7.4.6 GSH estimation

Reduced levels of GSH have been linked to chronic hyperglycemia. Consequently, we aimed to examine the GSH levels in the kidney and skin tissues of male diabetic rats following the administration of Sinapic acid at doses of 20 mg/kg and 40 mg/kg. Our results showed that non-diabetic non-wounded control rats receiving NPD had higher levels of GSH in kidney and skin tissues i.e. 1.55E-06±7.45E-08 U/mg and 3.80E-06±8.46E-08 U/mg, whereas the feeding of NPD to non-diabetic wounded rats had reduced level of GSH i.e. 1.22E-06±1.21E-08 U/mg and 2.84E-06±4.13E-07 U/mg respectively. Similarly, compared to non-diabetic wounded rats (1.22E-06±1.21E-08 U/mg and 2.84E-06±4.13E-07 U/mg), the level of GSH in kidney and skin tissues (1.41E-06±5.46E-08 U/mg and 3.30E-06±4.27E-07 U/mg) was increased upon receiving the treatment of Sinapic acid at 20 mg/kg, and these levels were not much increased upon receiving Sinapic acid treatment at 40 mg/kg doses i.e. 1.33E-06±1.22E-07E U/mg and 3.10E-06±9.98E-08 U/mg. On the contrary, the feeding of HFD to diabetic rats exhibited lower levels of GSH in kidney, and skin tissues up to 5.63E-07±2.69E-08 U/mg and 1.29E-06±3.78E-10E U/mg, when compared to non-diabetic rats i.e. 1.22E-06±1.21E-08 U/mg and 2.84E-06±4.13E-07 U/mg. In addition, the levels of GSH in kidney and skin tissues of diabetic wounded rats were significantly increased upon receiving the treatment of Sinapic acid at both 20 mg/kg and 40 mg/kg i.e. 1.11E-06±9.29E-08 U/mg, 1.01E-06±4.76E-08 U/mg, and 2.89E-06±1.74E-08E U/mg, 2.73E-06±4.13E-09 U/mg, compared to diabetic wounded rats receiving HFD treatment i.e. to 5.63E-07±2.69E-08 U/mg and 1.29E-06±3.78E-10E U/mg (Fig 6.63). In summary, our findings indicate that the Sinapic acid at both dosage levels significantly diminished the risk of oxidative stress by enhancing GSH activity in diabetic rats. Notably, more substantial results were observed with the administration of Sinapic acid at a dose of 20 mg/kg.
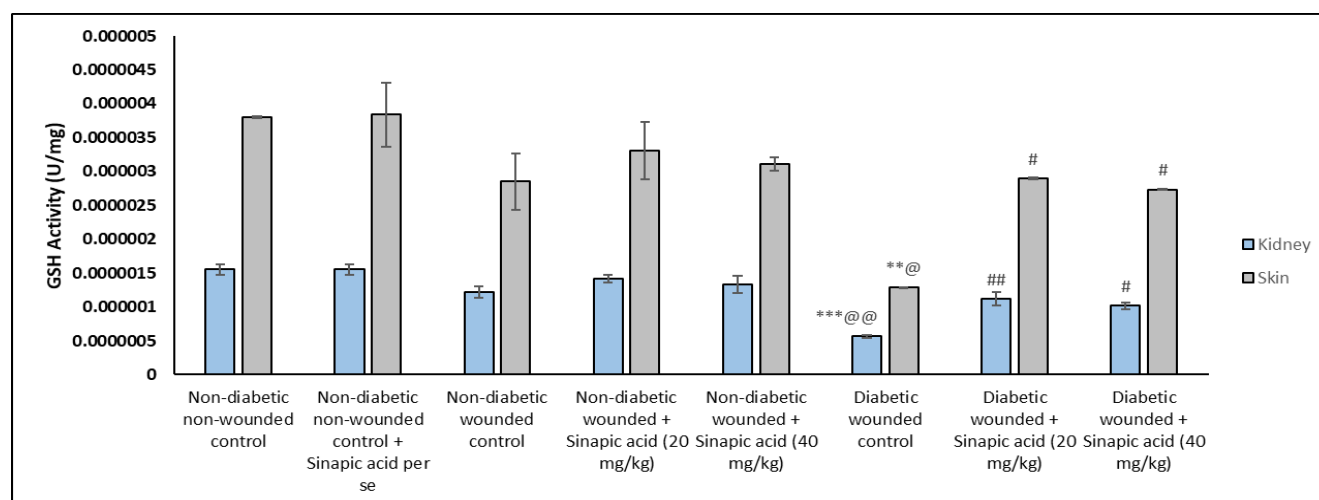
Fig 6.63: Graph showing variation in GSH levels in kidney and skin tissues of different treatment groups.

The data is represented as Mean ± S.E.M. (n=3), ***symbolises $p < 0.001$, and **symbolises $p < 0.01$, when in comparison with the non-diabetic non-wounded control group; @@symbolises $p < 0.01$, and @symbolizes $p < 0.05$, when in comparison to the non-diabetic wounded control group; ##symbolises $p < 0.01$, and #symbolises $p < 0.05$, when in comparison to the diabetic wounded control group.

6.7.5 Effect of Sinapic acid on wound area

A healing response referred to as wound contraction attempts to reduce the extent of the tissue defect and, as a result, reduces the volume of injured tissue and mediates the healing process. Wound healing may be delayed in people with diabetes due to several conditions related to the disease, including reduced blood flow, neuropathy (damage to the nerves), and a weakened immune system. With this purpose, we create wounds in different treatment groups and analyze the ability of Sinapic acid in reducing wound area and enhancing wound contraction. Our results showed that on day 3, group 6 i.e. diabetic wounded control group receiving HFD had a higher open wound area (164%) than group 3 i.e. non-diabetic wounded control group (154%). Whereas compared to group 6, the lesion area was greater in animals receiving low and high doses of Sinapic acid (group 7 and group 8), i.e., 143.5% and 161%, respectively. In contrast, compared to day 3, the wound area in group 6 was decreased up to 124.5% on day 7. Meanwhile, compared to the third day, the wound area in diabetic animals receiving Sinapic acid at low and high doses (groups 7 and 8) was reduced by 53% and 100.5%, respectively. Furthermore, on day 14, only groups 6 and 8 were reported to have 98% and 26.5% open wound area compared to the other groups (Fig 6.64). According to this, the group treated with HFD had impaired wound healing parameters such as epithelialization, fibroblast proliferation, collagen production, increased angiogenesis and granulation tissue formation. Nevertheless, therapy of 20 mg/kg and 40 mg/kg Sinapic acid was able to restore all these parameters and accelerate wound healing by reducing wound area.
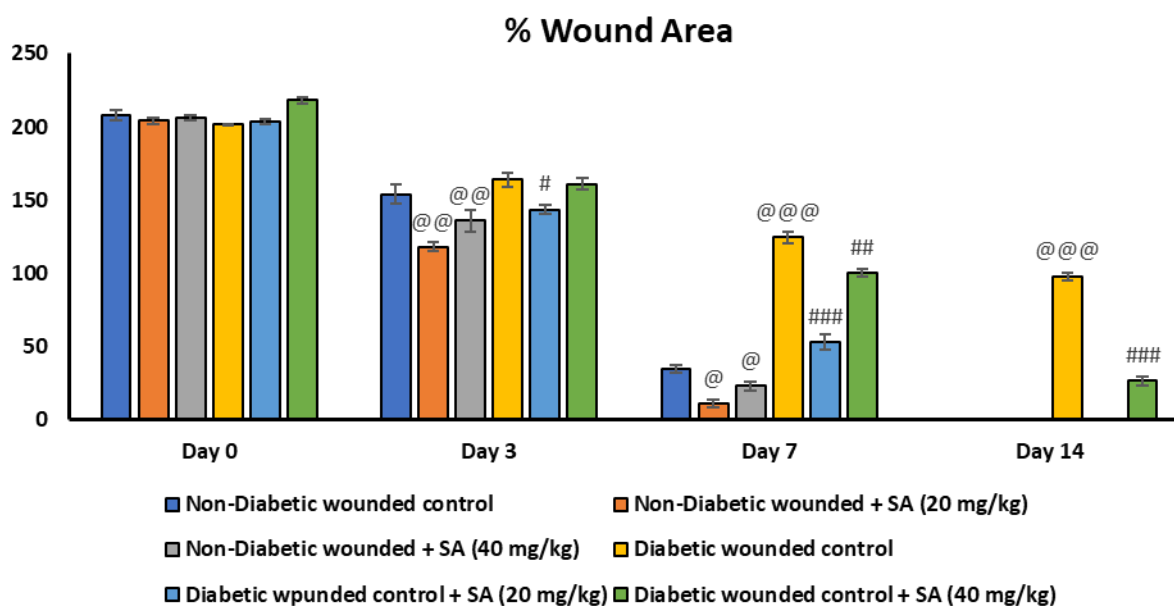
Fig 6.64: Graph showing variation in wound area of different treatment groups.
The data is represented as Mean ± S.E.M. @@@symbolises $p < 0.001$, @@symbolises $p < 0.01$, and @symbolises $p < 0.05$, when in comparison to the non-diabetic wounded control group; ###symbolises $p < 0.001$, ##symbolises $p < 0.01$, and #symbolises $p < 0.05$, when in comparison to the diabetic wounded control group.

6.7.6. Effect of Sinapic acid on wound contraction

Our results showed that on day 3, group 6 i.e. diabetic wounded control group receiving HFD had a lower wound contraction (18.41%) than group 3 i.e. non-diabetic wounded control group (27.01%). Whereas compared to group 6, the wound contraction was greater in animals receiving low and high doses of Sinapic acid (group 7 and group 8), i.e., 30.32% and 25.63%, respectively. In contrast, compared to day 3, the wound contraction in group 6 was more up to 37.90% on day 7. Meanwhile, compared to the third day, the wound contraction in diabetic animals receiving Sinapic acid at low and high doses (groups 7 and 8) was increased by 73.82% and 53.33%, respectively. Furthermore, on day 14, only groups 6 and 8 were reported to have 51.12% and 87.82% open wound area compared to the other groups (Fig 6.65 and 6.66). As a result, we found that treatment of Sinapic acid at 20 mg/kg and 40 mg/kg was able to accelerate wound healing by restoring all wound healing parameters that typically hinder diabetic wound control treated with a HFD. These parameters included epithelialization, fibroblast proliferation, collagen production, enhanced angiogenesis, and granulation tissue formation. In addition, it was found that Sinapic acid at 20 mg/kg produced better wound healing results than a 40 mg/kg dose.
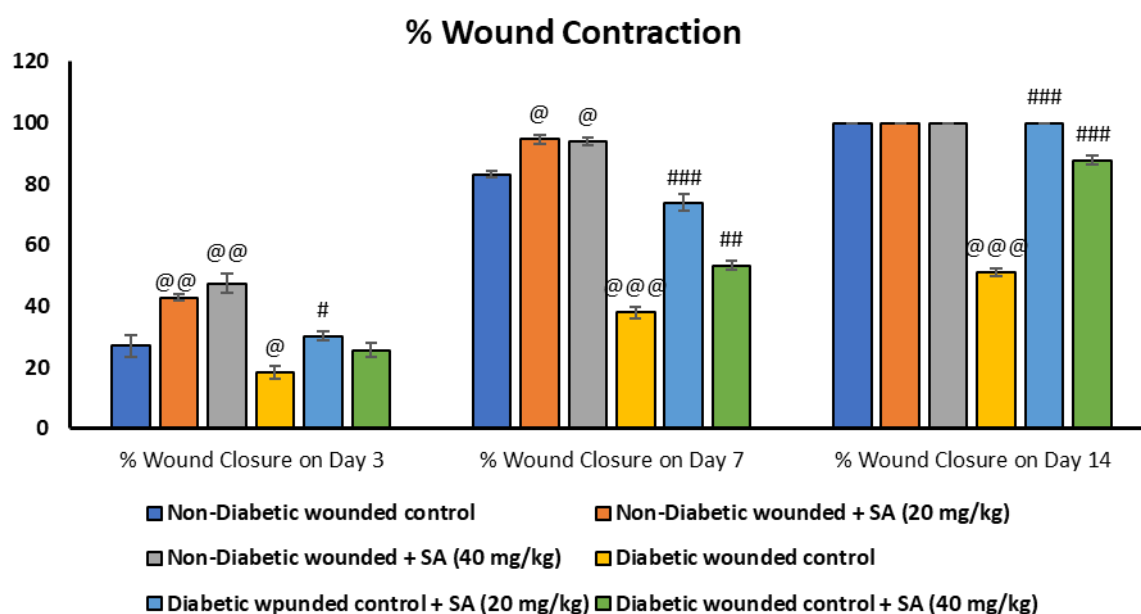
Fig 6.65: Graph showing variation in wound contraction of different treatment groups.

The data is represented as Mean ± S.E.M. @@@symbolises $p < 0.001$, @@symbolises $p < 0.01$, and @symbolises $p < 0.05$, when in comparison to the non-diabetic wounded control group; ###symbolises $p < 0.001$, ##symbolises $p < 0.01$, and #symbolises $p < 0.05$, when in comparison to the diabetic wounded control group.
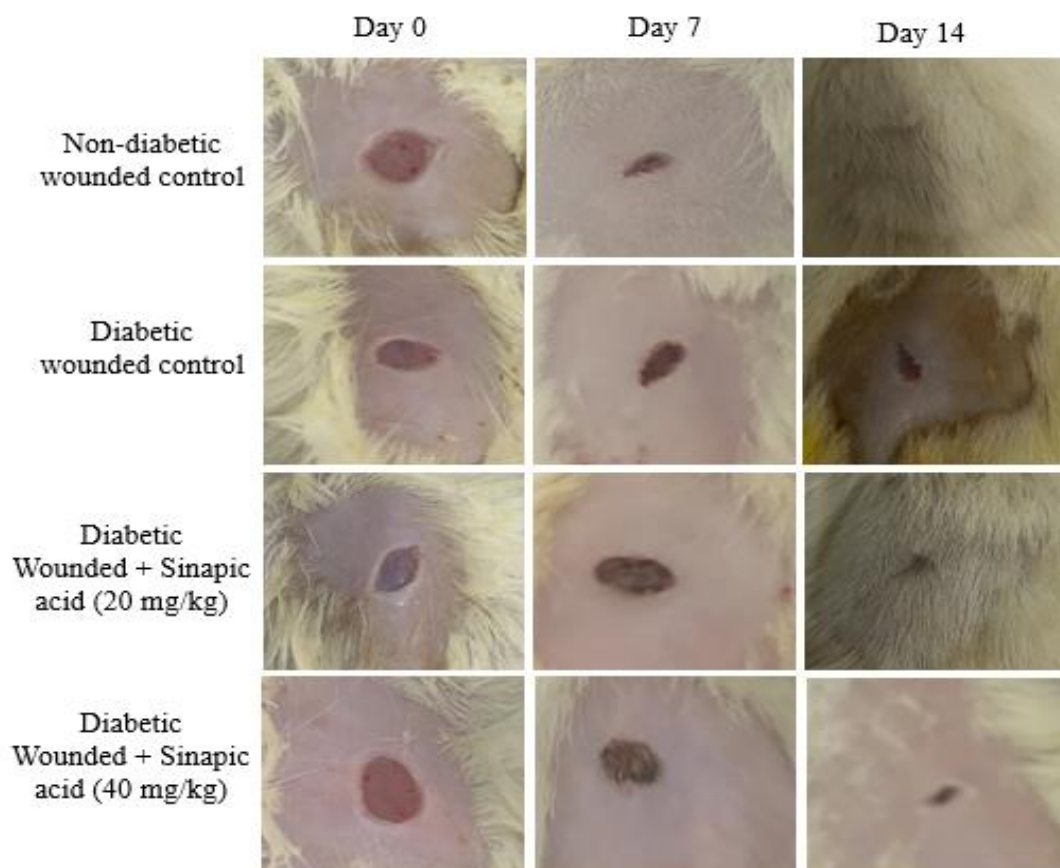
Fig 6.66: Photographic representation of wound contraction on different days (day 0, 7 and 14) for the normal control, diabetic control and treatment groups.

6.7.7 Histopathology results

In the present study, histopathology was performed on wounded tissues on different groups to analyze the extent of healing when Sinapic acid was given in low and high doses. The tissue underwent staining with H&E dye and was subsequently examined under a magnification of 10X. Our findings showed that both the non-diabetic non-wounded Sinapic acid group and the non-diabetic non-wounded control group had complete dermal remodeling as well as thickening and stratification of the epithelium. On the contrary, the non-diabetic wounded group exhibited changes in epithelialization and skin. Nonetheless, administering Sinapic acid 20 mg/kg and 40 mg/kg doses to non-diabetic wounded groups led to improved re-epithelialization, dermis remodeling, and increased angiogenesis. Additionally, critical parameters crucial for effective wound healing, including re-epithelialization, thickening of the epidermis and dermis, and the maturation of fully developed granulation tissues, were observed to be disturbed in the diabetic wounded control group. Conversely, after providing Sinapic acid at varying doses (20 mg/kg and 40 mg/kg), there was an enhanced re-epithelization, mature and fully-grown granular tissues, and new blood vessels in wounded tissues. Nevertheless, in comparison of diabetic wounds treated with 40 mg/kg Sinapic acid group and diabetic wound control groups, 20 mg/kg dose of Sinapic acid was efficient in restoring all these parameters and accelerating wound healing (Fig 6.67).
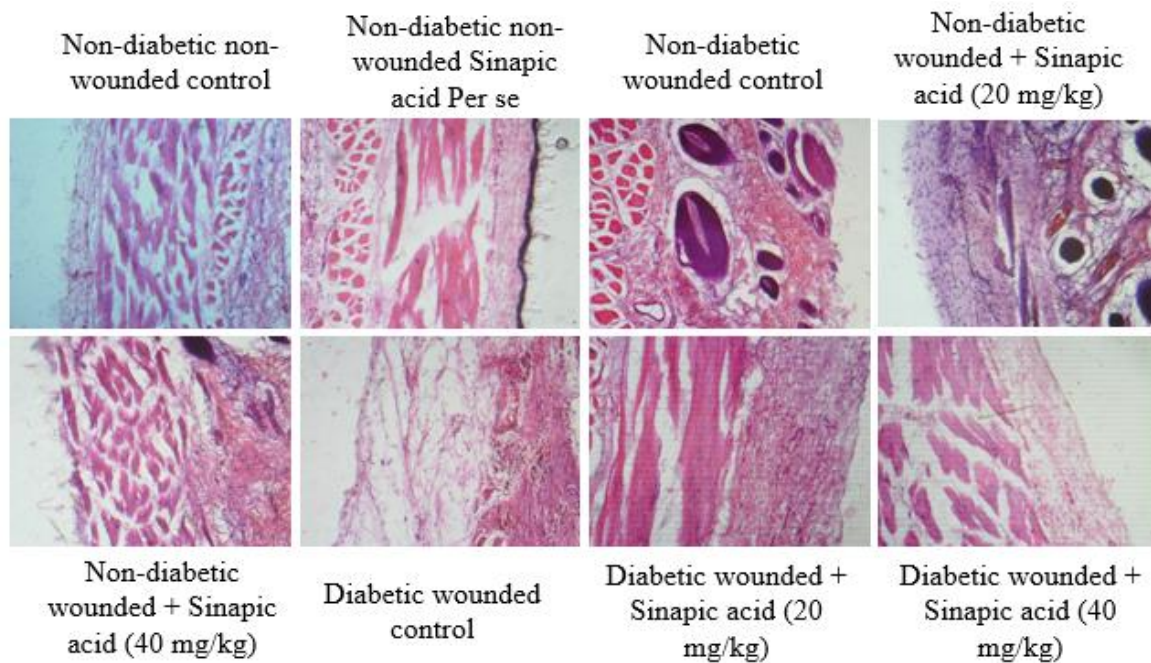
Fig 6.67: Histopathological evaluation of diabetic wound healing process before and after treatment in different groups

6.7.8 SIRT1 activity

Our results showed that non-diabetic non-wounded control rats receiving NPD had higher expression of SIRT1 i.e. 1.24 ± 0.002 ng/ml, whereas the feeding of NPD to non-diabetic wounded control had lower SIRT1 expression i.e. 0.91 ± 0.008 ng/ml. In comparison to both the non-diabetic non-wounded and non-diabetic wounded groups, the expression of SIRT1 increased upon administration of Sinapic acid, measuring 1.74 ± 0.007 ng/ml. On the contrary, the feeding of HFD to diabetic rats exhibit reduced expression of SIRT1 up to 0.48 ± 0.005 ng/ml, whereas these expressions were significantly increased in non-diabetic wounded animals receiving Sinapic acid treatment at 20 mg/kg and 40 mg/kg doses i.e. 1.09 ± 0.006 ng/ml and 0.98 ± 0.004 ng/ml. Compared to diabetic wounded animals (0.48 ± 0.005 ng/ml), the expression of SIRT1 was notably restored upon receiving the Sinapic acid therapy at 20 mg/kg and 40 mg/kg i.e. 1.34 ± 0.011 ng/ml and 1.20 ± 0.01 ng/ml respectively (Fig 6.68). In summary, our results indicate that the administration of Sinapic acid at both dosage levels significantly enhanced SIRT1 expression in diabetic rats. Notably, more pronounced results were observed with the Sinapic acid at a dose of 20 mg/kg.
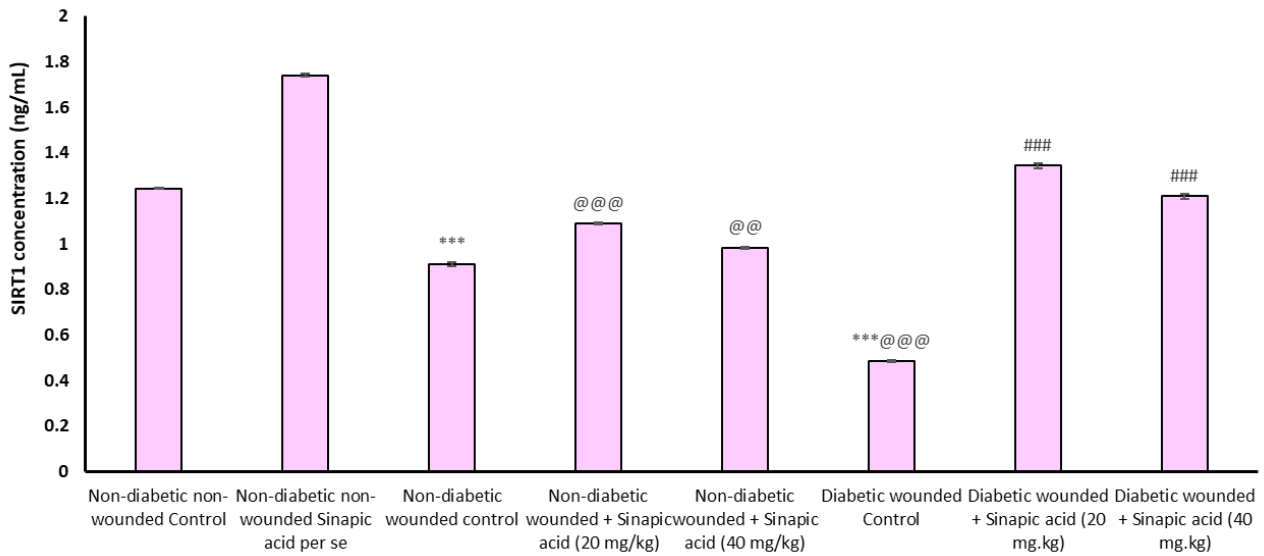
Fig 6.68: Expression of SIRT1 in the different treatment groups.

The data is represented as Mean ± S.E.M. ***symbolises p<0.001, when in comparison with the non-diabetic non-wounded control group; @@@symbolises p<0.001, and @@symbolizes p<0.01, when in comparison to the non-diabetic wounded control group; ###symbolises p<0.01, when in comparison to the diabetic wounded control group.

CHAPTER 7

DISCUSSION

The prevalence of T2D mellitus, a persistent metabolic disorder, is steadily on the rise globally. According to the latest survey conducted by the International Diabetes Federation, there are currently 537 million people globally diagnosed with diabetes. Projections suggest this number will escalate to 643 million by 2030 and further increase to 783 million by 2045 (1). High blood sugar levels are a hallmark of this condition, which is caused by a deficiency of insulin, a pancreatic hormone involved in controlling glycemia. This metabolic condition progresses over time to long-term, life-threatening microvascular, macrovascular, and neuropathic consequences. The inclination towards a sedentary lifestyle is likely the primary factor contributing to the escalating number of diabetic patients worldwide. Projections suggest that this figure is anticipated to reach 366 million among the elderly population (i.e., above 65 years) by the year 2030 (368).

The term DFU refers to an ulcer that often appears on the plantar part of the foot and is a devastating and serious symptom of uncontrolled and persistent diabetes. In a comprehensive cohort study involving individuals with DFU in China, the annual ulcer incidence rate stood at 8.1% for diabetic patients. Moreover, the annual rate of new ulcer occurrences was recorded at 31.6% among patients with DFU. During the one-year follow-up period, the study reported an annual amputation rate of 5.1%, along with respective annual mortality rates of 2.8% and 14.4% (369).

DFU constitutes the leading cause of hospitalization, amputation, reduced quality of life, and mortality among patients, they impose a significant financial burden on the medical and healthcare system. Globally, it holds the tenth position in terms of economic impact (370). A robust correlation exists between diabetes and neuropathy, signifying that prolonged elevated blood sugar levels can result in diverse complications. Among these complications, diabetic neuropathy plays a pivotal role in the initiation of DFU. This condition notably affects nerves throughout the body, especially those in the legs and feet. Peripheral neuropathy, a type of diabetic neuropathy, is extensively studied as a precursor to the development of foot ulcers. In essence, diabetic neuropathy results in nerve damage, leading to various symptoms such as tingling, numbness, and pain in the extremities, particularly the feet. People may find it difficult to recognize wounds or damage to the feet, such as blisters, cuts, or sores, as a result of a lack of sensation in their feet. People with diabetic neuropathy may continue to put pressure and shear stress on particular parts of their foot as they are unable to feel pain or discomfort which further leads to the development of blisters, open wounds, and calluses. As a result, if these problems are left abandoned, they may eventually worsen into sores and ulcers. These ulcers can be challenging to heal due to inadequate blood flow and the concomitant presence of nerve damage. Therefore, preventing and controlling DFU in people with diabetes requires controlling blood sugar levels, monitoring and caring for the feet, and seeking medical attention to avoid disease progression.

Medically accessible drugs like metformin are used to treat and prevent diabetes, however, these synthetic drugs have a long list of adverse effects. In response to this challenge, our research focus on the identification of phytochemicals through a comprehensive approach encompassing in silico, in vitro, and in vivo experiments. Recent research indicates that molecules sharing similar structures may exhibit comparable biological activities, making them candidates for subsequent testing to evaluate their potential in disease treatment. In the present study, a total of 16 natural phytochemicals have been selected from previously published research that served as the basis for the query structure for similarity search. These include **Quercetin, Resveratrol, Ellagic acid, Naringenin, Baicalein, Glabridin, Naringin, Capsaicin, Diosgenin, Amygdalin, Kaempferol, Ferulic acid, Vanillic acid, Coumaric acid, Apigenin, and Genistein.** These natural molecules were further processed for in silico and ADME study to investigate the potent molecule on the basis of high binding energy and good pharmacokinetic profile.

Extended exposure of diabetic wounds to elevated glucose levels leads to a debilitating condition, contributing to the progression of diabetes and its associated complications, including the delayed healing of diabetic wounds. These conditions may further cause death or amputation in diabetic patients. SIRT, is a homolog of Sir2 protein that belongs to class III histone/protein deacetylases in *S. cerevisiae*. Abundant evidence on diabetic wounds has revealed the significant potential of SIRT1 in promoting angiogenesis, mitochondrial biogenesis and reducing inflammation. However, all these aspects are reversed under conditions of low SIRT1 expression, potentially contributing to the delayed healing of diabetic wounds. For instance, a recent study emphasized that the activation of SIRT1 expedites the healing of diabetic wounds by promoting angiogenesis and suppressing oxidative stress (39). Hence, to explore a potent SAC, we initiate the docking process of selected molecules with the SIRT1 protein (PDB ID: 4ZZJ). The outcomes of the molecular docking involving all-natural compounds with the SIRT1 (4ZZJ protein) are presented in the Fig 6.2 to 6.23.

The pursuit of chemical entities with medicinal potential is referred to as drug discovery. Identifying new molecular entities that could prove beneficial in treating diseases, particularly those addressing unmet medical needs, stands as a primary goal in drug development programs. The key phases of drug discovery encompass target identification, target validation, lead optimization, preclinical testing, clinical trials, regulatory considerations, post-market surveillance, and market introduction. The ultimate aim of each stage in the drug development process is the creation and commercialization of novel, promising drugs to address a diverse array of medical conditions. Furthermore, a molecule must reach its target site while still exhibiting minimal toxicity, biodistribution, and high biological activity should be of greater concern when discovering a new compound. According to studies, early Pharmacokinetic testing of the molecule has been found to reduce the likelihood of Pharmacokinetic-related clinical phase failures. Since resources and availability are an issue, in silico models have been widely used as an alternative to experimental methods to predict ADME.

For a molecule to be efficacious, it must persist in the bioactive state at the target site within the body for an extended duration to exert its biological activity. Evaluating ADME becomes essential in the early stages of drug discovery when there is a high number of potential compounds but limited physical sample access. During these initial phases, where numerous chemical structures are explored but only a few compounds are available, computer models were advocated as a viable alternative to experimental approaches for predicting the ADME profile of biologically active drug candidates. In this study, we employed the SwissADME web tool to anticipate diverse attributes of the drug candidate, including kinetics, drug-likeness, and physicochemical characteristics. The main goal of the study is to explore the characteristics of BBB, human intestinal absorption (HIA), and P-gp permeability for selected compounds using SwissADME predictions.

To date, solubility remains one of the biggest hurdles in drug research and development, which needs to be tackled at the earliest. If the drug is to be administered by a method other than oral administration to deliver the appropriate amount of active substance, it must be highly soluble in water. The rate and amount at which a therapeutic ingredient is absorbed into the circulation and reaches its target site is called bioavailability, which is affected by the low solubility of the drug, leading to ineffective therapeutic treatment. Additionally, the solubility of a drug affects the type of dosage form it takes, such as tablet, capsule, or liquid suspension. Therefore, scientists working on pharmaceutical formulations are actively paying attention to this issue to increase the solubility of less soluble substances, which can result in the creation of potent and practical dosage forms.

Lately, the term cytochrome P450 has been crucial in the realms of pharmacology, toxicology, and clinical drug development, showcasing its capability to eliminate toxic compounds from the body. Although the liver is the primary location for cytochrome P450 enzymes, they can also be found in other tissues and organs, including the intestine. Many different compounds are oxidized and broken down by them, which makes them more water-soluble and less difficult for the body to expel. According to prior research, 5 main CYP isoforms (CYP2C19, CYP1A2, CYP2D6, CYP3A4, CYP2C9) comprise a substrate for 50–90% of chemical entities. Consequently, a critical aspect of drug-drug interactions involves the inhibition of these enzymes. It is crucial to foresee the potential interaction of specific compounds with a drug by inhibiting CYP, as a variety of inhibitors affecting CYP have been identified. Some exhibit a general impact on CYP, while others demonstrate selectivity for specific isoenzymes. Since the docking results suggest that the majority of these compounds exhibit favourable binding energy with SIRT1 protein and also demonstrate good ADME properties according to Lipinski's rule, we selected two phytochemicals based on cost and resource availability to ensure feasibility and practical application. These two compounds were Sinapic acid and o-Coumaric acid, which were further investigated for their potential in improving diabetes-associated wound healing using in vitro and in vivo approaches.

The DPPH test is a commonly used experiment to evaluate a compound's ability as an antioxidant. It is now well-established that hyperglycemia is a recognized factor in elevated plasma free radical levels. Globally, studies have shown that oxidative stress, which can cause nephropathy, retinopathy, and delayed wound healing, complicates the etiology of diabetes-related vascular problems. These free radicals can be eliminated by substances with antioxidant capacity, thereby reducing their effect on the body. Hence, it is of utmost significance for us to identify naturally occurring bioactive phenolic compounds with antioxidant potential. Therefore, we assessed the in vitro antioxidant capacity of Sinapic acid and o-Coumaric acid to neutralize free radicals after selecting these potential therapeutic candidates based on molecular docking and ADME studies. We found that Sinapic acid was found to exhibit antioxidant potential by scavenging 50% of DPPH radicals at 35.6 µg/mL, while o-Coumaric acid shows 50% inhibition at 106 µg/mL. In comparison to Sinapic acid and o-Coumaric acid, Ascorbic acid as a standard was found to show 50% inhibition at 44.26 µg/mL (Fig 6.28 to 6.30). Therefore, our results are consistent with previously published reports, where both compounds were found to exhibit antioxidant potential by scavenging DPPH radicals (371-375). This suggests that as the concentrations of both Sinapic acid and o-Coumaric acid increase, the antioxidant capacity of these compounds also rises. This heightened antioxidant capability enables them to effectively scavenge free radicals and alleviate oxidative stress associated with diabetes and its complications.

Additionally, it is essential to investigate the cytotoxic potential of the compound on normal and malignant cells before animal studies. Although, predicting the toxicity of compounds in animal models has pre-clinical significance as it leads to the introduction of tested compounds in human clinical settings for disease treatment; however, despite this, it is recommended to predict toxicity under in vitro conditions. There are several reasons to evaluate the toxicity on cell line models, some of which are low cost and zero human mortality (376). In general, monocytes produced from peripheral blood mononuclear cells (PBMCs) are tested using the MTT assay to determine the viability of the cells. Briefly, the MTT test is a colorimetric assay that identifies the presence of metabolically active cells when the color of the tetrazolium dye changes from yellow to purple due to the synthesis of formazan. Our results showed that IC_{50} values for Sinapic acid and o-Coumaric acid were found to be 467µM and 427µM. Therefore, our results are consistent with previously published reports where both compounds were observed to have cytotoxicity on malignant cells rather than on normal cells (377, 378). This indicates that Sinapic acid and o-Coumaric acid have no cytotoxic effect on L929 cells and are significantly safe for proceeding on animal studies.

The phenomenon responsible for the creation of new blood vessels to facilitate the development of tissues or organs is known as angiogenesis. These newly formed blood vessels (endothelial cells) act as a chief source of nutrients and oxygen to tissues for enhancing wound healing (379-381). Since angiogenesis and endothelial functioning is a beneficial process, it remains altered under hyperglycemic conditions. For instance, the lack of nutrient and oxygen supply and reduction in proliferation or migration of endothelial cells to the wounded site impair angiogenesis, by which wounds remain open for a long time. Hence, there is a crucial need to look

for the effect of phytochemicals on endothelial cells to elucidate their function. In this study, we assessed the capability of Sinapic acid and o-Coumaric acid to promote angiogenesis under HG conditions through tube formation. Our results showed that cells receiving HG treatment have a reduced number of branches, and thickening of capillaries, whereas treatment of Sinapic acid and o-Coumaric acid significantly enhanced branching number and capillary thickness, thereby supporting angiogenesis, and diabetic wound healing (Fig 6.33 to 6.35). These findings suggest that Sinapic acid and o-Coumaric acid may promote wound healing by improving vascularization, which is crucial for effective tissue repair. Enhanced capillary branching and thickness contribute to better oxygen and nutrient supply to the wound site, facilitating faster and more efficient healing. Moreover, the improved angiogenic response observed with these compounds highlights their potential as therapeutic agents in managing diabetic wounds, where compromised angiogenesis often impairs healing.

Since wound healing is a complex process, a series of events are initiated at the injury site to facilitate restoration of the skin's original shape and structure. A critical stage in this process involves cell migration, a pivotal factor in tissue repair and regeneration. The migration of epithelial cells toward the injured site fosters wound healing and serves as a protective barrier, preventing infections in the affected area. Furthermore, a vital cellular component, the fibroblast, assumes a crucial role in the wound healing process by producing granulation tissue. Significantly, it has been noted that granulation tissue is marked by a substantial presence of blood vessels, promoting angiogenesis at the injury site and contributing to the swift healing of wounds. Our findings of the cell scratch assay, indicate a decrease in cell migration under hyperglycemic conditions, as shown in Figures 6.36 to 6.38. This reduced migration was reversed when cells were cultured under normoglycemic conditions. Notably, the administration of Sinapic acid and o-Coumaric acid in hyperglycemic environments significantly increased cell migration. These results suggest that diabetes impairs wound healing primarily by delaying cell migration, a critical process for effective tissue repair. The improvement in cell migration observed with normal glucose treatment and phytochemical administration highlights the potential of these compounds to counteract the detrimental effects of hyperglycemia. The increased migratory capacity of cells treated with Sinapic acid and o-Coumaric acid suggests that these phytochemicals may enhance wound repair mechanisms by promoting more effective cell movement, which is essential for closing wounds and restoring tissue integrity. The findings of our study are consistent with previous research, which has shown that hyperglycemic conditions decrease cell migration and impair wound healing (65, 66, 382, 383). By demonstrating that Sinapic acid and o-Coumaric acid can counteract this effect, our results provide additional support for the therapeutic potential of these compounds in managing diabetic wounds.

Maintaining an equilibrium between oxidants and antioxidants is essential for the proper functioning of the biological system. However, an imbalance in these factors leads to the progression of oxidative stress by intensifying the generation of free radicals. Elevated levels of ROS disrupt the balance of antioxidants and the normal physiological functioning of biological macromolecules, including DNA, lipids, and proteins. In

addition, increased LPO (MDA levels) and rupturing of the mitochondrial membrane due to breakage of lipids impact the cell membrane fluidity and permeability (384). In a clinical and pre-clinical studies, it was found that the level of MDA was high in diabetic subjects, whereas their level was reduced in non-diabetic subjects (385, 386). Another report showed that Sinapic acid derived from rapeseed significantly inhibits LPO by reducing the expression of MDA. On the contrary, another research revealed that the administration of p-hydroxycinnamic acid to diabetic rats reduced MDA levels (387). In accordance with prior research, our data also showed increased MDA levels in the diabetic group (388-391), whereas these levels were found to be reduced upon treatment with Sinapic acid and o-Coumaric acid. Furthermore, the observed decrease in MDA levels with these treatments suggests that Sinapic acid and o-Coumaric acid exert a significant impact on reducing oxidative damage. Their ability to lower oxidative stress highlights their promising role as therapeutic agents in combating the adverse effects of hyperglycemia on cellular health.

As oxidative stress arises from an imbalance between the body's detoxification capacity and the rate of ROS production, antioxidant enzymes become crucial in alleviating the detrimental effects of this condition. Natural byproducts of cellular metabolism include ROS, such as superoxide radicals, hydrogen peroxide, and hydroxyl radicals. While too much ROS can result in oxidative stress and damage to cellular components, including proteins, lipids, and DNA, these molecules are vital for many physiological activities (392-394).

An antioxidant enzyme called GST is primarily responsible for maintaining glutathione homeostasis, phase II detoxification reactions, and reduction of hydrogen peroxide. The homeostasis of GSH and GST plays an essential role in various biological activities such as oxidative stress, signal transduction, and inflammation. Accumulating evidence from the research showed that the levels of GST were significantly reduced upon feeding a HFD (395). Another series of research highlighted that oral feeding of STZ to rats induced diabetes with the dysregulation of antioxidation enzymes such as GST, catalase, and SOD (396-398). This highlighted that the level of antioxidant enzymes was reduced, which further caused the development of oxidative stress in diabetes. Similarly, they also showed that administration of p-coumaric acid to diabetic rats restores the expression of GST and thereby reduces the risk of oxidative stress (399). On the contrary, the administration of Sinapic acid was found to mitigate oxidative stress by enhancing the expression of GST (400, 401). In our study, we investigated the protective effect of Sinapic acid and o-Coumaric acid in a diabetic model using L929 cells. Our findings were consistent with previously published research, which demonstrated that both Sinapic acid and o-Coumaric acid significantly restored GST levels in diabetic conditions (402-404). Compared to the control hyperglycemia group, which showed reduced GST activity, our results indicate that treatment with Sinapic acid and o-Coumaric acid led to a notable increase in GST levels. This restoration of GST activity is particularly important as it highlights the potential of these compounds in mitigating oxidative stress associated with diabetes. Elevated oxidative stress is a key contributor to the progression of diabetic complications, and by enhancing GST levels, Sinapic acid and o-Coumaric acid may help counteract this harmful process.

Besides this, SOD is another antioxidant enzyme that shields the biological system from the attack of oxidative stress. This enzyme works on the principle that the dismutation of superoxide anion into free radical and hydrogen peroxide prevents peroxynitrite generation and further supports the antioxidant defence mechanism. Since the level of free radicals is extensively increased due to the progression of oxidative stress, finding novel natural treatment strategies that can enhance the activity of this enzyme will be highly beneficial for human welfare. Over the past decades, several researchers have claimed that the level of this enzyme has decreased under hyperglycemic conditions. For instance, a study by Madi et al. unveiled that diabetic subjects had lower levels of SOD, indicating that hyperglycemia impairs the antioxidant defence system (405). To tackle this, researchers across the globe increased the use of naturally occurring phytochemicals as they possess a vast array of therapeutic applications. For instance, Sinapic acid treatment significantly enhanced SOD levels in serum, liver, and kidney of diabetic rats (406). Similarly, another research demonstrates that the level of SOD was upregulated upon treating Sinapic acid in diabetic nephropathy rats, indicating the abolition of oxidative stress (407). On the contrary, the effect of p-Coumaric acid, a chemical compound belonging to the hydroxycinnamic acid class was also found to lower oxidative stress by increasing the level of SOD in diabetic rats (399). In this investigation, we also observed that the administration of Sinapic acid and o-Coumaric acid alleviates oxidative stress by significantly elevating the levels of SOD in the diabetic model of L929 cells. By increasing SOD activity, Sinapic acid and o-Coumaric acid help to enhance the cellular antioxidant defence system, thereby neutralizing harmful free radicals more effectively. These findings are consistent with previous reports that highlight the potential of these compounds in reducing oxidative stress. Our results reinforce the notion that Sinapic acid and o-Coumaric acid can mitigate oxidative damage by boosting key antioxidant enzymes like SOD. This mechanism not only supports the restoration of oxidative balance but also provides additional evidence of their therapeutic potential in managing oxidative stress-related complications in diabetes. Overall, the elevation of SOD levels observed in our study emphasizes the beneficial effects of Sinapic acid and o-Coumaric acid in protecting cells from oxidative damage. This further solidifies their potential as effective agents in reducing oxidative stress and improving cellular health in diabetic conditions.

Catalase is one of the essential enzymes that work as a shielding agent by protecting the cells from damage induced by a form of ROS called hydrogen peroxide. The catalase functions by dissociating hydrogen peroxide into water and oxygen and helps restore a normal antioxidant defence system. As this enzyme plays a crucial role as a vital antioxidant in the biological system, its absence could lead to oxidative damage in living cells. Diminished catalase levels contribute to heightened hydrogen peroxide levels, thereby inducing further oxidative damage to DNA, lipids, and proteins. Several studies have shown that the levels of catalase are lower during episodes of chronic hyperglycemia (408-411). As these studies provide evidence of causing oxidative damage due to diabetes, thus it is highly needed to look for an alternative to manage glycaemic index as it acts as a key for the progression of other diseases such as oxidative stress, and diabetes-related ailments. Therefore, we also evaluated the effect of Sinapic and o-Coumaric acid. Our results are consistent with previously

published reports that the administration of Sinapic acid and o-Coumaric acid restores catalase activity during hyperglycemia. To address this issue, researchers around the world use Sinapic acid to tackle the inhibition of diabetes-induced oxidative stress. Many studies provide evidence that administration of Sinapic acid and p-Coumaric acid to model organisms mimicking diabetic conditions significantly reduce hydrogen peroxide levels by restoring catalase activity (399, 407, 412). Our study confirms these observations by demonstrating that the administration of Sinapic acid and o-Coumaric acid to L929 cells cultured under hyperglycemic conditions resulted in significantly higher levels of catalase. This increase in catalase activity suggests that Sinapic acid and o-Coumaric acid effectively mitigate oxidative damage induced by elevated blood glucose levels. This finding is consistent with previous research indicating that these compounds can restore catalase activity and reduce oxidative stress in diabetic models. By improving the antioxidant defence system, these plant-based molecules may offer a complementary approach to conventional diabetes treatments, addressing oxidative damage and supporting overall cellular health.

As aforementioned, since both molecules selected after molecular docking and ADME studies, we evaluate their effect in in vitro conditions (L929 cells) by inducing hyperglycemic conditions. Considering the results of cytotoxic and antioxidant enzymatic studies, we claimed that both these compounds possess no cytotoxicity, and hold good cell migration and antioxidant potential by enhancing epithelial cell migration and antioxidant enzymes levels required by the body to maintain the homeostasis.

As mentioned previously, several synthetic anti-diabetic and wound healing medications have a vast array of drawbacks, some of which are high-cost, side-effects, multiple consumption, interference with human metabolic pathways (413-416). This highlights the crucial requirement for exploring an alternative plant-based natural therapy that is easily accessible to humans, capable of enhancing wound healing and minimizing side effects. Consequently, we conducted an in vivo study to assess their potential in mitigating delayed diabetic wound healing and oxidative stress, following the completion of in vitro studies. Since the results of Sinapic acid were better as compared to o-Coumaric acid, so Sinapic acid was chosen as the test compound for in vivo studies.

To accomplish an in vivo study, we first attempted to develop an animal model that mimics the diabetes-induced delayed wound healing conditions by purchasing SD rats (n=54) from the central house facility of Lovely Professional University, India. Following a one-week acclimatization period, the rats were assigned to two dietary regimens: either NPD or HFD containing 58% fat, 25% protein, and 17% carbohydrate, provided ad libitum for a duration of 4 weeks. On the 7th day, HFD-fed rats received a single dose of STZ. Blood glucose levels were assessed after 7 days, and rats with blood glucose exceeding 250 mg/dl were classified as diabetic. On the diabetic rats, an excision wound was created as per the reported procedure and it was considered as 0 day of wound (362). The next day was considered as day 1 of wounded diabetic rats and from day 1 to day 14 treatment was given as follows: HFD + Sinapic acid (low dose), HFD + Sinapic acid (high

dose). The test-treated groups were fed orally with 20 mg/kg and 40 mg/kg of Sinapic acid. The body weight was documented every week throughout the entire duration of the study. Blood glucose was measured at the start and at the end of the study for NPD groups and at the start, on day 14, and at the end of the study for HFD groups.

HFD can contribute to the development of obesity and diabetes through various physiological mechanisms. Consuming a high-fat meal can promptly result in an excess of calories, causing weight gain and diabetes (417-419). Therefore, we investigated the influence of Sinapic acid on glucose levels in diabetic rats that were fed a HFD. Our findings indicated no significant difference in the rats' body weight during the initial week (when all rats were on a NPD) and the second week (when diabetic group rats transitioned to a HFD). However, by the third week on the HFD, an increase in body weight was noted, and after 14 days of treatment, a reduction in body weight was observed. Additionally, animals receiving Sinapic acid treatment at 20 mg/kg (low dose) were found to have lower glucose levels compared to Sinapic acid treatment at the 40 mg/kg dose.

Liver injury or failure is often characterized by elevated levels of specific liver enzymes such as bilirubin, ALP, SGOT and SGPT. These enzymes serve as crucial biomarkers for assessing liver health and function. In our study, we observed a significant increase in the levels of these enzymes following the administration of a HFD, which is known to induce hepatic damage and exacerbate diabetes-related complications. However, the intervention with Sinapic acid demonstrated a notable protective effect against liver damage. When Sinapic acid was administered at dosages of 20 mg/kg and 40 mg/kg, there was a marked normalization of enzyme levels. This indicates a reduction in liver injury and an improvement in liver function. Specifically, Sinapic acid effectively countered the enzyme elevations caused by the HFD, thereby ameliorating diabetes-associated liver damage. These findings are consistent with those from previously published studies, which have reported that the administration of natural molecules, including various phytochemicals, can positively impact liver enzyme levels in diabetic models. Research has shown that such interventions can lead to improved liver marker function and overall liver health in diabetic rats. For instance, several studies have highlighted similar effects, where natural compounds have provided therapeutic benefits by normalizing liver enzyme levels and reducing hepatic injury in diabetic conditions (420-422). Overall, our results underscore the potential of Sinapic acid as a therapeutic agent for mitigating liver damage associated with diabetes, aligning with existing literature that supports the role of natural compounds in liver protection.

Renal injury or failure may be indicated by elevated levels of certain parameters, including uric acid, creatinine, urea, and blood urea nitrogen (BUN). Long-term exposure to elevated uric acid levels can lead to the development of crystals in the kidneys, which can lead to kidney stones, or in the joints, which can aggravate arthritis (423-426). Persistent hyperuricemia is linked to an increased risk of developing chronic renal disease. Similarly, elevated blood creatinine levels may indicate impaired kidney function, as the kidneys play a vital role in creatinine excretion. A common indicator of a decreased glomerular filtration rate, a

measure of kidney function, is an increased creatinine level. Raised creatinine levels can be the result of several conditions, including chronic or acute kidney disease. Conversely, increased levels of urea nitrogen in the blood may indicate poor kidney function. Elevated BUN levels may be caused by acute kidney injury, chronic kidney disease, or dehydration. In our study, we investigated the impact of Sinapic acid on diabetes-related renal impairment, focusing on key indicators of kidney function. We found that Sinapic acid treatment effectively mitigated renal dysfunction, as evidenced by improved renal function markers, which aligns with findings reported in previous studies (427, 428). Specifically, our results demonstrated that treatment with Sinapic acid, at both 20 mg/kg and 40 mg/kg doses, significantly reduced levels of uric acid, creatinine, and urea. These markers are crucial for assessing kidney health and function. Elevated levels of uric acid, creatinine, and urea are commonly associated with impaired kidney function, as the kidneys are responsible for filtering and eliminating these waste products from the bloodstream. Under conditions of diabetes-related renal impairment, the kidneys' ability to filter waste materials is compromised, leading to their accumulation in the blood. This results in increased levels of these biomarkers, signaling renal dysfunction. However, Sinapic acid treatment reversed this trend by enhancing the kidney's ability to filter and expel waste, thereby reducing the elevated levels of uric acid, creatinine, and urea. The observed improvements in renal function with Sinapic acid therapy highlight its potential as a therapeutic agent for managing diabetes-induced kidney damage. This is consistent with earlier reports indicating that natural compounds can positively influence renal function and ameliorate kidney-related complications in diabetic models. In summary, our study supports the efficacy of Sinapic acid in protecting against renal impairment by restoring normal levels of critical renal function markers.

Lipotoxicity refers to a condition where an excess of lipids in tissues leads to oxidative stress and inflammation, which can contribute to insulin resistance and metabolic disorders such as T2D. High levels of cholesterol, LDL, VLDL are vital for lipid metabolism, but their excessive presence or certain forms can lead to significant health issues. LDL cholesterol, often referred to as "bad" cholesterol, can cause the formation of atherosclerotic plaques in artery walls. These plaques, composed of calcium, fat deposits, and cholesterol, thicken and harden the arteries, leading to atherosclerosis. This condition narrows the arteries and increases the risk of cardiovascular diseases, including heart disease. Our study's findings are particularly significant in the context of managing diabetes and cardiovascular health. Consistent with previous reports (429-431), we observed that animals on a HFD had elevated levels of LDL cholesterol, which is a well-documented risk factor for cardiovascular diseases associated with diabetes. The critical aspect of our results is the observation that Sinapic acid treatment led to a significant reduction in LDL cholesterol levels. This reduction is crucial because elevated LDL cholesterol contributes to the development of atherosclerosis, a condition that can lead to heart disease. By lowering LDL cholesterol levels, Sinapic acid potentially mitigates the risk of cardiovascular complications associated with diabetes.

The importance of these findings lies in the potential for Sinapic acid to offer dual benefits in diabetes management, such as improving glycemic control and reducing renal impairment, while also addressing one of the key risk factors for heart disease. This comprehensive effect underscores the therapeutic potential of Sinapic acid in enhancing overall metabolic health and reducing the risk of complications in diabetic patients. In summary, our study supports the therapeutic value of Sinapic acid in lowering LDL cholesterol and, consequently, in reducing the risk of diabetes-related heart disease. This aligns with and extends previous research, reinforcing the relevance of natural compounds in addressing multiple facets of diabetes and its associated complications.

The connection between antioxidants and oxidative stress is intricate, particularly when considering cellular and physiological functions. Prolonged or excessive oxidative stress is linked to a range of diseases, including cancer, heart disease, and neurological issues, leading to cellular damage. The immune system uses a complex network of both non-enzymatic and enzymatic antioxidants to fight oxidative damage. Enzymatic systems like catalase and SOD promptly neutralize free radicals, while non-enzymatic antioxidants eliminate and capture them. By neutralizing ROS and lipid peroxides, antioxidant enzymes (such as glutathione peroxidase, catalase, and SOD) along with non-enzymatic antioxidants (such as vitamins C and E) work to prevent LPO in cells. Comprehending the interaction between antioxidants and oxidative stress is essential for improving overall health and reducing the risk of diseases associated with excessive oxidative damage (432-434). Consistent with our in vitro results, the diabetic wounded control group exhibited significantly elevated levels of LPO, a marker of oxidative stress, along with reduced levels of key antioxidant enzymes. This imbalance between oxidative stress and antioxidant defence mechanisms is a hallmark of diabetic wounds, contributing to impaired wound healing. However, our study demonstrated that the administration of Sinapic acid at doses of 20 and 40 mg/kg effectively restored the levels of antioxidant enzymes and reduced LPO in the treated groups. These findings are particularly important as they reinforce the role of Sinapic acid in combating oxidative stress, which is a major factor in the progression of diabetic complications. By replenishing antioxidant enzyme levels, Sinapic acid not only helps to neutralize ROS but also supports the body's natural defence systems, thereby promoting better wound healing outcomes. This is consistent with previous studies that have highlighted the potent antioxidant properties of Sinapic acid, demonstrating its ability to restore antioxidant enzyme levels and mitigate oxidative damage in various pathological conditions (435). These results underscore the therapeutic potential of Sinapic acid in managing oxidative stress-related complications in diabetes, particularly in enhancing wound healing.

Wound contraction is the process by which a wound contracts and shrinks in size along the edges. Peripheral vascular disease, a disorder marked by decreased blood flow to the limbs, can be caused by diabetes. Insufficient blood flow can hinder the wound site's ability to receive oxygen and nutrients, which can impede the healing process and prevent wound contraction (436-439). Angiogenesis, or the formation of new blood vessels from existing vessels, is essential for the healing of wounds. It is essential that blood supply be restored

in order for damaged tissues to receive nutrition, oxygen and immune cells to heal properly. Myofibroblasts, which are specialized cells that bring the edges of a wound together, contract in response to the newly formed blood vessels, which aids the healing process. Effective wound contraction relies on the function of white blood cells, the formation of new blood vessels, and the synthesis of collagen, all of which are hindered by elevated glucose levels (440, 441). As a result, diabetes management and blood sugar control are essential to minimize the impact on wound healing. In the present study, we also sought to analyze the potential of Sinapic acid in healing the diabetic wound by reducing wound size and increasing wound contraction. The strength of our study lies in its comprehensive assessment of the wound healing process in a diabetic model, particularly under the influence of Sinapic acid treatment. Our findings demonstrated that while a HFD alone led to diminished wound contraction and impaired healing parameters, the administration of Sinapic acid at both 20 mg/kg and 40 mg/kg doses effectively reversed these detrimental effects. Notably, Sinapic acid not only enhanced wound contraction and reduced wound size but also restored critical wound healing parameters such as epithelization, fibroblast proliferation, collagen production, angiogenesis, and granulation tissue formation. The study further highlighted that the lower dose of Sinapic acid (20 mg/kg) produced superior wound healing outcomes compared to the higher dose (40 mg/kg), emphasizing the efficacy of lower doses in promoting optimal healing. Our results are consistent with the previous published report where Kaltalioglu showed that Sinapic acid-loaded gel at low dose (1% and 2%) exhibit higher rate of wound healing by reducing wound area than Sinapic acid-loaded gel at 3% (435). This leads to the conclusion that diabetic animals receiving Sinapic acid therapy had the potential to restore wound morphology by restoring the wound healing process. This strength underlines the potential of Sinapic acid as a promising therapeutic agent for accelerating wound healing in diabetic conditions, particularly in cases where wound healing is significantly compromised. The ability of Sinapic acid to restore multiple aspects of the healing process demonstrates its broad therapeutic potential and supports its use as a targeted treatment to improve clinical outcomes in diabetic wound management.

For several reasons, histopathological examination is essential in preclinical in vivo research because it provides important information about how experimental treatments affect the tissues and organs of living organisms. For instance, researchers can predict a safe and effective dosage range by analyzing animal tissues subjected to different doses of a test drug and identifying the point at which undesirable effects occur (376). Researchers can assess different stages of wound healing, such as inflammation, tissue regeneration and remodeling, using histopathology (442). It helps evaluate the effectiveness of diabetic wound healing treatments by providing a comprehensive perspective of the cellular and structural changes occurring at the wound site across time. Due to the fact that diabetic wounds often show reduced collagen deposition, tissue granulation, impaired epithelialization, tissue regeneration, and vasculature, microscopic and cellular investigation of these parameters by histopathological analysis becomes possible (80, 443).

In this study, we found that non-diabetic non-wounded group had thick epithelium layer, dermal remodeling, and good vasculature; whereas the diabetic wounded control group had poor wound healing due to altered epithelial and dermal layer, immature granular tissues. On the other hand, there was a distorted epithelial layer in the non-diabetic wounded group due to poor vascularization; whereas the treatment of Sinapic acid to non-diabetic wounded group at 20 mg/kg and 40 mg/kg helped the animals to heal wound by enhancing new blood vessels and granular tissue formation. The development of new blood vessels aids the skin in recovering its original structure and morphology by enhancing the processes of re-epithelization and dermal remodeling. Likewise, our findings suggest that the introduction of Sinapic acid at both concentrations fosters angiogenesis, dermal remodeling, re-epithelialization, and the formation of granulation tissue, collectively contributing to an expedited wound healing process. Although Sinapic acid demonstrated significant potential for wound healing at both low and high doses, the use of a lower dose (20 mg/kg) resulted in swifter healing of diabetic wounds compared to the higher dose (40 mg/kg). Our findings align with previously published reports indicating the positive impact of Sinapic acid on wound healing. Despite the overall efficacy, our study highlights significant results associated with the lower dose of Sinapic acid (435). In conclusion, our findings not only confirm the therapeutic potential of Sinapic acid in promoting wound healing but also emphasize the advantage of using a lower dose for more rapid recovery in diabetic wounds. This study contributes valuable insights into the dose-dependent effects of Sinapic acid and underscores its role in enhancing the wound healing process, making it a promising candidate for further research and clinical application in wound management.

A substantial reduction in SIRT1 expression has been observed in wounds of diabetic patients. This reduction in SIRT1 levels contributes to the modification of the molecular environment associated with diabetes, which may affect multiple cellular functions and interfere with the normal treatment response. Low SIRT1 expression in diabetic lesions may be due to a variety of signaling pathways, complex interactions with diabetes-specific variables, or epigenetic changes. This reflects the complex interaction between SIRT1 and diabetes-associated decreased wound healing ability. A previous published report showed that SIRT1 expression was reduced in diabetic animals and results in impaired angiogenesis (39). In conclusion, our study reinforces the critical role of SIRT1 in the healing of diabetic wounds, consistent with previous findings that indicate a decrease in SIRT1 expression in such conditions. Importantly, we observed that the administration of Sinapic acid at both 20 mg/kg and 40 mg/kg doses effectively enhanced SIRT1 expression, with more pronounced results at the lower dose. This suggests that upregulating SIRT1 expression may accelerate wound healing in diabetic patients, likely through the promotion of angiogenesis. These findings highlight the therapeutic potential of Sinapic acid in improving wound healing outcomes in diabetic contexts, particularly by targeting pathways that enhance vascularization and tissue repair.

CHAPTER 8

CONCLUSION

Diabetes is a metabolic disorder characterized by elevated plasma glucose levels resulting from deficiencies in insulin action, insulin secretion, or a combination of both. Individuals with diabetes are at an increased risk of developing chronic wounds, especially in the foot region, referred to as DFU. Approximately 15–20 % of patients with diabetes develop DFU annually and almost 15 % of the health budget yearly is used to treat patients with diabetes and its complications worldwide. The abnormal glucose metabolism was thought to affect the wound-healing process in individuals with diabetes, contributing to the formation of chronic wounds. The elevated level of blood glucose leads to poor blood flow due to which essential nutritional components are unable to reach the wounded area and impair the healing mechanism. Chronic inflammation and increased oxidative stress are characteristics of chronic wounds that result in causing extensive host tissue damage.

The clearance of anti-diabetic wound medications from the FDA has accelerated the use of synthetic medications for the treatment of DFU globally, and the majority of these medications are known to have adverse side effects. As an alternative, the use of herbal supplements for primary health care has increased significantly during the last thirty years. Consequently, to reduce the use of synthetic drugs and their associated side effects and to promote the use of natural phytochemical-based drugs to reach clinical trials, we selected various phytochemical compounds which were previously reported for their anti-diabetic properties. Among all these, we chose a natural phytochemical called Sinapic acid based on its high binding energy, ADME results and cost-effectiveness. The strength of our study lies in the innovative evaluation of Sinapic acid, a novel compound with demonstrated antioxidant properties, in the context of diabetes. Additionally, our study provides conclusive evidence of its potential role in enhancing wound healing associated with diabetes. Earlier investigations have indicated that the inclusion of this compound in fruits, vegetables, spices, oilseeds, and plants enhances its therapeutic potential for treating various diseases.

Oxidative stress, characterized by harm to macromolecules due to an imbalance between ROS generation and antioxidant defence, was assessed through the DPPH free radical analysis assay. Sinapic acid demonstrated robust scavenging effects in a dose-dependent manner, indicating its potent antioxidant properties. Sinapic acid was tested for toxicity on proliferating normal skin cells (L929 cells) using a cell viability assay (MTT assay), and it was discovered that the substance did not exhibit any toxicity when exposed to the cells. Sinapic acid improved HUVEC cell migration and endothelium growth in hyperglycemic environment. Furthermore, administration of Sinapic acid into L929 cells effectively reduced oxidative stress by restoring the levels of SOD, catalase and GST and reducing LPO. This implies that Sinapic acid may be employed to diminish oxidative stress linked to diabetes by decreasing free radical production and enhancing antioxidant enzyme levels. It has been demonstrated that oxidative stress damages pancreatic cells, impairing insulin secretion and potentially leading to diabetes. According to our research, Sinapic acid has a strong antioxidant capacity and

can restore damaged pancreatic cells as well as irregular insulin secretion. Sinapic acid emerges as a promising novel compound for the management of diabetes and diabetic wounds, given our in vitro findings that demonstrate its potential to improve oxidative wound healing and alleviate oxidative stress associated with diabetes.

To investigate changes in glucose and injured tissues, we created an in vivo diabetic wound healing model. This is the first research to demonstrate how antioxidant enzyme levels and wound healing parameters are restored when Sinapic acid is administered orally at different dosages, such as 20 mg/kg and 40 mg/kg, protecting animals against oxidative stress and delayed wound healing caused by a HFD. Additionally, after consuming Sinapic acid, blood sugar and body weight increased by high-fat meals normalized. Similarly, our test compound was found to reduce wound area and increase wound contraction in a group suffering from diabetes. Our histopathologic analysis showed that Sinapic acid treatment enhanced re-epithelialization, dermal remodeling, and angiogenesis as compared to the diabetic injured control group.

In view of the present study, our results suggest that SIRT1 activators, such as Sinapic acid, may play a role in enhancing diabetes-related wound healing. The outcomes derived from in silico approach have provided insights into the role of Sinapic acid as a SIRT1 activator in the treatment of diabetic wounds. SIRT1 is known to modulate epigenetic changes by deacetylating histones and other transcriptional regulators, leading to the activation or repression of genes involved in wound healing processes. Based on this information, we explored the potential of Sinapic acid in diabetic wound healing models, utilizing both in vitro and in vivo approaches with varying doses of Sinapic acid. We examined the effects of administering Sinapic acid orally in vivo, for the first time, at dosages of 20 and 40 mg/kg.

We employed a HFD model to demonstrate its potential utility in diabetes and diabetic wounds treatment. Although the impact of Sinapic acid or formulations containing Sinapic acid on diabetic wound healing is already established, the distinct effect of orally administered Sinapic acid at 20 and 40 mg/kg on an in vivo diabetic wound model has not been investigated, which makes this study unique. Our in vivo findings from this study are significant, as they conclusively demonstrated that Sinapic acid treatment at a lower dose (20 mg/kg) yielded superior results compared to the higher dose (40 mg/kg). Furthermore, the strength of our study is further bolstered by its comprehensive methodology, which includes wound closure assessments, detailed antioxidant experiments, histopathological evaluations, and monitoring of body weight and blood glucose levels, and analysis of SIRT1 expression. However, while we assessed SIRT1 expression in different treatment groups, an in-depth investigation of SIRT1 as an epigenetic regulator remains unexplored. Additionally, our study did not examine the effects of Sinapic acid on inflammatory markers or gene expression related to diabetic wound healing.

Despite these limitations, the multifaceted approach used in this study provides a holistic view of Sinapic acid's therapeutic potential, ensuring that both efficacy and safety are considered. By demonstrating that a

lower dose achieves superior results, our study offers valuable guidance for optimizing dosage in clinical settings, potentially leading to more effective and safer treatments for diabetic wounds. To advance this compound to clinical trials and enhance its therapeutic relevance, future studies should focus on elucidating the mechanisms through which Sinapic acid influences epigenetic regulators and pathways involved in diabetic wound healing at the cellular, molecular, and biochemical levels.

BIBLIOGRAPHY

1. Atlas D. International diabetes federation. IDF Diabetes Atlas, 7th edn Brussels, Belgium: International Diabetes Federation. 2015;33(2).
2. Reiber G, Lipsky B, Gibbons G. The burden of diabetic foot ulcers. The American journal of surgery. 1998;176(2):5S-10S.
3. Raghav A, Khan ZA, Labala RK, Ahmad J, Noor S, Mishra BK. Financial burden of diabetic foot ulcers to world: a progressive topic to discuss always. Therapeutic advances in endocrinology and metabolism. 2018;9(1):29-31.
4. Greenhalgh DG. Wound healing and diabetes mellitus. Clinics in plastic surgery. 2003;30(1):37-45.
5. Stewart PS, Franklin MJ. Physiological heterogeneity in biofilms. Nature Reviews Microbiology. 2008;6(3):199-210.
6. MacLeod AS, Mansbridge JN. The innate immune system in acute and chronic wounds. Advances in wound care. 2016;5(2):65-78.
7. Wang X, Li R, Zhao H. Enhancing angiogenesis: innovative drug delivery systems to facilitate diabetic wound healing. Biomedicine & Pharmacotherapy. 2024;170:116035.
8. Lee SH, Kim SH, Kim KB, Kim HS, Lee YK. Factors Influencing Wound Healing in Diabetic Foot Patients. Medicina. 2024;60(5):723.
9. Davis FM, Kimball A, Boniakowski A, Gallagher K. Dysfunctional wound healing in diabetic foot ulcers: new crossroads. Current diabetes reports. 2018;18:1-8.
10. Han X, Ju LS, Irudayaraj J. Oxygenated wound dressings for hypoxia mitigation and enhanced wound healing. Molecular pharmaceutics. 2023;20(7):3338-55.
11. Ghahremani-Nasab M, Del Bakhshayesh AR, Akbari-Gharalari N, Mehdipour A. Biomolecular and cellular effects in skin wound healing: the association between ascorbic acid and hypoxia-induced factor. Journal of Biological Engineering. 2023;17(1):62.
12. Cheng P, Xie X, Hu L, Zhou W, Mi B, Xiong Y, et al. Hypoxia endothelial cells-derived exosomes facilitate diabetic wound healing through improving endothelial cell function and promoting M2 macrophages polarization. Bioactive Materials. 2024;33:157-73.
13. Chinaroonchai K. Oxygen therapy to enhance wound healing after revascularization. The International Journal of Lower Extremity Wounds. 2024;23(1):49-54.
14. Qin S, Bie F, Chen S, Xu Y, Chen L, Shu B, et al. Targeting S100A12 to improve angiogenesis and accelerate diabetic wound healing. Inflammation. 2024:1-16.
15. Nirenjen S, Narayanan J, Tamilanban T, Subramaniyan V, Chitra V, Fuloria NK, et al. Exploring the contribution of pro-inflammatory cytokines to impaired wound healing in diabetes. Frontiers in immunology. 2023;14:1216321.
16. Pal D, Das P, Mukherjee P, Roy S, Chaudhuri S, Kesh SS, et al. Biomaterials-Based Strategies to Enhance Angiogenesis in Diabetic Wound Healing. ACS Biomaterials Science & Engineering. 2024;10(5):2725-41.
17. Xu J, Gao J, Li H, Zhu Z, Liu J, Gao C. The risk factors in diabetic foot ulcers and predictive value of prognosis of wound tissue vascular endothelium growth factor. Scientific Reports. 2024;14(1):14120.
18. Yadav JP, Singh AK, Grishina M, Pathak P, Verma A, Kumar V, et al. Insights into the mechanisms of diabetic wounds: pathophysiology, molecular targets, and treatment strategies through conventional and alternative therapies. Inflammopharmacology. 2024;32(1):149-228.
19. Veith AP, Henderson K, Spencer A, Sligar AD, Baker AB. Therapeutic strategies for enhancing angiogenesis in wound healing. Advanced drug delivery reviews. 2019;146:97-125.
20. An Y, Xu B-t, Wan S-r, Ma X-m, Long Y, Xu Y, et al. The role of oxidative stress in diabetes mellitus-induced vascular endothelial dysfunction. Cardiovascular Diabetology. 2023;22(1):237.
21. Xie W, Hu W, Huang Z, Li M, Zhang H, Huang X, et al. Betulinic acid accelerates diabetic wound healing by modulating hyperglycemia-induced oxidative stress, inflammation and glucose intolerance. Burns & Trauma. 2022;10:tkac007.
22. Potenza MA, Gagliardi S, Nacci C, Carratu MR, Montagnani M. Endothelial dysfunction in diabetes: from mechanisms to therapeutic targets. Current medicinal chemistry. 2009;16(1):94-112.
23. Lobmann R, Zemlin C, Motzkau M, Reschke K, Lehnert H. Expression of matrix metalloproteinases and growth factors in diabetic foot wounds treated with a protease absorbent dressing. Journal of Diabetes and its Complications. 2006;20(5):329-35.
24. Deng L, Du C, Song P, Chen T, Rui S, Armstrong DG, et al. The role of oxidative stress and antioxidants in diabetic wound healing. Oxidative medicine and cellular longevity. 2021;2021.

25.   Catrina S-B, Zheng X. Hypoxia and hypoxia-inducible factors in diabetes and its complications. Diabetologia. 2021;64:709-16.

26.   Tesfaye S, Stevens L, Stephenson J, Fuller J, Plater M, Ionescu-Tirgoviste C, et al. Prevalence of diabetic peripheral neuropathy and its relation to glycaemic control and potential risk factors: the EURODIAB IDDM Complications Study. Diabetologia. 1996;39:1377-84.

27.   Kim JH, Ruegger PR, Lebig EG, VanSchalkwyk S, Jeske DR, Hsiao A, et al. High levels of oxidative stress create a microenvironment that significantly decreases the diversity of the microbiota in diabetic chronic wounds and promotes biofilm formation. Frontiers in cellular and infection microbiology. 2020;10:259.

28.   Prabhakar PK, Singh K, Kabra D, Gupta J. Natural SIRT1 modifiers as promising therapeutic agents for improving diabetic wound healing. Phytomedicine. 2020;76:153252.

29.   Chen B, Zang W, Wang J, Huang Y, He Y, Yan L, et al. The chemical biology of sirtuins. Chemical Society Reviews. 2015;44(15):5246-64.

30.   Michan S, Sinclair D. Sirtuins in mammals: insights into their biological function. Biochemical Journal. 2007;404(1):1-13.

31.   Jęśko H, Wencel P, Strosznajder RP, Strosznajder JB. S irtuins and Their Roles in Brain Aging and Neurodegenerative Disorders. Neurochemical research. 2017;42:876-90.

32.   Grabowska W, Sikora E, Bielak-Zmijewska A. Sirtuins, a promising target in slowing down the ageing process. Biogerontology. 2017;18:447-76.

33.   Dai H, Sinclair DA, Ellis JL, Steegborn C. Sirtuin activators and inhibitors: Promises, achievements, and challenges. Pharmacology & therapeutics. 2018;188:140-54.

34.   Zhao L, Cao J, Hu K, He X, Yun D, Tong T, et al. Sirtuins and their biological relevance in aging and age-related diseases. Aging and disease. 2020;11(4):927.

35.   Iside C, Scafuro M, Nebbioso A, Altucci L. SIRT1 activation by natural phytochemicals: an overview. Frontiers in pharmacology. 2020;11:1225.

36.   Strycharz J, Rygielska Z, Swiderska E, Drzewoski J, Szemraj J, Szmigiero L, et al. SIRT1 as a therapeutic target in diabetic complications. Current medicinal chemistry. 2018;25(9):1002-35.

37.   Meng T, Qin W, Liu B. SIRT1 antagonizes oxidative stress in diabetic vascular complication. Frontiers in endocrinology. 2020;11:568861.

38.   Potente M, Ghaeni L, Baldessari D, Mostoslavsky R, Rossig L, Dequiedt F, et al. SIRT1 controls endothelial angiogenic functions during vascular growth. Genes & development. 2007;21(20):2644-58.

39.   Li X, Wu G, Han F, Wang K, Bai X, Jia Y, et al. SIRT1 activation promotes angiogenesis in diabetic wounds by protecting endothelial cells against oxidative stress. Archives of biochemistry and biophysics. 2019;661:117-24.

40.   Blume P, Bowlby M, Schmidt BM, Donegan R. Safety and efficacy of Becaplermin gel in the treatment of diabetic foot ulcers. Chronic Wound Care Management and Research. 2014:11-4.

41.   Steed DL. Clinical evaluation of recombinant human platelet-derived growth factor for the treatment of lower extremity ulcers. Plastic and reconstructive surgery. 2006;117(7S):143S-9S.

42.   Smiell JM. Clinical safety of becaplermin (rhPDGF-BB) gel. The American journal of surgery. 1998;176(2):68S-73S.

43.   Wieman TJ, Smiell JM, Su Y. Efficacy and safely of a topical gel formulation of recombinant human platelet-derived growth factor-BB (becaplermin) in patients with chronic neuropathic diabetic ulcers: a phase III randomized placebo-controlled double-blind study. Diabetes care. 1998;21(5):822-7.

44.   Fang RC, Galiano RD. A review of becaplermin gel in the treatment of diabetic neuropathic foot ulcers. Biologics: Targets and Therapy. 2008;2(1):1-12.

45.   Ling C, Rönn T. Epigenetics in human obesity and type 2 diabetes. Cell Metab. 2019;29(5):1028-44.

46.   Organization WH. Guideline daily iron supplementation in infants and children: World Health Organization; 2016.

47.   Prevention C. National diabetes statistics report: estimates of diabetes and its burden in the United States, 2014. US Department of Health and Human Services, Atlanta, GA. 2014.

48.   Gordois A, Scuffham P, Shearer A, Oglesby A, Tobian JA. The health care costs of diabetic peripheral neuropathy in the US. Diabetes Care. 2003;26(6):1790-5.

49.   Singh N, Armstrong DG, Lipsky BA. Preventing foot ulcers in patients with diabetes. JAMA. 2005;293(2):217-28.

50.   Wu SC, Driver VR, Wrobel JS, Armstrong DG. Foot ulcers in the diabetic patient, prevention and treatment. Vasc Health Risk Manag. 2007;3(1):65.

51.   Ling C, Groop L. Epigenetics: a molecular link between environmental factors and type 2 diabetes. Diabetes. 2009;58(12):2718-25.

52.   Theilgaard-Mönch K, Knudsen S, Follin P, Borregaard N. The transcriptional activation program of human neutrophils in skin lesions supports their important role in wound healing. J Immunol. 2004;172(12):7684-93.

53.   Wynn TA, Vannella KM. Macrophages in tissue repair, regeneration, and fibrosis. Immunity. 2016;44(3):450-62.

54.   Maruyama K, Asai J, Ii M, Thorne T, Losordo DW, D'Amore PA. Decreased macrophage number and activation lead to reduced lymphatic vessel formation and contribute to impaired diabetic wound healing. Am J Pathol. 2007;170(4):1178-91.

55.   Willenborg S, Lucas T, Van Loo G, Knipper JA, Krieg T, Haase I, et al. CCR2 recruits an inflammatory macrophage subpopulation critical for angiogenesis in tissue repair. Blood. 2012;120(3):613-25.

56.   Italiani P, Boraschi D. From monocytes to M1/M2 macrophages: phenotypical vs. functional differentiation. Front Immunol. 2014;5:514.

57.   Boniakowski AE, Kimball AS, Jacobs BN, Kunkel SL, Gallagher KA. Macrophage-mediated inflammation in normal and diabetic wound healing. J Immunol. 2017;199(1):17-24.

58.   Gallagher KA, Joshi A, Carson WF, Schaller M, Allen R, Mukerjee S, et al. Epigenetic changes in bone marrow progenitor cells influence the inflammatory phenotype and alter wound healing in type 2 diabetes. Diabetes. 2015;64(4):1420-30.

59.   Kimball AS, Joshi A, Carson WF, Boniakowski AE, Schaller M, Allen R, et al. The histone methyltransferase MLL1 directs macrophage-mediated inflammation in wound healing and is altered in a murine model of obesity and type 2 diabetes. Diabetes. 2017;66(9):2459-71.

60.   Wang X, Cao Q, Yu L, Shi H, Xue B, Shi H. Epigenetic regulation of macrophage polarization and inflammation by DNA methylation in obesity. JCI Insight. 2016;1(19).

61.   Yan J, Tie G, Wang S, Tutto A, DeMarco N, Khair L, et al. Diabetes impairs wound healing by Dnmt1-dependent dysregulation of hematopoietic stem cells differentiation towards macrophages. Nat Commun. 2018;9(1):1-13.

62.   De Santa F, Totaro MG, Prosperini E, Notarbartolo S, Testa G, Natoli G. The histone H3 lysine-27 demethylase Jmjd3 links inflammation to inhibition of polycomb-mediated gene silencing. Cell. 2007;130(6):1083-94.

63.   Peppa M, Brem H, Ehrlich P, Zhang J-G, Cai W, Li Z, et al. Adverse effects of dietary glycotoxins on wound healing in genetically diabetic mice. Diabetes. 2003;52(11):2805-13.

64.   Zhu P, Yang C, Chen L-H, Ren M, Lao G-j, Yan L. Impairment of human keratinocyte mobility and proliferation by advanced glycation end products-modified BSA. Arch Dermatol Res. 2011;303(5):339-50.

65.   Lerman OZ, Galiano RD, Armour M, Levine JP, Gurtner GC. Cellular dysfunction in the diabetic fibroblast: impairment in migration, vascular endothelial growth factor production, and response to hypoxia. The American journal of pathology. 2003;162(1):303-12.

66.   Xuan YH, Huang BB, Tian HS, Chi LS, Duan YM, Wang X, et al. High-glucose inhibits human fibroblast cell migration in wound healing via repression of bFGF-regulating JNK phosphorylation. PloS one. 2014;9(9):e108182.

67.   Zhang J, Yang C, Wang C, Liu D, Lao G, Liang Y, et al. AGE-induced keratinocyte MMP-9 expression is linked to TET2-mediated CpG demethylation. Wound Repair Regen. 2016;24(3):489-500.

68.   Ling L, Ren M, Yang C, Lao G, Chen L, Luo H, et al. Role of site-specific DNA demethylation in TNFa-induced. Endocrinology. 2013;50:279-90.

69.   Park LK, Maione AG, Smith A, Gerami-Naini B, Iyer LK, Mooney DJ, et al. Genome-wide DNA methylation analysis identifies a metabolic memory profile in patient-derived diabetic foot ulcer fibroblasts. Epigenetics. 2014;9(10):1339-49.

70.   Bowler P, Duerden B, Armstrong DG. Wound microbiology and associated approaches to wound management. Clinical microbiology reviews. 2001;14(2):244-69.

71.   Velnar T, Bailey T, Smrkolj V. The wound healing process: an overview of the cellular and molecular mechanisms. Journal of international medical research. 2009;37(5):1528-42.

72.   Golebiewska EM, Poole AW. Platelet secretion: From haemostasis to wound healing and beyond. Blood reviews. 2015;29(3):153-62.

73.   Weisel JW, Litvinov RI. Fibrin formation, structure and properties. Fibrous proteins: structures and mechanisms. 2017:405-56.

74.   Kingsley K, Huff J, Rust W, Carroll K, Martinez A, Fitchmun M, et al. ERK1/2 mediates PDGF-BB stimulated vascular smooth muscle cell proliferation and migration on laminin-5. Biochemical and biophysical research communications. 2002;293(3):1000-6.

75.   Dong J, Chen L, Zhang Y, Jayaswal N, Mezghani I, Zhang W, et al. Mast cells in diabetes and diabetic wound healing. Advances in Therapy. 2020;37(11):4519-37.

76.   Kolaczkowska E, Kubes P. Neutrophil recruitment and function in health and inflammation. Nature reviews immunology. 2013;13(3):159-75.

77.   Van der Veer W, Van Egmond M, Niessen F, Beelen R. Macrophages in skin injury and repair. Immunobiology. 2011;216(7):753-62.

78.   Barrientos S, Stojadinovic O, Golinko MS, Brem H, Tomic-Canic M. Growth factors and cytokines in wound healing. Wound repair and regeneration. 2008;16(5):585-601.

79.   Campbell L, Saville CR, Murray PJ, Cruickshank SM, Hardman MJ. Local arginase 1 activity is required for cutaneous wound healing. Journal of Investigative Dermatology. 2013;133(10):2461-70.

80.   Wilkinson HN, Hardman MJ. Wound healing: Cellular mechanisms and pathological outcomes. Open biology. 2020;10(9):200223.

81.   Landén NX, Li D, Ståhle M. Transition from inflammation to proliferation: a critical step during wound healing. Cellular and Molecular Life Sciences. 2016;73:3861-85.

82.   Szabo I, Simon M, Hunyadi J. Plasmin promotes keratinocyte migration and phagocytic-killing accompanied by suppression of cell proliferation which may facilitate re-epithelialization of wound beds. Clinical and Developmental Immunology. 2004;11(3-4):233-40.

83.   Olczyk P, Mencner Ł, Komosinska-Vassev K. The role of the extracellular matrix components in cutaneous wound healing. BioMed research international. 2014;2014.

84.   Huang S-P, Wu M-S, Shun C-T, Wang H-P, Hsieh C-Y, Kuo M-L, et al. Cyclooxygenase-2 increases hypoxia-inducible factor-1 and vascular endothelial growth factor to promote angiogenesis in gastric carcinoma. Journal of biomedical science. 2005;12:229-41.

85.   Poché RA, Hsu C-W, McElwee ML, Burns AR, Dickinson ME. Macrophages engulf endothelial cell membrane particles preceding pupillary membrane capillary regression. Developmental biology. 2015;403(1):30-42.

86.   Darby IA, Laverdet B, Bonté F, Desmoulière A. Fibroblasts and myofibroblasts in wound healing. Clinical, cosmetic and investigational dermatology. 2014:301-11.

87.   Mathew-Steiner SS, Roy S, Sen CK. Collagen in wound healing. Bioengineering. 2021;8(5):63.

88.   Duca L, Floquet N, Alix AJ, Haye B, Debelle L. Elastin as a matrikine. Critical reviews in oncology/hematology. 2004;49(3):235-44.

89.   Dunne Jr WM. Bacterial adhesion: seen any good biofilms lately? Clinical microbiology reviews. 2002;15(2):155-66.

90.   Liang Z, Rybtke M, Kragh KN, Johnson O, Schicketanz M, Zhang YE, et al. Transcription of the Alginate Operon in Pseudomonas aeruginosa Is Regulated by c-di-GMP. Microbiology Spectrum. 2022;10(4):e00675-22.

91.   Hay ID, Rehman ZU, Moradali MF, Wang Y, Rehm BH. Microbial alginate production, modification and its applications. Microbial biotechnology. 2013;6(6):637-50.

92.   Boyd A, Chakrabarty A. Pseudomonas aeruginosa biofilms: role of the alginate exopolysaccharide. Journal of industrial microbiology and biotechnology. 1995;15(3):162-8.

93.   Ibanez de Aldecoa AL, Zafra O, González-Pastor JE. Mechanisms and regulation of extracellular DNA release and its biological roles in microbial communities. Frontiers in microbiology. 2017;8:1390.

94.   Schulze A, Mitterer F, Pombo JP, Schild S. Biofilms by bacterial human pathogens: Clinical relevance-development, composition and regulation-therapeutical strategies. Microbial Cell. 2021;8(2):28.

95.   Feng G, Cheng Y, Wang S-Y, Borca-Tasciuc DA, Worobo RW, Moraru CI. Bacterial attachment and biofilm formation on surfaces are reduced by small-diameter nanoscale pores: how small is small enough? npj Biofilms and Microbiomes. 2015;1(1):1-9.

96.   Koczan JM, Lenneman BR, McGrath MJ, Sundin GW. Cell surface attachment structures contribute to biofilm formation and xylem colonization by Erwinia amylovora. Applied and Environmental Microbiology. 2011;77(19):7031-9.

97.   Rosenberg M, Bayer EA, Delarea J, Rosenberg E. Role of thin fimbriae in adherence and growth of Acinetobacter calcoaceticus RAG-1 on hexadecane. Applied and Environmental Microbiology. 1982;44(4):929-37.

98.   Bullitt E, Makowski L. Structural polymorphism of bacterial adhesion pili. Nature. 1995;373(6510):164-7.

99.   Caiazza NC, O'Toole GA. SadB is required for the transition from reversible to irreversible attachment during biofilm formation by Pseudomonas aeruginosa PA14. Am Soc Microbiol; 2004.

100.   Hinsa SM, Espinosa-Urgel M, Ramos JL, O'Toole GA. Transition from reversible to irreversible attachment during biofilm formation by Pseudomonas fluorescens WCS365 requires an ABC transporter and a large secreted protein. Molecular microbiology. 2003;49(4):905-18.

101.   Nwodo UU, Green E, Okoh AI. Bacterial exopolysaccharides: functionality and prospects. International journal of molecular sciences. 2012;13(11):14002-15.

102.   Rutherford ST, Bassler BL. Bacterial quorum sensing: its role in virulence and possibilities for its control. Cold Spring Harbor perspectives in medicine. 2012;2(11):a012427.

103.   Rasmussen TB, Bjarnsholt T, Skindersoe ME, Hentzer M, Kristoffersen P, Kote M, et al. Screening for quorum-sensing inhibitors (QSI) by use of a novel genetic system, the QSI selector. Journal of bacteriology. 2005;187(5):1799-814.

104.   Bouyahya A, Dakka N, Et-Touys A, Abrini J, Bakri Y. Medicinal plant products targeting quorum sensing for combating bacterial infections. Asian Pacific journal of tropical medicine. 2017;10(8):729-43.

105.   Rasmussen TB, Givskov M. Quorum sensing inhibitors: a bargain of effects. Microbiology. 2006;152(4):895-904.

106.   Hong K-W, Koh C-L, Sam C-K, Yin W-F, Chan K-G. Quorum quenching revisited—from signal decays to signalling confusion. Sensors. 2012;12(4):4661-96.

107.   Yang Q, Aamdal Scheie A, Benneche T, Defoirdt T. Specific quorum sensing-disrupting activity (AQSI) of thiophenones and their therapeutic potential. Scientific reports. 2015;5(1):18033.

108.   Kaur B, Gupta J, Sharma S, Sharma D, Sharma S. Focused review on dual inhibition of quorum sensing and efflux pumps: a potential way to combat multi drug resistant Staphylococcus aureus infections. International Journal of Biological Macromolecules. 2021;190:33-43.

109.   Hannigan GD, Grice EA. Microbial ecology of the skin in the era of metagenomics and molecular microbiology. Cold Spring Harbor perspectives in medicine. 2013;3(12).

110.   Huber B, Riedel K, Hentzer M, Heydorn A, Gotschlich A, Givskov M, et al. The cep quorum-sensing system of Burkholderia cepacia H111 controls biofilm formation and swarming motility. Microbiology. 2001;147(9):2517-28.

111.   Ganesh PS, Rai VR. Attenuation of quorum-sensing-dependent virulence factors and biofilm formation by medicinal plants against antibiotic resistant Pseudomonas aeruginosa. Journal of traditional and complementary medicine. 2018;8(1):170-7.

112.   Khatoon Z, McTiernan CD, Suuronen EJ, Mah T-F, Alarcon EI. Bacterial biofilm formation on implantable devices and approaches to its treatment and prevention. Heliyon. 2018;4(12).

113.   Alves PM, Al-Badi E, Withycombe C, Jones PM, Purdy KJ, Maddocks SE. Interaction between Staphylococcus aureus and Pseudomonas aeruginosa is beneficial for colonisation and pathogenicity in a mixed biofilm. Pathogens and disease. 2018;76(1):fty003.

114.   Waldrop R, McLaren A, Calara F, McLemore R. Biofilm growth has a threshold response to glucose in vitro. Clinical Orthopaedics and Related Research®. 2014;472:3305-10.

115.   Hsu C-Y, Shu J-C, Lin M-H, Chong K-Y, Chen C-C, Wen S-M, et al. High glucose concentration promotes vancomycin-enhanced biofilm formation of vancomycin-non-susceptible Staphylococcus aureus in diabetic mice. PLoS One. 2015;10(8):e0134852.

116.   Kirker KR, Secor PR, James GA, Fleckman P, Olerud JE, Stewart PS. Loss of viability and induction of apoptosis in human keratinocytes exposed to Staphylococcus aureus biofilms in vitro. Wound Repair and Regeneration. 2009;17(5):690-9.

117.   Zhao G, Hochwalt PC, Usui ML, Underwood RA, Singh PK, James GA, et al. Delayed wound healing in diabetic (db/db) mice with Pseudomonas aeruginosa biofilm challenge: a model for the study of chronic wounds. Wound Repair and Regeneration. 2010;18(5):467-77.

118.   Schierle CF, De la Garza M, Mustoe TA, Galiano RD. Staphylococcal biofilms impair wound healing by delaying reepithelialization in a murine cutaneous wound model. Wound repair and regeneration. 2009;17(3):354-9.

119.   Tottoli EM, Dorati R, Genta I, Chiesa E, Pisani S, Conti B. Skin wound healing process and new emerging technologies for skin wound care and regeneration. Pharmaceutics. 2020;12(8):735.

120.   Pastar I, Nusbaum AG, Gil J, Patel SB, Chen J, Valdes J, et al. Interactions of methicillin resistant Staphylococcus aureus USA300 and Pseudomonas aeruginosa in polymicrobial wound infection. PloS one. 2013;8(2):e56846.

121.   Watters C, DeLeon K, Trivedi U, Griswold JA, Lyte M, Hampel KJ, et al. Pseudomonas aeruginosa biofilms perturb wound resolution and antibiotic tolerance in diabetic mice. Medical microbiology and immunology. 2013;202:131-41.

122.   Horner W, Helbling A, Salvaggio J, Lehrer S. Fungal allergens. Clinical microbiology reviews. 1995;8(2):161-79.

123. Kalan L, Loesche M, Hodkinson BP, Heilmann K, Ruthel G, Gardner SE, et al. Redefining the chronic-wound microbiome: fungal communities are prevalent, dynamic, and associated with delayed healing. MBio. 2016;7(5):10.1128/mbio. 01058-16.

124. Eckhard M, Lengler A, Liersch J, Bretzel R, Mayser P. Fungal foot infections in patients with diabetes mellitus–results of two independent investigations. Mycoses. 2007;50:14-9.

125. Raiesi O, Siavash M, Mohammadi F, Chabavizadeh J, Mahaki B, Maherolnaghsh M, et al. Frequency of cutaneous fungal infections and azole resistance of the isolates in patients with diabetes mellitus. Advanced biomedical research. 2017;6.

126. Chellan G, Shivaprakash S, Karimassery Ramaiyar S, Varma AK, Varma N, Thekkeparambil Sukumaran M, et al. Spectrum and prevalence of fungi infecting deep tissues of lower-limb wounds in patients with type 2 diabetes. Journal of clinical microbiology. 2010;48(6):2097-102.

127. Bokulich NA, Mills DA. Improved selection of internal transcribed spacer-specific primers enables quantitative, ultra-high-throughput profiling of fungal communities. Applied and environmental microbiology. 2013;79(8):2519-26.

128. Kalan LR, Brennan MB. The role of the microbiome in nonhealing diabetic wounds. Annals of the New York Academy of Sciences. 2019;1435(1):79-92.

129. Krzyszczyk P, Schloss R, Palmer A, Berthiaume F. The role of macrophages in acute and chronic wound healing and interventions to promote pro-wound healing phenotypes. Frontiers in physiology. 2018;9:419.

130. Guan Y, Niu H, Liu Z, Dang Y, Shen J, Zayed M, et al. Sustained oxygenation accelerates diabetic wound healing by promoting epithelialization and angiogenesis and decreasing inflammation. Science Advances. 2021;7(35):eabj0153.

131. Frantz S, Vincent KA, Feron O, Kelly RA. Innate immunity and angiogenesis. Circulation research. 2005;96(1):15-26.

132. Bermudez DM, Xu J, Herdrich BJ, Radu A, Mitchell ME, Liechty KW. Inhibition of stromal cell-derived factor-1α further impairs diabetic wound healing. Journal of vascular surgery. 2011;53(3):774-84.

133. Brem H, Tomic-Canic M. Cellular and molecular basis of wound healing in diabetes. The Journal of clinical investigation. 2007;117(5):1219-22.

134. Miricescu D, Badoiu SC, Stanescu-Spinu I-I, Totan AR, Stefani C, Greabu M. Growth Factors, Reactive Oxygen Species, and Metformin—Promoters of the Wound Healing Process in Burns? International Journal of Molecular Sciences. 2021;22(17):9512.

135. Nouvong A, Ambrus AM, Zhang ER, Hultman L, Coller HA. Reactive oxygen species and bacterial biofilms in diabetic wound healing. Physiological genomics. 2016;48(12):889-96.

136. Baidamshina DR, Koroleva VA, Trizna EY, Pankova SM, Agafonova MN, Chirkova MN, et al. Anti-biofilm and wound-healing activity of chitosan-immobilized Ficin. International Journal of Biological Macromolecules. 2020;164:4205-17.

137. Mudge BP, Harris C, Gilmont RR, Adamson BS, Rees RS. Role of glutathione redox dysfunction in diabetic wounds. Wound repair and regeneration. 2002;10(1):52-8.

138. Dhall S, Do DC, Garcia M, Kim J, Mirebrahim SH, Lyubovitsky J, et al. Generating and reversing chronic wounds in diabetic mice by manipulating wound redox parameters. Journal of diabetes research. 2014;2014.

139. Long M, Rojo de la Vega M, Wen Q, Bharara M, Jiang T, Zhang R, et al. An essential role of NRF2 in diabetic wound healing. Diabetes. 2016;65(3):780-93.

140. Okamoto A, Iwamoto Y, Maru Y. Oxidative stress-responsive transcription factor ATF3 potentially mediates diabetic angiopathy. Molecular and cellular biology. 2006;26(3):1087-97.

141. Badr G, Hozzein WN, Badr BM, Al Ghamdi A, Saad Eldien HM, Garraud O. Bee venom accelerates wound healing in diabetic mice by suppressing activating transcription factor-3 (ATF-3) and inducible nitric oxide synthase (iNOS)-mediated oxidative stress and recruiting bone marrow-derived endothelial progenitor cells. Journal of cellular physiology. 2016;231(10):2159-71.

142. Wu M, Lu Z, Wu K, Nam C, Zhang L, Guo J. Recent advances in the development of nitric oxide-releasing biomaterials and their application potentials in chronic wound healing. Journal of Materials Chemistry B. 2021;9(35):7063-75.

143. Chong HC, Chan JSK, Goh CQ, Gounko NV, Luo B, Wang X, et al. Angiopoietin-like 4 stimulates STAT3-mediated iNOS expression and enhances angiogenesis to accelerate wound healing in diabetic mice. Molecular Therapy. 2014;22(9):1593-604.

144.   Kim JH, Yang B, Tedesco A, Lebig EGD, Ruegger PM, Xu K, et al. High levels of oxidative stress and skin microbiome are critical for initiation and development of chronic wounds in diabetic mice. Scientific reports. 2019;9(1):19318.

145.   Moosavi A, Ardekani AM. Role of epigenetics in biology and human diseases. Iran Biomed J. 2016;20(5):246.

146.   Tycko B, Ashkenas J. Epigenetics and its role in disease. J Clin Investig. 2000;105(3):245-6.

147.   Zullo A, Sommese L, Nicoletti G, Donatelli F, Mancini FP, Napoli C. Epigenetics and type 1 diabetes: mechanisms and translational applications. Transl Res. 2017;185:85-93.

148.   Sommese L, Zullo A, Mancini FP, Fabbricini R, Soricelli A, Napoli C. Clinical relevance of epigenetics in the onset and management of type 2 diabetes mellitus. Epigenetics. 2017;12(6):401-15.

149.   Picascia A, Grimaldi V, Pignalosa O, De Pascale MR, Schiano C, Napoli C. Epigenetic control of autoimmune diseases: from bench to bedside. Clin Immunol. 2015;157(1):1-15.

150.   Li E, Beard C, Jaenisch R. Role for DNA methylation in genomic imprinting. Nature. 1993;366(6453):362-5.

151.   Hansen RS, Stöger R, Wijmenga C, Stanek AM, Canfield TK, Luo P, et al. Escape from gene silencing in ICF syndrome: evidence for advanced replication time as a major determinant. Hum Mol Genet. 2000;9(18):2575-87.

152.   Waterland RA, Jirtle RL. Transposable elements: targets for early nutritional effects on epigenetic gene regulation. Mol Cell Biol. 2003;23(15):5293-300.

153.   Jia D, Jurkowska RZ, Zhang X, Jeltsch A, Cheng X. Structure of Dnmt3a bound to Dnmt3L suggests a model for de novo DNA methylation. Nature. 2007;449(7159):248-51.

154.   Rougier N, Bourc'his D, Gomes DM, Niveleau A, Plachot M, Pàldi A, et al. Chromosome methylation patterns during mammalian preimplantation development. Genes Dev. 1998;12(14):2108-13.

155.   He Y-F, Li B-Z, Li Z, Liu P, Wang Y, Tang Q, et al. Tet-mediated formation of 5-carboxylcytosine and its excision by TDG in mammalian DNA. Science. 2011;333(6047):1303-7.

156.   Tahiliani M, Koh KP, Shen Y, Pastor WA, Bandukwala H, Brudno Y, et al. Conversion of 5-methylcytosine to 5-hydroxymethylcytosine in mammalian DNA by MLL partner TET1. Science. 2009;324(5929):930-5.

157.   Ito S, Shen L, Dai Q, Wu SC, Collins LB, Swenberg JA, et al. Tet proteins can convert 5-methylcytosine to 5-formylcytosine and 5-carboxylcytosine. Science. 2011;333(6047):1300-3.

158.   Jaenisch R, Bird A. Epigenetic regulation of gene expression: how the genome integrates intrinsic and environmental signals. Nat Genet. 2003;33(3):245-54.

159.   Tammen SA, Friso S, Choi S-W. Epigenetics: the link between nature and nurture. Mol Aspects Med. 2013;34(4):753-64.

160.   Maunakea AK, Nagarajan RP, Bilenky M, Ballinger TJ, D'Souza C, Fouse SD, et al. Conserved role of intragenic DNA methylation in regulating alternative promoters. Nature. 2010;466(7303):253-7.

161.   Hodges E, Molaro A, Dos Santos CO, Thekkat P, Song Q, Uren PJ, et al. Directional DNA methylation changes and complex intermediate states accompany lineage specificity in the adult hematopoietic compartment. Mol Cell. 2011;44(1):17-28.

162.   Schmidl C, Klug M, Boeld TJ, Andreesen R, Hoffmann P, Edinger M, et al. Lineage-specific DNA methylation in T cells correlates with histone methylation and enhancer activity. Genome Res. 2009;19(7):1165-74.

163.   Hirst M, Marra MA. Epigenetics and human disease. Int J Biochem Cell Biol. 2009;41(1):136-46.

164.   Suzuki MM, Bird A. DNA methylation landscapes: provocative insights from epigenomics. Nat Rev Genet. 2008;9(6):465-76.

165.   Eckhardt F, Lewin J, Cortese R, Rakyan VK, Attwood J, Burger M, et al. DNA methylation profiling of human chromosomes 6, 20 and 22. Nat Genet. 2006;38(12):1378-85.

166.   Lande-Diner L, Zhang J, Ben-Porath I, Amariglio N, Keshet I, Hecht M, et al. Role of DNA methylation in stable gene repression. J Biol Chem. 2007;282(16):12194-200.

167.   Fuks F, Hurd PJ, Wolf D, Nan X, Bird AP, Kouzarides T. The methyl-CpG-binding protein MeCP2 links DNA methylation to histone methylation. J Biol Chem. 2003;278(6):4035-40.

168.   Tazi J, Bird A. Alternative chromatin structure at CpG islands. Cell. 1990;60(6):909-20.

169.   Agalioti T, Lomvardas S, Parekh B, Yie J, Maniatis T, Thanos D. Ordered recruitment of chromatin modifying and general transcription factors to the IFN-β promoter. Cell. 2000;103(4):667-78.

170.   McEwen KR, Ferguson-Smith AC. Distinguishing epigenetic marks of developmental and imprinting regulation. Epigenetics Chromatin. 2010;3(1):1-13.

171.   Ling C, Poulsen P, Simonsson S, Rönn T, Holmkvist J, Almgren P, et al. Genetic and epigenetic factors are associated with expression of respiratory chain component NDUFB6 in human skeletal muscle. J Clin Investig. 2007;117(11):3427-35.

172.   Rönn T, Poulsen P, Hansson O, Holmkvist J, Almgren P, Nilsson P, et al. Age influences DNA methylation and gene expression of COX7A1 in human skeletal muscle. Diabetologia. 2008;51(7):1159-68.

173.   Schübeler D. Function and information content of DNA methylation. Nature. 2015;517(7534):321-6.

174.   Yang BT, Dayeh TA, Volkov PA, Kirkpatrick CL, Malmgren S, Jing X, et al. Increased DNA methylation and decreased expression of PDX-1 in pancreatic islets from patients with type 2 diabetes. Mol Endocrinol. 2012;26(7):1203-12.

175.   Ishikawa K, Tsunekawa S, Ikeniwa M, Izumoto T, Iida A, Ogata H, et al. Long-term pancreatic beta cell exposure to high levels of glucose but not palmitate induces DNA methylation within the insulin gene promoter and represses transcriptional activity. PLoS One. 2015;10(2):e0115350.

176.   Dayeh T, Volkov P, Salö S, Hall E, Nilsson E, Olsson AH, et al. Genome-wide DNA methylation analysis of human pancreatic islets from type 2 diabetic and non-diabetic donors identifies candidate genes that influence insulin secretion. PLoS Genet. 2014;10(3):e1004160.

177.   Ling C, Del Guerra S, Lupi R, Rönn T, Granhall C, Luthman H, et al. Epigenetic regulation of PPARGC1A in human type 2 diabetic islets and effect on insulin secretion. Diabetologia. 2008;51(4):615-22.

178.   Alibegovic AC, Sonne MP, Højbjerre L, Bork-Jensen J, Jacobsen S, Nilsson E, et al. Insulin resistance induced by physical inactivity is associated with multiple transcriptional changes in skeletal muscle in young men. Am J Physiol Endocrinol Metab. 2010;299(5):E752-E63.

179.   Nasrin N, Wu X, Fortier E, Feng Y, Bare OC, Chen S, et al. SIRT4 regulates fatty acid oxidation and mitochondrial gene expression in liver and muscle cells. J Biol Chem. 2010;285(42):31995-2002.

180.   Cox EJ, Marsh SA. Exercise and diabetes have opposite effects on the assembly and O-GlcNAc modification of the mSin3A/HDAC1/2 complex in the heart. Cardiovasc Diabetol. 2013;12(1):1-15.

181.   Liu Z-Z, Zhao X-Z, Zhang X-S, Zhang M. Promoter DNA demethylation of Keap1 gene in diabetic cardiomyopathy. Int J Clin Exp Pathol. 2014;7(12):8756.

182.   Mishra M, Kowluru RA. Epigenetic modification of mitochondrial DNA in the development of diabetic retinopathy. Invest Ophthalmol Vis Sci. 2015;56(9):5133-42.

183.   Chen Y-T, Liao J-W, Tsai Y-C, Tsai F-J. Inhibition of DNA methyltransferase 1 increases nuclear receptor subfamily 4 group A member 1 expression and decreases blood glucose in type 2 diabetes. Oncotarget. 2016;7(26):39162.

184.   Hall E, Dayeh T, Kirkpatrick CL, Wollheim CB, Nitert MD, Ling C. DNA methylation of the glucagon-like peptide 1 receptor (GLP1R) in human pancreatic islets. BMC Med Genet. 2013;14(1):1-7.

185.   Mönkemann H, De Vriese A, Blom H, Kluijtmans L, Heil S, Schild H, et al. Early molecular events in the development of the diabetic cardiomyopathy. Amino Acids. 2002;23(1-3):331-6.

186.   Xu F, Zhang C, Graves DT. Abnormal cell responses and role of TNF-in impaired diabetic wound healing. Biomed Res Int. 2013;2013.

187.   Bouwmeester T, Bauch A, Ruffner H, Angrand P-O, Bergamini G, Croughton K, et al. A physical and functional map of the human TNF-α/NF-κB signal transduction pathway. Nat Cell Biol. 2004;6(2):97-105.

188.   Lu W, Li J, Ren M, Zeng Y, Zhu P, Lin L, et al. Role of the mevalonate pathway in specific CpG site demethylation on AGEs-induced MMP9 expression and activation in keratinocytes. Mol Cell Endocrinol. 2015;411:121-9.

189.   Zhou L, Wang W, Yang C, Zeng T, Hu M, Wang X, et al. GADD45a promotes active DNA demethylation of the MMP-9 promoter via base excision repair pathway in AGEs-treated keratinocytes and in diabetic male rat skin. Endocrinology. 2018;159(2):1172-86.

190.   Zhu P, Ren M, Yang C, Hu YX, Ran JM, Yan L. Involvement of RAGE, MAPK and NF-κB pathways in AGEs-induced MMP-9 activation in HaCaT keratinocytes. Exp Dermatol. 2012;21(2):123-9.

191.   Wolffe AP, Hayes JJ. Chromatin disruption and modification. Nucleic Acids Res. 1999;27(3):711-20.

192.   Thomas JO, Kornberg RD. Cleavable cross-links in the analysis of histone—histone associations. FEBS Lett. 1975;58(1-2):353-8.

193.   McGhee JD, Rau DC, Charney E, Felsenfeld G. Orientation of the nucleosome within the higher order structure of chromatin. Cell. 1980;22(1):87-96.

194.   Allshire RC, Madhani HD. Ten principles of heterochromatin formation and function. Nature reviews Molecular cell biology. 2018;19(4):229.

195.   Strahl BD, Allis CD. The language of covalent histone modifications. Nature. 2000;403(6765):41-5.

196.   Jenuwein T, Allis CD. Translating the histone code. Science. 2001;293(5532):1074-80.

197.   Luger K, Richmond TJ. The histone tails of the nucleosome. Curr Opin Genet Dev. 1998;8(2):140-6.

198.	Winer DA, Luck H, Tsai S, Winer S. The intestinal immune system in obesity and insulin resistance. Cell Metab. 2016;23(3):413-26.
199.	Hotamisligil GS, Shargill NS, Spiegelman BM. Adipose expression of tumor necrosis factor-alpha: direct role in obesity-linked insulin resistance. Science. 1993;259(5091):87-91.
200.	Olefsky JM, Glass CK. Macrophages, inflammation, and insulin resistance. Annu Rev Physiol. 2010;72:219-46.
201.	Biddinger SB, Kahn CR. From mice to men: insights into the insulin resistance syndromes. Annu Rev Physiol. 2006;68:123-58.
202.	Yun J-M, Jialal I, Devaraj S. Epigenetic regulation of high glucose-induced proinflammatory cytokine production in monocytes by curcumin. J Nutr Biochem. 2011;22(5):450-8.
203.	Miao F, Gonzalo IG, Lanting L, Natarajan R. In vivo chromatin remodeling events leading to inflammatory gene transcription under diabetic conditions. J Biol Chem. 2004;279(17):18091-7.
204.	Kadiyala CSR, Zheng L, Du Y, Yohannes E, Kao H-Y, Miyagi M, et al. Acetylation of retinal histones in diabetes increases inflammatory proteins: effects of minocycline and manipulation of histone acetyltransferase (HAT) and histone deacetylase (HDAC). J Biol Chem. 2012;287(31):25869-80.
205.	Perrone L, Devi TS, Hosoya Ki, Terasaki T, Singh LP. Thioredoxin interacting protein (TXNIP) induces inflammation through chromatin modification in retinal capillary endothelial cells under diabetic conditions. J Cell Physiol. 2009;221(1):262-72.
206.	Crosson CE, Mani SK, Husain S, Alsarraf O, Menick DR. Inhibition of histone deacetylase protects the retina from ischemic injury. Invest Ophthalmol Vis Sci. 2010;51(7):3639-45.
207.	Tu P, Li X, Ma B, Duan H, Zhang Y, Wu R, et al. Liver histone H3 methylation and acetylation may associate with type 2 diabetes development. J Physiol Biochem. 2015;71(1):89-98.
208.	Guillam M-T, Hümmler E, Schaerer E, Wu J-Y, Birnbaum MJ, Beermann F, et al. Early diabetes and abnormal postnatal pancreatic islet development in mice lacking Glut-2. Nat Genet. 1997;17(3):327-30.
209.	Seyer P, Vallois D, Poitry-Yamate C, Schütz F, Metref S, Tarussio D, et al. Hepatic glucose sensing is required to preserve β cell glucose competence. J Clin Investig. 2013;123(4):1662-76.
210.	Yasuda H, Ohashi A, Nishida S, Kamiya T, Suwa T, Hara H, et al. Exendin-4 induces extracellular-superoxide dismutase through histone H3 acetylation in human retinal endothelial cells. J Clin Biochem Nutr. 2016;59(3):174-81.
211.	Zhong Q, Kowluru RA. Role of histone acetylation in the development of diabetic retinopathy and the metabolic memory phenomenon. J Cell Biochem. 2010;110(6):1306-13.
212.	Kim MS, Kwon HJ, Lee YM, Baek JH, Jang J-E, Lee S-W, et al. Histone deacetylases induce angiogenesis by negative regulation of tumor suppressor genes. Nat Med. 2001;7(4):437-43.
213.	Mottet D, Bellahcene A, Pirotte S, Waltregny D, Deroanne C, Lamour V, et al. Histone deacetylase 7 silencing alters endothelial cell migration, a key step in angiogenesis. Circ Res. 2007;101(12):1237-46.
214.	Patel T, Patel V, Singh R, Jayaraman S. Chromatin remodeling resets the immune system to protect against autoimmune diabetes in mice. Immunol Cell Biol. 2011;89(5):640-9.
215.	Spallotta F, Cencioni C, Straino S, Sbardella G, Castellano S, Capogrossi MC, et al. Enhancement of lysine acetylation accelerates wound repair. Commun Integr Biol. 2013;6(5):e25466.
216.	Melchionna R, Bellavia G, Romani M, Straino S, Germani A, Di Carlo A, et al. C/EBPγ regulates wound repair and EGF receptor signaling. J Invest Dermatol. 2012;132(7):1908-17.
217.	El-Osta A, Brasacchio D, Yao D, Pocai A, Jones PL, Roeder RG, et al. Transient high glucose causes persistent epigenetic changes and altered gene expression during subsequent normoglycemia. J Exp Med. 2008;205(10):2409-17.
218.	Na J, Shin JY, Jeong H, Lee JY, Kim BJ, Kim WS, et al. JMJD3 and NF-κB-dependent activation of Notch1 gene is required for keratinocyte migration during skin wound healing. Sci Rep. 2017;7(1):1-12.
219.	Shaw T, Martin P. Epigenetic reprogramming during wound healing: loss of polycomb-mediated silencing may enable upregulation of repair genes. EMBO Rep. 2009;10(8):881-6.
220.	Melton C, Judson RL, Blelloch R. Opposing microRNA families regulate self-renewal in mouse embryonic stem cells. Nature. 2010;463(7281):621-6.
221.	Yamakuchi M, Ferlito M, Lowenstein CJ. miR-34a repression of SIRT1 regulates apoptosis. Proceedings of the National Academy of Sciences. 2008;105(36):13421-6.
222.	Ferguson BS. Nutritional Epigenomics: Academic Press; 2019.
223.	Guay C, Jacovetti C, Nesca V, Motterle A, Tugay K, Regazzi R. Emerging roles of non-coding RNAs in pancreatic β-cell function and dysfunction. Diabetes, Obesity and Metabolism. 2012;14:12-21.

224.   Herrera B, Lockstone H, Taylor J, Ria M, Barrett A, Collins S, et al. Global microRNA expression profiles in insulin target tissues in a spontaneous rat model of type 2 diabetes. Diabetologia. 2010;53(6):1099-109.

225.   Poy M. A pancreatic islet-specific microRNA regulates insulin secretion. Nat. 432, 226–230. 2004.

226.   Xu G, Chen J, Jing G, Shalev A. Thioredoxin-interacting protein regulates insulin transcription through microRNA-204. Nat Med. 2013;19(9):1141-6.

227.   Bolmeson C, Esguerra JL, Salehi A, Speidel D, Eliasson L, Cilio CM. Differences in islet-enriched miRNAs in healthy and glucose intolerant human subjects. Biochem Biophys Res Commun. 2011;404(1):16-22.

228.   Sebastiani G, Po A, Miele E, Ventriglia G, Ceccarelli E, Bugliani M, et al. MicroRNA-124a is hyperexpressed in type 2 diabetic human pancreatic islets and negatively regulates insulin secretion. Acta Diabetol. 2015;52(3):523-30.

229.   Tattikota SG, Rathjen T, McAnulty SJ, Wessels H-H, Akerman I, Van De Bunt M, et al. Argonaute2 mediates compensatory expansion of the pancreatic β cell. Cell Metab. 2014;19(1):122-34.

230.   Ofori JK, Salunkhe VA, Bagge A, Vishnu N, Nagao M, Mulder H, et al. Elevated miR-130a/miR130b/miR-152 expression reduces intracellular ATP levels in the pancreatic beta cell. Sci Rep. 2017;7(1):1-15.

231.   Belgardt B-F, Ahmed K, Spranger M, Latreille M, Denzler R, Kondratiuk N, et al. The microRNA-200 family regulates pancreatic beta cell survival in type 2 diabetes. Nat Med. 2015;21(6):619-27.

232.   Nesca V, Guay C, Jacovetti C, Menoud V, Peyot M-L, Laybutt DR, et al. Identification of particular groups of microRNAs that positively or negatively impact on beta cell function in obese models of type 2 diabetes. Diabetologia. 2013;56(10):2203-12.

233.   Latreille M, Hausser J, Stützer I, Zhang Q, Hastoy B, Gargani S, et al. MicroRNA-7a regulates pancreatic β cell function. J Clin Investig. 2014;124(6):2722-35.

234.   Hanna J, Hossain GS, Kocerha J. The potential for microRNA therapeutics and clinical research. Front Genet. 2019;10:478.

235.   Chan YC, Roy S, Khanna S, Sen CK. Downregulation of endothelial microRNA-200b supports cutaneous wound angiogenesis by desilencing GATA binding protein 2 and vascular endothelial growth factor receptor 2. Arterioscler Thromb Vasc Biol. 2012;32(6):1372-82.

236.   Sinha M, Ghatak S, Roy S, Sen CK. microRNA–200b as a switch for inducible adult angiogenesis. Antioxid Redox Signal. 2015;22(14):1257-72.

237.   Detich N, Hamm S, Just G, Knox JD, Szyf M. The methyl donor S-adenosylmethionine inhibits active demethylation of DNA: a candidate novel mechanism for the pharmacological effects of S-adenosylmethionine. J Biol Chem. 2003;278(23):20812-20.

238.   Koh TJ, DiPietro LA. Inflammation and wound healing: the role of the macrophage. Expert Rev Mol Med. 2011;13.

239.   Barrows LR, Magee PN. Nonenzymatic methylation of DNA by S-adenosylmethionine in vitro. Carcinogenesis. 1982;3(3):349-51.

240.   Spijkerman A, Smulders Y, Kostense P, Henry R, Becker A, Teerlink T, et al. S-adenosylmethionine and 5-methyltetrahydrofolate are associated with endothelial function after controlling for confounding by homocysteine: the Hoorn Study. Arterioscler Thromb Vasc Biol. 2005;25(4):778-84.

241.   Kim SY, Hong SW, Kim M-O, Kim H-S, Jang JE, Leem J, et al. S-adenosyl methionine prevents endothelial dysfunction by inducing heme oxygenase-1 in vascular endothelial cells. Mol Cells. 2013;36(4):376-84.

242.   Taganov KD, Boldin MP, Chang K-J, Baltimore D. NF-κB-dependent induction of microRNA miR-146, an inhibitor targeted to signaling proteins of innate immune responses. Proceedings of the National Academy of Sciences. 2006;103(33):12481-6.

243.   Tili E, Michaille J-J, Cimino A, Costinean S, Dumitru CD, Adair B, et al. Modulation of miR-155 and miR-125b levels following lipopolysaccharide/TNF-α stimulation and their possible roles in regulating the response to endotoxin shock. J Immunol. 2007;179(8):5082-9.

244.   Villeneuve LM, Kato M, Reddy MA, Wang M, Lanting L, Natarajan R. Enhanced levels of microRNA-125b in vascular smooth muscle cells of diabetic db/db mice lead to increased inflammatory gene expression by targeting the histone methyltransferase Suv39h1. Diabetes. 2010;59(11):2904-15.

245.   Kuehbacher A, Urbich C, Zeiher AM, Dimmeler S. Role of Dicer and Drosha for endothelial microRNA expression and angiogenesis. Circ Res. 2007;101(1):59-68.

246.   Wang S, Olson EN. AngiomiRs—key regulators of angiogenesis. Curr Opin Genet Dev. 2009;19(3):205-11.

247.   Yang WJ, Yang DD, Na S, Sandusky GE, Zhang Q, Zhao G. Dicer is required for embryonic angiogenesis during mouse development. J Biol Chem. 2005;280(10):9330-5.

248.	Shilo S, Roy S, Khanna S, Sen CK. Evidence for the involvement of miRNA in redox regulated angiogenic response of human microvascular endothelial cells. Arterioscler Thromb Vasc Biol. 2008;28(3):471-7.

249.	Poliseno L, Tuccoli A, Mariani L, Evangelista M, Citti L, Woods K, et al. MicroRNAs modulate the angiogenic properties of HUVECs. Blood. 2006;108(9):3068-71.

250.	Biswas S, Roy S, Banerjee J, Hussain S-RA, Khanna S, Meenakshisundaram G, et al. Hypoxia inducible microRNA 210 attenuates keratinocyte proliferation and impairs closure in a murine model of ischemic wounds. Proceedings of the National Academy of Sciences. 2010;107(15):6976-81.

251.	Chang WY, Bryce DM, D'Souza SJ, Dagnino L. The DP-1 transcription factor is required for keratinocyte growth and epidermal stratification. J Biol Chem. 2004;279(49):51343-53.

252.	Huang X, Sun J, Chen G, Niu C, Wang Y, Zhao C, et al. Resveratrol promotes diabetic wound healing via SIRT1-FOXO1-c-Myc signaling pathway-mediated angiogenesis. Frontiers in pharmacology. 2019;10:421.

253.	Wahedi HM, Chae JK, Subedi L, Kang MC, Cho H, Kim S, et al. NED416, a novel synthetic Sirt1 activator, promotes cutaneous wound healing via the MAPK/Rho pathway. International Journal of Molecular Medicine. 2020;46(1):149-58.

254.	Valente S, Mellini P, Spallotta F, Carafa V, Nebbioso A, Polletta L, et al. 1, 4-Dihydropyridines active on the SIRT1/AMPK pathway ameliorate skin repair and mitochondrial function and exhibit inhibition of proliferation in cancer cells. Journal of Medicinal Chemistry. 2016;59(4):1471-91.

255.	Zhang P, He L, Zhang J, Mei X, Zhang Y, Tian H, et al. Preparation of novel berberine nano-colloids for improving wound healing of diabetic rats by acting Sirt1/NF-κB pathway. Colloids and Surfaces B: Biointerfaces. 2020;187:110647.

256.	Shi R, Jin Y, Hu W, Lian W, Cao C, Han S, et al. Exosomes derived from mmu_circ_0000250-modified adipose-derived mesenchymal stem cells promote wound healing in diabetic mice by inducing miR-128-3p/SIRT1-mediated autophagy. American Journal of Physiology-Cell Physiology. 2020;318(5):C848-C56.

257.	Dubey R, Prabhakar PK, Gupta J. Identification of Structurally Similar Phytochemicals to Quercetin with High SIRT1 Binding Affinity and Improving Diabetic Wound Healing by Using In silico Approaches. Biointerface Res Appl Chem. 2021;12:7621-32.

258.	Zhou G, Han X, Wu Z, Shi Q, Bao X. Rosiglitazone accelerates wound healing by improving endothelial precursor cell function and angiogenesis in db/db mice. PeerJ. 2019;7:e7815.

259.	Steed DL. The role of growth factors in wound healing. Surgical Clinics of North America. 1997;77(3):575-86.

260.	Zhu Y, Wang Y, Jia Y, Xu J, Chai Y. Roxadustat promotes angiogenesis through HIF-1α/VEGF/VEGFR2 signaling and accelerates cutaneous wound healing in diabetic rats. Wound repair and regeneration. 2019;27(4):324-34.

261.	Smiell JM, Wieman TJ, Steed DL, Perry BH, Sampson AR, Schwab BH. Efficacy and safety of becaplermin (recombinant human platelet-derived growth factor-BB) in patients with nonhealing, lower extremity diabetic ulcers: a combined analysis of four randomized studies. Wound Repair and Regeneration. 1999;7(5):335-46.

262.	Huang Y-W, Zhu Q-Q, Yang X-Y, Xu H-H, Sun B, Wang X-J, et al. Wound healing can be improved by (—)-epigallocatechin gallate through targeting Notch in streptozotocin-induced diabetic mice. The FASEB Journal. 2019;33(1):953-64.

263.	Kim H, Kawazoe T, Han DW, Matsumara K, Suzuki S, Tsutsumi S, et al. Enhanced wound healing by an epigallocatechin gallate-incorporated collagen sponge in diabetic mice. Wound repair and regeneration. 2008;16(5):714-20.

264.	Kant V, Jangir BL, Sharma M, Kumar V, Joshi VG. Topical application of quercetin improves wound repair and regeneration in diabetic rats. Immunopharmacology and Immunotoxicology. 2021;43(5):536-53.

265.	Kant V, Sharma M, Jangir BL, Kumar V. Acceleration of wound healing by quercetin in diabetic rats requires mitigation of oxidative stress and stimulation of the proliferative phase. Biotechnic & Histochemistry. 2022;97(6):461-72.

266.	Mi Y, Zhong L, Lu S, Hu P, Pan Y, Ma X, et al. Quercetin promotes cutaneous wound healing in mice through Wnt/β-catenin signaling pathway. Journal of Ethnopharmacology. 2022;290:115066.

267.	Sidhu GS, Mani H, Gaddipati JP, Singh AK, Seth P, Banaudha KK, et al. Curcumin enhances wound healing in streptozotocin induced diabetic rats and genetically diabetic mice. Wound repair and regeneration. 1999;7(5):362-74.

268.	Kulac M, Aktas C, Tulubas F, Uygur R, Kanter M, Erboga M, et al. The effects of topical treatment with curcumin on burn wound healing in rats. Journal of molecular histology. 2013;44:83-90.

269.	Kant V, Gopal A, Kumar D, Pathak NN, Ram M, Jangir BL, et al. Curcumin-induced angiogenesis hastens wound healing in diabetic rats. Journal of Surgical Research. 2015;193(2):978-88.

270.   Kant V, Gopal A, Pathak NN, Kumar P, Tandan SK, Kumar D. Antioxidant and anti-inflammatory potential of curcumin accelerated the cutaneous wound healing in streptozotocin-induced diabetic rats. International immunopharmacology. 2014;20(2):322-30.

271.   Yang DJ, Moh SH, Son DH, You S, Kinyua AW, Ko CM, et al. Gallic acid promotes wound healing in normal and hyperglucidic conditions. Molecules. 2016;21(7):899.

272.   Chen L-Y, Cheng H-L, Kuan Y-H, Liang T-J, Chao Y-Y, Lin H-C. Therapeutic potential of luteolin on impaired wound healing in streptozotocin-induced rats. Biomedicines. 2021;9(7):761.

273.   Wu Z, Zheng X, Gong M, Li Y. Myricetin, a potent natural agent for treatment of diabetic skin damage by modulating TIMP/MMPs balance and oxidative stress. Oncotarget. 2016;7(44):71754.

274.   Kerr J. The use of essential oils in healing wounds. International Journal of Aromatherapy. 2002;12(4):202-6.

275.   Ayuningtyas NF, Hendarti HT, Soebadi B, Surboyo MDC, Hadi P, Ganesha R, et al. Expression of VEGF and CD-31 in traumatic ulcer of diabetic Wistar rats after application of Citrus limon peel essential oil. Journal of Oral Biology and Craniofacial Research. 2023;13(3):380-5.

276.   Ganesha R, Hernawan I, Hendarti HT, Radithia D, Hadi P, Ayuningtyas NF, et al. Expression of FGF-2 and fibronectin in citrus limon fruit peel malang essential oil gel treated traumatic ulcer in diabetic wistar rats (Rattus novergicus). Research Journal of Pharmacy and Technology. 2019;12(7):3350-4.

277.   Andjić M, Draginić N, Kočović A, Jeremić J, Vučićević K, Jeremić N, et al. Immortelle essential oil-based ointment improves wound healing in a diabetic rat model. Biomedicine & Pharmacotherapy. 2022;150:112941.

278.   Andjić M, Božin B, Draginić N, Kočović A, Jeremić JN, Tomović M, et al. Formulation and evaluation of Helichrysum italicum essential oil-based topical formulations for wound healing in diabetic rats. Pharmaceuticals. 2021;14(8):813.

279.   Ibaokurgil F, Yildirim BA, Yildirim S. Effects of Hypericum scabrum L. essential oil on wound healing in streptozotocin-induced diabetic rats. Cutaneous and Ocular Toxicology. 2022;41(2):137-44.

280.   Betul AY, Semin G. Wound healing effects of Nigella sativa L. essential oil in streptozotocin induced in diabetic rats. GSC Biological and Pharmaceutical Sciences. 2019;7(3):-.

281.   Mahboubi M, Taghizadeh M, Khamechian T, Tamtaji OR, Mokhtari R, Talaei SA. The wound healing effects of herbal cream containing Oliveria decumbens and Pelargonium graveolens essential oils in diabetic foot ulcer model. World journal of plastic surgery. 2018;7(1):45.

282.   Mori H-M, Kawanami H, Kawahata H, Aoki M. Wound healing potential of lavender oil by acceleration of granulation and wound contraction through induction of TGF-β in a rat model. BMC complementary and alternative medicine. 2016;16:1-11.

283.   Bigliardi PL, Alsagoff SAL, El-Kafrawi HY, Pyon J-K, Wa CTC, Villa MA. Povidone iodine in wound healing: A review of current concepts and practices. International Journal of Surgery. 2017;44:260-8.

284.   Kushwaha A, Goswami L, Kim BS. Nanomaterial-based therapy for wound healing. Nanomaterials. 2022;12(4):618.

285.   Gupta NK, Joshi P, Srivastava V, Quraishi M. Chitosan: A macromolecule as green corrosion inhibitor for mild steel in sulfamic acid useful for sugar industry. International journal of Biological macromolecules. 2018;106:704-11.

286.   Teaima MH, Elasaly MK, Omar SA, El-Nabarawi MA, Shoueir KR. Wound healing activities of polyurethane modified chitosan nanofibers loaded with different concentrations of linezolid in an experimental model of diabetes. Journal of Drug Delivery Science and Technology. 2022;67:102982.

287.   Wang T, Zheng Y, Shen Y, Shi Y, Li F, Su C, et al. Chitosan nanoparticles loaded hydrogels promote skin wound healing through the modulation of reactive oxygen species. Artificial cells, nanomedicine, and biotechnology. 2018;46(sup1):138-49.

288.   Wang L, Yang B, Jiang H, Yu G, Feng M, Lu X, et al. The molecular mechanism study of insulin in promoting wound healing under high-glucose conditions. Journal of cellular biochemistry. 2019;120(9):16244-53.

289.   Ribeiro MC, Correa VLR, da Silva FKL, Casas AA, das Chagas AdL, de Oliveira LP, et al. Wound healing treatment using insulin within polymeric nanoparticles in the diabetes animal model. European Journal of Pharmaceutical Sciences. 2020;150:105330.

290.   Hajimiri M, Shahverdi S, Esfandiari MA, Larijani B, Atyabi F, Rajabiani A, et al. Preparation of hydrogel embedded polymer-growth factor conjugated nanoparticles as a diabetic wound dressing. Drug development and industrial pharmacy. 2016;42(5):707-19.

291.   Thangavel P, Ramachandran B, Chakraborty S, Kannan R, Lonchin S, Muthuvijayan V. Accelerated healing of diabetic wounds treated with L-glutamic acid loaded hydrogels through enhanced collagen deposition and angiogenesis: an in vivo study. Scientific reports. 2017;7(1):10701.

292.   Tallapaneni V, Pamu D, Mude L, Karri VVSR. Dual-Drug Loaded Biomimetic Chitosan-Collagen Hybrid Nanocomposite Scaffolds for Ameliorating Potential Tissue Regeneration in Diabetic Wounds. bioRxiv. 2022:2022.02. 16.480700.

293.   Shah SA, Sohail M, Karperien M, Johnbosco C, Mahmood A, Kousar M. Chitosan and carboxymethyl cellulose-based 3D multifunctional bioactive hydrogels loaded with nano-curcumin for synergistic diabetic wound repair. International journal of biological macromolecules. 2023;227:1203-20.

294.   Arantes VT, Faraco AA, Ferreira FB, Oliveira CA, Martins-Santos E, Cassini-Vieira P, et al. Retinoic acid-loaded solid lipid nanoparticles surrounded by chitosan film support diabetic wound healing in in vivo study. Colloids and Surfaces B: Biointerfaces. 2020;188:110749.

295.   Correa VLR, Martins JA, de Souza TR, Rincon GdCN, Miguel MP, de Menezes LB, et al. Melatonin loaded lecithin-chitosan nanoparticles improved the wound healing in diabetic rats. International Journal of Biological Macromolecules. 2020;162:1465-75.

296.   Bardill JR, Laughter MR, Stager M, Liechty KW, Krebs MD, Zgheib C. Topical gel-based biomaterials for the treatment of diabetic foot ulcers. Acta biomaterialia. 2022;138:73-91.

297.   Dumville JC, Lipsky BA, Hoey C, Cruciani M, Fiscon M, Xia J. Topical antimicrobial agents for treating foot ulcers in people with diabetes. Cochrane Database of Systematic Reviews. 2017(6).

298.   Huang Y-Y, Lin C-W, Cheng N-C, Cazzell SM, Chen H-H, Huang K-F, et al. Effect of a novel macrophage-regulating drug on wound healing in patients with diabetic foot ulcers: a randomized clinical trial. JAMA network open. 2021;4(9):e2122607-e.

299.   Louise Holmen Terkelsen AE-J, Hanne Kjeldsen, John Howard Barker, Vibeke Elisabeth Hjortdal, Anni. Topical application of cod liver oil ointment accelerates wound healing: an experimental study in wounds in the ears of hairless mice. Scandinavian journal of plastic and reconstructive surgery and hand surgery. 2000;34(1):15-20.

300.   Khazaeli P, Alaei M, Khaksarihadad M, Ranjbar M. Preparation of PLA/chitosan nanoscaffolds containing cod liver oil and experimental diabetic wound healing in male rats study. Journal of Nanobiotechnology. 2020;18(1):1-9.

301.   Li C, Jiang T, Zhou C, Jiang A, Lu C, Yang G, et al. Injectable self-healing chitosan-based POSS-PEG hybrid hydrogel as wound dressing to promote diabetic wound healing. Carbohydrate Polymers. 2023;299:120198.

302.   St-Gelais F, Jomphe C, Trudeau L-É. The role of neurotensin in central nervous system pathophysiology: what is the evidence? Journal of Psychiatry and Neuroscience. 2006;31(4):229-45.

303.   Moura LI, Dias AM, Leal EC, Carvalho L, de Sousa HC, Carvalho E. Chitosan-based dressings loaded with neurotensin—an efficient strategy to improve early diabetic wound healing. Acta biomaterialia. 2014;10(2):843-57.

304.   Sheir MM, Nasra MM, Abdallah OY. Chitosan alginate nanoparticles as a platform for the treatment of diabetic and non-diabetic pressure ulcers: Formulation and in vitro/in vivo evaluation. International Journal of Pharmaceutics. 2021;607:120963.

305.   Li F, Shi Y, Liang J, Zhao L. Curcumin-loaded chitosan nanoparticles promote diabetic wound healing via attenuating inflammation in a diabetic rat model. Journal of biomaterials applications. 2019;34(4):476-86.

306.   Qadir MI, Naqvi STQ, Muhammad SA, Qadir M, Naqvi ST. Curcumin: a polyphenol with molecular targets for cancer control. Asian pacific journal of cancer prevention. 2016;17(6):2735-9.

307.   Sohn S-I, Priya A, Balasubramaniam B, Muthuramalingam P, Sivasankar C, Selvaraj A, et al. Biomedical applications and bioavailability of curcumin—An updated overview. Pharmaceutics. 2021;13(12):2102.

308.   Karri VVSR, Kuppusamy G, Talluri SV, Mannemala SS, Kollipara R, Wadhwani AD, et al. Curcumin loaded chitosan nanoparticles impregnated into collagen-alginate scaffolds for diabetic wound healing. International journal of biological macromolecules. 2016;93:1519-29.

309.   Habibi Y, Lucia LA, Rojas OJ. Cellulose nanocrystals: chemistry, self-assembly, and applications. Chemical reviews. 2010;110(6):3479-500.

310.   Zheng L, Li S, Luo J, Wang X. Latest advances on bacterial cellulose-based antibacterial materials as wound dressings. Frontiers in Bioengineering and Biotechnology. 2020;8:593768.

311.   Loh EYX, Mohamad N, Fauzi MB, Ng MH, Ng SF, Mohd Amin MCI. Development of a bacterial cellulose-based hydrogel cell carrier containing keratinocytes and fibroblasts for full-thickness wound healing. Scientific reports. 2018;8(1):2875.

312.   Wang Y, Xiao D, Tang Y, Xia Y, Zhong Y, Zhang L, et al. Carboxymethyl cellulose-based injectable hydrogel loaded with a composite of melatonin and γ-cyclodextrin with antioxidant property for diabetic wound repair. Cellulose. 2023;30(3):1791-810.

313.   Alfassi G, Rein DM, Shpigelman A, Cohen Y. Partially acetylated cellulose dissolved in aqueous solution: Physical properties and enzymatic hydrolysis. Polymers. 2019;11(11):1734.

314. Pilehvar-Soltanahmadi Y, Dadashpour M, Mohajeri A, Fattahi A, Sheervalilou R, Zarghami N. An overview on application of natural substances incorporated with electrospun nanofibrous scaffolds to development of innovative wound dressings. Mini reviews in medicinal chemistry. 2018;18(5):414-27.

315. Gushiken LFS, Beserra FP, Bastos JK, Jackson CJ, Pellizzon CH. Cutaneous wound healing: An update from physiopathology to current therapies. Life. 2021;11(7):665.

316. Dos Santos AEA, Dos Santos FV, Freitas KM, Pimenta LPS, de Oliveira Andrade L, Marinho TA, et al. Cellulose acetate nanofibers loaded with crude annatto extract: Preparation, characterization, and in vivo evaluation for potential wound healing applications. Materials Science and Engineering: C. 2021;118:111322.

317. Anjum A, Chung P-Y, Ng S-F. PLGA/xylitol nanoparticles enhance antibiofilm activity via penetration into biofilm extracellular polymeric substances. RSC advances. 2019;9(25):14198-208.

318. Kalishwaralal K, BarathManiKanth S, Pandian SRK, Deepak V, Gurunathan S. Silver nanoparticles impede the biofilm formation by Pseudomonas aeruginosa and Staphylococcus epidermidis. Colloids and Surfaces B: Biointerfaces. 2010;79(2):340-4.

319. Satish L, Santhakumari S, Gowrishankar S, Pandian SK, Ravi AV, Ramesh M. Rapid biosynthesized AgNPs from Gelidiella acerosa aqueous extract mitigates quorum sensing mediated biofilm formation of Vibrio species—an in vitro and in vivo approach. Environmental Science and Pollution Research. 2017;24:27254-68.

320. Li J-J, Hu Y, Hu B, Wang W, Xu H, Hu X-Y, et al. Lactose azocalixarene drug delivery system for the treatment of multidrug-resistant pseudomonas aeruginosa infected diabetic ulcer. Nature Communications. 2022;13(1):6279.

321. McLaughlin S, Ahumada M, Franco W, Mah T-F, Seymour R, Suuronen EJ, et al. Sprayable peptide-modified silver nanoparticles as a barrier against bacterial colonization. Nanoscale. 2016;8(46):19200-3.

322. Lazurko C, Khatoon Z, Goel K, Sedlakova V, Eren Cimenci C, Ahumada M, et al. Multifunctional nano and collagen-based therapeutic materials for skin repair. ACS Biomaterials Science & Engineering. 2019;6(2):1124-34.

323. Richter K, Facal P, Thomas N, Vandecandelaere I, Ramezanpour M, Cooksley C, et al. Taking the silver bullet colloidal silver particles for the topical treatment of biofilm-related infections. ACS applied materials & interfaces. 2017;9(26):21631-8.

324. Ambrogi V, Pietrella D, Donnadio A, Latterini L, Di Michele A, Luffarelli I, et al. Biocompatible alginate silica supported silver nanoparticles composite films for wound dressing with antibiofilm activity. Materials Science and Engineering: C. 2020;112:110863.

325. Paterson TE, Bari A, Bullock AJ, Turner R, Montalbano G, Fiorilli S, et al. Multifunctional copper-containing mesoporous glass nanoparticles as antibacterial and proangiogenic agents for chronic wounds. Frontiers in Bioengineering and Biotechnology. 2020;8:246.

326. Yang X, Wei Q, Shao H, Jiang X. Multivalent aminosaccharide-based gold nanoparticles as narrow-spectrum antibiotics in vivo. ACS applied materials & interfaces. 2019;11(8):7725-30.

327. Mir M, Permana AD, Tekko IA, McCarthy HO, Ahmed N, Donnelly RF. Microneedle liquid injection system assisted delivery of infection responsive nanoparticles: a promising approach for enhanced site-specific delivery of carvacrol against polymicrobial biofilms-infected wounds. International journal of pharmaceutics. 2020;587:119643.

328. Sancineto L, Piccioni M, De Marco S, Pagiotti R, Nascimento V, Braga AL, et al. Diphenyl diselenide derivatives inhibit microbial biofilm formation involved in wound infection. BMC microbiology. 2016;16:1-10.

329. Khan ST, Ahamed M, Musarrat J, Al-Khedhairy AA. Anti-biofilm and antibacterial activities of zinc oxide nanoparticles against the oral opportunistic pathogens R othia dentocariosa and R othia mucilaginosa. European Journal of Oral Sciences. 2014;122(6):397-403.

330. Park JW, Hwang SR, Yoon I-S. Advanced growth factor delivery systems in wound management and skin regeneration. Molecules. 2017;22(8):1259.

331. Al-Dwairi A. Low serum epidermal growth factor level is associated with lack of diabetic control in type 2 diabetes mellitus in diabetic patients in Jordan. Diabetologie und Stoffwechsel. 2022;17:S46-S.

332. Lev-Ran A, Hwang DL, Miller JD, Josefsberg Z. Excretion of epidermal growth factor (EGF) in diabetes. Clinica chimica acta. 1990;192(3):201-6.

333. Qi X, Huan Y, Si H, Zou J, Mu Z. Study of the effect epidermal growth factor nanoparticles in the treatment of diabetic rat ulcer skin and regeneration. Journal of Nanoscience and Nanotechnology. 2021;21(5):3028-34.

334. Chereddy KK, Lopes A, Koussoroplis S, Payen V, Moia C, Zhu H, et al. Combined effects of PLGA and vascular endothelial growth factor promote the healing of non-diabetic and diabetic wounds. Nanomedicine: Nanotechnology, Biology and Medicine. 2015;11(8):1975-84.

335. Li S, Tang Q, Xu H, Huang Q, Wen Z, Liu Y, et al. Improved stability of KGF by conjugation with gold nanoparticles for diabetic wound therapy. Nanomedicine. 2019;14(22):2909-23.

336.   Chen X, Thibeault SL. Role of tumor necrosis factor–α in wound repair in human vocal fold fibroblasts. The Laryngoscope. 2010;120(9):1819-25.

337.   Liu R, Bal HS, Desta T, Behl Y, Graves DT. Tumor necrosis factor-α mediates diabetes-enhanced apoptosis of matrix-producing cells and impairs diabetic healing. The American journal of pathology. 2006;168(3):757-64.

338.   Frank J, Born K, Barker JH, Marzi I. In vivo effect of tumor necrosis factor alpha on wound angiogenesis and epithelialization. European Journal of Trauma. 2003;29:208-19.

339.   Kasiewicz LN, Whitehead KA. Lipid nanoparticles silence tumor necrosis factor α to improve wound healing in diabetic mice. Bioengineering & translational medicine. 2019;4(1):75-82.

340.   Zhang W, Chen L, Xiong Y, Panayi AC, Abudulibaier A, Hu Y, et al. Antioxidant therapy and antioxidant-related bionanomaterials in diabetic wound healing. Frontiers in Bioengineering and Biotechnology. 2021;9:707479.

341.   Xu Z, Liu Y, Ma R, Chen J, Qiu J, Du S, et al. Thermosensitive hydrogel incorporating Prussian blue nanoparticles promotes diabetic wound healing via ROS scavenging and mitochondrial function restoration. ACS applied materials & interfaces. 2022;14(12):14059-71.

342.   Azlan AYHN, Katas H, Zin NM, Fauzi MB. Dual action gels containing DsiRNA loaded gold nanoparticles: Augmenting diabetic wound healing by promoting angiogenesis and inhibiting infection. European Journal of Pharmaceutics and Biopharmaceutics. 2021;169:78-90.

343.   Singh BR, Singh BN, Singh A, Khan W, Naqvi AH, Singh HB. Mycofabricated biosilver nanoparticles interrupt Pseudomonas aeruginosa quorum sensing systems. Scientific reports. 2015;5(1):13719.

344.   Chu Y, Yu D, Wang P, Xu J, Li D, Ding M. Nanotechnology promotes the full-thickness diabetic wound healing effect of recombinant human epidermal growth factor in diabetic rats. Wound repair and regeneration. 2010;18(5):499-505.

345.   Grosdidier A, Zoete V, Michielin O. SwissDock, a protein-small molecule docking web service based on EADock DSS. Nucleic acids research. 2011;39(suppl_2):W270-W7.

346.   Ferreira LG, Dos Santos RN, Oliva G, Andricopulo AD. Molecular docking and structure-based drug design strategies. Molecules. 2015;20(7):13384-421.

347.   Trott O, Olson AJ. AutoDock Vina: improving the speed and accuracy of docking with a new scoring function, efficient optimization, and multithreading. Journal of computational chemistry. 2010;31(2):455-61.

348.   Bashary R, Khatik GL. Design, and facile synthesis of 1, 3 diaryl-3-(arylamino) propan-1-one derivatives as the potential alpha-amylase inhibitors and antioxidants. Bioorganic chemistry. 2019;82:156-62.

349.   Selvaraj G, Kaliamurthi S, Thirugnanasambandam R. Molecular docking studies on potential PPAR-γ agonist from Rhizophora apiculata. ||| Bangladesh Journal of Pharmacology. 2014;9(3):298-302.

350.   Daina A, Michielin O, Zoete V. SwissADME: a free web tool to evaluate pharmacokinetics, drug-likeness and medicinal chemistry friendliness of small molecules. Scientific reports. 2017;7(1):42717.

351.   Wu F, Zhou Y, Li L, Shen X, Chen G, Wang X, et al. Computational approaches in preclinical studies on drug discovery and development. Frontiers in chemistry. 2020;8:726.

352.   Sharma OP, Bhat TK. DPPH antioxidant assay revisited. Food chemistry. 2009;113(4):1202-5.

353.   Gerlier D, Thomasset N. Use of MTT colorimetric assay to measure cell activation. Journal of immunological methods. 1986;94(1-2):57-63.

354.   Lee H, Kang K-T. Advanced tube formation assay using human endothelial colony forming cells for in vitro evaluation of angiogenesis. The Korean Journal of Physiology & Pharmacology. 2018;22(6):705-12.

355.   Kauanova S, Urazbayev A, Vorobjev I. The frequent sampling of wound scratch assay reveals the "opportunity" window for quantitative evaluation of cell motility-impeding drugs. Frontiers in cell and developmental biology. 2021;9:640972.

356.   Classics Lowry O, Rosebrough N, Farr A, Randall R. Protein measurement with the Folin phenol reagent. J biol Chem. 1951;193(1):265-75.

357.   Chance B, Maehly A. [136] Assay of catalases and peroxidases. 1955.

358.   Habig WH, Pabst MJ, Jakoby WB. Glutathione S-transferases: the first enzymatic step in mercapturic acid formation. Journal of biological Chemistry. 1974;249(22):7130-9.

359.   Buege JA, Aust SD. [30] Microsomal lipid peroxidation. Methods in enzymology. 52: Elsevier; 1978. p. 302-10.

360.   Kono Y. Generation of superoxide radical during autoxidation of hydroxylamine and an assay for superoxide dismutase. Archives of biochemistry and biophysics. 1978;186(1):189-95.

361.   Gaikwad AB, Gupta J, Tikoo K. Epigenetic changes and alteration of Fbn1 and Col3A1 gene expression under hyperglycaemic and hyperinsulinaemic conditions. Biochemical Journal. 2010;432(2):333-41.

362.   Ahmed OM, Mohamed T, Moustafa H, Hamdy H, Ahmed RR, Aboud E. Quercetin and low level laser therapy promote wound healing process in diabetic rats via structural reorganization and modulatory effects on inflammation and oxidative stress. Biomedicine & Pharmacotherapy. 2018;101:58-73.

363.   Rahman I, Kode A, Biswas SK. Assay for quantitative determination of glutathione and glutathione disulfide levels using enzymatic recycling method. Nature protocols. 2006;1(6):3159-65.

364.   Kumar A, Zhang KY. Advances in the development of shape similarity methods and their application in drug discovery. Frontiers in chemistry. 2018;6:315.

365.   Katiyar C, Gupta A, Kanjilal S, Katiyar S. Drug discovery from plant sources: An integrated approach. Ayu. 2012;33(1):10.

366.   Carracedo-Reboredo P, Liñares-Blanco J, Rodríguez-Fernández N, Cedrón F, Novoa FJ, Carballal A, et al. A review on machine learning approaches and trends in drug discovery. Computational and structural biotechnology journal. 2021;19:4538-58.

367.   Lowry O, Rosebrough N, Farr AL, Randall R. Protein measurement with the Folin phenol reagent. Journal of biological chemistry. 1951;193(1):265-75.

368.   Wild S, Roglic G, Green A, Sicree R, King H. Global prevalence of diabetes: estimates for the year 2000 and projections for 2030. Diabetes care. 2004;27(5):1047-53.

369.   Jiang Y, Wang X, Xia L, Fu X, Xu Z, Ran X, et al. A cohort study of diabetic patients and diabetic foot ulceration patients in China. Wound Repair and Regeneration. 2015;23(2):222-30.

370.   Boulton AJ, Vileikyte L, Ragnarson-Tennvall G, Apelqvist J. The global burden of diabetic foot disease. The Lancet. 2005;366(9498):1719-24.

371.   Nenadis N, Tsimidou M. Observations on the estimation of scavenging activity of phenolic compounds using rapid 1, 1-diphenyl-2-picrylhydrazyl (DPPH•) tests. Journal of the American Oil Chemists' Society. 2002;79:1191-5.

372.   Zhang W, Lan Y, Dang B, Zhang J, Zheng W, Du Y, et al. Polyphenol Profile and In Vitro Antioxidant and Enzyme Inhibitory Activities of Different Solvent Extracts of Highland Barley Bran. Molecules. 2023;28(4):1665.

373.   Keskin C. Antioxidant, anticancer and anticholinesterase activities of flower, fruit and seed extracts of Hypericum amblysepalum HOCHST. Asian Pac J Cancer Prev. 2015;16(7):2763-9.

374.   Nićiforović N, Abramovič H. Sinapic acid and its derivatives: natural sources and bioactivity. Comprehensive reviews in food science and food safety. 2014;13(1):34-51.

375.   Kalinowska M, Płońska A, Trusiak M, Gołębiewska E, Gorlewska-Pietluszenko A. Comparing the extraction methods, chemical composition, phenolic contents and antioxidant activity of edible oils from Cannabis sativa and Silybum marianu seeds. Scientific Reports. 2022;12(1):20609.

376.   Van Norman GA. Limitations of animal studies for predicting toxicity in clinical trials: is it time to rethink our current approach? JACC: Basic to Translational Science. 2019;4(7):845-54.

377.   Hameed H, Aydin S, Başaran AA, Başaran N. Assessment of cytotoxic properties of sinapic acid in vitro. Turk J Pharm Sci. 2016;13(2):225-32.

378.   Kim Y-O, Lee S-W, Oh M-S, Lee HJ. Effects of sinapic Acid of 4 vessel occlusion model-induced ischemia and cognitive impairments in the rat. Clinical Psychopharmacology and Neuroscience. 2011;9(2):86.

379.   Akbarian M, Bertassoni LE, Tayebi L. Biological aspects in controlling angiogenesis: Current progress. Cellular and Molecular Life Sciences. 2022;79(7):349.

380.   Everts PA, Lana JF, Onishi K, Buford D, Peng J, Mahmood A, et al. Angiogenesis and Tissue Repair Depend on Platelet Dosing and Bioformulation Strategies Following Orthobiological Platelet-Rich Plasma Procedures. A Narrative Review. 2023.

381.   Dudley AC, Griffioen AW. Pathological angiogenesis: mechanisms and therapeutic strategies. Angiogenesis. 2023:1-35.

382.   Herion NJ, Kruger C, Staszkiewicz J, Kappen C, Salbaum JM. Embryonic cell migratory capacity is impaired upon exposure to glucose in vivo and in vitro. Birth defects research. 2019;111(14):999-1012.

383.   Buranasin P, Mizutani K, Iwasaki K, Pawaputanon Na Mahasarakham C, Kido D, Takeda K, et al. High glucose-induced oxidative stress impairs proliferation and migration of human gingival fibroblasts. PloS one. 2018;13(8):e0201855.

384.   Dix TA, Aikens J. Mechanisms and biological relevance of lipid peroxidation initiation. Chemical research in toxicology. 1993;6(1):2-18.

385.   de Souza Bastos A, Graves DT, de Melo Loureiro AP, Júnior CR, Corbi SCT, Frizzera F, et al. Diabetes and increased lipid peroxidation are associated with systemic inflammation even in well-controlled patients. Journal of Diabetes and its Complications. 2016;30(8):1593-9.

386.   Jain SK, Levine SN, Duett J, Hollier B. Elevated lipid peroxidation levels in red blood cells of streptozotocin-treated diabetic rats. Metabolism. 1990;39(9):971-5.

387.   Ambika S, Saravanan R, Thirumavalavan K. Antidiabetic and antihyperlipidemic effect of p-hydroxycinnamic acid on streptozotocin-induced diabetic Wistar rats. Biomedicine & Aging Pathology. 2013;3(4):253-7.

388.   Mahreen R, Mohsin M, Nasreen Z, Siraj M, Ishaq M. Significantly increased levels of serum malonaldehyde in type 2 diabetics with myocardial infarction. International journal of diabetes in developing countries. 2010;30(1):49.

389.   Noberasco G, Odetti P, Boeri D, Maiello M, Adezati L. Malondialdehyde (MDA) level in diabetic subjects. Relationship with blood glucose and glycosylated hemoglobin. Biomedicine & pharmacotherapy. 1991;45(4-5):193-6.

390.   Kar K, Bhattacharyya A, Paria B. Elevated MDA Level Correlates with Insulin Resistance in Prediabetes. Journal of Clinical & Diagnostic Research. 2018;12(8).

391.   Nacítarhan S, Özben T. Serum and urine malondialdehyde levels in NIDDM patients with and without hyperlipidemia. Free Radical Biology and Medicine. 1995;19(6):893-6.

392.   Schieber M, Chandel NS. ROS function in redox signaling and oxidative stress. Current biology. 2014;24(10):R453-R62.

393.   Aranda-Rivera AK, Cruz-Gregorio A, Arancibia-Hernández YL, Hernández-Cruz EY, Pedraza-Chaverri J. RONS and oxidative stress: An overview of basic concepts. Oxygen. 2022;2(4):437-78.

394.   Forman HJ, Zhang H. Targeting oxidative stress in disease: Promise and limitations of antioxidant therapy. Nature Reviews Drug Discovery. 2021;20(9):689-709.

395.   Noeman SA, Hamooda HE, Baalash AA. Biochemical study of oxidative stress markers in the liver, kidney and heart of high fat diet induced obesity in rats. Diabetology & metabolic syndrome. 2011;3(1):1-8.

396.   Peluso I, Palmery M, Drummen G. Biomarkers of oxidative stress in experimental models and human studies with nutraceuticals: Measurement, interpretation, and significance 2017. Hindawi; 2017.

397.   Gilani SJ, Bin-Jumah MN, Al-Abbasi FA, Nadeem MS, Afzal M, Sayyed N, et al. Fustin ameliorates hyperglycemia in streptozotocin induced type-2 diabetes via modulating glutathione/Superoxide dismutase/Catalase expressions, suppress lipid peroxidation and regulates histopathological changes. Saudi Journal of Biological Sciences. 2021;28(12):6963-71.

398.   Tunali S, Yanardag R. Protective effect of vanadyl sulfate on skin injury in streptozotocin-induced diabetic rats. Human & experimental toxicology. 2013;32(11):1206-12.

399.   Mani A, Kushwaha K, Khurana N, Gupta J. p-Coumaric acid attenuates high-fat diet-induced oxidative stress and nephropathy in diabetic rats. Journal of Animal Physiology and Animal Nutrition. 2022;106(4):872-80.

400.   Koriem KM, Gad IB. Sinapic acid restores blood parameters, serum antioxidants, and liver and kidney functions in obesity. Journal of Diabetes & Metabolic Disorders. 2022;21(1):293-303.

401.   Altındağ F, Rağbetli MÇ, Özdek U, Koyun N, Alhalboosi JKI, Elasan S. Combined treatment of sinapic acid and ellagic acid attenuates hyperglycemia in streptozotocin-induced diabetic rats. Food and Chemical Toxicology. 2021;156:112443.

402.   Giebułtowicz J, Sołobodowska S, Bobilewicz D, Wroczyński P. Blood ALDH1 and GST activity in diabetes type 2 and its correlation with glycated hemoglobin. Experimental and Clinical Endocrinology & Diabetes. 2014;122(01):55-9.

403.   Sharma M, Gupta S, Singh K, Mehndiratta M, Gautam A, Kalra OP, et al. Association of glutathione-S-transferase with patients of type 2 diabetes mellitus with and without nephropathy. Diabetes & Metabolic Syndrome: Clinical Research & Reviews. 2016;10(4):194-7.

404.   Tesauro M, Nisticò S, Noce A, Tarantino A, Marrone G, Costa A, et al. The possible role of glutathione-S-transferase activity in diabetic nephropathy. International Journal of Immunopathology and Pharmacology. 2015;28(1):129-33.

405.   Madi M, Babu S, Kumari S, Shetty S, Achalli S, Madiyal A, et al. Status of serum and salivary levels of superoxide dismutase in type 2 diabetes mellitus with oral manifestations: a case control study. Ethiopian journal of health sciences. 2016;26(6):523-32.

406.   Kanchana G, Shyni WJ, Malini P, Rajadurai M. Effect of sinapic acid on antiperoxidative and antioxidant potential in normal and streptozotocin-induced diabetes in wistar rats. Int J Pharm Clin Res. 2011;3(1):5-9.

407.   Alaofi AL. Sinapic acid ameliorates the progression of streptozotocin (STZ)-induced diabetic nephropathy in rats via NRF2/HO-1 mediated pathways. Frontiers in Pharmacology. 2020;11:1119.

408.   Mestry SN, Dhodi JB, Kumbhar SB, Juvekar AR. Attenuation of diabetic nephropathy in streptozotocin-induced diabetic rats by Punica granatum Linn. leaves extract. Journal of traditional and complementary medicine. 2017;7(3):273-80.

409.   Promyos N, Phienluphon PP, Wechjakwen N, Lainampetch J, Prangthip P, Kwanbunjan K. Inverse Correlation of Superoxide Dismutase and Catalase with Type 2 Diabetes among Rural Thais. Nutrients. 2023;15(9):2071.

410.   Góth L. Reactive oxygen species, hydrogen peroxide, catalase and diabetes mellitus. Redox Report. 2006;11(6):281-2.

411.   Takemoto K, Tanaka M, Iwata H, Nishihara R, Ishihara K, Wang D-H, et al. Low catalase activity in blood is associated with the diabetes caused by alloxan. Clinica Chimica Acta. 2009;407(1-2):43-6.

412.   Raish M, Ahmad A, Jardan YAB, Shahid M, Alkharfy KM, Ahad A, et al. Sinapic acid ameliorates cardiac dysfunction and cardiomyopathy by modulating NF-κB and Nrf2/HO-1 signaling pathways in streptozocin induced diabetic rats. Biomedicine & pharmacotherapy. 2022;145:112412.

413.   Bharti SK, Krishnan S, Kumar A, Kumar A. Antidiabetic phytoconstituents and their mode of action on metabolic pathways. Therapeutic Advances in Endocrinology and metabolism. 2018;9(3):81-100.

414.   Chaudhury A, Duvoor C, Reddy Dendi VS, Kraleti S, Chada A, Ravilla R, et al. Clinical review of antidiabetic drugs: implications for type 2 diabetes mellitus management. Frontiers in endocrinology. 2017;8:6.

415.   Sagandira CR, Khasipo AZ, Sagandira MB, Watts P. An overview of the synthetic routes to essential oral anti-diabetes drugs. Tetrahedron. 2021;96:132378.

416.   Alam S, Sarker MMR, Sultana TN, Chowdhury MNR, Rashid MA, Chaity NI, et al. Antidiabetic phytochemicals from medicinal plants: prospective candidates for new drug discovery and development. Frontiers in endocrinology. 2022;13:800714.

417.   Cani PD, Bibiloni R, Knauf C, Waget A, Neyrinck AM, Delzenne NM, et al. Changes in gut microbiota control metabolic endotoxemia-induced inflammation in high-fat diet–induced obesity and diabetes in mice. Diabetes. 2008;57(6):1470-81.

418.   Wang C-Y, Liao JK. A mouse model of diet-induced obesity and insulin resistance. Mtor: Methods and Protocols. 2012:421-33.

419.   Konda PY, Poondla V, Jaiswal KK, Dasari S, Uyyala R, Surtineni VP, et al. Pathophysiology of high fat diet induced obesity: impact of probiotic banana juice on obesity associated complications and hepatosteatosis. Scientific Reports. 2020;10(1):16894.

420.   Pathak K, Das A, Shakya A, Saikia R, Sarma H. Evaluation of Anti-Diabetic and Anti-Hyperlipidemic Activity of Isolated Bioactive Compounds of Leaves of Annona reticulata Linn. The Natural Products Journal. 2021;11(3):414-21.

421.   Farzaei MH, Zobeiri M, Parvizi F, El-Senduny FF, Marmouzi I, Coy-Barrera E, et al. Curcumin in liver diseases: a systematic review of the cellular mechanisms of oxidative stress and clinical perspective. Nutrients. 2018;10(7):855.

422.   El-Beshbishy HA, Mohamadin AM, Nagy AA, Abdel-Naim AB. Amelioration of tamoxifen-induced liver injury in rats by grape seed extract, black seed extract and curcumin. 2010.

423.   Manoeuvrier G, Bach-Ngohou K, Batard E, Masson D, Trewick D. Diagnostic performance of serum blood urea nitrogen to creatinine ratio for distinguishing prerenal from intrinsic acute kidney injury in the emergency department. BMC nephrology. 2017;18(1):1-7.

424.   Liu Y-M, Xie J, Chen M-M, Zhang X, Cheng X, Li H, et al. Kidney function indicators predict adverse outcomes of COVID-19. Med. 2021;2(1):38-48. e2.

425.   Lan Q, Zheng L, Zhou X, Wu H, Buys N, Liu Z, et al. The value of blood urea nitrogen in the prediction of risks of cardiovascular disease in an older population. Frontiers in Cardiovascular Medicine. 2021;8:614117.

426.   Pandya D, Nagrajappa AK, Ravi K. Assessment and correlation of urea and creatinine levels in saliva and serum of patients with chronic kidney disease, diabetes and hypertension–a research study. Journal of clinical and diagnostic research: JCDR. 2016;10(10):ZC58.

427.   Al-Naimi MS, Rasheed HA, Hussien NR, Al-Kuraishy HM, Al-Gareeb AI. Nephrotoxicity: Role and significance of renal biomarkers in the early detection of acute renal injury. Journal of advanced pharmaceutical technology & research. 2019;10(3):95.

428.   Edelstein CL. Biomarkers in acute kidney injury. Biomarkers of Kidney Disease. 2017:241-315.

429.   Hassan MM, Uddin S, Bhowmik A, Ashraf A, Islam MM, Rokeya B. Phytochemical screening and antidiabetic effects of fruit rind of Momordica dioica roxb. on streptozocin induced type 2 diabetic rats. Heliyon. 2022;8(1).

430.   Komeili G, Hashemi M, Bameri-Niafar M. Evaluation of antidiabetic and antihyperlipidemic effects of Peganum harmala seeds in diabetic rats. Cholesterol. 2016;2016.

431.   Eilam Y, Pintel N, Khattib H, Shagug N, Taha R, Avni D. Regulation of Cholesterol Metabolism by Phytochemicals Derived from Algae and Edible Mushrooms in Non-Alcoholic Fatty Liver Disease. International Journal of Molecular Sciences. 2022;23(22):13667.

432.   Sharifi-Rad M, Anil Kumar NV, Zucca P, Varoni EM, Dini L, Panzarini E, et al. Lifestyle, oxidative stress, and antioxidants: Back and forth in the pathophysiology of chronic diseases. Frontiers in physiology. 2020;11:694.

433.   Tan BL, Norhaizan ME, Liew W-P-P, Sulaiman Rahman H. Antioxidant and oxidative stress: a mutual interplay in age-related diseases. Frontiers in pharmacology. 2018;9:1162.

434.   Jomova K, Raptova R, Alomar SY, Alwasel SH, Nepovimova E, Kuca K, et al. Reactive oxygen species, toxicity, oxidative stress, and antioxidants: Chronic diseases and aging. Archives of toxicology. 2023;97(10):2499-574.

435.   Kaltalioglu K. Sinapic acid-loaded gel accelerates diabetic wound healing process by promoting re-epithelialization and attenuating oxidative stress in rats. Biomedicine & Pharmacotherapy. 2023;163:114788.

436.   Guo Sa, DiPietro LA. Factors affecting wound healing. Journal of dental research. 2010;89(3):219-29.

437.   Rodrigues M, Kosaric N, Bonham CA, Gurtner GC. Wound healing: a cellular perspective. Physiological reviews. 2019;99(1):665-706.

438.   Velnar T, Bailey T, Smrkolj V. The wound healing process: an overview of the cellular and molecular mechanisms. J Int Med Res. 2009;37(5):1528-42.

439.   Okur ME, Karantas ID, Şenyiğit Z, Üstündağ Okur N, Siafaka PI. Recent trends on wound management: New therapeutic choices based on polymeric carriers. Asian J Pharm Sci. 2020;15(6):661-84.

440.   Ramamurthy NS, Zebrowski EJ, Golub LM. The effect of alloxan diabetes on gingival collagen metabolism in rats. Arch Oral Biol. 1972;17(11):1551-60.

441.   Arul V, Masilamoni JG, Jesudason EP, Jaji PJ, Inayathullah M, Dicky John DG, et al. Glucose oxidase incorporated collagen matrices for dermal wound repair in diabetic rat models: a biochemical study. J Biomater Appl. 2012;26(8):917-38.

442.   Gupta A, Kumar P. Assessment of the histological state of the healing wound. Plastic and Aesthetic Research. 2015;2:239-42.

443.   Chakraborty R, Borah P, Dutta PP, Sen S. Evolving spectrum of diabetic wound: Mechanistic insights and therapeutic targets. World Journal of Diabetes. 2022;13(9):696.